



RNA Degradation using Small Molecule- Based Recruiters of RNase L

Dissertation

For the achievement of the academic degree of the
Doctor in Natural Sciences
(Doctor Rerum Naturalium)

Submitted to

Faculty of Chemistry and Chemical Biology
Technical University of Dortmund

by

Carl Leonard Stenbratt

from Fässberg, Sweden

Dortmund 2021

The work presented in this thesis was performed from October 2018 to October 2021 under supervision of Prof. Dr. Herbert Waldmann and Dr. Peng Wu at the Max Planck Institute of Molecular Physiology and the Chemical Genomics Centre of the Max Planck Society.

1st Examiner: Prof. Dr. Herbert Waldmann

2nd Examiner: Dr. Andreas Brunschweiler

*Nog finns det mål och mening i vår färd -
men det är vägen, som är mödan värd*

Karin Boye

Table of contents

Abstract	1
Zusammenfassung	2
1. Introduction	4
1.1. RNA as a Target in Drug Discovery	4
1.2. Targeted RNA Cleavage and Degradation.....	13
2. Aim of the Thesis	31
3. Results and Discussion	32
3.1. Small Molecule RNase L Activators.....	32
3.1.1. <i>Thienopyrimidinones</i>	32
3.1.2. <i>Thienodiazepines</i>	34
3.1.3. <i>Thiophenones</i>	39
3.1.4. <i>Biochemical Evaluation</i>	41
3.2. RNA Interactome Targeting Chimera	43
3.2.1. <i>WDR5 Inhibitors</i>	44
3.2.2. <i>Chemical Synthesis of WDR5 Inhibitors</i>	49
3.2.3. <i>Biochemical Evaluation</i>	55
3.2.4. <i>Bifunctional Molecules</i>	56
3.3. Ribonuclease Targeting Chimera.....	59
3.3.1. <i>HIV-1 TAR Ligands</i>	59
3.3.2. <i>Chemical Synthesis of HIV-1 TAR Ligands</i>	62
3.3.3. <i>Bifunctional Molecules</i>	65
4. Conclusion	67
5. Perspective	69

6. Experimental	71
6.1. General Information	71
6.2. Synthesis of Thiophenes	72
6.3. Synthesis of Benzonitriles	73
6.4. Synthesis of Thienopyrimidinones	76
6.5. Synthesis of <i>N</i> -Boc Thiophene Dipeptides	79
6.6. Synthesis of Thiophene Dipeptides	84
6.7. Synthesis of Thienodiazepines	88
6.8. Synthesis of Thiophenones	88
6.9. Synthesis of WDR5 Inhibitors	93
6.10. Synthesis of RITACs	103
6.11. Synthesis of HIV TAR Ligands	107
6.12. Synthesis of RIBOTACs	114
6.13. Biochemical Evaluation	117
7. References	118
8. Appendix	143
8.1. List of Abbreviations	143
8.2. Acknowledgements	151
8.3. Eidesstattliche Versicherung (Affidavit)	152

Abstract

The human genome is mainly transcribed into non-coding RNAs that are not translated into proteins. With increasing understanding of function through continued research it has become evident that parts of the transcriptome are disease-related. RNAs are becoming increasingly important targets for the development of novel medicines using chemical modalities such as small molecules, bifunctional molecules, peptides, oligonucleotides and conjugates. Yet we have only discovered part of what is possible to achieve by targeting non-coding RNAs that allows for modifications of cellular processes beyond of what is capable by targeting proteins.

Described in this thesis are strategies targeting RNAs for degradation and the synthesis of lead compounds in the development of novel tools and therapeutics. Catalytically acting therapeutics offer advantages including lower drug dosage and longer lasting effect. This may allow them to serve as tools for target elucidation in biological studies. The main results are divided into three chapters. First, the design, synthesis and characterization of 2-aminothiophene-containing heterocyclic molecules with the introduction of functional groups were allowing for appendage conjugation. Compounds were evaluated in an RNase L activation assay to identify thiophenones as the most suitable for incorporation in heterobifunctional molecules to recruit RNase L. Second, evolution of the novel RITAC strategy to target the RNA interactome of RNA-binding proteins for degradation is described here. As proof-of-concept, targeted degradation of the RNA interactome of the RNA-binding protein WDR5 using heterobifunctional molecules may serve to identify new protein-RNA interactions as well as to develop therapeutics for the treatment of acute myeloid leukemia. Design, synthesis and characterization of heterobifunctional molecules containing thiophenones for recruitment of RNase L and reported small molecules for selected targets were performed. Third, RIBOTACs were developed from thienopyridines to recruit RNase L for degradation of the HIV-1 RNA genome by binding to the transactivation response element. Obtained compounds are to be evaluated for their application in potentially addressing HIV-1 infections.

This thesis shows the design and synthesis of small molecule-based heterobifunctional molecules (Figure 1) for targeted RNA degradation via the recruitment of RNase L, and the potential that the synthesized compounds have to be used as tools and therapeutics.

Zusammenfassung

Der Großteil des menschlichen Genoms wird in sogenannte *non-coding RNAs* transkribiert, die nie in Proteine translatiert werden. Die Forschung zeigt, dass Teile des Transkriptoms eine Rolle in der Entstehung von Krankheiten spielen. *RNA* wird daher zu einem immer wichtigeren Ziel für die Entwicklung neuartiger Medikamente unter Verwendung chemischer Modalitäten wie *small molecules*, bifunktionelle Moleküle, Peptide und Oligonukleotide. Bis jetzt wurde jedoch nur einen Teil dessen entdeckt, was durch das Targeting von *non-coding RNAs* erreicht werden kann und das Adressieren von *RNA* wird Modifikationen zellulärer Prozesse ermöglichen, die über das hinausgehen, was durch das Targeting von Proteinen möglich ist.

In dieser Arbeit werden Strategien zum selektiven Abbau von *RNAs* beschrieben, die Leitstrukturen für die Entwicklung neuer molekularer Werkzeuge und Therapeutika bieten. Katalytisch wirkende Therapeutika haben den Vorteil, dass sie eine geringere Medikamentendosis benötigen und gleichzeitig eine länger anhaltende Wirkung aufweisen. Zudem können sie als Werkzeug für den *Target-Knockdown* in biologischen Studien dienen. Die wichtigsten Ergebnisse sind in drei Kapitel unterteilt. Zunächst werden Design, Synthese und Charakterisierung von 2-Aminothiophen enthaltenden heterocyclischen Molekülen mit Einführung funktioneller Gruppen, die eine Konjugation ermöglichen, beschrieben. Diese Verbindungen wurden in einem *RNase L FRET*-Aktivierungsassay evaluiert. Thiophenone sind damit am geeignetsten für den Einbau in heterobifunktionelle Moleküle zur Rekrutierung von *RNase L*. Zweitens wird hier die Entwicklung der neuartigen *RITAC* Strategie zum gezielten Abbau des *RNA*-Interaktoms *RNA* bindender Proteine aufgezeigt. Der gezielte Abbau des *WDR5-RNA*-Interaktoms unter Verwendung heterobifunktioneller Moleküle könnte als Werkzeug zur Identifizierung neuer Protein-*RNA*-Interaktionen sowie als Therapeutikum zur Behandlung der akuten myeloischen Leukämie dienen. Design, Synthese und Charakterisierung heterobifunktioneller Moleküle, die einerseits Thiophenone für die Rekrutierung von *RNase L* und andererseits bekannte *small molecules* für ausgewählte Targets enthalten, wurden durchgeführt. Drittens wurden *RIBOTACs* aus Thienopyridinen für die Rekrutierung von *RNase L* zur *TAR RNA* für den teilweisen oder vollständigen Abbau des *HIV-1 RNA*-Genoms entwickelt. Die gewonnenen Verbindungen sollen

in Zukunft auf ihr Anwendungspotenzial bei der Bekämpfung von *HIV-1*-Infektionen untersucht werden.

Die Arbeit in dieser Dissertation zeigt das Design und die Synthese von heterobifunktionellen Molekülen (Figure 1) auf Basis von *small molecules* für den gezielten *RNA*-Abbau durch Rekrutierung der Endonuklease *RNase L* sowie das Potenzial, dass die synthetisierten Verbindungen als *tools* und Therapeutika verwendet werden können.

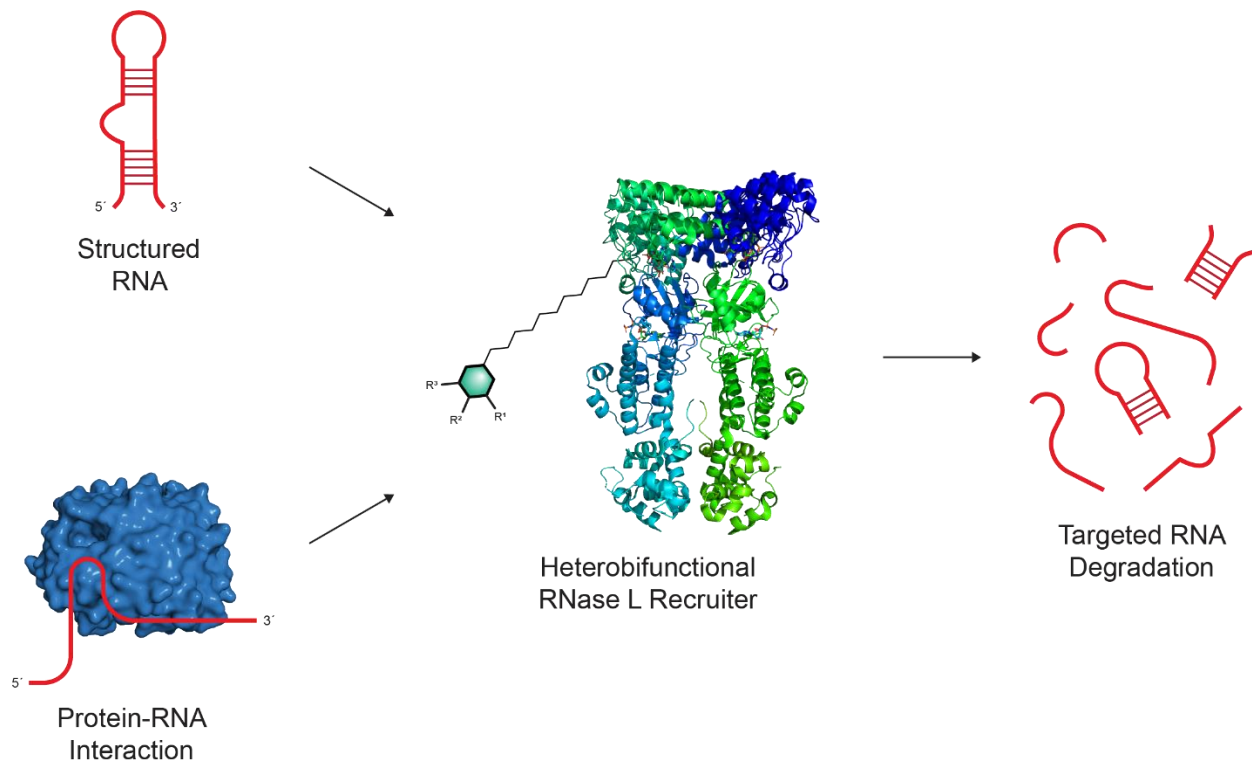


Figure 1. Recruitment of RNase L using small molecule-based heterobifunctional molecules for targeted degradation of disease-causing RNAs.

1. Introduction

Development of therapeutics based on different chemical modalities, such as small molecules, peptides and peptidomimetics, nucleotides and nucleic acids, are important for advancing the treatment of human diseases.^[1] In parallel, identification of new drug targets and strategies utilizing new mode of actions has promoted the progression of therapeutics in past decades.^[2]

1.1. RNA as a Target in Drug Discovery

The human genome is, to the greatest extent, transcribed into RNAs without protein-coding regions, often referred to as non-coding RNAs (ncRNAs). Despite that just 1.5% of human genome is translated, most efforts in the development of pharmaceuticals have been focused on a small number of proteins. Out of all ~20 000 human proteins, less than 700 have been targeted with approved drugs, meaning that less than 0.05% of the human genome has been addressed by currently available pharmaceuticals (Figure 2).^[3, 4] Like proteins, ncRNAs regulate gene expression through numerous mechanisms and their dysregulation has been related to a wide range of human diseases, which makes ncRNAs a promising target class in drug discovery.^[5] Targeting ncRNAs offers a wide variety of opportunities to modulate cellular processes, inaccessible when targeting proteins, in the search for new medicines.

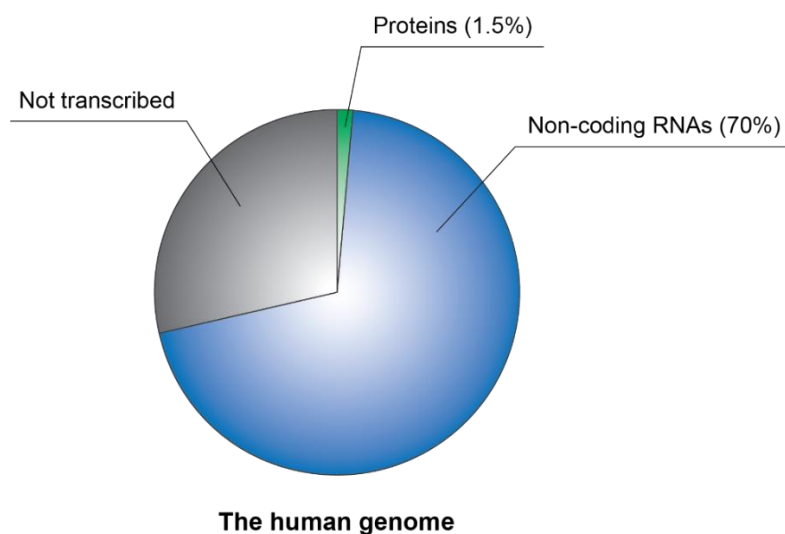


Figure 2. Overview of the human DNA sequence containing ~3 billion base pairs storing the genetic information regarding transcription of protein-coding and non-coding RNAs.

The four nucleic bases cytosine, guanine, adenine, and uracil are the natural building blocks of RNA with a backbone of ribose units connected by phosphodiester (Figure 3A). Compared to proteins, which are composed of 20 different natural amino acids, the diversity of natural bases is low and it was for a long time uncertain if RNA formed stable tertiary structures from the linear sequence (Figure 3B). Post-transcriptional modifications further extend the variety of natural nucleic bases and impact folding.^[6] Numerous stable RNA structures have now experimentally been determined using NMR spectroscopy,^[7] small-angle X-ray scattering^[8] or cryo-EM,^[9] suggesting that RNAs can be targeted by various chemical modalities depending on tertiary folded structures (Figure 3D).

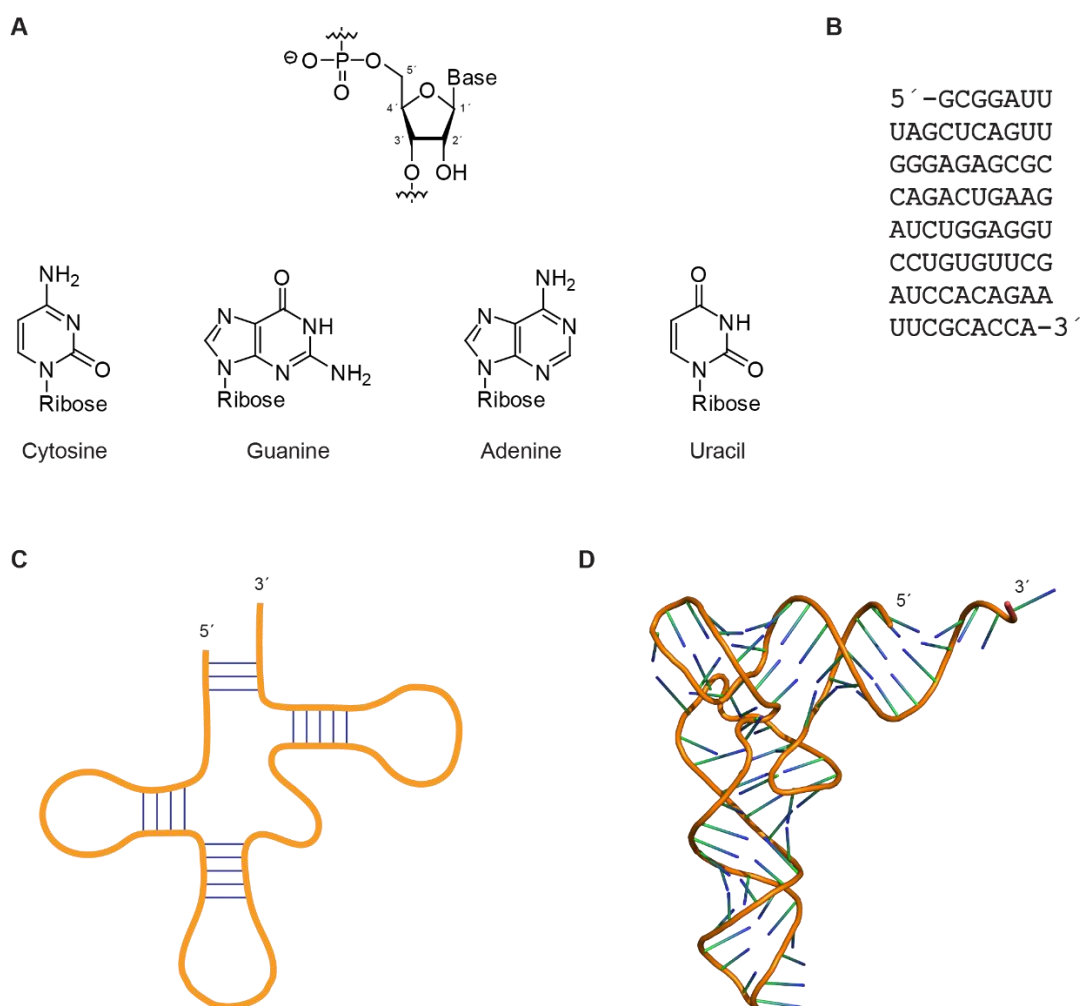


Figure 3. Structure of RNA. **A:** Elements of ribonucleic acids; ribose, phosphate, nucleic bases. **B:** Primary structure is the sequence of nucleic acids, displayed is the sequence of tRNA. **C:** Base pairing form RNA motifs in the secondary structure of tRNA resembling a cloverleaf structure. **D:** Tertiary structure of tRNA (crystal structure, PDB: 1EHZ) folded into an L-shape stabilized by intramolecular interactions.

Conserved structures observed in RNAs include hairpins, internal loops, bulges, pseudoknots and G-quadruplexes. They can be efficiently recognized and bound by small molecules, peptides and RNA-binding proteins (RBPs).^[10] Continued efforts to elucidate the function of RNA networks and identification of suitable chemical modalities indicate a resurrection in targeting RNAs in drug discovery.

1.1.1. Oligonucleotide Therapeutics

High selectivity and potency in targeting RNAs can be achieved by the use of synthetic nucleic acid polymers through Watson-Crick base pairing with unstructured regions of endogenously expressed transcripts. Limited metabolic stability, off-target cytotoxicity and challenging drug delivery, due to poor cell permeability, are issues required to overcome for successful development of oligonucleotide-based therapeutics.^[11, 12] While oligonucleotides efficiently hybridize with linear RNA, it is demanding to target highly structured regions of RNA,^[13] where small molecules, peptides and proteins are more suitable chemical modalities.

Chemical modifications of the oligonucleotide backbone linkage, sugar moiety, base pairs and terminal conjugates have been employed for stabilization of oligonucleotides to avoid cleavage by nucleases.^[14] Certain modifications improve cellular uptake, such as conjugation to trivalent *N*-acetylgalactosamine (GalNAc) that mediates active membrane transport through interaction with asialoglycoprotein receptor (ASGPR).^[15] Targeted delivery to adipocytes can also be achieved using neuropeptide Y receptor Y1 (NPY1R) ligands^[16] and folate as a ligand of the folate receptor to mediate transport to tumour cells.^[17] Conjugation to glucagon-like peptide 1 (GLP1) has also been successful for targeted delivery to beta-cells promoting the development of treatments for diabetes.^[18] Formulation of oligonucleotides is essential for efficient drug delivery and can solve issues related to metabolic stability, cytotoxicity and adsorption. Administration of nanoparticles has been successful for the delivery of unmodified oligonucleotides to tumours and simultaneously provides protection from nucleases and undesired cytotoxicity.^[19]

The first synthetic oligonucleotides were developed in the 1970's.^[20] Despite decades of research on nucleic acids it was not until recently that the first therapeutics were approved.^[21] With a deoxyribose backbone, antisense oligonucleotides (ASOs) (Section 1.2.1.), can form RNA-DNA duplexes, which are substrates for human ribonuclease H (RNase H) resulting in cleavage of the

target RNA backbone. Targeted RNA degradation by ASOs causes suppressed gene expression.^[22] There is a growing number of ASO therapeutics approved for drug use (Table 1), including Milasen developed for a single patient with a rare disease.^[23] Additionally, several ASOs are undergoing clinical trials.^[24]

The mechanism of RNA interference (RNAi) (Section 1.2.2.) using synthetic small interfering RNA (siRNA) is gaining interest in the pharmaceutical industry. Three siRNAs have already been approved for drug use (Table 1). Numerous siRNA therapeutics are also in clinical trials.^[25]

Table 1. Clinically approved oligonucleotide-based therapeutics targeting RNAs.

Drug	Approval year	Target	Indication
Antisense oligonucleotides			
Fomivirsen ^[26]	1998	CMV UL123	CMV retinitis
Mipomersen ^[27]	2013	apoB-100	HoFH
Nusinersen ^[28]	2016	SMN2	SMA
Eteplirsen ^[28]	2016	DMD exon 51	DMD
Inotersen ^[29]	2018	TTR	hATTR
Golodirsen ^[30]	2018	DMD exon 53	DMD
Milasen ^[23]	2019	CLN7	Batten disease
Volanesorsen ^[31]	2019	apoC-III	FCS
Viltolarsen ^[32]	2020	DMD exon 53	DMD
Casimersen ^[33]	2021	DMD exon 45	DMD
Small interfering RNAs			
Patisiran ^[34]	2018	TTR	hATTR
Givosiran ^[35]	2019	ALAS1	AHP
Lumasiran ^[36]	2020	HAO1	PH1

This chemical modality has attracted attention in the pharmaceutical industry to develop therapeutics for targets that have not been accessible using small molecule-based strategies and thereby termed undruggable. Continued efforts in the development of oligonucleotide conjugates offers the advantage of targeted delivery *in vivo*.

1.1.2. Small Molecule Therapeutics

The advantages of using small molecule-based therapeutics lies in favorable pharmacokinetic properties. This includes sufficient metabolic stability and cell permeability that allow oral bioavailability. Structurally stable binding sites within RNA are required for the development of selective small molecules, since binding mostly depends on non-covalent interactions, but can be challenging to determine due to the flexibility of RNA.^[37, 38]

Microarray assays have been successfully used in the identification of small molecule binders to specific RNAs. Aminoglycosides are polycationic small molecules and were one of the first compound classes discovered to bind RNA with high affinity and low selectivity.^[39] The observed antibacterial effect was caused by binding bacterial rRNA and blocking protein production.^[40] Two-dimensional combinatorial screening (2DCS) microarray assays later identified new classes of small molecules as selective binders of secondary RNA structures (Figure 3C).^[41, 42] This platform was used to build a database by scoring monitored quantified interactions between small molecules and RNA motifs, called structure-activity relationships through sequencing (StARTS).^[43] The software Inforna is based on the generated data and can now be used to predict structures of active small molecule binders to RNA motifs or larger RNAs based on sequence.^[44, 45] This powerful tool has successfully generated several small molecules that selectively bind to microRNAs (miRNAs),^[46-51] RNA repeats^[52, 53] and structured mRNAs^[54-56] with some examples inducing higher selectivity than the corresponding ASOs.^[44, 57] Databases using publicly available information are small molecule modulators of RNA (SMMRNA),^[58] nucleic acid ligand database (NALDB)^[59] and RNA-targeted bioactive ligand database (R-BIND),^[60] where information about small molecule structures, physicochemical properties and activities are collected.

Two examples of RNA-targeting small molecules are Ribocil that was screened as an antibacterial agent against riboswitches,^[61, 62] and Risdiplam that was recently approved for treatment of spinal muscular atrophy (SMA) (Figure 4).^[63] Riboswitches are structured regions located within the 5′

untranslated region (UTR) of bacterial mRNAs with the ability to sense small molecule metabolites. Interaction with a metabolite, such as Ribocil, shifts the 3D-conformation and thereby regulates gene expression.^[64, 65] Risdiplam modulates the splicing pattern for the survival of motor neuron 2 (SMN2) pre-mRNA by binding structured regions in intron 7 and exon 7. This stabilizes the interaction with U1 small nuclear ribonucleoprotein (U1 snRNP) for alternative splicing, resulting in increased levels of the SMN2 protein.^[66, 67] With the preferred oral administration, compared to intrathecal injection required for the oligonucleotide Nusinersen, the new small molecule-based drugs are likely to take over part of the market for treatment of SMA.

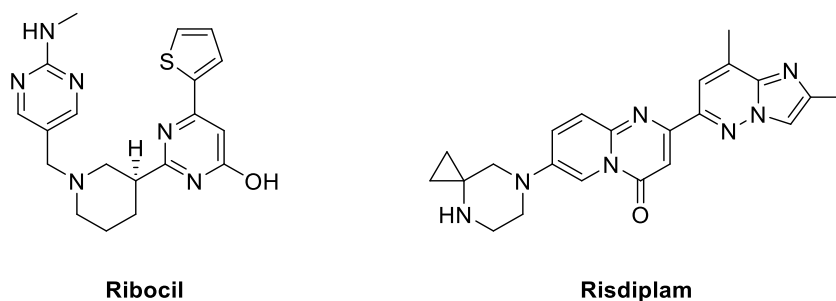


Figure 4. Examples of RNA-binding small molecules with therapeutic applications.

RNA-binding small molecules tend to be enriched in sp^2 hybridized atoms and aromatic fragments resulting in a flat conformation to allow hydrogen bond formation and stacking between nucleic bases at the interaction surface. Fragments repeatedly found in RNA targeting small molecules include aminopyrimidines, benzimidazoles, diphenylfurans, naphthalenes, purines, quinazolines and thiazoles.^[50, 68, 69] In terms of physicochemical properties, this generally results in higher lipophilicity, fewer aliphatic atoms, fewer chiral centers, more hydrogen bond donors and acceptors as well as increased positive charge compared to protein ligands. Such molecular structures allow hydrogen bonding and electrostatic interaction with the nucleic bases respectively the phosphodiester backbone.^[4, 70] Enrichment of sp^3 hybridized atoms in small molecules targeting proteins normally enhances selectivity^[71] and the lack thereof in small molecules targeting RNA might be an explanation for the issues obtaining high selectivity in addition to the increased flexibility and low diversity of natural bases in RNA.

1.1.3. Peptide-Based Modalities

Peptides have been identified as a suitable chemical modality to develop RNA ligands, similar to small molecules. Partially because of their higher molecular weights, larger interaction surfaces can be accessed by peptides that lead to increased potency and selectivity. Like oligonucleotides, peptides suffer from poor metabolic stability and in some cases limited cell permeability, which can be addressed by using unnatural amino acids and cyclisation strategies.^[72]

Various peptide collections have been explored in the search of RNA ligands, such as a dynamic combinatorial library for discovery of the first RNA repeat ligands inhibiting the interaction with muscle blind-like splicing regulator 1 (MBNL1).^[73] A microarray assay was used for the discovery of miRNA-155 binding peptides,^[74] while phage display libraries were employed for the identification of peptides inhibiting miRNA-21 processing.^[75, 76] A combinatorial library of peptide-nucleic acid hybrids was prepared by using a mixture of amino acids with natural or nucleic base-containing side chains and screening identified molecules interacting with RNA hairpins as an alternative to hybridisation of oligonucleotides through base pairing.^[77]

Another approach to develop RNA-binding peptides is the extraction of the RNA-binding domain (RBD) of various RBPs. Arginine-rich peptides derived from trans-activator of transcription (Tat) have been used as ligands of transactivation response (TAR).^[78-80] Cyclic peptides derived from the tomato aspermy virus 2b (TAV2b) have been used to target pre-miRNA-21 by interaction with the major groove of double stranded regions.^[81] Conjugation of such peptides with DNA allows additional interaction with target RNA through base pairing, which has further expanded the toolbox for targeting ssRNA.^[82]

1.1.4. RNA-Binding Proteins

Using small molecules to target proteins is an established strategy that has been used successfully in the development of selective therapeutics, aided by the rigid structure and well-defined pockets found in proteins. An alternative strategy to target RNAs with small molecules is indirectly through RBPs. These are proteins with RBDs, commonly containing positively charged amino acids forming strong electrostatic interactions with the negatively charged backbone of RNA. Types of RBDs are RNA recognition motifs (RRMs),^[83] arginine-rich motifs (ARMs),^[84] K homology (KH) domains,^[85] DEAD motifs,^[86] cold-shock domains (CSDs),^[87, 88] zinc-finger domains (ZFDs)^[89]

and dsRNA-binding motifs.^[90-93] The electrostatic substrate identification often leads to promiscuous interactions and is the reason for the high number of RNA substrates for each RBP. Therefore, it may be difficult to target specific RNAs through interaction mediated by RBPs. Another issue with targeting RBPs is the high affinity to RNA, mainly caused by strong electrostatic interactions over large surfaces, making the development of small molecules with the ability to compete with RNA challenging. This could be an explanation as to why the potency of reported small molecules inhibiting protein-RNA interactions is relatively low. However, small molecules with unique biological function may be developed if these challenges can be solved, for example by targeting allosteric binding sites.

Human RBPs interact with a wide range of RNAs consisting mainly of mRNA (45%),^[94] but also rRNA (11%), pre-rRNA (8%), tRNA (10%) and ncRNAs (26%).^[95] RBPs can regulate the function of or be regulated by their RNA substrates to control cellular processes. Inhibition or stabilization of protein-RNA interactions can have therapeutic effects and have been identified as potential targets in drug discovery.^[96] Well-characterized RBPs for which small molecule inhibitors have been reported include abnormal cell lineage protein 28 (LIN28)^[97-104] and Toll-like receptor 3 (TLR3).^[105]

LIN28 was one of the first discovered and currently most studied RBP with a relatively high selectivity for RNA substrates, limited to the miRNA *let-7* family (Figure 5A).^[106] The interaction with RNA is supported by a CSD and two ZFDs which are connected by a flexible linker, where the major part of the RNA-binding capacity is contributed by the affinity of the CSD to *let-7*.^[107] LIN28 has been found upregulated in numerous human cancers and involved in cell differentiation making it a relevant therapeutic target in oncology.^[108]

TLR3 is activated upon interaction with dsRNA forming a dimer (Figure 5B) as a viral response, facilitated using ectodomains stabilizing the complex. The horseshoe shape is induced by leucine-rich repeats found in the RBDs. Activation by dsRNA induces inflammatory signaling by expression of type I interferons and pro-inflammatory cytokines. Activation can be triggered by treating cells with poly(I:C), a synthetic dsRNA that also target other RBPs.^[109-111] Inhibition of TLR3-dsRNA interaction may serve as treatment for inflammatory diseases and viral infections by reducing inflammatory signaling.^[112]

Additionally, small molecule inhibitors of RBP-RNA complexes have also been discovered for METTL3,^[113, 114] MSI1/2,^[115-121] RNA-dependent protein kinase (PKR),^[122-124] WD (Trp-Asp)-40 repeat protein 5 (WDR5) (Section 3.2.1.) and others.^[125-139]

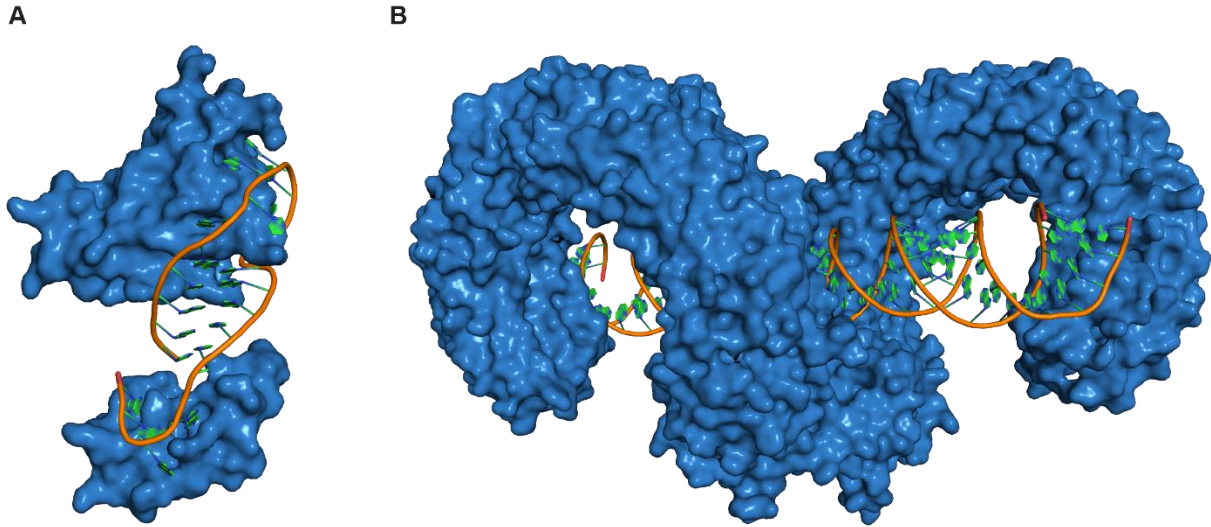


Figure 5. Crystal structures of RBPs in complex with substrate RNAs. **A:** LIN28-*let7* interaction (PDB: 3T50). **B:** TLR3-dsRNA interaction (PDB: 3CIY).

1.2. Targeted RNA Cleavage and Degradation

Degradation of disease-related targets is more advantageous in comparison to inhibiting them from interacting with other partners in signaling pathways. Inhibitors may stabilize the target resulting in increased half-life and in return accumulation.^[70] Molecules inducing catalytic degradation provide a more sustained reduction in signaling, longer duration of response and allow lower drug dosage in comparison with an inhibitor. Proteolysis targeting chimeras (PROTACs) have been successfully applied for targeted protein degradation using proximity-inducing bifunctional molecules that recruit a ubiquitin E3 ligase for ubiquitination and subsequent degradation of the target protein by the proteasome.^[140, 141] Furthermore proximity-induced degradation has shown increased selectivity over the monomeric inhibitor, supported by specific interactions with the recruited degrader.^[142] Presented here are methods for targeted cleavage or degradation of RNA.

1.2.1. Ribonuclease H

Endogenously expressed RNase H is an essential enzyme found in most eukaryotic cells. It is a type of endonuclease involved in cleaving the RNA within RNA-DNA duplexes with low sequence specificity. This mechanism supports DNA replication by degrading RNA primers on Okazaki DNA fragments remaining from processing by DNA polymerases and allows further ligation.^[143] Single stranded ASOs can modulate gene expression through several mechanisms depending on the target RNA, the sequence and chemical modifications introduced during the synthesis of the oligonucleotide. Maturation of pre-mRNA can be sterically blocked by ASOs hindering interaction with splicing factors. Targeting mature mRNAs can in similar fashion inhibit translation by sterically blocking interactions with the ribosome.^[144]

RNase H1 is present in both the cytoplasm and nucleus of mammalian cells and catalytically cleaves RNA by hydrolysis of the phosphodiester backbone, leaving the ASO component intact (Figure 6). The endonuclease enzyme contains a DEDD motif chelating two Mg^{2+} ions crucial for stabilization of transition states that forms the cleaved RNA products with 3'-hydroxyl and 5'-phosphate termini.^[145] Chemical modifications of the ribose building block in ASOs offer solutions to increase metabolic stability. However, it has been shown that RNase H1 do not cleave duplexes formed using ASOs carrying modification of the 2'-hydroxyl, such as 2'-OMe, peptide nucleic acids and locked nucleic acids. ASOs have been modified on the flanking regions, while the central

part consisting of DNA can recruit RNase H1 for targeted RNA degradation in a concept termed gapmer strategy. Combined with improved metabolic stability this strategy may offer enhanced affinity to target RNA.^[146]

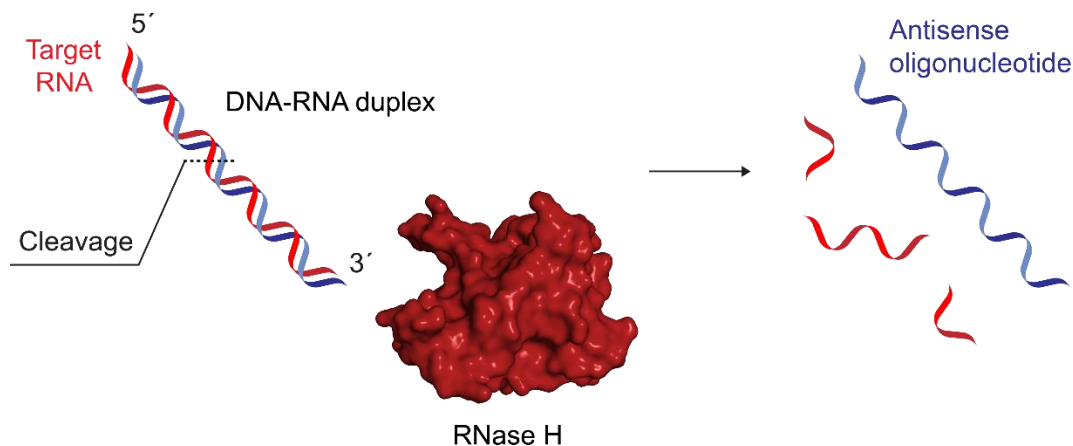


Figure 6. Antisense oligonucleotide-mediated degradation of RNA by recognition of RNase H.

1.2.2. RNA Interference

The gene silencing mechanism of RNAi by oligonucleotides was first described by Andrew Fire and Craig Mello^[147] and honored with the Nobel prize in Physiology or Medicine 2006. Silencing of mRNA transcripts is achieved by dimerization with a complementary RNA strand, which can be an administered synthetic siRNA or an endogenous miRNA, resulting in catalytic cleavage of target mRNA by the RNA-induced silencing complex (RISC) (Figure 7). Pri-miRNAs are transcribed from the human genome by RNA polymerase II to form capped and polyadenylated hairpin structures. They are further processed in the cell nucleus by RNA ribonuclease III Drosha in complex with DiGeorge syndrome critical region 8 (DGCR8) to form single hairpins of pre-miRNAs. Exportin 5 transport the transcripts into the cytoplasm, where they are processed into mature miRNA by Ribonuclease III Dicer in complex with TAR RNA-binding protein (TRBP). These double stranded 20-25 nucleotide long mature miRNAs are loaded onto Argonaute 2 (Ago2) that select the guide strand, while the passenger strand is discarded. The RISC is formed to degrade target mRNAs with complementary sequence to the miRNA.^[148]

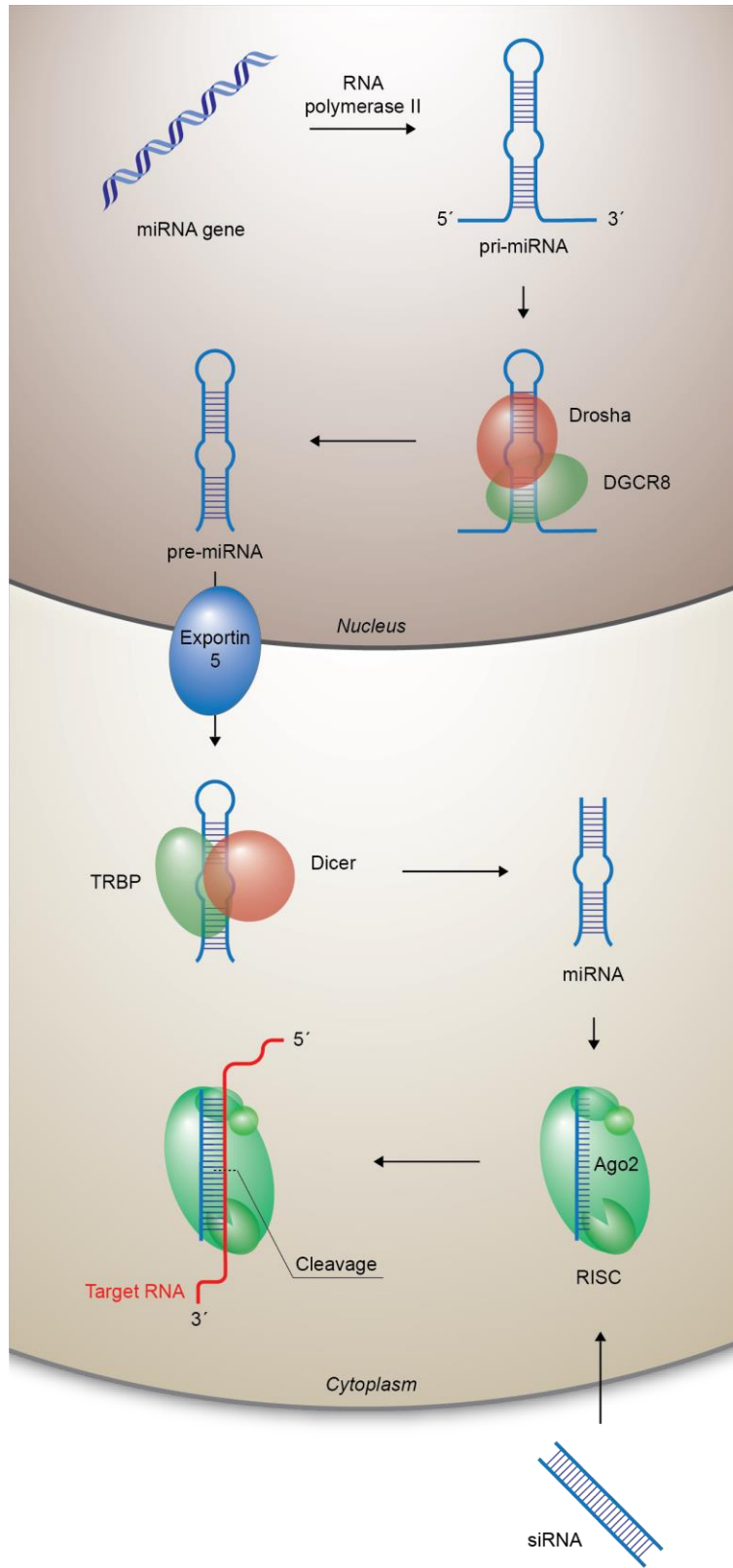


Figure 7. Mechanism of RNAi. Endogenous miRNA or synthetic siRNA can downregulate gene expression by degradation of mRNA in the RISC.

Synthetic siRNAs on the other hand can be prepared and administered as double stranded oligonucleotides, which are directly loaded onto the RISC after cell uptake without processing. Downregulation of protein expression by RNAi has proven useful, but comes with challenges. Critical factors to achieve specific and sufficient downregulation are length of siRNA and sequence selection.^[149] siRNAs with over 30 nucleotide sequences tend to bind RNA-binding proteins with affinity for dsRNA, such as PKR, TLRs, oligoadenylate synthetase (OAS), retinoic acid-inducible gene I (RIG-I) and melanoma differentiation-associated gene 5 (MDA-5). This results in activation of an immune response as an off-target effect causing cytotoxicity.^[150] Since siRNA compete with endogenous miRNA for binding of Ago2, the RISC machinery can be saturated if siRNA is dosed at too high concentration resulting in loss of regulatory function.^[151] Both strands of siRNAs can be loaded onto the RISC, however it is crucial that the complementary strand is selected as a guide strand for degradation of target mRNA. The selection process can be enhanced using chemical modifications and an AU rich sequence in the 5' end.^[152]

1.2.3. Ribozymes

Ribozymes are RNA-based macromolecules with enzymatic activities and have been studied in detail by Sidney Altman and Thomas Cech who were rewarded with the Nobel prize in Chemistry 1989. Many types of ribozymes have been applied for targeted degradation of RNAs, for example hammerhead,^[153] hairpin,^[154] hepatitis delta,^[155] varkud satellite^[156] and ribonuclease P (RNase P) ribozymes.^[157] DNA-based enzymes (deoxyribozymes) and other nucleotide modifications have been incorporated to improve metabolic stability and reactivity. For example, “10-23” share a similar RNA cleavage mechanism with the hammerhead ribozyme. The “10-23” deoxyribozyme contains two arms binding target RNA by base pairing and a 15 nucleotide catalytic core chelating Mg^{2+} that mediates RNA cleavage forming a terminal 2',3'-cyclic phosphate (Figure 8A).^[158] Incorporation of a hammerhead ribozyme binding sequence in ASOs showed cleavage of target RNA directly after hybridization. Cleaved products have 5'-hydroxy and 2',3'-cyclic phosphates termini with inversed stereochemistry.^[159]

External guide sequences (EGS) are derived from natural tRNA sequences and can be used for recruitment of endogenous RNase P that cleave target RNA. The RNase P ribozyme catalyses phosphodiester hydrolysis to remove the leader sequence of precursor tRNA and is responsible for 5' maturation of tRNA. Hybridization with target RNA and formation of a double stranded hybrid

with the EGS to mimic the secondary structure of pre-tRNAs is required in order to be recognized by RNase P (Figure 8B).^[160]

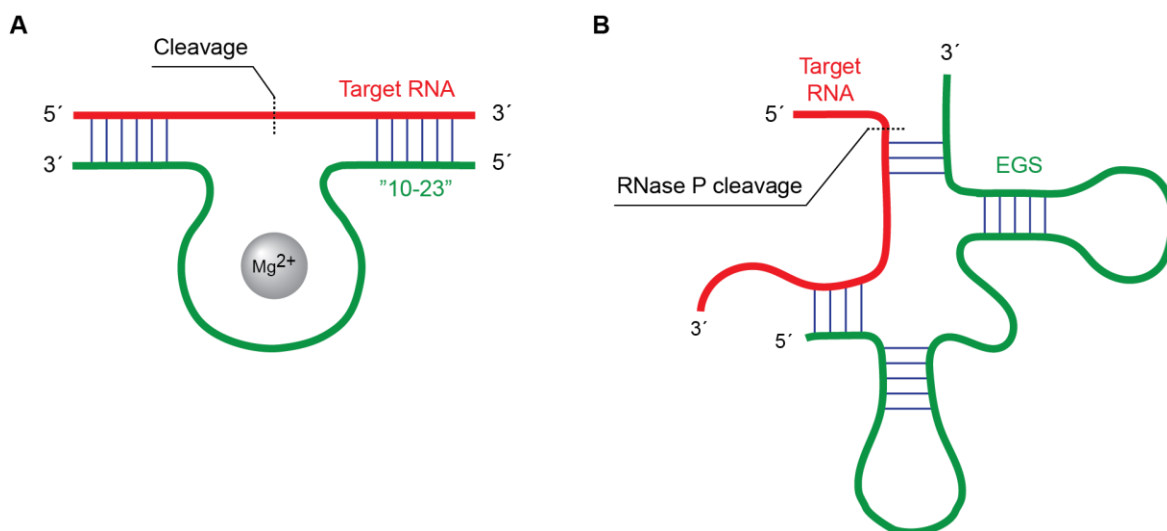


Figure 8. Targeted RNA degradation by enzymatic nucleic acid polymers. **A:** Mg²⁺-dependent RNA cleavage by deoxyribozyme "10-23". **B:** Triggering RNase P to cleave target mRNA by incorporation of external guide sequence (EGS).

1.2.4. RNA Exosome

The RNA exosome can be compared to the proteasome as a recycling center, where the exosome degrades RNAs and the proteasome degrades proteins. Both machineries consist of a complex of hydrolytic enzymes to cleave biomolecules into smaller fragments for reuse or excretion.^[161] ASOs binding the 3'-UTR of pre-mRNAs have been tethered with the sequence of U1 adaptors. Including this 10 nucleotide sequence derived from U1 small nuclear RNA (snRNA) in the final ASO results in formation of the U1 snRNP complex together with target pre-mRNA (Figure 9). The formed complex sterically hinders polyadenylation and since the mRNA fails to mature it is degraded by the RNA exosome.^[162, 163]

A small molecule, binding CUG RNA repeats, was shown to inhibit protein interaction with MBNL1 (Figure 9) leading to splicing of the transcript coding for dystrophin protein kinase (DMPK). RNA repeats located in the introns subsequently were degraded by the endogenous RNA exosome.^[164]

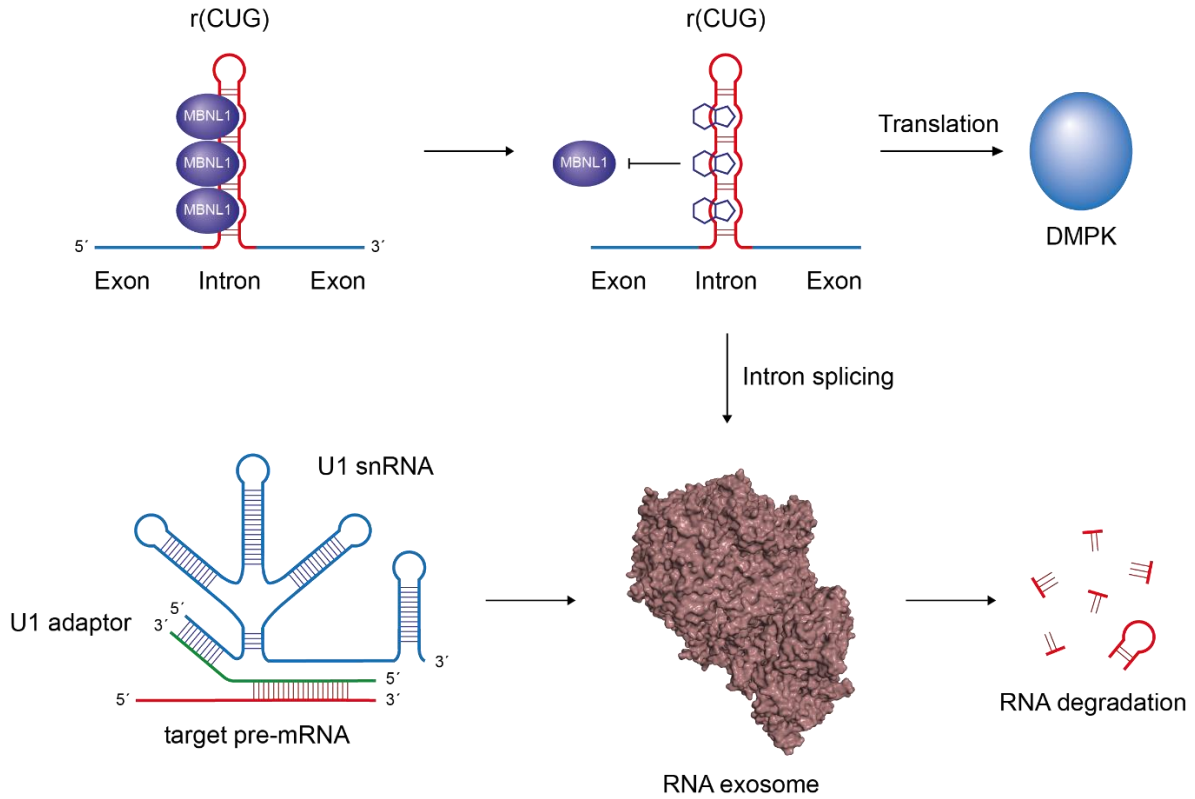


Figure 9. RNA exosome (PDB: 4IFD) machinery for recycling of unprocessed RNA.

1.2.5. Hybrid Nucleases

Conjugation of nucleases catalysing unselective RNA cleavage to ASOs has allowed the development of hybrid nucleases where induced proximity promote targeted RNA degradation (Figure 10). This strategy may also enhance efficacy of ASOs relying on recruitment of RNase H, which requires optimization of sequence and chemical modifications to achieve target knockdown.

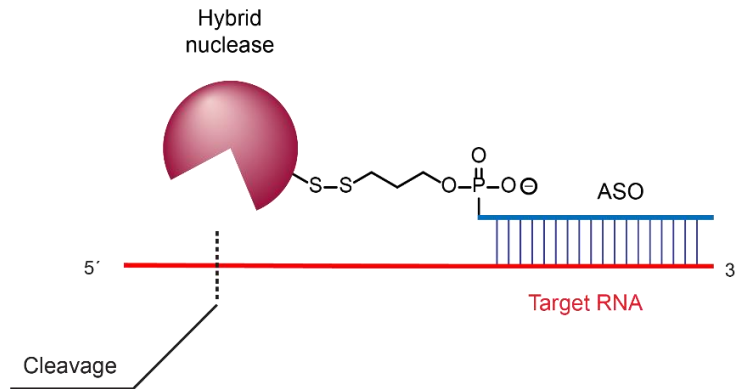


Figure 10. Hybrid nuclease composed of a peptide or protein with hydrolytic function and ASO with complementary sequence to the oligonucleotide for degradation of target RNA.

The Ca²⁺-dependent staphylococcal nuclease (SNase) has been conjugated with ASOs for directing degradation to AU-rich ssRNA with complementary sequence. Cleavage occurs 2-3 bases from 3' termini of the ASO and generate phosphates with free hydroxyls at 3' and 5'. Mutation of Lys-116 to Cys-116 in the nuclease allowed disulfide formation with the ASO carrying a propyl linker, forming a hybrid nuclease. This methodology has been used for degradation of *E. coli* M1 RNA, 16S rRNA and Phe-tRNA *in vitro*.^[165, 166] This method required hybrid nucleases present in stoichiometric quantities since catalytic degradation has not been achieved with SNase. However, authors mentioned that catalytic degradation may be possible in combination with other nucleases and has been proven possible with cleavage of ssDNA.^[167] Although a valuable tool for biological studies in cell free environments, this conjugate would not pass cell membranes. The conditions where the hybrid nuclease is active (60 °C) are also far from physiological conditions making applications further limited.

Comparable strategies using oligonucleotides for RNA binding have been developed by conjugation to other molecules possessing hydrolytic activity, which may be used under milder conditions. The S peptide, modified by changing Lys-1 to Cys-1, allowed conjugation with oligonucleotides by the same principle as described for the SNase hybrid nucleases. This strategy recruited RNase S for selective cleavage of RNA one base from the 3' oligonucleotide binding site.^[168] Mutation of Glu-135 to Cys-135 in RNase H allowed conjugation by Michael addition to maleimide-modified ASOs forming a hybrid nuclease with improved selectivity over wild-type RNase H.^[169] Peptides containing (Arg-Leu)_n repeats conjugated with ASOs have been shown to induce cleavage of RNA hybridized with DNA, thereby forming another type of hybrid nuclease^[170-174] with expanded application scope including cellular activity^[175] and effect in animal models.^[176] Arginine fork domains can also be found in RBPs, but without hydrolytic activity.^[177, 178] Peptide-based nucleases used in this strategy have been shown not to be dependent on metal ions for catalytic activity by addition of excess EDTA,^[179] but synergistically inducing RNA degradation by RNase H recognition of the DNA-RNA duplex.^[180]

1.2.6. CRISPR

Genome editing is currently standardized by clustered regularly interspaced short palindromic repeat (CRISPR) technologies. This prokaryotic machinery is used as a defense system by bacteria to cleave nucleic acid strands of bacteriophages and has been adapted to biological research using various CRISPR-associated (Cas) proteins with endonucleolytic activity as RNA guiding enzymes.^[181] The work by Emmanuelle Charpentier and Jennifer Doudna was awarded with the Nobel prize in Chemistry 2020. The CRISPR-Cas13 system has been used to modify RNA with high precision, where, especially the Cas13b ortholog has been reported to be stable and efficient in mammalian cells. Cas13 family members can process their own pre-crRNA using another nuclease domain allowing generation of mature crRNA to bind Cas13 to initiate degradation of target RNA. Dual higher eukaryotes and prokaryotes nucleotide-binding (HEPN) nuclease domains within Cas13 catalyse cleavage of target ssRNA encoded within the palindromic repeat (Figure 11).^[182] CRISPR interference (CRISPRi) methods have also been used with dCas13, which lack nuclease activity, to sterically block processing or translation of transcripts.^[183] However, there are still issues with non-specific collateral degradation of proximal transcripts that needs to be addressed before developing a therapeutic. Another challenge for development of medicines based on CRISPR technologies is efficient delivery of the machinery *in vivo*.^[184]

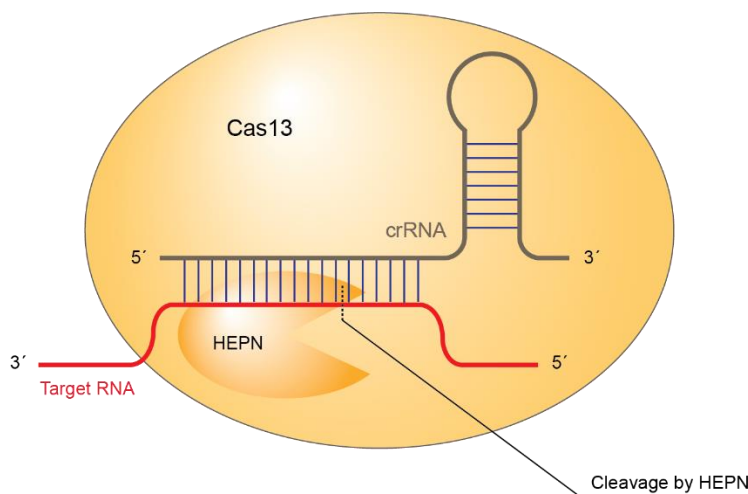


Figure 11. CRISPR-Cas13 targeting RNA for cleavage.

1.2.7. Photo-Induced Radical Formation

N-hydroxypyridine-2(1*H*)-thione (HPT) (Figure 12) has been conjugated to a small molecule^[185] binding to a specific RNA sequence. Upon irradiation with UV light, a hydroxyl radical forms that subsequently degrades the RNA by a cascade reaction leading to cleavage of the proximal nucleic acid polymers. Despite a phenotypic effect, controlling radical formation was problematic. Another disadvantage of this strategy is that it is not catalytic.^[186, 187] The RNA cleavage mechanism caused by the hydroxy radicals is complex with many possible outcomes depending on the base and position of radical insertion.

Conjugation of a tris(bipyridine)ruthenium(II) complex to an RNA-binding small molecule resulted in oxidation of proximal guanosines into 8-oxo-7,8-dihydroguanosine within an RNA repeat upon irradiation. Subsequent treatment with aniline resulted in cleavage of modified RNA in cell-free environment. However, degradation of RNA repeats in cells could not be achieved using this 2-step approach.^[188]

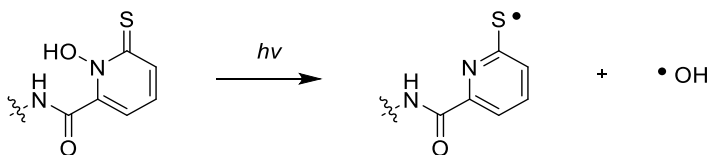


Figure 12. Photo-induced formation of hydroxy radical using HPTs.

1.2.8. Synthetic Metallonucleases

Footprinting experiments have been performed to determine sequences of DNA or RNA that interact with proteins. Several approaches to non-selectively degrade nucleic acid polymers, except from the sequences bound and protected by proteins, have been established. Synthetic metallonucleases, such as EDTA, phenanthroline and other metal chelating molecules (Figure 13A), have been investigated for footprinting applications. Generation of hydroxyl radicals from hydrogen peroxide and reducing agents resulted in the cleavage of nucleic acid polymers.^[189] Coordination complexes of divalent transition metal ions (Cu^{2+} , Fe^{2+} , Zn^{2+}) or trivalent lanthanide metal ions have been conjugated to RNA-binding modalities such as ASOs^[190-193] and peptides^[194, 195] for targeted degradation of proximal RNAs. Aminoglycosides have been shown not only to bind, but also to catalyse hydrolysis of DNA and RNA by formation of metal coordination complexes.^[196] Conjugation of neamine to peptide nucleic acids (PNAs) induced degradation of

TAR RNA.^[197-199] Synthetic metallonuclease conjugates has the disadvantage of lacking selectivity in targeting RNA over DNA, which may cause severe off-target effects.

Introduction of a propargyl modification in cellular RNAs has been achieved by using a propargyl substituted S-adenosyl methionine substrate of m⁶A modifying methyltransferases METTL3 and METTL16. Copper(I)-catalyzed click chemistry was applied for conjugation with an imidazole (Figure 13B) and was able to degrade modified RNAs. The imidazole mimics the conserved histidine in ribonucleases by acting as a base to catalyse deprotonation of 2'-hydroxyl.^[200-202] Although targeted only for RNA interactome of methyltransferases, this methodology offers a novel method of studying RNA modifications in cells.

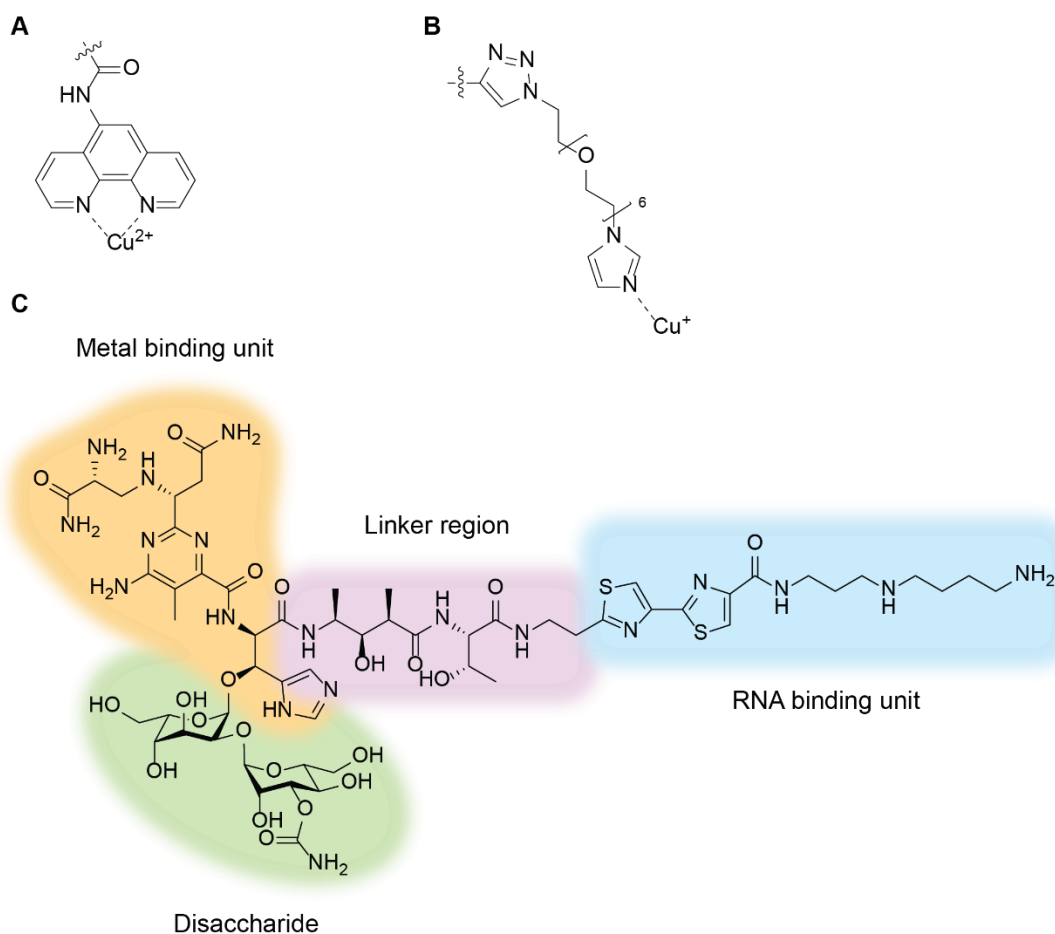


Figure 13. Radical generating compounds inducing RNA cleavage. **A:** Copper(II) bis-phenantroline complex. **B:** Imidazole-based ligand for Cu(I) targeting RNA interactome of methyl transferases. **C:** Natural product bleomycin A5 divided into four groups; metal binding unit, RNA binding unit, linker region and carbohydrate disaccharide.

The glycopeptide natural product family of bleomycins has been shown to degrade DNA and RNA *in vitro* by a related, but not completely determined mechanism forming radicals from cellular oxygen.^[203] The molecule consists of a metal chelator, a nucleic acid-binding group, a linker region connecting previously mentioned domains and a carbohydrate. Total synthesis has afforded several analogues with varying activity.^[204-207] The Fe²⁺ chelating functionality is essential to generate radicals that cleave phosphodiester. However, the domain interacting with the nucleic acid polymer can be modified to alter the preference of binding RNA over DNA by removing charged functionalities and increase hydrophobicity of the C-terminal as found in bleomycin A5 (Figure 13C).^[208-210] The carbohydrate group improves cellular uptake, but removal resulted in increased preference of degrading RNA over DNA. Applying acquired knowledge on bleomycin resulted in the modified peptide-polyketide deglycobleomycin A5.^[211] These bleomycin analogues were conjugated with ASOs^[212] targeting unstructured RNA as well as small molecules binding RNA repeats,^[52, 57, 213, 214] pri-miR-96^[215] and the pri-miRNA 17-92 cluster^[216] respectively and showed therapeutic activity by degradation of target RNAs. Degradation of DNA would be detrimental for any therapeutic and may cause mutations of the genome, resulting in various side-effects.

1.2.9. Ribonuclease L

OAS is an RBP able to sense dsRNA upon viral infections, which trigger ATP-dependent synthesis of the short and unique oligonucleotide p_xA(2'p5'A)_n (2-5A), where x = 1 - 3 and n = 2 - 4.^[217, 218] The only reported function of 2-5A is to activate ribonuclease L (RNase L),^[219] which is expressed as a latent monomer at basal levels of most mammalian cells.^[220] The endonuclease RNase L consist of an ankyrin repeat domain, a pseudokinase domain and an ribonuclease domain. 2-5A binds ankyrin repeats 2 and 4 of RNase L^[221] with K_d = 40 pM^[222] and EC₅₀ = 0.5 nM^[223] that induce a fold change within the protein exposing surfaces allowing for dimerization.^[224] In addition the RNase L dimer is stabilized by binding of ATP or ADP to its pseudokinase domain, which lacks enzymatic function.^[225] When dimerized and thereby activated RNase L use its catalytic ribonuclease domain to cleave single stranded regions of RNA (Figure 14) with moderate selectivity to sites 3' of UN[^]N (^ marks the cleavage site, N = C, G, A or U).^[226, 227] The mechanism of RNA cleavage catalysed by RNase L is not fully determined. The RNase domain has high sequence similarity with inositol-requiring enzyme 1 (IRE1) and it is likely to follow the same mechanism (Figure 15) resulting in cleavage products with terminal 2',3'-cyclic

phosphates.^[228] Detection of RNA containing 2',3'-cyclic phosphates can be performed with RNA sequencing (RNA-Seq) using RtcB ligase and thereby mapping the RNA interactome of RNase L.^[229] The result of RNase L activation is an antiviral response by degradation of viral and ribosomal RNA that hinder the virus from replicating. Overactivation of RNase L leads to caspase-dependent apoptosis.^[230, 231] The RNase L pathway is tightly regulated, where phosphodiesterases rapidly hydrolyze 2-5A that stop RNA degradation.^[232, 233]

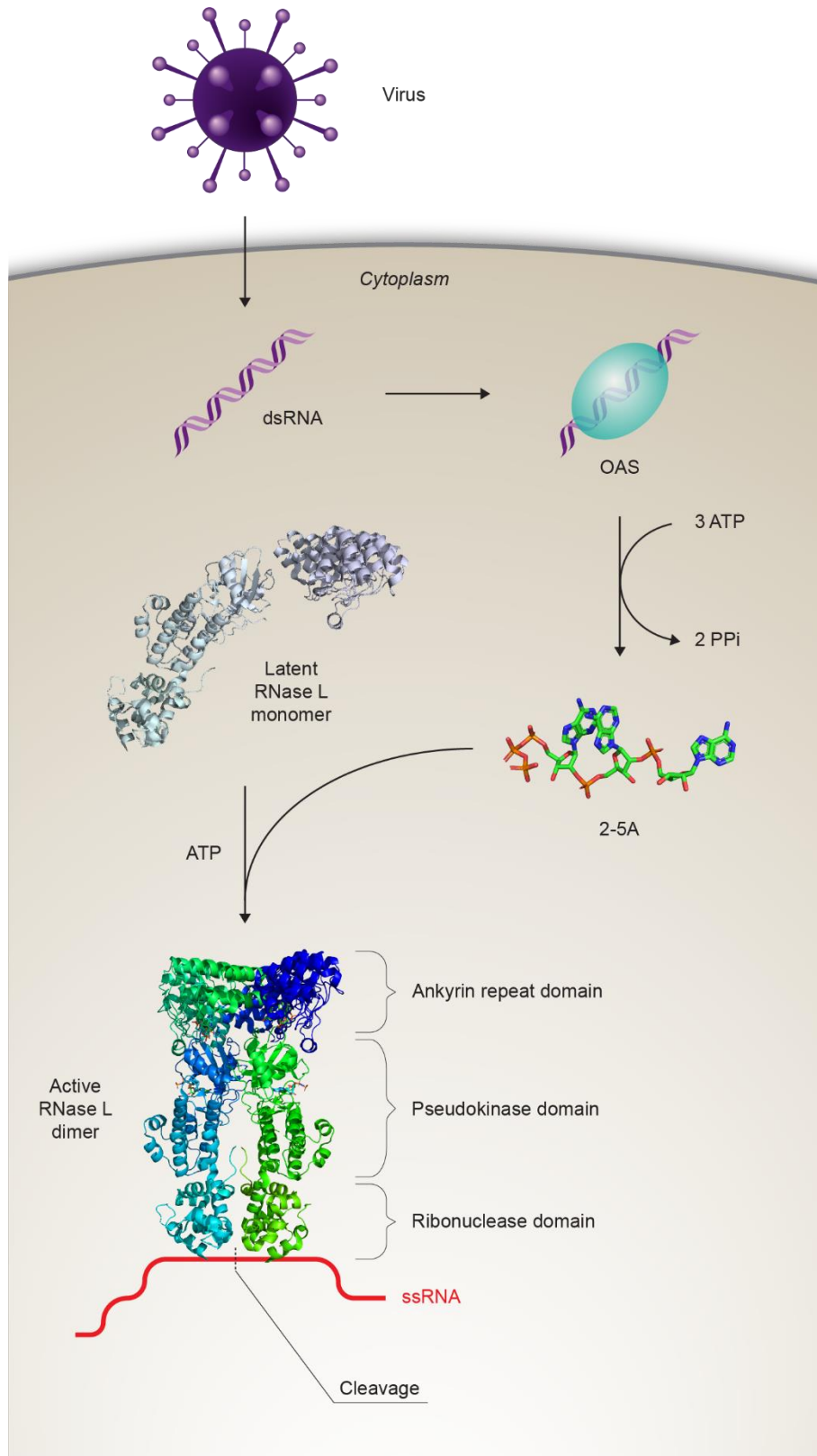


Figure 14. Natural pathway of RNase L with x-ray crystal structure of active form bound to two 2-5A and two ATP mimetics (PDB: 4O1P).

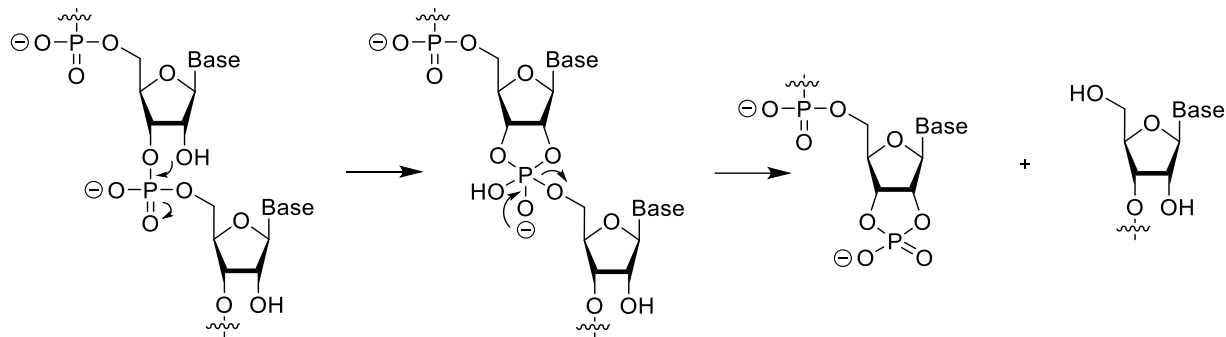


Figure 15. RNA cleavage mechanism generating 2',3'-cyclic phosphates.

Hijacking the natural pathway of RNase L has been achieved by conjugating ASOs targeting mRNAs of disease-causing proteins to 2-5A (Figure 17A) via alkane phosphate or PEG linkers.^[234] The chimeric constructs activate and recruit RNase L for cleavage of target mRNAs. The antisense sequence used to bind targets is DNA-based to avoid cleavage by RNase L and modifications of the backbone have proven that degradation is independent of RNase H (Section 1.2.1.). Other chemical modifications, such as incorporation of phosphorothioates, have also been applied to improve metabolic stability and reduce cytotoxicity of both the ASO and 2-5A.^[234] Several examples of this methodology showed selective and catalytic degradation of target mRNAs (Table 2). 2-5A antisense chimeras have been shown effective in cells, which indicate that constructs were cell permeable to some extent. Up to 100-fold loss in activation of RNase L *in vitro* has been reported for many 2-5A antisense chimeras compared to the unmodified 2-5A tetramer, while conjugates still perform well in cellular assays by efficient degradation of target mRNAs. This is explained by steric effects of the construct, but could as well be related to reduced cell permeability. Despite the loss in activity the 2-5A antisense chimeras were still highly efficient in degradation of target RNA. The sequence preference of RNase L was absent when activated by chimeras, meaning that any sequence could be cleaved by 2-5A antisense chimeras.^[234]

Disney and co-workers further developed this approach by conjugating tetrameric 2-5A via PEG-based linkers to molecules binding target RNAs for degradation by recruitment of RNase L, a strategy termed ribonuclease targeting chimera (RIBOTAC). The method was again proven to be selective and catalytic with turnover of 3.1 moles of pri-miRNA-96^[235] or 9.7 moles of pre-miRNA-210^[236] respectively per mole of RIBOTAC. Degradation efficiency depending on linker length was assessed to find that the shortest linker was most effective.^[235] Ability to activate RNase L using RIBOTAC targeting pri-miRNA-96 was evaluated using an oligomerization assay and

found to be reduced by 50% compared to 2-5A,^[235] while the RIBOTAC targeting pre-miRNA-210 was nearly as effective as 2-5A.^[236] Cell permeability of RIBOTACs was assessed by flow cytometry that showed 50-60% reduced permeability compared to the free RNA-binding molecules. Confocal microscopy was used to determine the localization of RIBOTAC targeting pre-miRNA-210, which was in the cytoplasm while the RNA-binding molecule was mainly located in the nucleus.^[236] Treatment of breast cancer cells with RIBOTACs was found to induce apoptosis in line with the theory of degrading pri-miRNA-96 or pre-miRNA-210, whereas same concentration of 2-5A alone did not induce apoptosis.^[235, 236] RIBOTAC did not induce apoptosis in healthy breast epithelial cells indicating that the effect was indeed due to targeted RNA degradation.^[235] RNase L knockdown using siRNA showed that RIBOTACs lost activity and thus are dependent on endogenously expressed RNase L.^[235, 236]

Thiophenone **C-5966451** and thienopyrimidinones **C-5950331** and **C-6474572** (Figure 16) were discovered as small molecule activators of RNase L from a high-throughput screening (HTS) of 31 990 compounds using a fluorescence resonance energy transfer (FRET)-based RNA cleavage assay. Activation of RNase L by 2-5A is triggered by viral infection in higher vertebrates to hinder further replication of the virus. Antiviral activity of the novel small molecule RNase L activators was confirmed by suppressing growth of cells infected with encephalomyocarditis virus, vesicular stomatitis virus, human parainfluenza virus type 3 and other viruses. In contrast to 2-5A the small molecules did not induce apoptosis, showed high cell permeability and stability making them useful drug leads.^[223]

Synthesis of thiophenone and thienopyrimidinone analogues for structure-activity relationship (SAR) studies to improve activity and identify suitable linker attachment sites recently resulted in discovery of **C1-3** and **C2-3** (Figure 16), however activity of reported thienopyrimidinones could not be reproduced in the FRET assay.^[49] Thiophenone **C1-3** was the most potent activator and basis of the small molecule-based RIBOTACs conjugated by linker attachment at the 4-hydroxy functionality for retained RNase L activity and efficient RNA degradation (Figure 17B).^[237] The fully small molecule-based RIBOTAC possessed improved pharmacokinetic properties compared to using 2-5A as RNase L activator. Negative control compound with reduced RNase L activation ability was prepared by conjugation of the RNA-binding small molecule to 3-hydroxy group on the thiophenone. Proof-of-concept was done by selective and catalytic turnover of 26 moles of pre-

miRNA-21 per mole RIBOTAC in breast cancer cells. Targeted degradation by RIBOTAC compared to the RNA binding small molecule, which inhibits processing by Dicer, was more potent, faster acting and had a prolonged effect on reducing mature miRNA-21 levels. Selectivity of the RIBOTAC was also improved compared to the RNA binding small molecule in a study of miRNA levels. Similarly to PROTACs this conclude that recruitment of RNase L may improve selectivity by formation of a ternary complex between RNA-RIBOTAC-RNase L. RIBOTAC based on thiophenone as activator of RNase L did not induce innate immune response, while 2-5A upregulated mRNA levels of immune response biomarkers. When comparing targeted RNA degradation by RIBOTAC with corresponding conjugate of bleomycin A5 it was reported that the enzymatic cleavage was 10-fold more efficient. In an animal model of breast cancer metastasis RIBOTAC had a clear effect on reducing metastasis to lungs showing the great therapeutic potential of bifunctional degraders targeting RNA. Additionally degradation of pre-miRNA-210 was possible with RIBOTAC based on thiophenone for activation of RNase L.^[49]

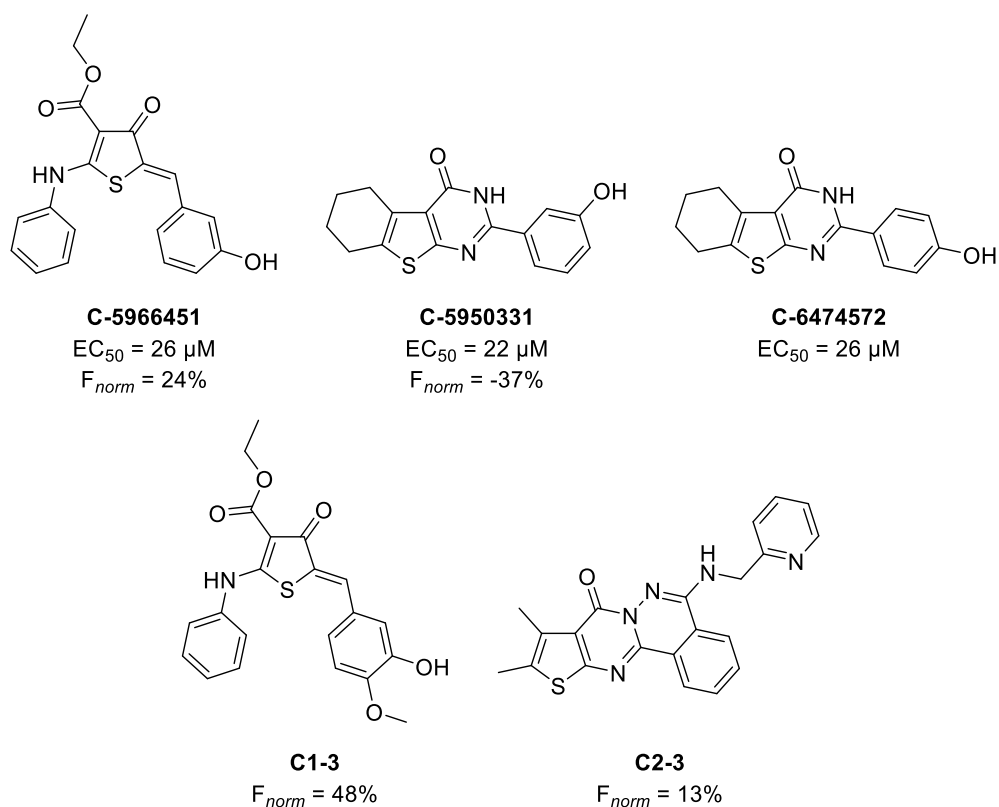


Figure 16. Small molecule RNase L activators.

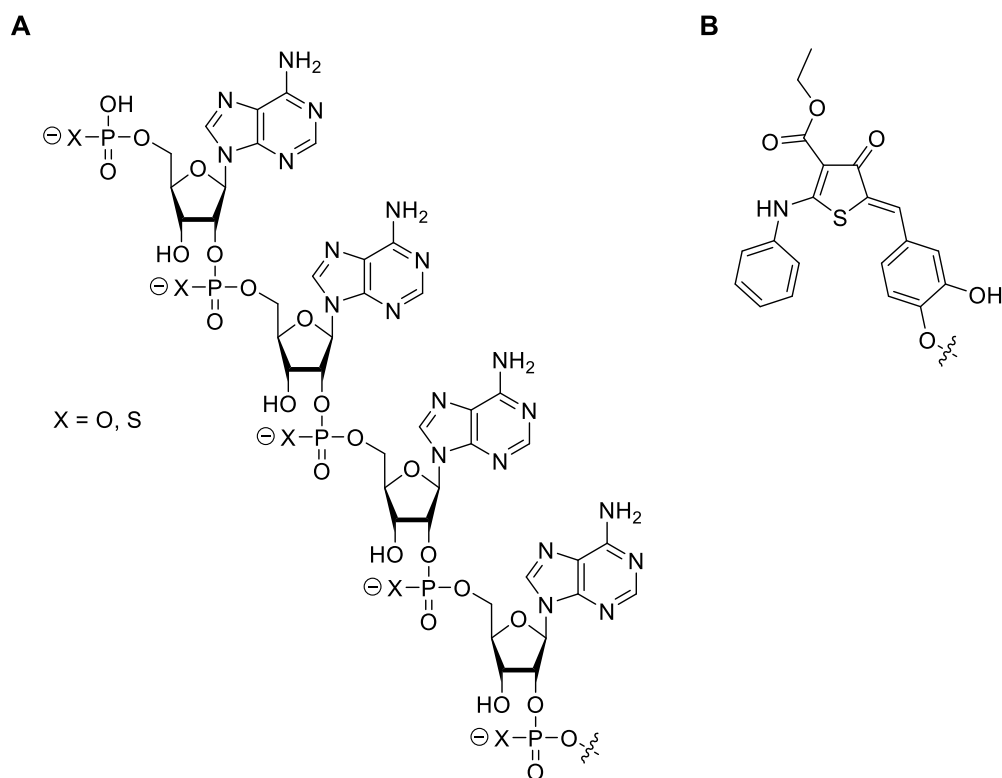


Figure 17. RNase L recruiters used in heterobifunctional molecules for targeted RNA degradation. **A:** 2'-5'A₄ analogues. **B:** Thiophenone-based RIBOTACs.

Further use of the thiophenone RNase L recruiter in RIBOTAC strategies found that degradation of the pri-miRNA 17-92 cluster was not possible due to the nuclear localization of target RNA while RNase L mainly was cytoplasmic in selected cell line. Instead degradation of pre-miRNA 17, 18a and 20a was found after processing and transportation to the cytoplasm, which indicate that RIBOTACs may be more suitable for targeting RNAs in the cytoplasm than in the nucleus.^[216] The Inforna software was used for identification of a small molecule selectively binding the RNA genome of SARS-CoV-2 and subsequently conjugated with thiophenone for recruitment of RNase L. Catalytic turnover of target RNA could be detected and potency of the RIBOTAC was increased by at least 10-fold compared to the small molecule alone.^[56] In another example the kinase inhibitor Dovitinib was identified to interact with the A bulge of pre-miRNA-21 with moderate selectivity over other RNAs. However, when conjugated with thiophenone as RNase L recruiter the chimeric RIBOTAC possessed increased selectivity in degradation of pre-miRNA-21 and lost kinase inhibitory effect.^[238]

Table 2. Heterobifunctional molecules used for targeted RNA degradation.

RNase L recruiter	RNA ligand	Linker	Target
2-5A	ASO	Bu-PO ₄ -Bu (11 atoms)	poly(A) ^[239]
2-5A	ASO	Bu-PO ₄ -Bu (11 atoms)	HIV-1 TAR-A ₂₅ -vif ^[240]
2-5A	ASO	Bu-PO ₄ -Bu (11 atoms)	PKR ^[241-245]
2-5A	ASO	Bu-PO ₄ -Bu (11 atoms)	RSV ^[246-248]
2-5A	ASO	Bu-PO ₄ -Bu (11 atoms)	Telomerase ^[249-251]
2-5A	ASO	Hex (6 atoms)	VSV ^[252]
2-5A	ASO	Bu-PO ₄ -Bu (11 atoms)	BCR-ABL ^[244, 253]
2-5A	ASO	Bu-PO ₄ -Bu (11 atoms)	HIV-1 <i>gag</i> ^[254]
2-5A	ASO	PEG ₆ (17 atoms)	SARS-CoV-2 ^[255]
2-5A	Small molecule	PEG ₃ + Gly (11 atoms)	pri-miRNA-96 ^[235]
2-5A	Small molecule	Amide ether (12 atoms)	pre-miRNA-210 ^[236]
Thiophenone	Small molecule	PEG ₄ (11 atoms)	pre-miRNA-21 ^[49]
Thiophenone	Small molecule	PEG ₄ (11 atoms)	pre-miRNA-17, -18a, -20a ^[216]
Thiophenone	Small molecule	PEG ₄ (11 atoms)	SARS-CoV-2 ^[56]
Thiophenone	Small molecule	PEG ₄ + urea (16 atoms)	pre-miRNA-21 ^[238]

2. Aim of the Thesis

Drug discovery efforts have mainly been focused on proteins as therapeutic targets and thereby limited to the coding part of the human genome that is considered druggable by small molecules. The role of ncRNA in diseases is becoming more evident as researchers are pushing the boundaries of science in transcriptomics. The ability of using small molecules to bind RNA opens new possibilities of modulating cellular processes not accessible by targeting proteins. Development of medicines with novel mode of actions covering clinical unmet needs will benefit current biomedical research.

Methods to selectively degrade disease-causing RNA has recently been expanded by the recruitment of RNase L using small molecule-based strategies. In contrast to oligonucleotide-based therapeutics, small molecules possess pharmacokinetic properties allowing oral administration. This thesis focuses to address three aims as listed below.

Firstly, to design and synthesize reported and novel compounds with the ability to activate RNase L. The introduction of functional groups at varied positions is used to identify suitable linker attachment positions. Furthermore, a scaffold hopping approach, based on reported RNase L activators, aims to retain or improve activity, increase aqueous solubility and enhance selectivity by increasing the fraction of sp^3 hybridized atoms as a strategy in targeting proteins.

Second, the most promising small molecule RNase L activator is conjugated with a small molecule inhibitor of a selected RBP. Such proximity-inducing heterobifunctional molecules aim to induce targeted RNA degradation through quaternary complex formation between heterobifunctional molecule, RNase L, RBP and RNA. Synthesis of such heterobifunctional compounds may serve as a tool to study the RNA interactome of RBPs, identify novel protein-RNA interactions and be used as therapeutic for diseases where transcripts are upregulated.

Third, extending the scope of small molecule-based RIBOTACs for targeted degradation of the HIV-1 genome by synthesis of heterobifunctional molecules containing thienopyridine ligands binding to the TAR element of HIV-1 RNA may offer a therapeutic solution for patients suffering from HIV infection.

3. Results and Discussion

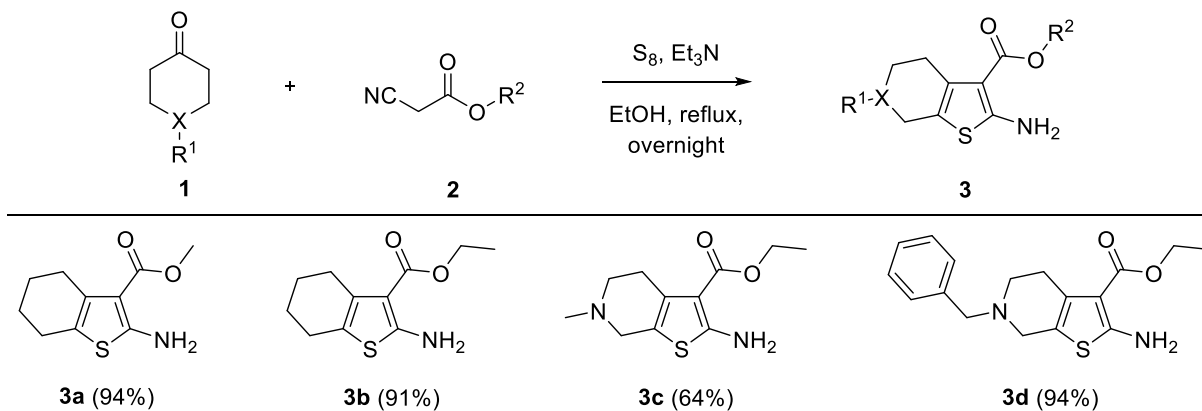
The identification of small molecule RNase L activators would allow the construction of heterobifunctional molecules for targeted degradation of disease-causing RNAs. Three compound classes have been synthesized and the introduction of linkers allows for further conjugation performed for the activation of RNase L. When used to target RBPs the methodology may be used as a tool to map the protein-RNA interactomes. Extending the scope of the RIBOTAC strategy was achieved by conjugation with small molecules targeting viral RNA.

3.1. Small Molecule RNase L Activators

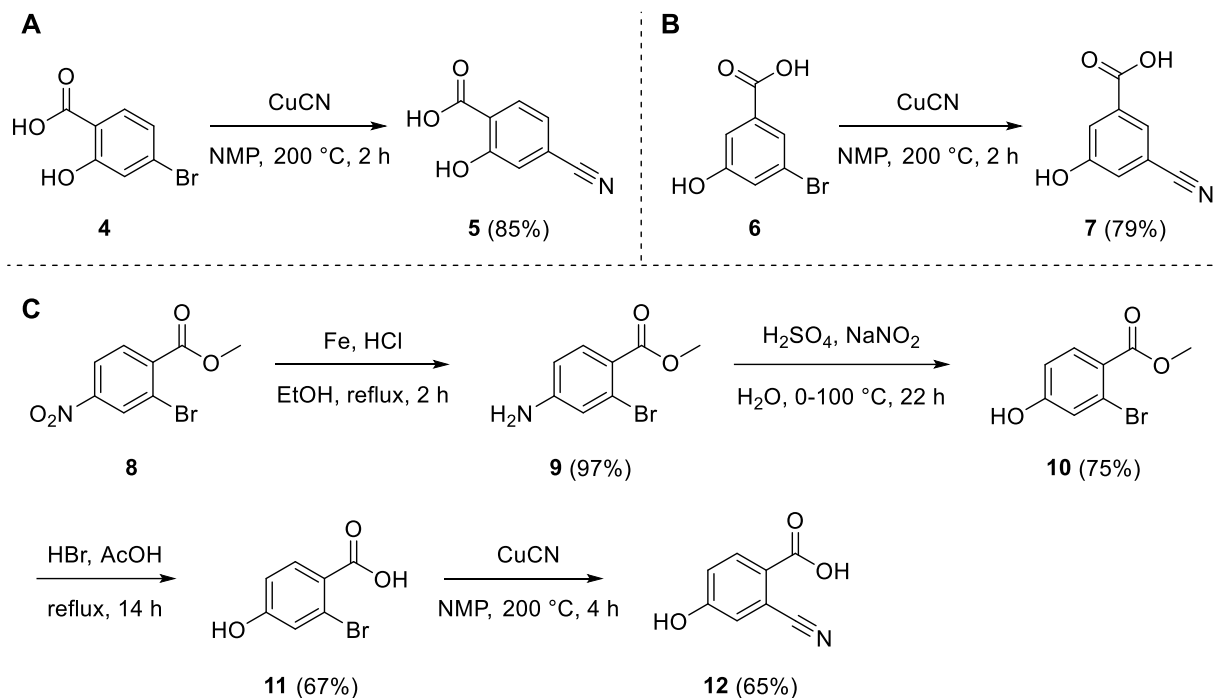
Synthesis of reported compounds and analogues with the introduction of functional groups allowing linker attachment through amide couplings was performed to explore the thienopyrimidinone scaffold for activation of RNase L. Scaffold hopping^[256] through a ring distortion approach^[257, 258] generated thienodiazepines with improved solubility. Furthermore, thiophenones were prepared for conjugation strategies.

3.1.1. Thienopyrimidinones

Thiophene synthesis was performed using the Gewald multicomponent reaction first reported in 1961^[259] providing a robust procedure for obtaining 2-aminothiophenes (Scheme 1). Knoevenagel condensation between cyclic ketones **1** and α -cyanoesters **2** initiates the reaction and elemental sulfur allows the formation of 2-aminothiophenes **3a-d** including the pharmaceutical agent Tinoridine (**3d**) containing a benzyl-protected amine as handle for potential linker attachment.^[260]



Scheme 1. Synthesis of thiophenes via the multicomponent Gewald reaction.



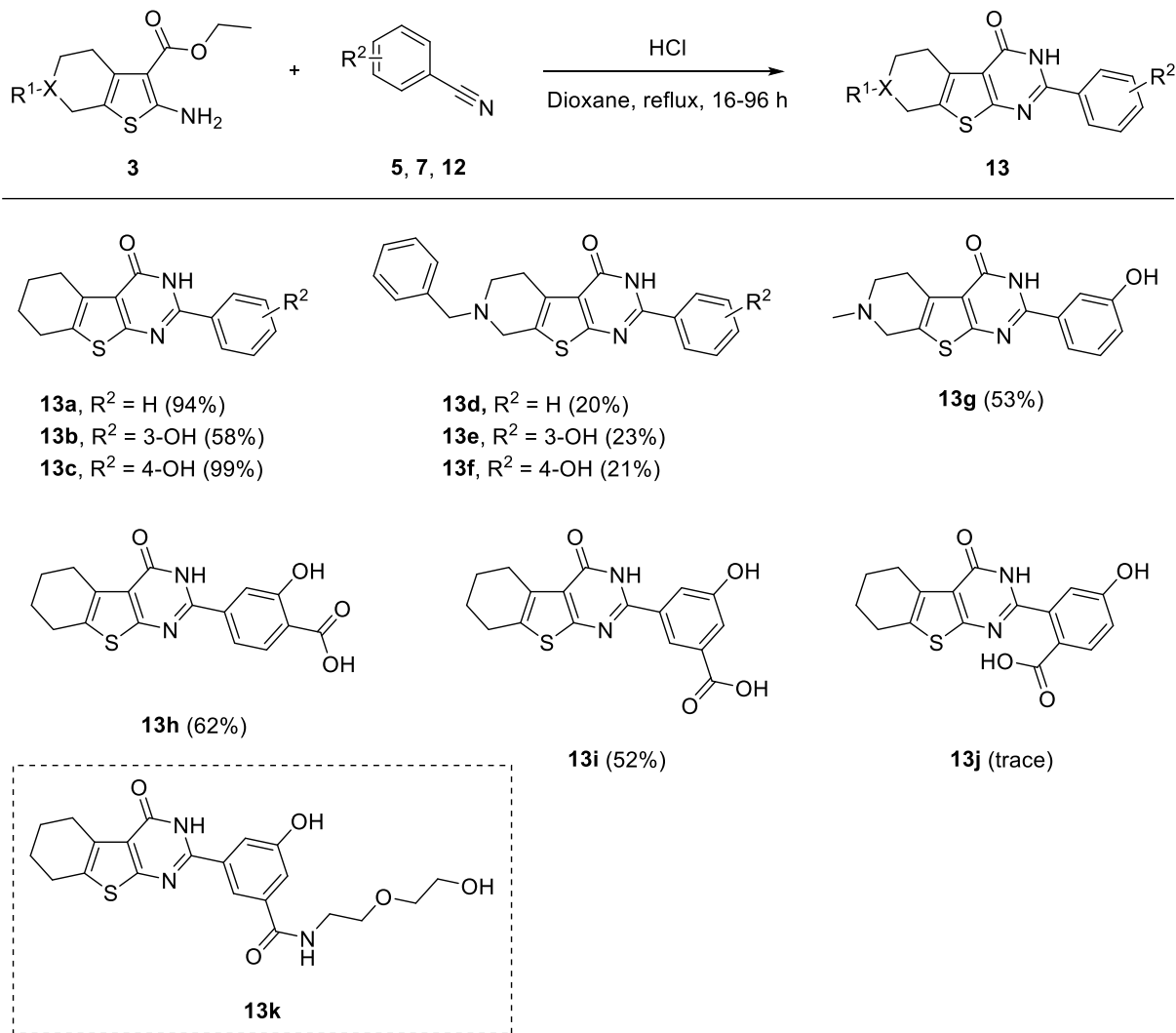
Scheme 2. Synthesis of benzonitriles with variations in carboxylic acid position.

A: 4-carboxybenzonitrile. **B:** 3-carboxybenzonitrile. **C:** 2-carboxybenzonitrile.

Introduction of a carboxylic acid was used as a handle on the thienopyrimidinones for linker attachment. A carboxylic acid in position 2 was prepared by using the corresponding nitro-substituted methyl ester **8** as the starting material. Nitro-reduction afforded aniline **9** that underwent diazonium salt formation followed by hydrolysis to generate phenol **10**. Ester hydrolysis afforded desired bromobenzene **11**. Benzonitriles **5**, **7** and **12** were prepared from the corresponding bromobenzenes **4**, **6** and **11** using copper(I) cyanide via nucleophilic aromatic substitution under microwave irradiation (Scheme 2). Prepared 2-aminothiophenes **3b-3d** and benzonitriles **5**, **7** and **12** were reacted under acidic conditions to form the corresponding thienopyrimidinones **13a-13j** that were collected by precipitation in water or purified by MPLC resulting in lower yields (Scheme 3).

The overall low solubility of the thienopyrimidinones was a limitation in biological evaluation as **13a**, **13d** and **13h** were not soluble at 20 mM in DMSO. Functional groups were introduced at various positions allowing linker attachment using amide couplings. Benzyl removal can be carried out with **13d**, **13e** and **13f** by treatment with palladium hydroxide on active charcoal under hydrogenation to generate secondary amines suitable for coupling with carboxylic acids.^[261]

Similarly, aromatic carboxylic acids on **13h**, **13i** and **13j** were suitable for coupling with amines to attach linkers. One example was prepared by coupling a PEG₂ linker with terminal amine to **13i** resulting in **13k**. Unfortunately, amide coupling of **13h** was not successful.

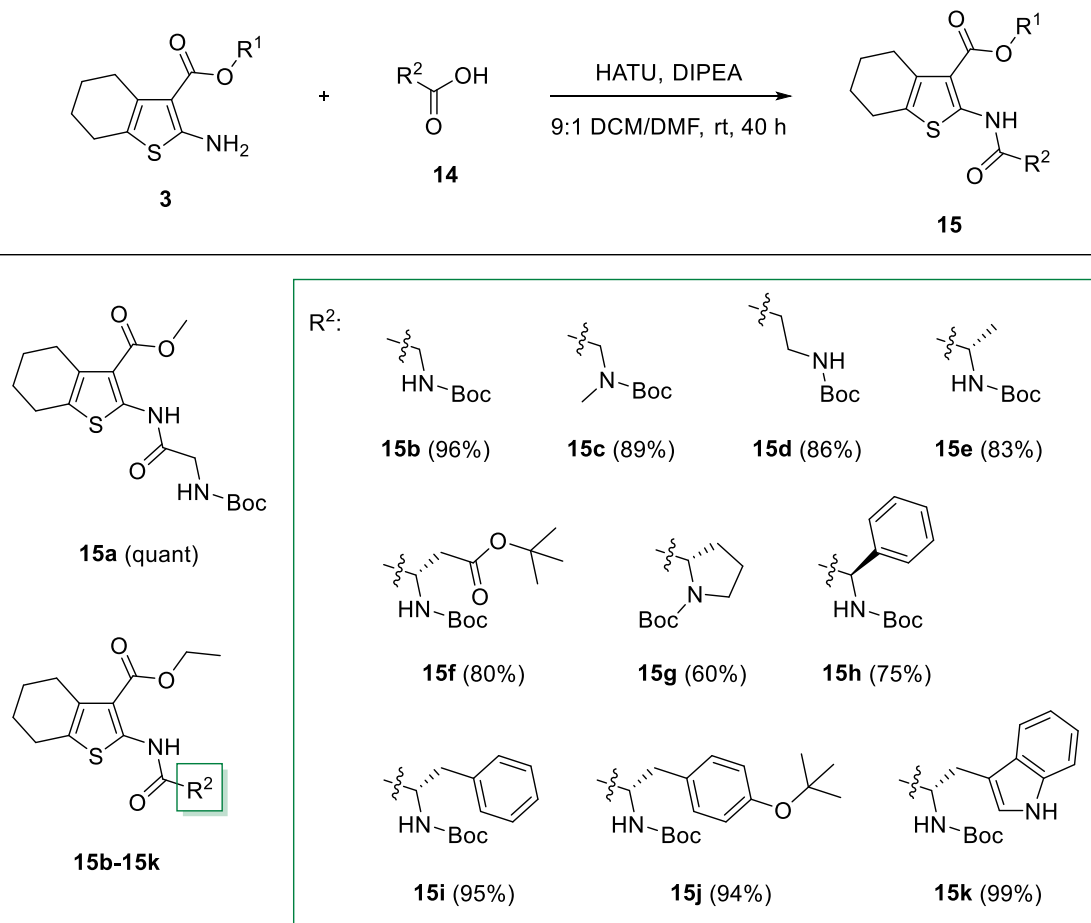


Scheme 3. Synthesis of thienopyrimidinones through condensation of Gewald products with benzonitriles.

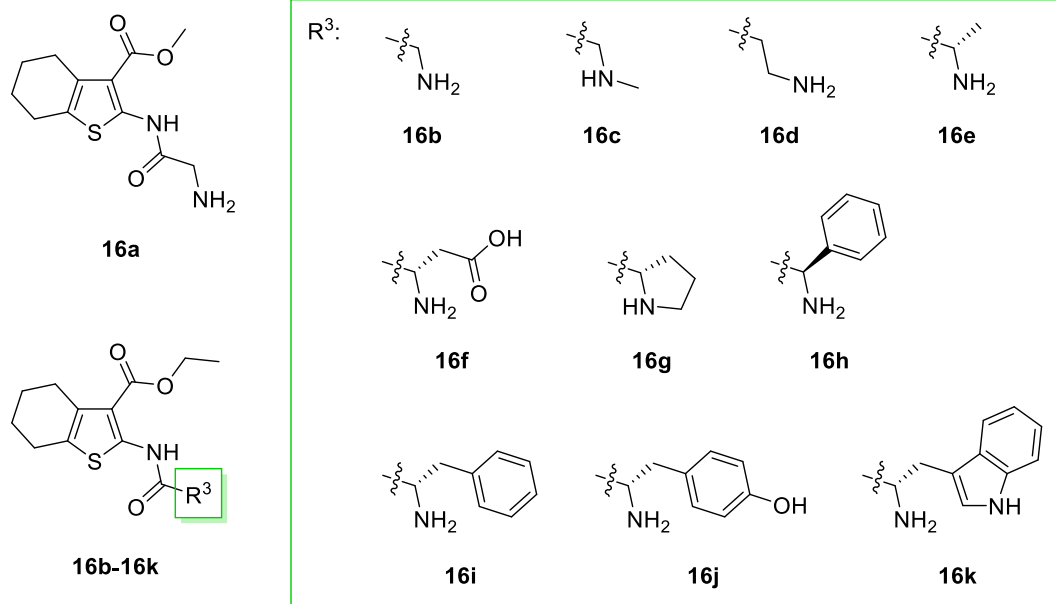
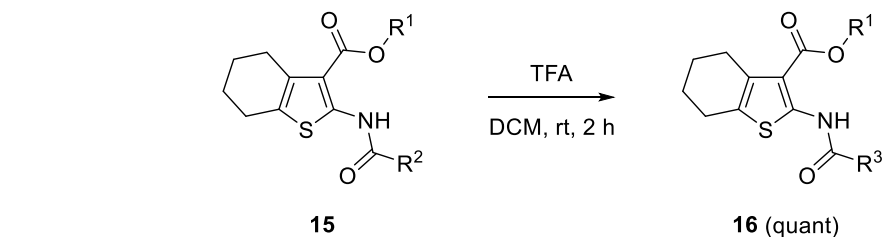
3.1.2. Thienodiazepines

Amide coupling of commercially available amino acids **14**, containing *N*-Boc and corresponding side chain protecting groups hinder undesired reactions. Reaction with 2-aminothiophenes **3** was optimized with HATU as a coupling reagent. Screening of solvent mixtures showed that a mixture of 9:1 DCM/DMF resulted in sufficient solubility for the coupling reagent to afford Boc-protected dipeptides **15a-15k** in good to high yields (Scheme 4). Using HOBT^[262] as the additive to avoid

racemization of the stereogenic center resulted in decreased yield. Removal of Boc and *tert*-butyl protecting groups from dipeptides was performed in a 1:1 mixture of TFA/DCM to afford free amines **16a-16k** (Scheme 5).



Scheme 4. Amide coupling of amino acids to 2-aminothiophenes.

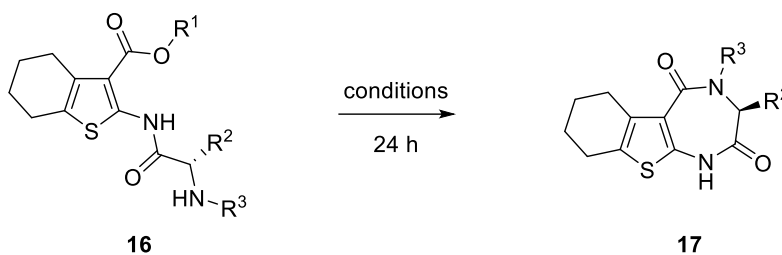


Scheme 5. Removal of Boc protecting group.

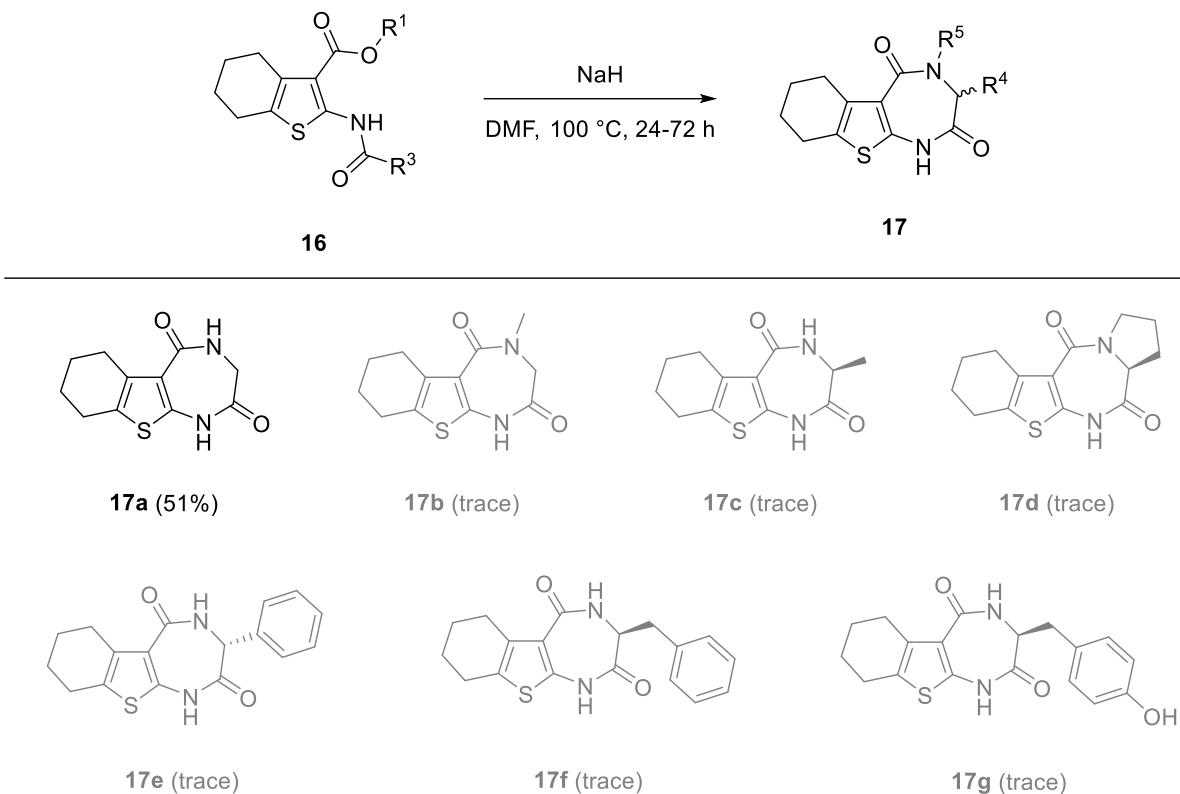
Intramolecular cyclization was achieved through condensation of amine with ester forming an amide bond. Sodium methoxide prepared fresh from sodium metal dissolved in methanol was initially used based on reports of the synthesis of amides from esters^[263] including intramolecular cyclization generating benzodiazepines,^[264] but no product was observed (Table 3, Entry 1-2). Sodium hydride was used inspired by the synthesis of cyclic dipeptides,^[265] and was basic enough to deprotonate the amine allowing the intramolecular cyclization to take place in DMF (Table 3, Entry 3-4) in high conversion. Ethyl ester proved to be beneficial in the formation of the thienodiazepine over methyl ester (Table 3, Entry 4-5), leading interest towards exploring better leaving groups. However, such esters would also be prone to hydrolysis during the former acidic Boc deprotection step. *N*-Alkylation represented by a methylated amine was examined to see effects of increased nucleophilicity of the amine, but probably steric hindrance reduced yield of the reaction compared to the unsubstituted analogue (Table 3, Entry 4 and 6). Optimal reaction conditions (Table 3, Entry 4) did not give comparable conversion with the phenylalanine-based

dipeptide and required further optimization. Screening of organic solvents, with the ability to dissolve starting material whilst having boiling points higher than the generated alcohol, was performed with the phenylalanine-based dipeptide to detect conversion. However, the tested conditions (Table 3, Entry 7-10) did not improve conversion, indicating that DMF was the most suitable solvent. The optimal conditions led to **17a** with 51% isolated yield, while only trace of thienodiazepines **17b-17g** was obtained. Limitations of the reaction scope were detected when applying optimized reaction conditions (Scheme 6). Any substitutions of the amino acid side chain or amine greatly reduced the yield compared to the dipeptide based on glycine. Functionalities including carboxylic acid (**16f**) or amine (**16k**) within the amino acid side chain was not tolerated. The dipeptide **16d** based on β -alanine did not show any formation of expected 8-membered ring.

Table 3. Optimization of thienodiazepine synthesis through intramolecular cyclization. Reactions performed in 0.35 mmol scale at 0.2 M. Conversion determined by LC-MS.



Entry	Starting material	Solvent	Temperature	Base	Conversion
1	16b , R ¹ : Et, R ² : H, R ³ : H	THF	70 °C	NaOMe	-
2	16b , R ¹ : Et, R ² : H, R ³ : H	Dioxane	100 °C	NaOMe	-
3	16b , R ¹ : Et, R ² : H, R ³ : H	Dioxane	100 °C	NaH	-
4	16b , R ¹ : Et, R ² : H, R ³ : H	DMF	100 °C	NaH	86%
5	16a , R ¹ : Me, R ² : H, R ³ : H	DMF	100 °C	NaH	12%
6	16c , R ¹ : Et, R ² : H, R ³ : Me	DMF	100 °C	NaH	34%
7	16i , R ¹ : Et, R ² : Bn, R ³ : H	DMF	100 °C	NaH	27%
8	16i , R ¹ : Et, R ² : Bn, R ³ : H	DMA	100 °C	NaH	11%
9	16i , R ¹ : Et, R ² : Bn, R ³ : H	NMP	100 °C	NaH	10%
10	16i , R ¹ : Et, R ² : Bn, R ³ : H	DMSO	100 °C	NaH	trace



Scheme 6. Synthesis of thienodiazepines through intramolecular cyclization.

The goal of improving aqueous solubility was achieved as proven with reduced retention times in reverse phase HPLC correlating to aqueous solubility (Figure 18).^[266] Other methods may be more reliable in predicting solubility,^[267] but were not available at the time and would be less suitable considering the purity of thienodiazepines **17b-17g** obtained in trace amounts. The improved solubility of thienodiazepines likely originates from dearomatization of the thienopyrimidinone and change from a flat conformation into a three-dimensional chemical space inhibiting π - π stacking in the solid state, which may also contribute to improved selectivity when targeting proteins.^[71]

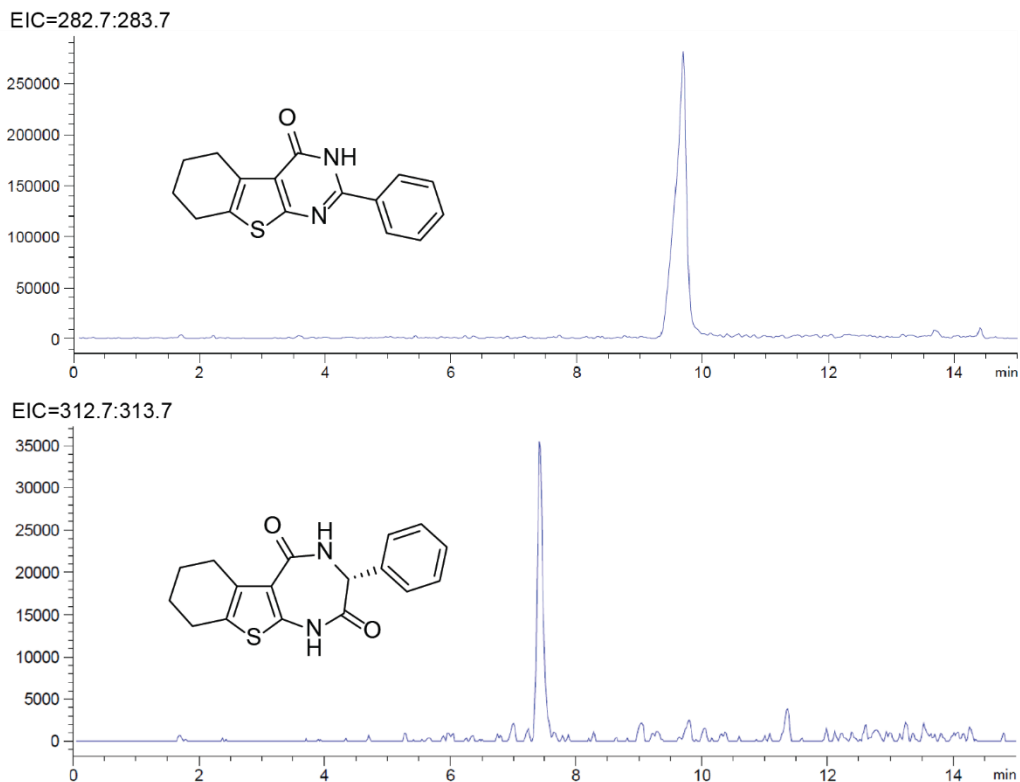


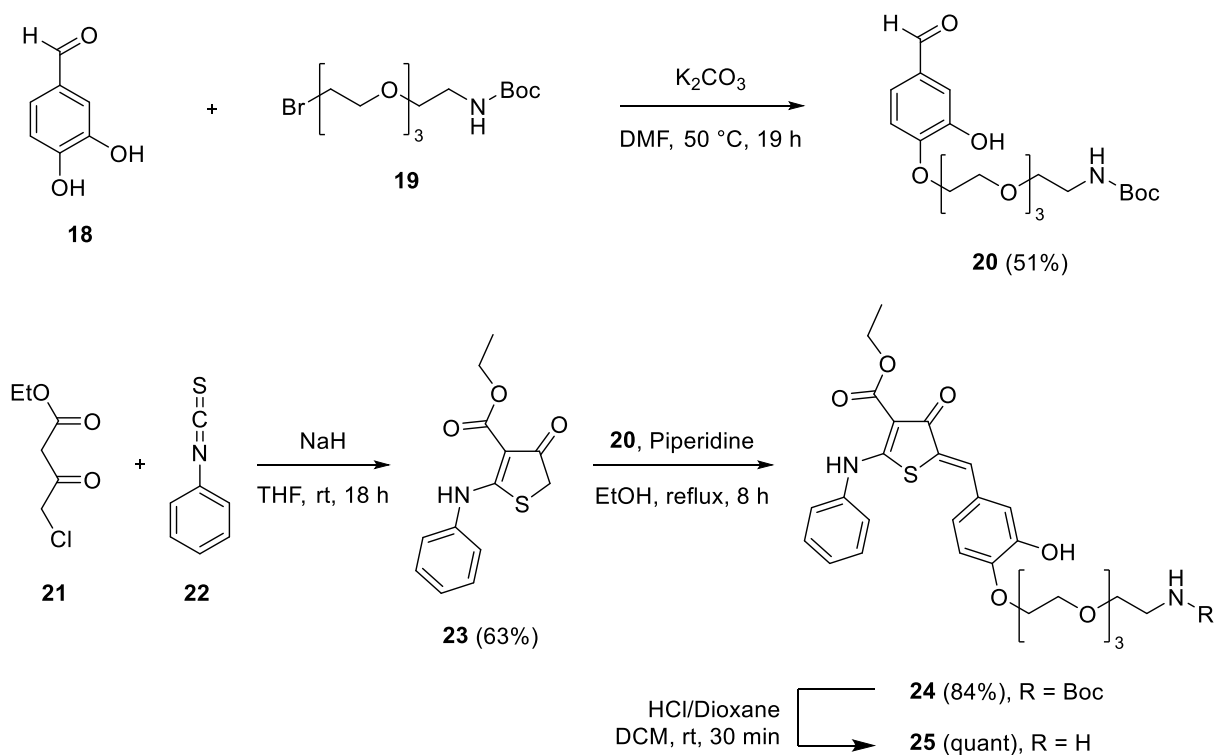
Figure 18. LC-MS elution times of direct analogues **13a** (9.67 min, 8.0% H₂O in MeCN with 0.1% TFA) and **17e** (7.47 min, 27.8% H₂O in MeCN with 0.1% TFA) indicating improved aqueous solubility of thienodiazepines compared to thienopyrimidinones.

Considering that the thienodiazepines or original thienopyrimidinones did not show significant activity against RNase L in-house, no further efforts to optimize reaction conditions to obtain a library of thienodiazepines was carried out. In case of further interest to explore thienodiazepines in the discovery of ligands for various targets, synthesis with incorporation of amino acids may be performed using solid phase synthesis to increase yields and reduce work load. Gewald reaction^[268] in combination with on-resin or solution phase cyclization would readily generate a library of thienodiazepines. Alternatively, various activated esters may be investigated for their tolerance to acidic environments allowing Boc deprotection in the previous step followed by intramolecular cyclization.

3.1.3. Thiophenones

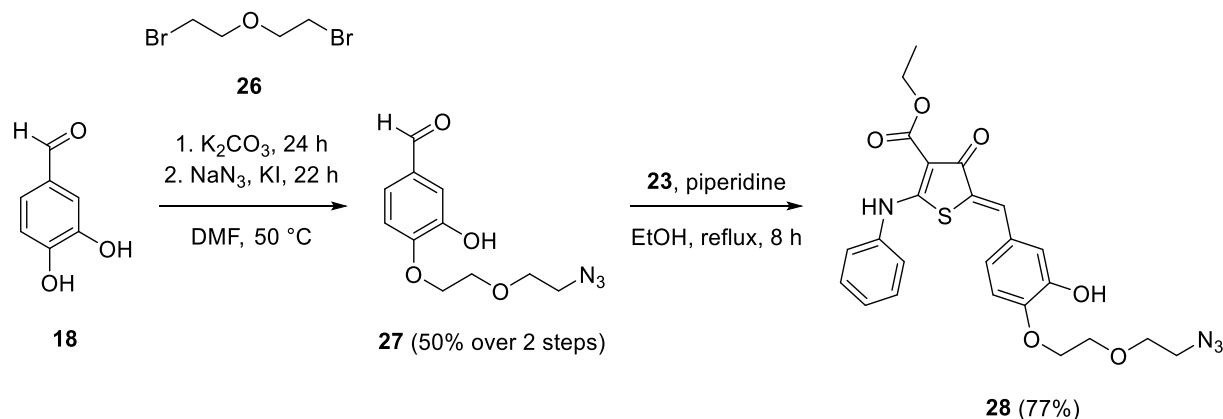
Based on the reported thiophenones as RNase L activators,^[49, 223] thiophenones were synthesized with linkers (Schemes 7, 8) for conjugation with small molecules binding to RBPs or RNAs allowing RNase L to be recruited for targeted RNA degradation. Protocatechuic aldehyde **18** was

selectively substituted at the 4-hydroxy position with brominated PEG₄ linker **19**. Regioselectivity of product **20** was confirmed by comparing with reported NMR spectra and characterization data.^[49] Cyclocondensation between ethyl 4-chloroacetoacetate **21** and phenyl isothiocyanate **22** generated thiophenone **23** that could further undergo aldol condensation with benzaldehyde **20** to introduce an amine as handle for conjugation. Deprotection of **24** under acidic conditions generated the primary amine **25** as a hydrochloric acid salt used for synthesis of conjugates and recruitment of RNase L.



Scheme 7. Synthesis of thiophenone with (PEG)₄ linker and terminal amine.

Protocatechuic aldehyde **18** was alkylated with **26** at 4-hydroxy position in an optimized one-pot two step reaction giving intermediate 4-(2-(2-bromoethoxy)ethoxy)-3-hydroxybenzaldehyde. Reaction conditions were compatible with direct substitution of the second bromide using sodium azide and catalytic potassium iodine to obtain benzaldehyde **27**. Introduction of the azide was strategically performed at a structure of higher molecular weight in order to avoid the explosive character of low molecular weight organic azides.^[269] Aldol condensation with thiophenone **23** generated RNase L recruiter **28** and regioselectivity of the substitution was confirmed by 2D NOESY NMR through coupling of the phenol hydrogen with the singlet hydrogen at 2 position.



Scheme 8. Synthesis of thiophenone with (PEG)₂ linker and terminal azide.

3.1.4. Biochemical Evaluation

The biochemical evaluation of RNase L activation of the synthesized compounds was performed by Lydia Borgelt and Neele Haacke. Given the reported RNase L activating potency of the thiophenones,^[49, 223] thienopyrimidinones and thienodiazepines were evaluated for their RNase L activating potency in a FRET assay.

Synthetic RNA forming two hairpin loops labelled with 6-FAM on 5' termini and IQ4 on 3' termini undergoes FRET when excited at 489 nm and emission of light is quenched. RNase L was activated by the addition of 2-5A or small molecule activators and the single stranded sections cleaved resulting in loss of FRET and emission of light from the 6-FAM probe at 525 nm (Figure 19). Since thienopyrimidinones **13b**, **13c**, **13e-13g** and **13i** nor thienodiazepine **17a** did not show any activity in the RNase L FRET activation assay (Figure 20), thiophenones **25** and **28** were used for conjugation strategies to degrade RNA.

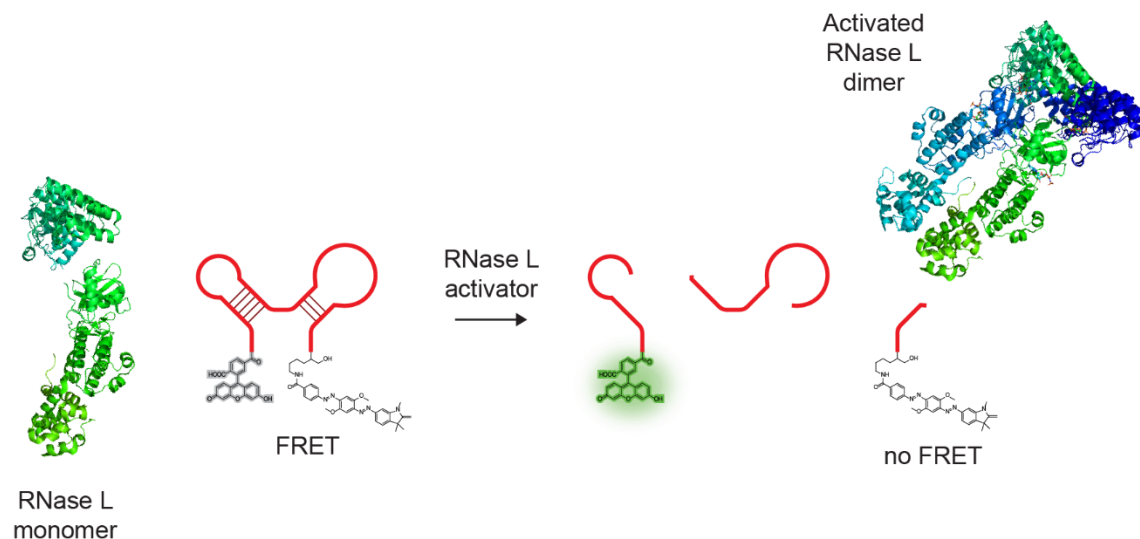


Figure 19. RNase L FRET activation assay.

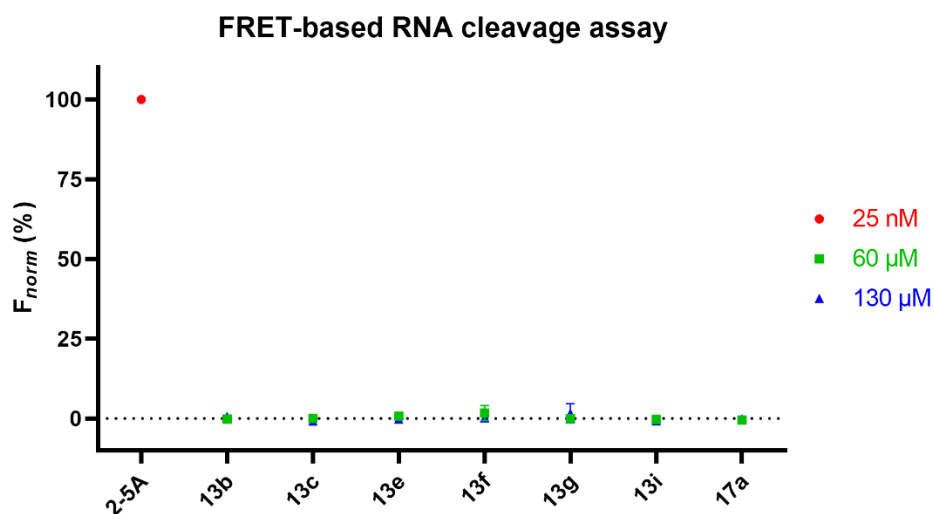


Figure 20. Evaluation of compounds (**13b**, **13c**, **13e-13g**, **13i**, **17a**) in RNase L FRET activation assay.

In summary, a collection of thienopyrimidinones have been synthesized using combinations of 2-aminothiophenes with benzonitriles for incorporation of functional groups allowing linker attachment at different positions. Thienodiazepines were synthesized from amino acids to increase aqueous solubility. However, RNase L activating potency of the synthetic compounds could not be observed in a biochemical assay measuring RNA cleavage. Established RIBOTAC methodology based on thiophenones was instead utilized to synthesize analogs with amine or azide functionalized linkers allowing conjugation.

3.2. RNA Interactome Targeting Chimera

Targeted RNA degradation strategies have so far only been achieved by using RNA-binding oligonucleotides or small molecules, which has rendered concern on target selectivity. A novel small molecule-based strategy is the recruitment of RNase L to an RBP leading to degradation of the RNA interactome (Figure 21). Such an approach has the potential to overcome selectivity concerns of current RNA degradation methods as high selectivity of small molecules targeting RBPs can be achieved. This strategy utilizing proximity-inducing bifunctional molecules is here described for the first time and may be applied as a tool to study and discover unreported protein-RNA interactions by using total RNA-Seq in cellular experiments for the identification of reduced levels of transcripts after compound treatment, but may also be therapeutically relevant in case of degradation of oncogenic RNAs. As seen with proximity-inducing PROTACs and RIBOTACs generation of novel complexes can enhance selectivity over monomeric ligands.^[238, 270, 271]

Another advantage of the RNA interactome targeting chimera (RITAC) approach is the feasibility of targeting long non-coding RNAs (lncRNAs). The defined structures of lncRNAs are challenging to determine, making it difficult to target lncRNAs directly with small molecule ligands. There are only a few examples of small molecules directly binding lncRNAs.^[272-275] The biological functions of lncRNAs have been increasingly well-characterized and connected to pathogenesis of multiple diseases, making lncRNAs potential drug targets.^[276, 277]

To synthesize the first examples of RITACs, reported small molecule inhibitors of an RBP were employed to recruit RNase L through conjugation with thiophenones. PEG linkers were used to increase flexibility and aqueous solubility of the heterobifunctional molecules. Considering that the RBP may sterically clash with RNase L if using a short inflexible linker, synthesis of the RITACs were based on previous reported heterobifunctional RNase L thiophenone recruiters (Table 2) using a minimum linker length of 11 atoms to recruit RNase L for targeted RNA degradation mediated by RBPs.

For proof-of-concept, the first RITAC was designed to target the RBP WDR5 based on reported inhibitors binding allosterically to the RNA-binding region. WDR5 interacts with oncogenic lncRNAs and complex formation with RNase L induced by RITACs would allow for cleavage of single stranded regions of the disease-causing RNA, which may serve as an anticancer strategy.

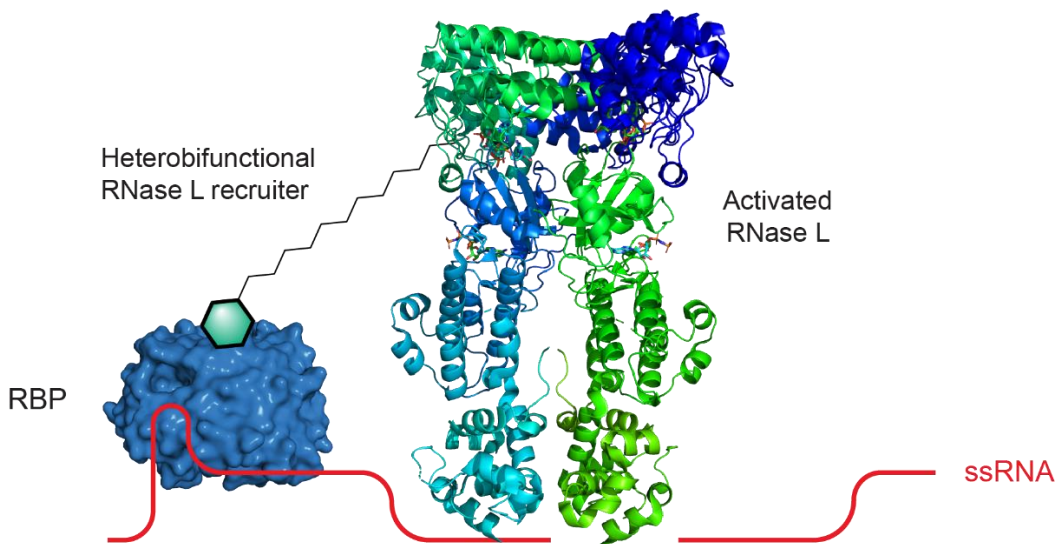


Figure 21. Concept of RITAC inducing quaternary complex formation.

3.2.1. WDR5 Inhibitors

The scaffolding protein WDR5 is required for the assembly and activity of the histone methyltransferase complex together with mixed lineage leukemia 1 (MLL1), retinoblastoma binding protein 5 (RbBP5) and absent small or homeotic-2-like (ASH2L) causing trimethylation of Lys-4 on histone H3, but also has other interaction partners for additional functions.^[278-280] Post-translational H3K4me3 modifications result in the activation of homeobox A (HOXA) gene expression, where upregulation has been associated with acute myeloid leukemia (AML).^[281-283]

WDR5 is a relatively small 37 kDa protein consisting of seven repeats forming a β -propeller doughnut-shaped protein with two major interaction sites, the WDR5-interaction (WIN) site and the WDR5-binding motif (WBM) (Figure 22A). The WIN site is located within the deep central cavity and allows protein-protein interaction (PPI) with histone H3^[284-287] and MLL1.^[288, 289] The WBM site is positively charged, located on the surface of the β -sheets and apart from protein interaction with RbBP5, WBM also facilitates interaction with lncRNAs such as HOXA transcript at the distal tip (HOTTIP)^[290], BLACAT2^[291], NeST^[292], GClnc1^[293], Linc1405^[294] and RAIN^[295]. The promiscuity in RNA-binding of WDR5 might suggest that the development of RITAC against this target would be more suitable as a tool to further study the interactome.^[296, 297] The same WBM binding site mediates PPI with the oncogenic transcription factor c-MYC^[298] making WDR5 an interesting target for treatment of cancers via small molecule PPI inhibitors.^[299, 300]

The HOTTIP gene is located at the 5' tip upstream of the HOXA genes and acts as a scaffold to transport and locate the complex in position for accurate methylation by direct interactions with target genes (Figure 22B).^[301] Knockdown of either WDR5^[302] or HOTTIP^[303-305] using RNAi resulted in reduced trimethylation levels of H3K4 as well as reduced transcription of HOXA genes. Neither secondary structure nor the sequence of HOTTIP interacting with WDR5 have been determined, but the use of RITACs has the potential to determine both RNA structure and sequence in proximity to the RBP. Upregulation of HOTTIP has been connected to gastric cancer,^[306] pancreatic cancer^[307] and prostate cancer^[308] amongst others, and HOTTIP levels used as biomarker to predict patient survival. Targeted degradation of HOTTIP has potential to serve as therapeutic strategy for treatment of several human cancers.

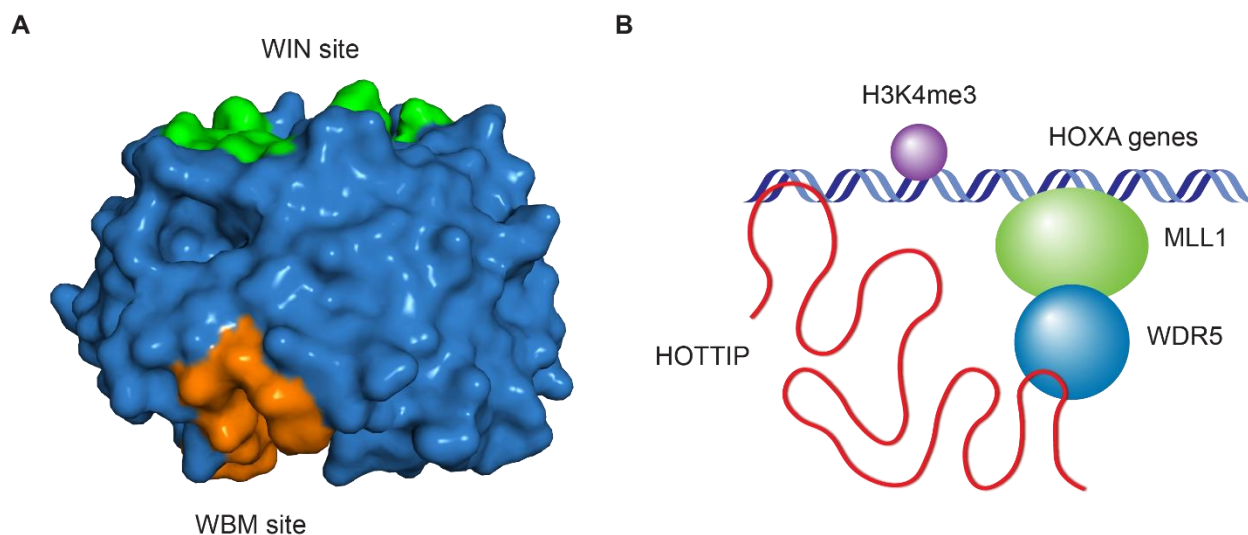


Figure 22. Interactions of the RBP WDR5. **A:** WDR5 (PDB: 3UR4) binding sites WIN respectively WBM. Key residues at the WIN site interacting with MLL1 are shown in green.^[285-289, 309, 310] Key residues at the WBM site interacting with RNAs are shown in orange.^[296, 311, 312] **B:** MLL1-WDR5-HOTTIP interaction with HOXA genes.

WDR5 is a suitable target for the development of the RITAC strategy due to (1) the allosteric nature of the RNA interaction of WDR5 to the extensively explored WIN binding site that would avoid competition between the RITAC and RNAs of binding to WDR5, (2) the interaction with at least partially single stranded pathologic RNAs that can be cleaved by RNase L and (3) the presence of reported ligands of the allosteric WIN site. Potentially challenging may be that WDR5 and its RNA interactome are mainly present in the nucleus, whereas RNase L is mainly located in the cytoplasm. However, targeted degradation of primary miRNA has been reported using the

RIBOTAC strategy indicating the nuclear presence of RNase L to some extent.^[235] The cellular localization of RNase L has also been seen depending on cell line, where in some cases RNase L was predominantly found in the nucleus.^[313, 314] This may offer additional selectivity to specific cells and tissues.

Properties of WDR5 WIN site inhibitors to be incorporated into the RITACs have been limited to compounds with (1) reported activity in cells, (2) available linker attachment site and (3) drug-like properties resulting in sufficient metabolic stability and cell permeability.

Peptides and peptidomimetics have been developed as potent inhibitors of the WDR5 WIN site hindering interaction with MLL1 and directly decreasing methylation activity.^[315-318] Peptides generally require optimization to afford stability and cell permeability including formulation strategies in the drug development space to achieve oral bioavailability.^[319] Although peptidomimetics like **MM-589** display improved metabolic stability and cell permeability compared to linear analogues,^[318] their high molecular weight makes it less suitable to be incorporated for the development of cell permeable heterobifunctional molecules.

Several small molecules have been developed for inhibition of the PPI between WDR5-MLL1 (Figure 23).^[320-325] A general chemotype can be defined by a benzene core substituted with a group positively charged at physiological pH (piperazine, imidazole or guanidine analogues) in *ortho* or *meta* position to an aromatic moiety connected by 2-3 atoms from the benzene. The first reported WDR5 inhibitor of such chemotype was **WDR5-0103** that forms a water-mediated hydrogen bond between the protonated *N*-methyl piperazine and the carbonyl of Cys-261 in the WIN site. This interaction directly replaces the position of Arg-3765 side chain from interaction with MLL1.^[320] Variation of aromatic substituents and replacement of the ester have further expanded the SAR and provided small molecules with improved activity.^[326, 327] Introduction of a biaryl fragment found in **OICR-9429**,^[322, 328] **DDO-2117**^[323] and other analogues^[329-334] further increased affinity to WDR5 by interaction with a hydrophobic patch near the solvent exposed regions allowing π - π stacking with Tyr-191, while retaining water-mediated hydrogen bonding between protonated piperazine and Cys-261. However, limited solubility has been observed for compounds containing the biaryl fragment.^[328]

WDR5 inhibitors with bicyclic scaffolds containing an imidazole or guanidine moiety affording higher affinity to the WIN site have recently been reported. Compounds containing the highly basic guanidine group also bear issues with limited cell permeability.^[324, 325, 335] By studying the complex formation of inhibitors “**6e**” and “**16**” with WDR5 (PDB: 6E22 and 6E23), the lack of solvent exposed functionalities suitable for linker attachment becomes evident and making this compound class less suitable to be incorporated for the synthesis of heterobifunctional molecules.

Proteomic studies have shown that WIN site inhibitors change the protein interactome of WDR5 indicating the possibility of RITACs binding the WIN site and recruiting RNase L may also affect the RNA interactome.^[336] Targets of RBPs identified by editing (TRIBE) is an established method^[337] to identify protein-RNA interactions by using RBPs fused to the catalytic domain of adenosine deaminases acting on RNA (ADAR). Altering of the RNA interactome compared to the endogenous RBP is likely during mapping of the RNA interactome by RNA-Seq. In comparison the RITAC strategy may be used directly on endogenously expressed RBPs and with ability to determine the RNA interactome with high precision.

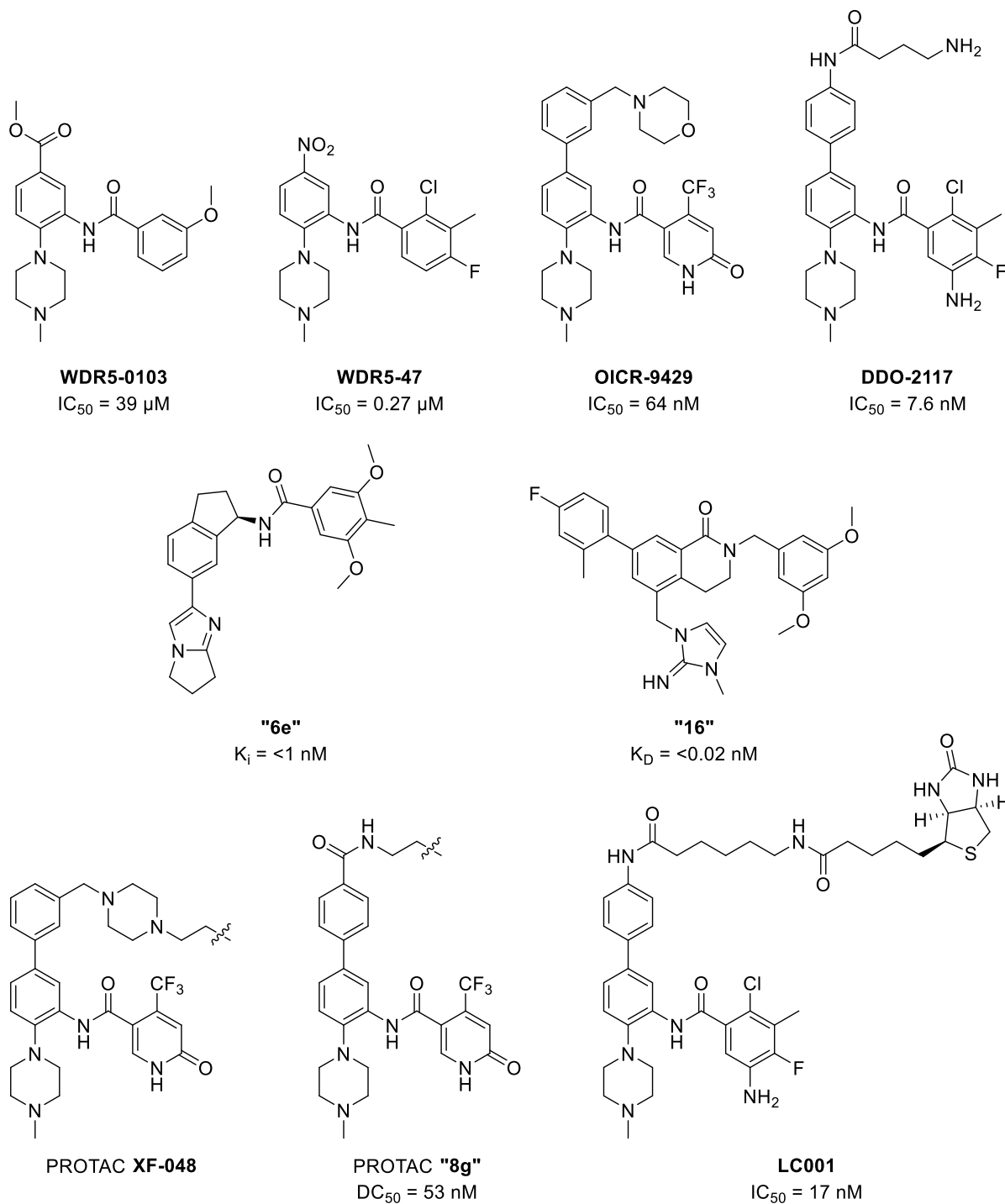


Figure 23. Representative small molecule WDR5 WIN site inhibitors.

WDR5-0103 presents a solvent exposed methyl ester in complex with WDR5 (Figure 24) suitable for linker attachment. The closely related analogue **WL-1** with modification of the aromatic substitution pattern likely forms similar interactions with WDR5 but offers improved affinity.^[326]

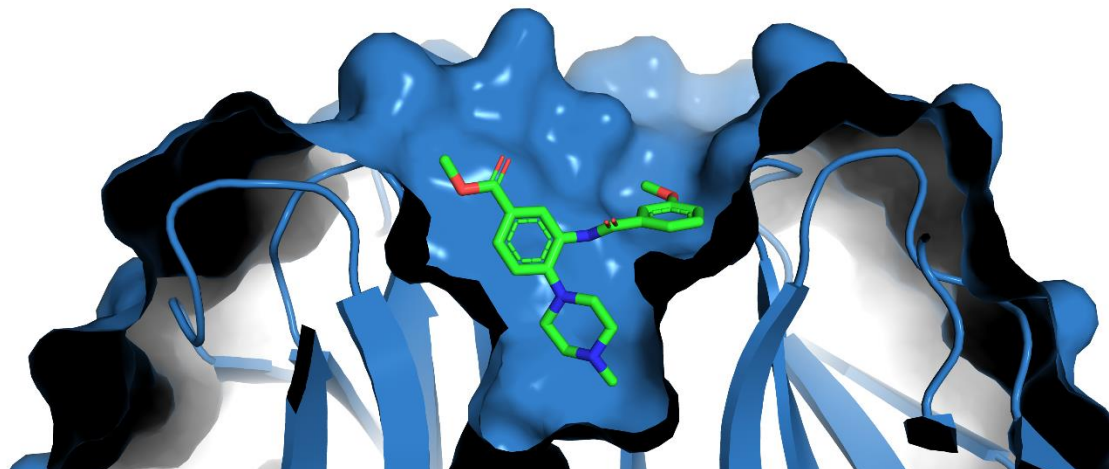


Figure 24. Co-crystal structure of **WDR5-0103** binding WIN site of WDR5 (PDB: 3UR4).

Linker attachment *para* to the biaryl fragment in WDR5 inhibitor **DDO-2084** for introduction of biotin as pull-down probe resulting in **LC001** barely affected binding affinity to WDR5 and has been used to show that selective pull-down of WDR5 from cell lysate is possible.^[338]

Recent development of WDR5 degrading PROTAC **XF-048** has been based on **OICR-9429**, where linker attachment was performed by replacing the morpholine group with a piperazine allowing substitution and conjugation with E3 ligase recruiters.^[339] Another set of PROTACs targeting WDR5 were based on **OICR-9429**, but lacking the morpholine moiety where linker attachment for conjugation with von Hippel-Lindau (VHL) E3 ligase recruiter was performed *para* to the biaryl fragment by introducing a *tert*-butyl ester. This compound possessed higher activity than **OICR-9249** by increasing the melting temperature of WDR5 during differential scanning fluorimetry measurements and served as starting point for amide coupling to obtain the bifunctional molecules. It was also found that bifunctional molecules containing PEG linkers had higher solubility than those prepared from aliphatic or aromatic linkers. However, most efficient WDR5 degradation in AML cell line MV4-11 was achieved using a short butane linker in “**8g**”.^[340] Indeed, this position has been proven to be suitable for modifications allowing retained activity of inhibitors of WDR5 and the use of PEG linkers enhanced aqueous solubility.

3.2.2. Chemical Synthesis of WDR5 Inhibitors

Available data on SAR and co-crystal structure of WDR5 inhibitors was analyzed to identify sites suitable for linker attachment to avoid loss of activity (Figure 25). Functional groups present in

selected WDR5 inhibitors were utilized for amide coupling and further conjugation strategies with thiophenones to induce complex formation with RNase L.

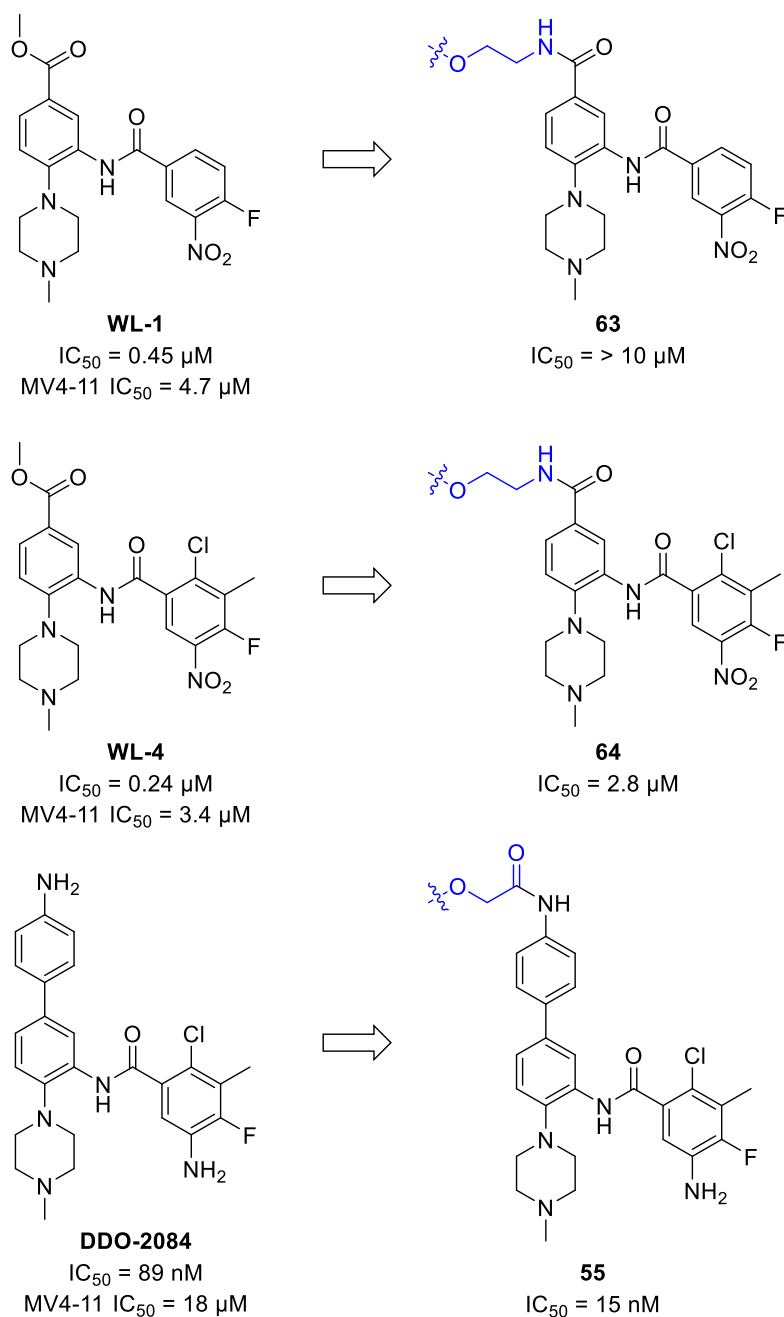
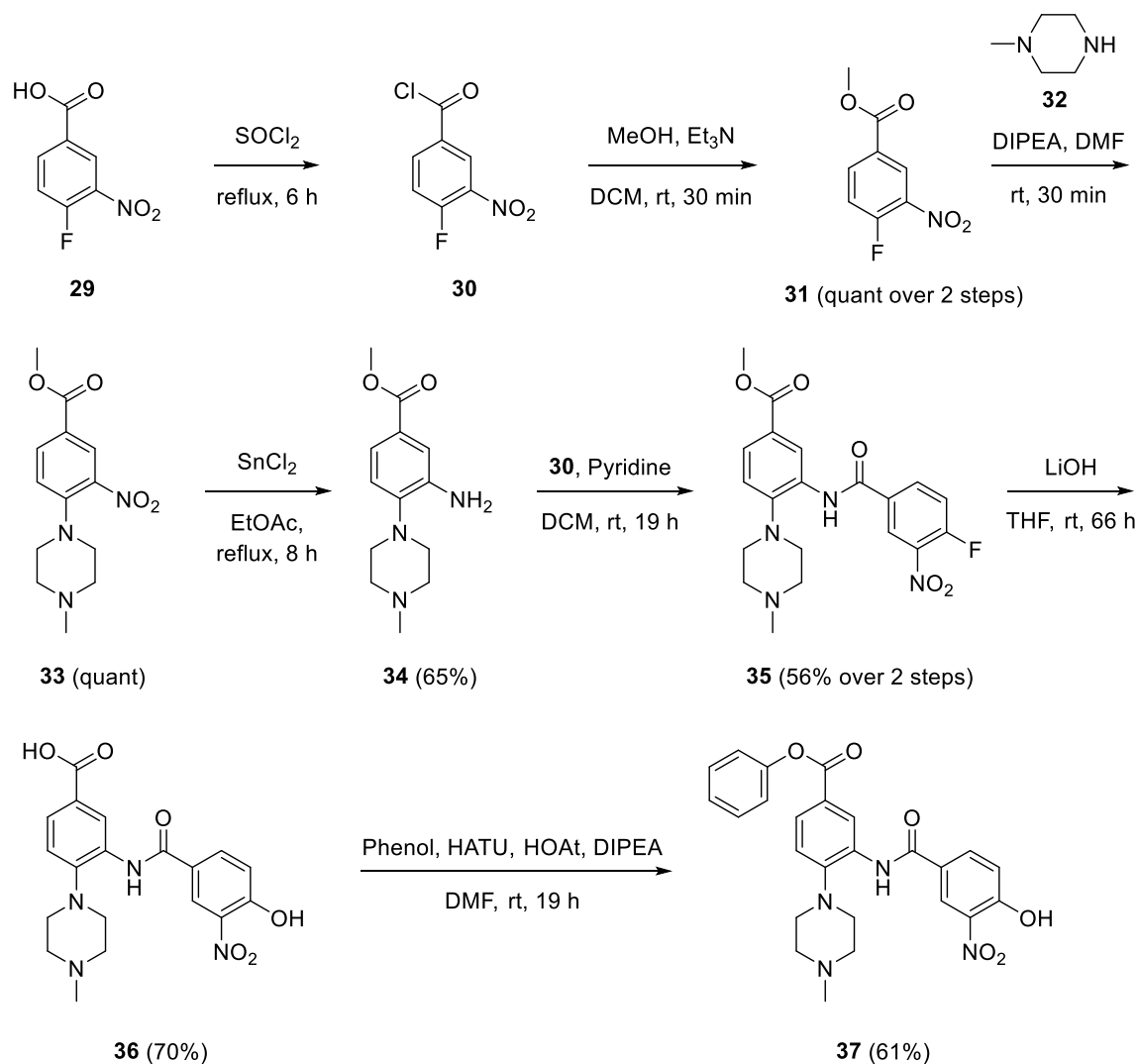


Figure 25. Linker attachment strategies on WDR5 inhibitors.

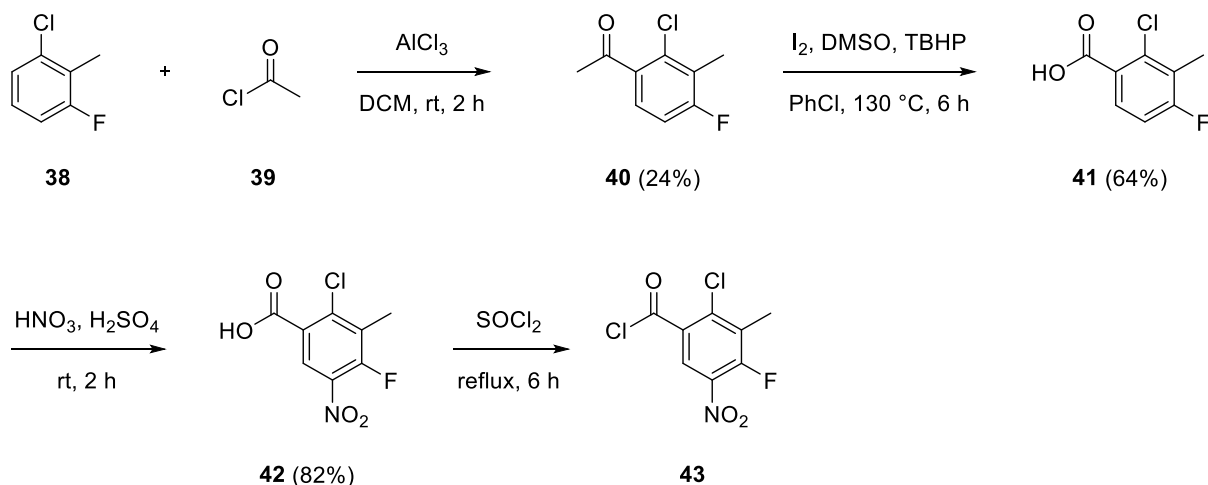
Synthesis of first selected WDR5 inhibitor was initiated by esterification of benzoic acid **29** to obtain **31** and subsequent substitution with *N*-methyl piperazine **32** gave **33**. Nitro group reduction with tin(II) chloride to **34** allowed amide coupling with acyl chloride **30** to obtain WDR5 inhibitor

35 (Scheme 9). Following literature procedure^[326] hydrolysis of the methyl ester was carried out with lithium hydroxide, but also resulted in hydrolysis of the fluoride. In fact, fluoride hydrolysis rate was higher than ester hydrolysis due to the electron deficient nature of the aromatic system, thereby making it impossible to obtain any sample with intact fluoride in combination with hydrolysed ester. Hydrolysis conditions used to afford a carboxylic acid from **WL-1** was falsely reported to result in an intact fluoride, but according to analytical data in the publication the obtained compound was identical to **36** meaning that authors also observed fluoride hydrolysis.^[326] To evaluate how fluoride hydrolysis affected activity of the compound series esterification with a phenol afforded **37**, a direct analogue of reported **WL-11** ($IC_{50} = 0.48 \mu M$) that has an intact fluoride atom and similar activity as **WL-1**.

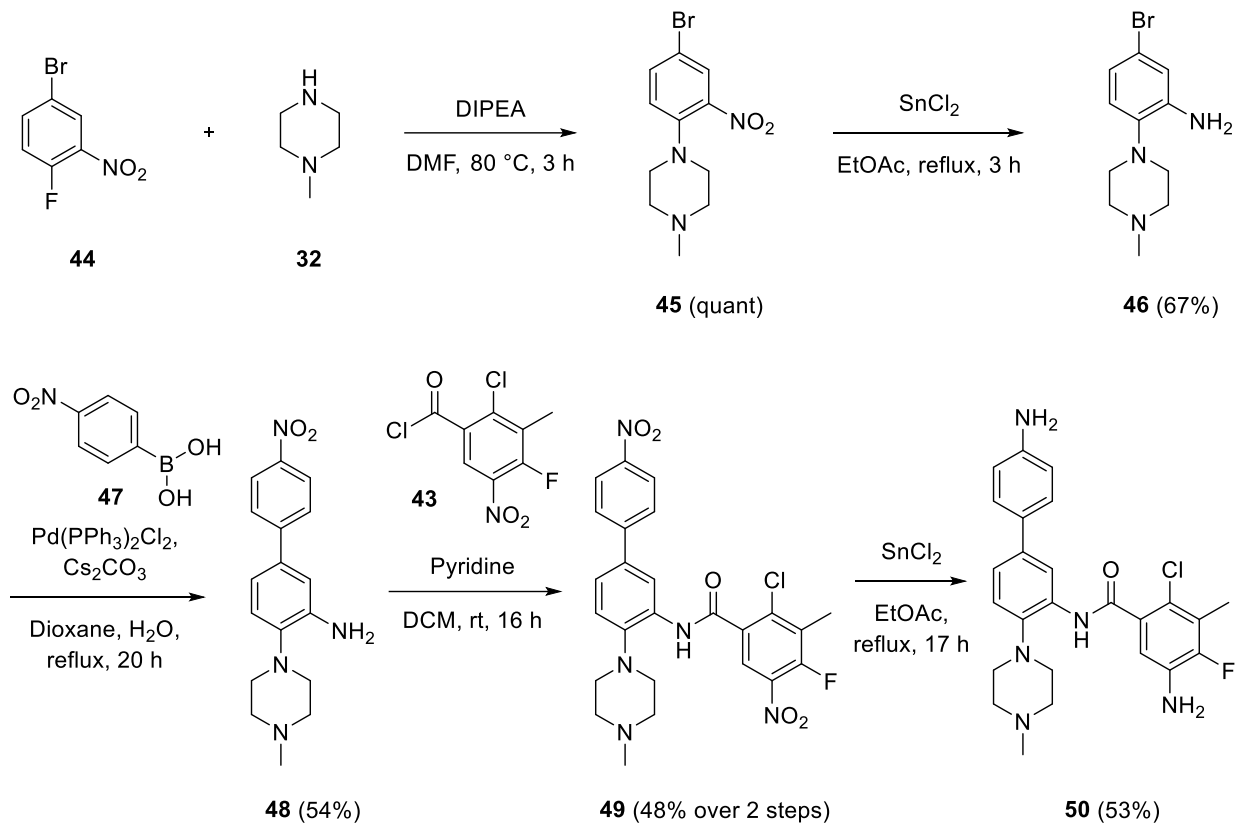


Scheme 9. Synthesis of WDR5 inhibitor analogues.

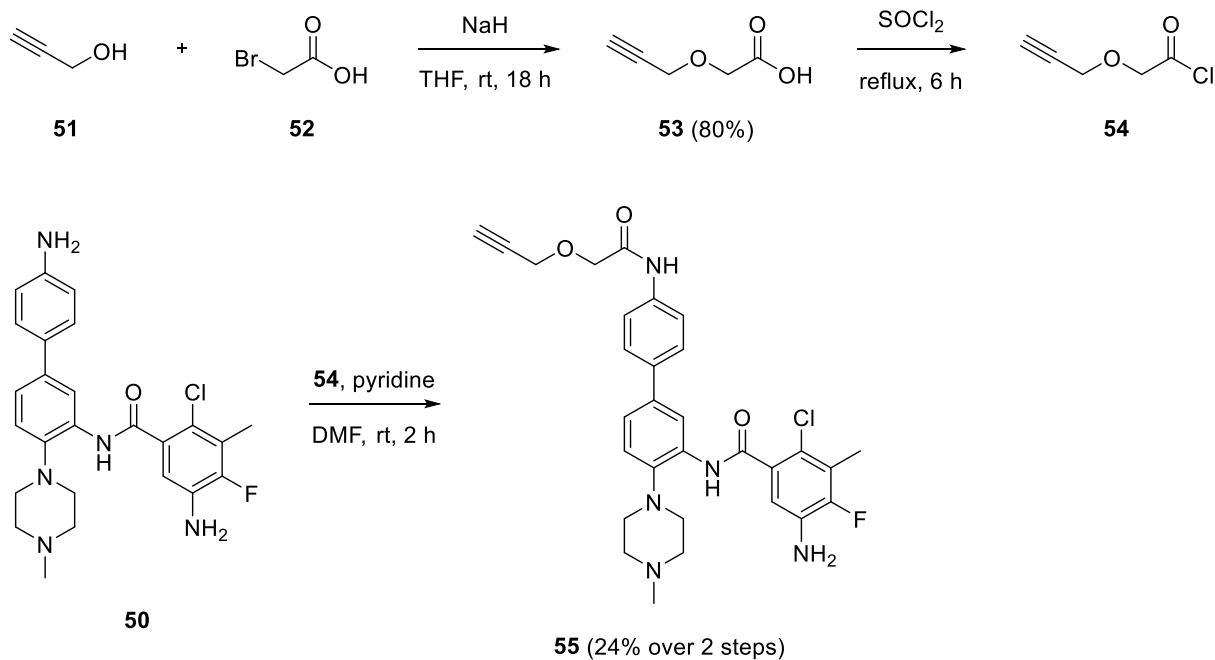
Synthesis of the fragment for amide coupling to the scaffold of biaryl WDR5 inhibitor **50** was modified from the reported synthetic route.^[327] Lewis acid mediated Friedel-Crafts acylation of **38** with acetyl chloride **39** generated aryl ketone **40** (Scheme 10) that could be oxidized into corresponding carboxylic acid **41** by DMSO and TBHP with catalytic iodine.^[341] Nitration yielded the desired carboxylic acid **42** that was transformed into acyl chloride **43** by reflux in thionyl chloride. Synthesis of the biaryl-based WDR5 inhibitor **50** was initiated by substitution of **44** with *N*-methyl piperazine **32** yielding **45**, followed by reduction of the nitro group to **46** (Scheme 11). The palladium catalysed Suzuki cross-coupling with boronic acid **47** gave the core biaryl scaffold **48**. Amide coupling of prepared fragment **43** generated **49**. Reduction of both nitro groups afforded WDR5 inhibitor **50**. Installation of the alkyne handle for conjugation with the RNase L recruiter was performed by synthesis of carboxylic acid **53** from substitution of bromoacetic acid **52** with propargyl alcohol **51**. Transformation into the corresponding acyl chloride **54** and selective amide coupling of **50** gave the alkyne handle at the northern amine due to the increased nucleophilic nature (Scheme 12). Small amounts of diacylated by-product were observed and separated from desired product **55** with purification by prep. HPLC. Analogues of **WL-1** and **WL-4** with alkyne handles were prepared by alkylation of alcohol **56** with propargyl bromide **57** giving **58**. Boc deprotection allowed amide coupling of amine **59** with acyl chloride **30**. Nucleophilic aromatic substitution of **60** with *N*-methyl piperazine **32** resulted in **61**, where further nitro group reduction gave core **62**. Using either acyl chloride **30** or **43** generated the alkyne tagged WDR5 inhibitors **63** respectively **64** (Scheme 13).



Scheme 10. Synthesis of 2-chloro-4-fluoro-3-methyl-5-nitro substituted building block.

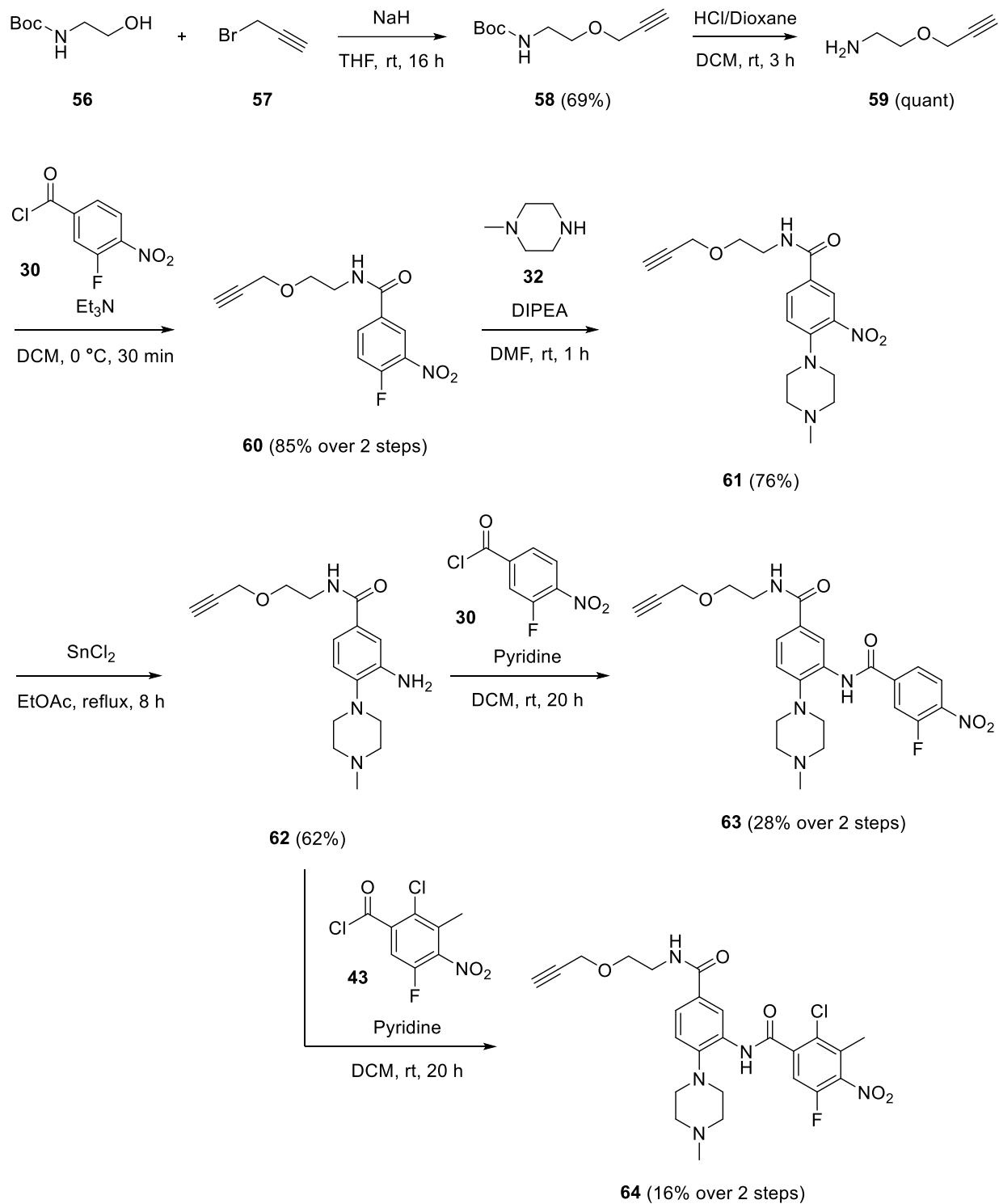


Scheme 11. Synthesis of WDR5 inhibitor analogues with biaryl fragment.



Scheme 12. Synthesis of WDR5 inhibitor with biaryl fragment and alkyne tag.

RESULTS AND DISCUSSION



Scheme 13. Synthesis of WDR5 inhibitor with alkyne tag.

3.2.3. Biochemical Evaluation

Biochemical evaluation of the WDR5 inhibitory activities of the synthesized compounds was performed by Jen-Yao Chang. Compounds aimed to target the WIN site of WDR5 were evaluated in a competitive fluorescence polarization (FP) assay using a 5-FAM-labelled peptide derived from MLL1. Reported assay conditions were adapted to be performed in 384 well plate format.^[315]

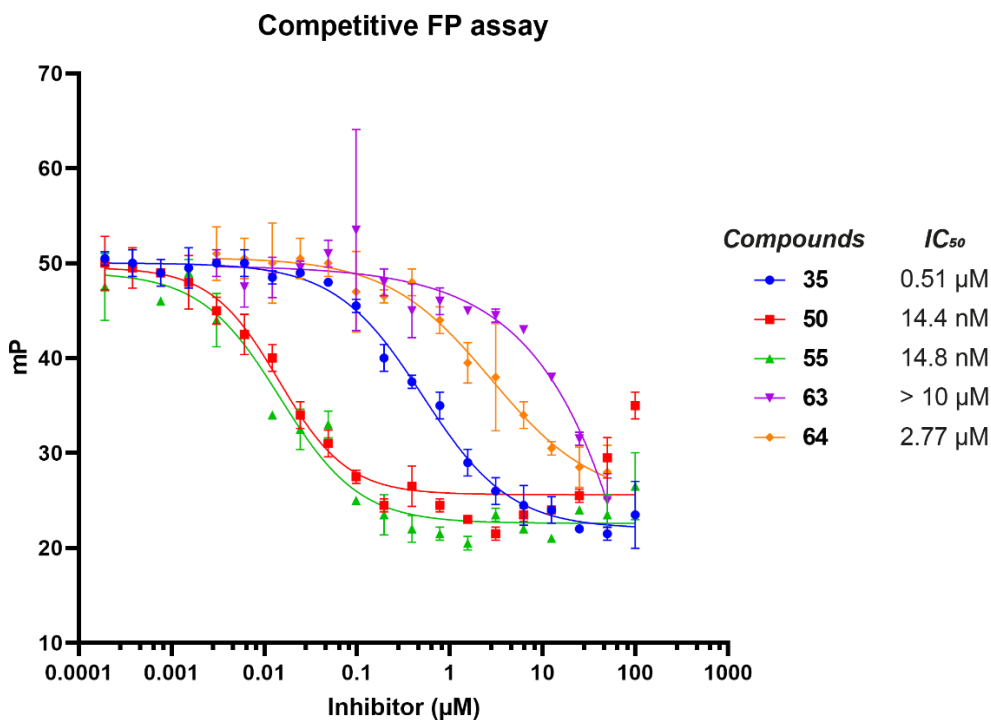


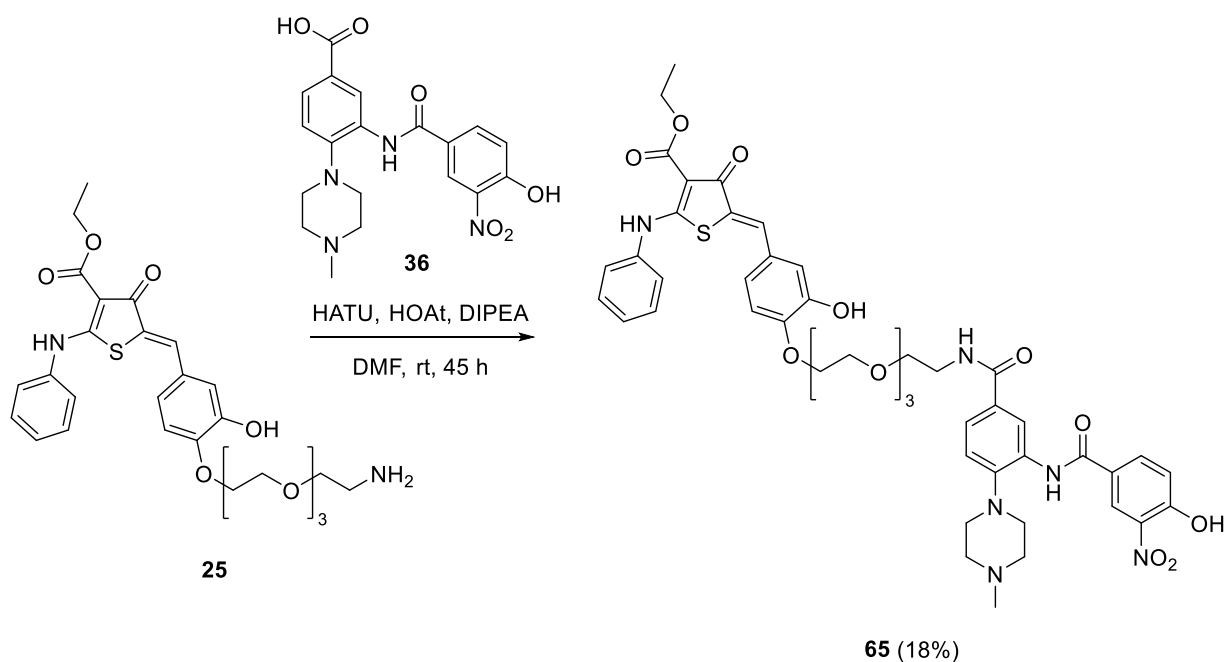
Figure 26. Biochemical evaluation of compounds (**35**, **50**, **55**, **63**, **64**) in competitive WDR5 FP assay.

Compounds were able to compete with the peptide after incubation with the protein indicating direct binding to the WIN site (Figure 26). Evaluation of **35** matched well with reported biological evaluation data of **WL-1**.^[326] The experimental IC₅₀ of compound **50** was found to be 7-fold lower than the reported value of **DDO-2084**,^[323] still within an acceptable error range. Overall the obtained results indicated a robust assay setup and compounds of high quality. Linker attachment site *para* to the biaryl scaffold did not affect WDR5 binding negatively with compound **55**. The IC₅₀ value is in line with both **DDO-2117**^[323] and **LC001**,^[338] indicating that this position is optimal for conjugation. Modification of the ester in **35** to an amide for linker attachment negatively affected the binding affinity more than for **55** indicating a less suitable linker attachment site. However, **64** still retained activity with 11.3-fold loss in IC₅₀ compared to original compound

WL-4^[326] indicating a suitable site for conjugation with RNase L recruiter. The binding affinity is not necessarily correlating to complex stability and degradation efficiency as seen with PROTACs.^[342]

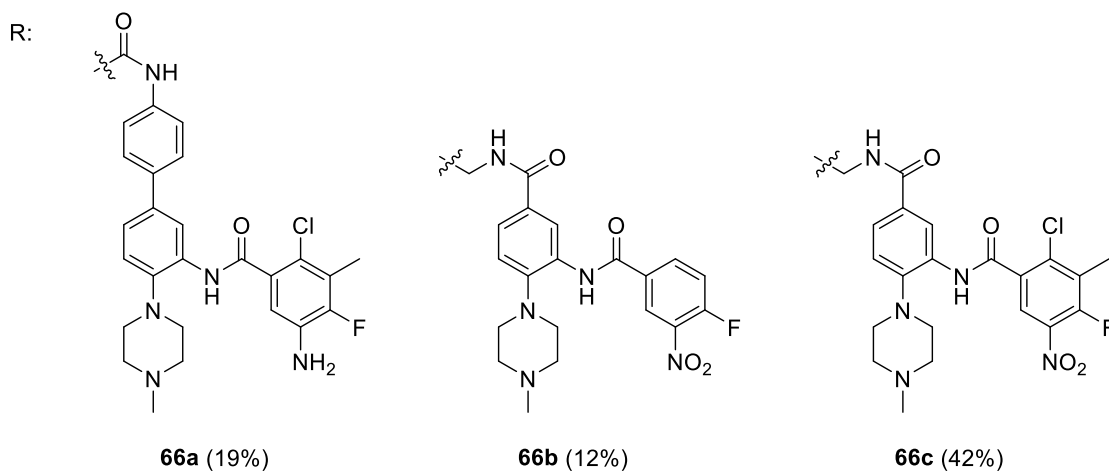
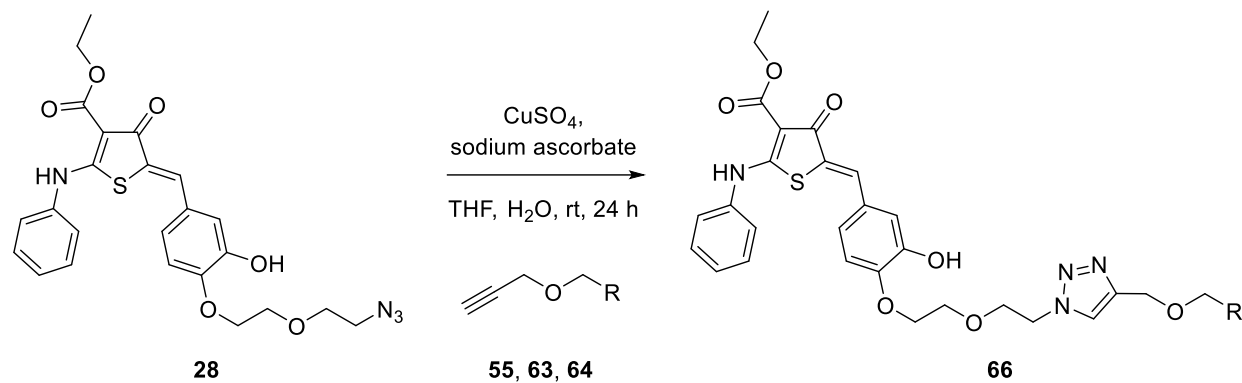
3.2.4. Bifunctional Molecules

Synthesis of heterobifunctional RITACs was performed using amide coupling or copper-catalyzed azide-alkyne cycloaddition (CuAAC) between the WDR5 inhibitor and the reported thiophenone RNase L recruiter. The first RITAC was synthesized by amide coupling between carboxylic acid **36** and amine **25** giving heterobifunctional molecule **65** conjugated via a PEG linker to enhance aqueous solubility (Scheme 14). The same linker length was used as in reported examples of small molecule-based RIBOTACs (Table 2) to ensure efficient recruitment of RNase L. Hydrolysis of the fluoride atom in **37** may have resulted in reduced affinity to WDR5, but was not evaluated in the competitive FP assay for WDR5. The aromatic substitution pattern in combination with intact methyl ester has not been evaluated for binding of WIN site nor proven active in cell-based assays making it uncertain if the obtained molecule will be successful in inducing proximity to WDR5.



Scheme 14. Synthesis of first RITAC containing PEG₄ linker by amide coupling.

To avoid issues with fluoride hydrolysis during ester hydrolysis a different synthetic route was designed for conjugation by Huisgen 1,3-dipolar cycloaddition forming 1,4-disubstituted 1,2,3-triazoles (Scheme 15). Copper(II) sulfate was used in combination with reducing agent sodium ascorbic acid to generate Cu(I) *in situ* for catalysis of the cycloaddition.^[343] A linker length of 12-13 atoms in the obtained heterobifunctional molecules **66a-66c** is in the range of reported RIBOTACs (Table 2) and should be suitable for recruitment of RNase L to induce degradation of RNA proximal to the small molecule binding site. Aqueous solubility was lower for **66a** due to the biaryl fragment causing increased lipophilicity, but also potency of precursor **55**. However, an overall acceptable solubility of **66a** was obtained by incorporation of the piperazine moiety, which becomes charged at physiological pH. How this affects cell permeability is to be determined. The substitution pattern of precursor **64** resulted in higher WDR5 inhibition than **63**, which indicates that **66c** will be more efficient than **66b** in stabilizing complex formation between WDR5 and RNase L. The balance between solubility and cell permeability has been shown to be an important factor for successful development of PROTACs.^[344-347]



Scheme 15. Synthesis of RITACs conjugated by click chemistry.

In summary, WDR5 inhibitors have been successfully modified with linkers, resulting in retained inhibitory activity of at least two compounds. Obtained inhibitors were conjugated with prepared thiophenone RNase L recruiters using amide coupling or click chemistry and thereby the first heterobifunctional RITAC molecules have been synthesized, isolated and characterized.

3.3. Ribonuclease Targeting Chimera

RIBOTACs (Section 1.2.9.) have been developed against several miRNA targets, but recently also for degradation of the SARS-CoV-2 RNA genome.^[56] 2-5A antisense chimera strategies (Table 3) have also been successful in degradation of the HIV-1 RNA genome by recruitment of RNase L to the *gag* gene^[254] and replacement with fully small molecule-based probes may serve as potent antiviral therapeutics allowing oral administration. RNase L inhibitor produced during HIV-1 infection might interfere with the catalytic cleavage, but has not yet been proven to be a concern in strategies to selectively degrade viral RNA.^[348] The HIV-1 genome has been targeted for degradation in this section to extend the application scope of RIBOTACs.

3.3.1. HIV-1 TAR Ligands

HIV-1 infection is a wide-spread infectious disease that affects millions of people leading to the serious condition AIDS.^[349] The virus recognizes C-C chemokine receptor type 5 (CCR5) located at the outer membrane of CD4⁺ T cells for entrance and makes use of endogenous machinery of the white blood host cell for replication and spreading, which ultimately leads to reduced immune response.^[350] The HIV-1 RNA genome contains nine genes encoding for proteins required in this process.^[351] Multiple proteins supporting the physical capsid structure common for retroviruses are encoded within the *gag* gene. Reverse transcriptase, integrase and HIV protease are expressed from the *pol* gene allowing viral RNA to be incorporated in the human DNA and proteolytic processing of viral precursory polyproteins. Glycoproteins are encoded in the *env* gene that detect CCR5 on the surface of host cells assisting entry.^[352] Tat is a small protein essential for induced expression of the virus by interaction of ARMs with the trinucleotide bulge of TAR RNA in both 5' and 3' UTRs (Figure 27). Tat is thereby recruiting endogenous proteins inducing the translation of the viral RNA genome. Similarly, Rev is another small RBP recognizing the RRE RNA within the *env* gene by an ARM resulting in complex formation with exportin-1 that transport viral transcripts to the cytoplasm for translation into proteins.^[353] The virus can stay latent for years caused by low levels of Tat protein amongst other factors.^[354] It has been shown that the TAR RNA can be processed by Dicer-TRBP complex to act as a miRNA and thereby downregulate endogenous proteins to prevent apoptosis.^[355-357] Genes *vif*, *vpr*, *vpu* and *nef* are coding for accessory proteins with the effect of resisting antiviral responses, for example through recruitment

of E3 ubiquitin ligases to induce polyubiquitination and proteasomal degradation of proteins implicating on the viral replication.^[358]

The RNA genome of HIV-1 contains several structurally determined sites suitable for binding of small molecules.^[359] The unstructured reading frame containing coding regions is more suitable for targeting using oligonucleotide-based strategies and has been explored in clinical trials.^[360, 361] Degradation of the viral RNA genome may serve as therapy in treatment of early stages of viral infections and hindering the virus from spreading. Using small molecule-based strategies allowing oral administration would significantly improve the situation of patients in comparison with current methods including bone marrow transplantation.^[362, 363]

Several small molecule ligands have been discovered to bind the bulge area of HIV-1 TAR RNA inhibiting interaction with the Tat protein. One of the first discovered scaffolds for targeting the TAR RNA is thienopyridine (Figure 28).^[364-366] Inhibitors of quinolone^[367-373] and amiloride^[374-378] scaffolds have been discovered and induced proliferative effect in HIV-infected cell lines, although cell permeability might be of concern when incorporated into heterobifunctional molecules due to the presence of readily ionizable functional groups. The selectivity profile of reported small molecule TAR ligands has not yet been fully determined and may cause unselective RNA degradation when incorporated in RIBOTACs.

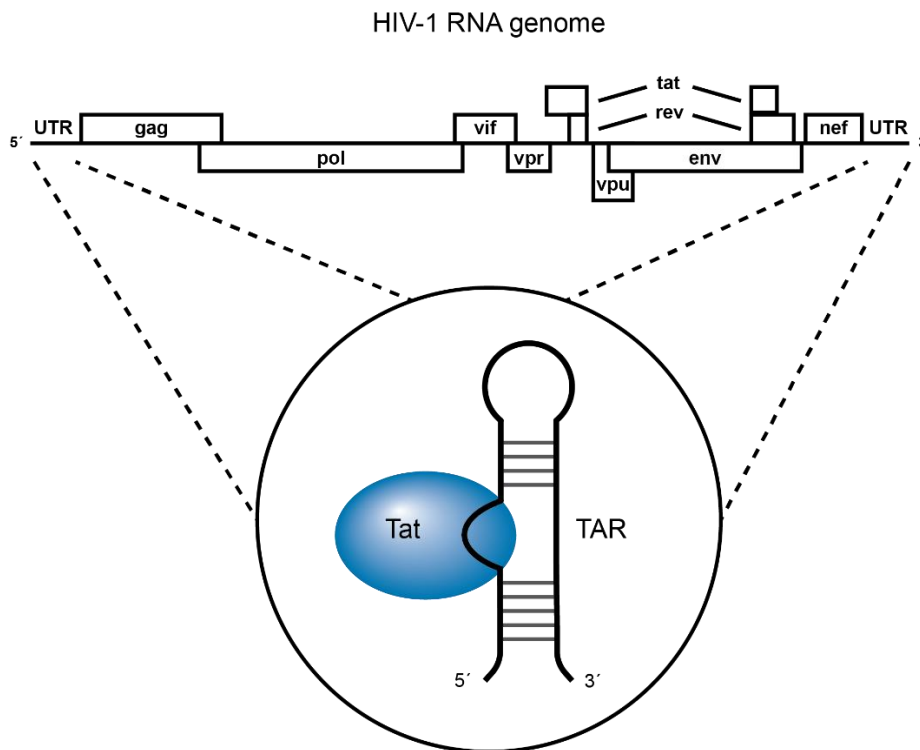


Figure 27. HIV-1 RNA genome with TAR-Tat interaction as a drug target.

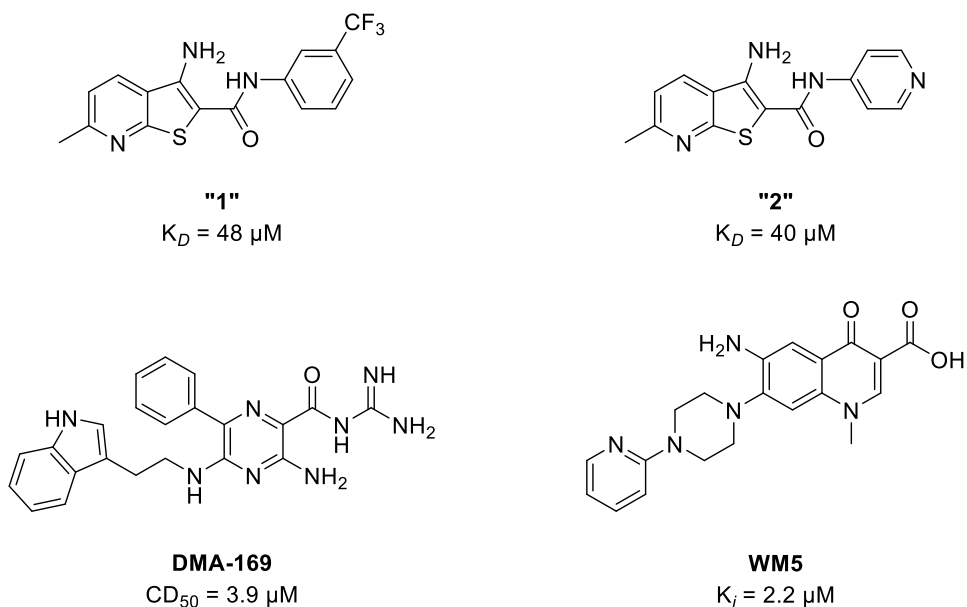


Figure 28. Representative small molecule HIV-1 TAR RNA ligands evaluated by FRET peptide displacement assays.

Based on reported SAR studies of thienopyridines as ligand of TAR RNA, substitutions of the pyridine ring are limited to small aliphatic groups and phenyls with small sized substituents. The

primary amine can not be modified and the amide only allow *N*-methylation or replacement with an oxadiazole. This leaves the aromatic substituent, which fortunately tolerates a wide range of modifications including phenyls with substituents at various positions as well as heterocycles including pyridines and benzimidazole.^[364-366] In conclusion, linker attachment site is likely most suitable at the aromatic region (Figure 29).

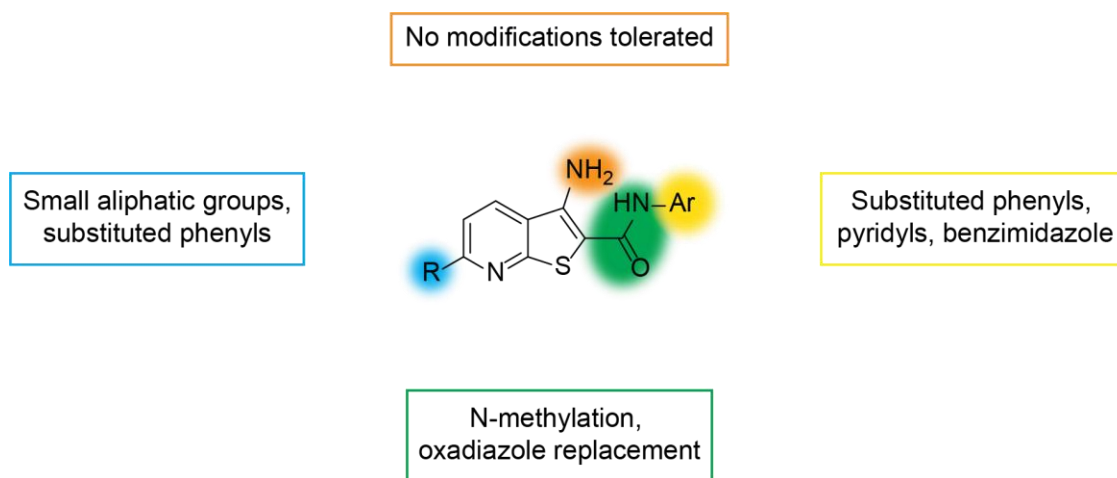
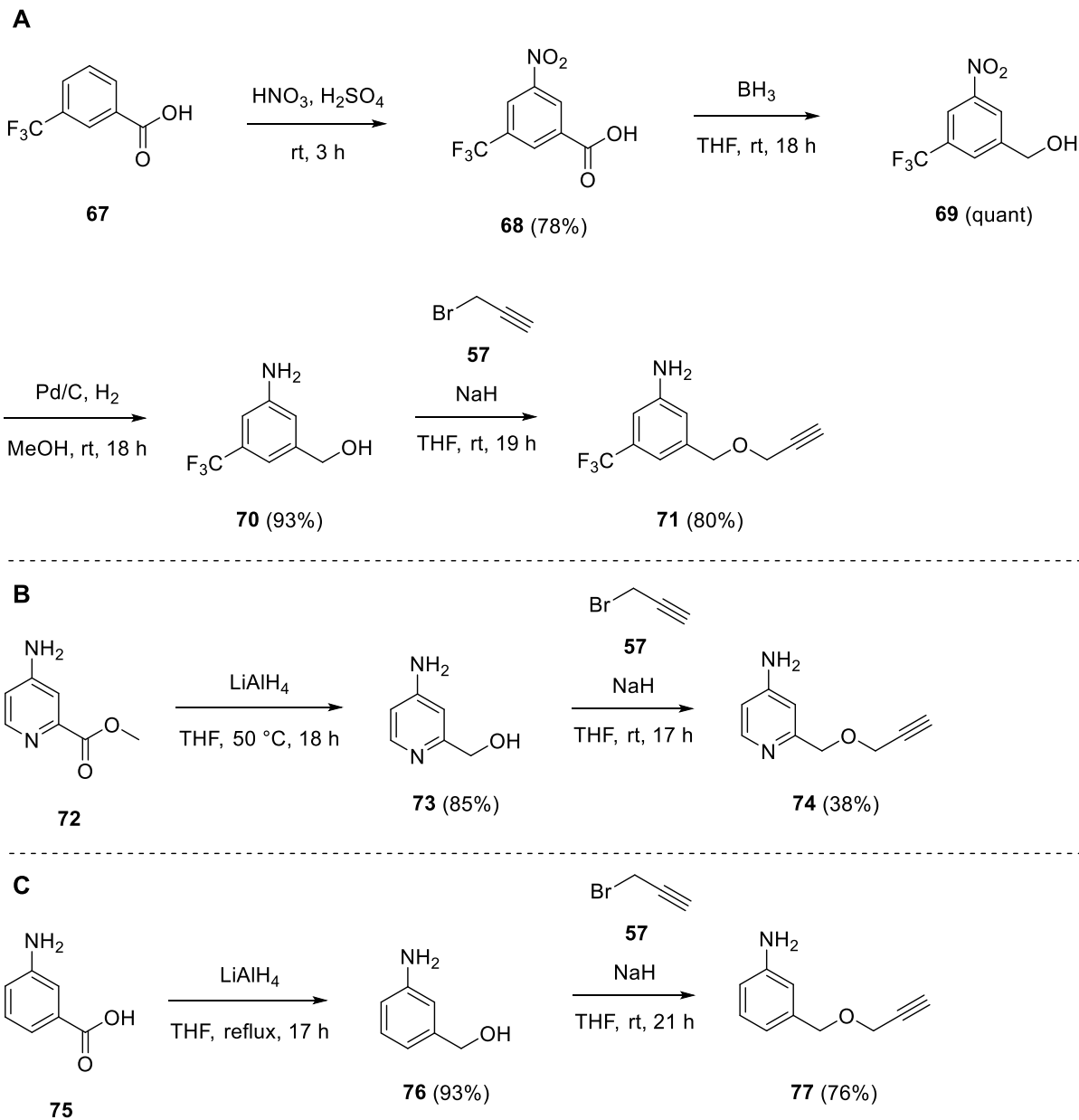


Figure 29. SAR of thienopyridines as TAR ligands.

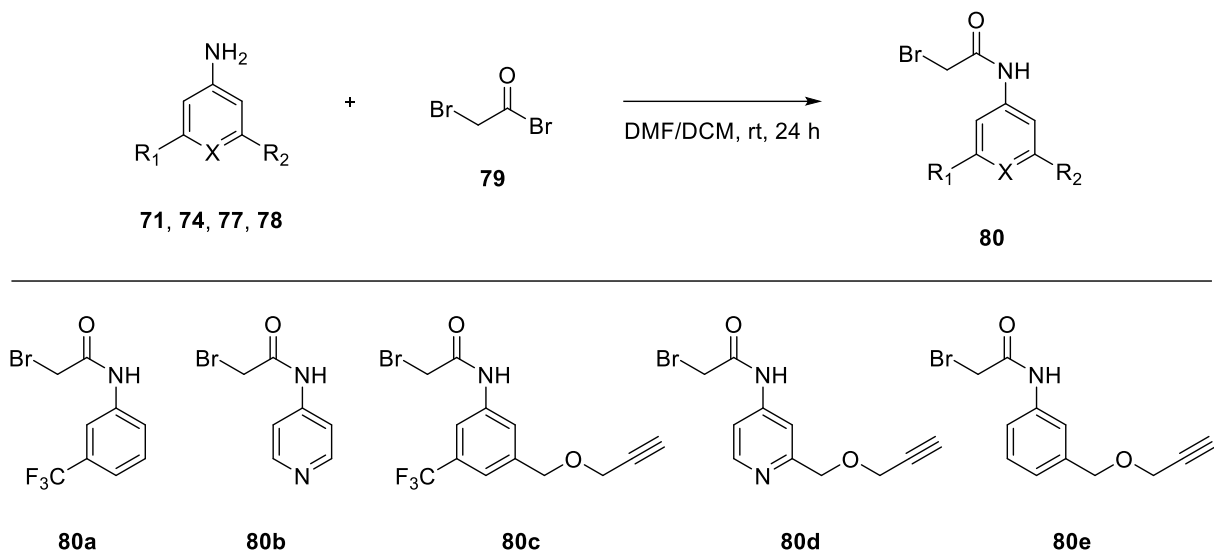
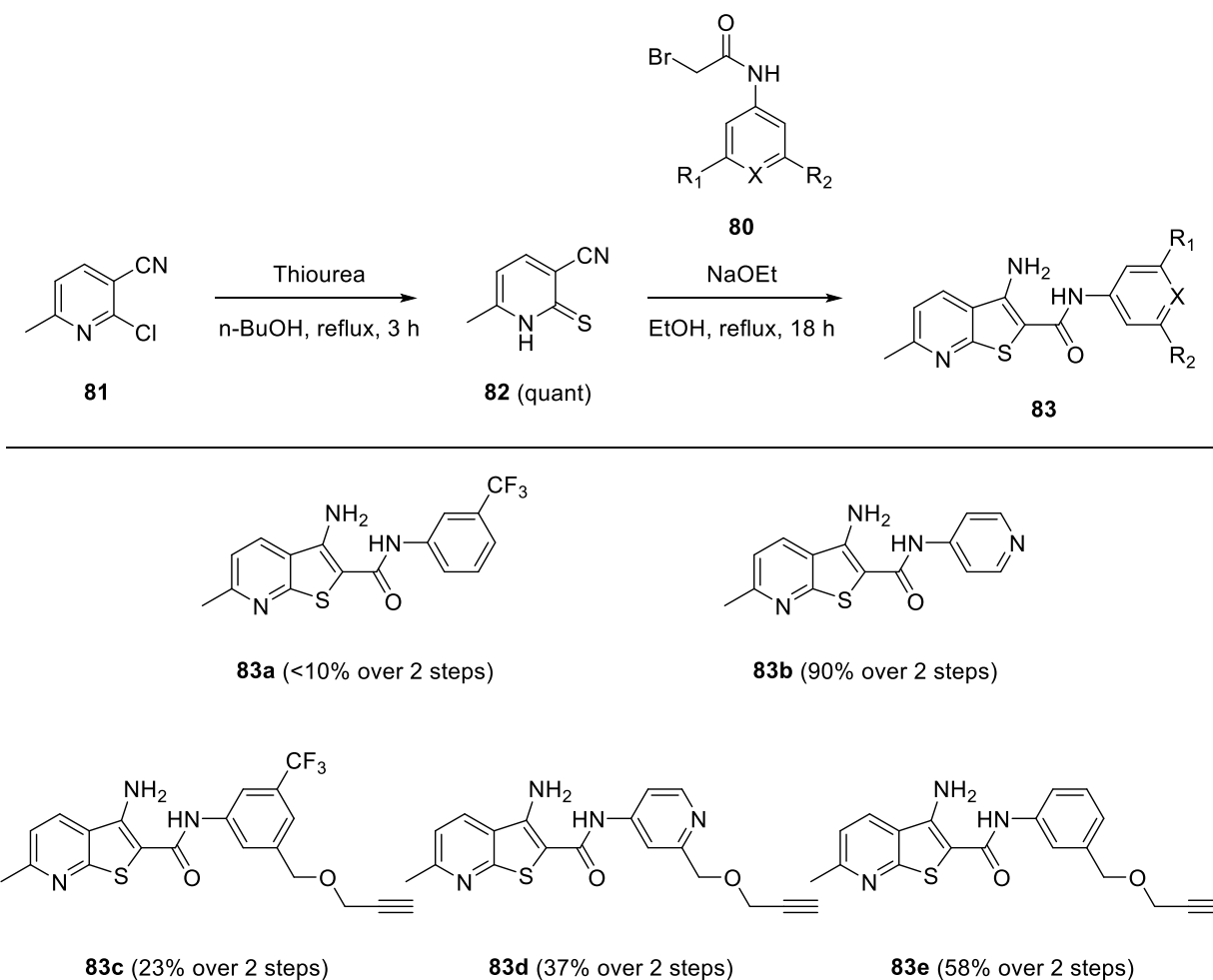
3.3.2. Chemical Synthesis of HIV-1 TAR Ligands

Alkyne tagged anilines were prepared for the synthesis of RIBOTACs. For the trifluoromethylated aniline, corresponding benzoic acid **67** was nitrated resulting in **68**, followed by reduction of first carboxylic acid into alcohol **69** and then nitro group yielding **70** (Scheme 16A). Propargyl bromide **57** was then used to introduce the alkyne handle in **71**. Methyl-4-aminopicolinate **72** was used for the pyridine analogue and reduced into corresponding primary alcohol **73** (Scheme 16B). Propargyl bromide **57** was then used to introduce the alkyne handle in **74**. 3-Aminobenzoic acid **75** was used for the unsubstituted analogue, where reduction lead to the primary alcohol **76** (Scheme 16C). Propargyl bromide **57** was then used to introduce the alkyne handle in **77**. Bromoacetyl bromide **79** was used to acylate the anilines **71**, **74**, **77**, **78a** and **78b** in high conversion to obtain bromoacetamides **80a-80e** after precipitation in Et_2O (Scheme 17). Product **80a** was found to be highly hydrophilic and substantially dissolved in the ether phase and in turn explaining the lower yield of **83a**. Efficient preparation of the thioxo-dihydropyridine **82** from **81** was performed by substitution using thiourea and collection of precipitated product by filtration (Scheme 18). Thienopyridines **83a-83e** were synthesized from prepared bromoacetamides **80a-**

80e and thioxo-dihydropyridine **82** under basic conditions allowing thiophene formation (Scheme 18).^[365] Position of the linker is in agreement with SAR studies and should result in retained binding affinity to TAR RNA.

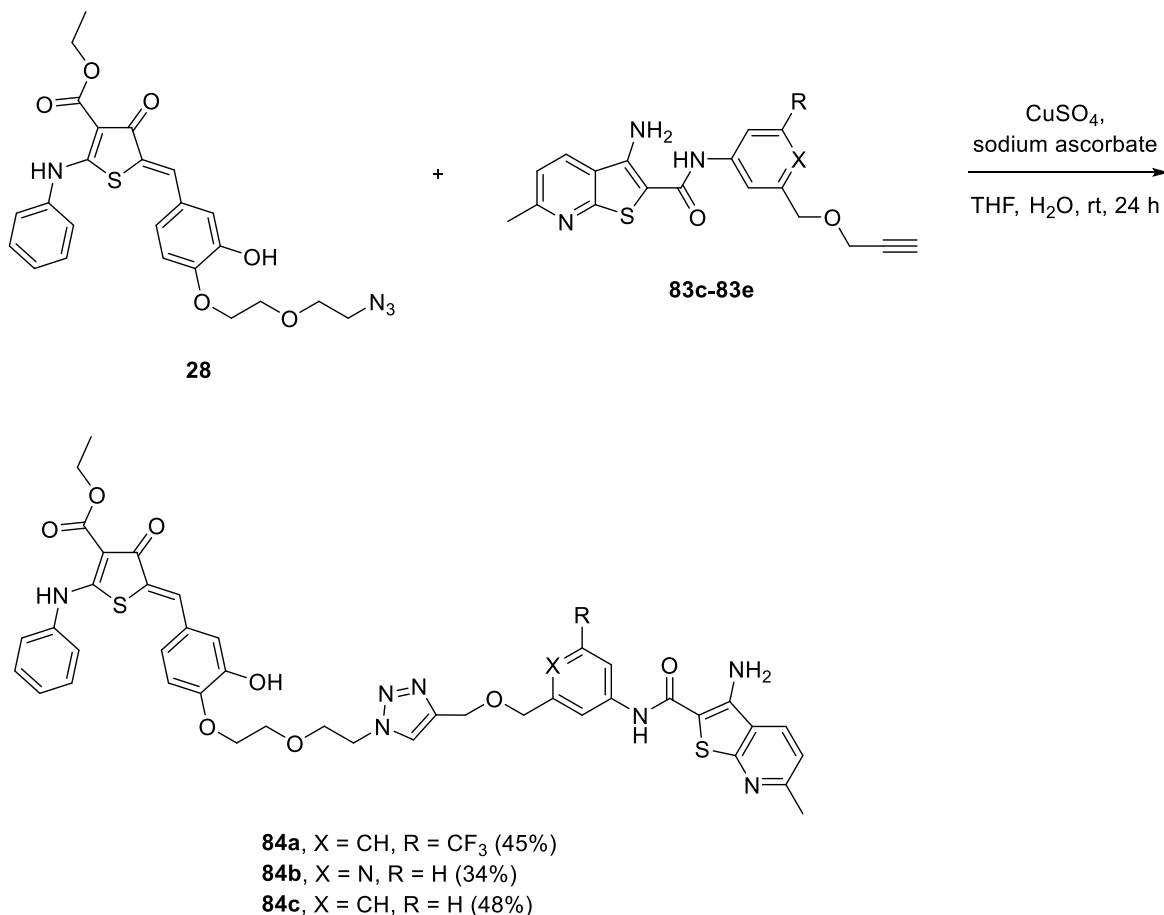


Scheme 16. Synthesis of alkyne tagged anilines. **A:** 3-trifluoromethylaniline. **B:** 4-aminopyridine. **C:** Aniline.

**Scheme 17.** Synthesis of bromoacetamides.**Scheme 18.** Synthesis of thienopyridine TAR ligands and analogues.

3.3.3. Bifunctional Molecules

Click chemistry was applied for conjugation of the alkyne tagged TAR RNA ligands **83c-83e** to azide tagged RNase L recruiter **28** to obtain three RIBOTAC compounds with variations in the RNA ligand (Scheme 19). Heterobifunctional molecules **84a** and **84b** are based on reported compounds “1” and “2” respectively, while **84c** contain an unsubstituted benzene ring with potential activity or otherwise useful as negative control in biological experiments.



Scheme 19. Synthesis of RIBOTACs.

Attachment of the linker through C-C bonds should have minimal impact on the original TAR ligands and if the positioning is located on solvent exposed positions it should be fully suitable for the development of RIBOTACs. The linker length of 11 atoms is consistent with reported RIBOTACs (Table 2). The high structural similarity of RIBOTACs **84a**, **84b** and **84c** with reported RIBOTAC targeting SARS-CoV-2 RNA genome^[56] indicate that efficient recruitment of RNase L is possible and that physiochemical properties will result in sufficient solubility and cell

permeability of obtained heterobifunctional molecules. Considering that pyridine containing parent compound “2” shows higher activity in combination with improved solubility, it makes this heterobifunctional compound a promising RIBOTAC for targeted degradation of the HIV RNA genome.

In summary, thienopyridines were functionalized with alkyne handles for conjugation with thiophenone RNase L recruiter using click chemistry. Obtained heterobifunctional molecules aiming to target HIV-1 TAR RNA will be used to extend the scope of RIBOTACs and evaluated for potential degradation of the HIV-1 RNA genome and ultimately treatment of HIV-1 infection.

4. Conclusion

In this study, synthetic organic chemistry methods were applied to obtain diverse bioactive compounds in three parts. Medicinal chemistry approaches were used to identify suitable linker attachment sites on small molecules with reported biological activity based on SAR and co-crystal structures. The aim was to obtain biologically active compounds to recruit RNase L for targeted degradation of RNAs via either small molecule binders to RBPs or RNAs.

The Gewald reaction was carried out for the synthesis of 2-aminothiophenes, which were subsequently used for the divergent synthesis of reported and novel thienopyrimidinones as well as thienodiazepines. Introduction of functional groups allowing linker attachment through amide coupling to thienopyrimidinones at different positions was achieved, as exemplified by the attachment of a PEG₂ linker. A route for the synthesis of thienodiazepines in three steps was established, albeit with limited scope of amino acid side chains amenable in the final intramolecular cyclization step. Aqueous solubility of thienodiazepines was improved compared to analogous thienopyrimidinones. No activity of the obtained compound classes could be detected in the RNase L FRET activation assay and consequently no further progression on the synthesized scaffolds was pursued. Lack of activity in thienopyrimidinones was in line with a recent report,^[49] but contradictory to the original report.^[223] Thiophenone **C-5966451** reported to activate RNase L *in vitro* and *in cellulo*^[49, 223] was instead used for regioselective introduction of an azide allowing another conjugation strategy using copper(I)-catalyzed click chemistry to obtain novel heterobifunctional molecules.

Development of RITAC as a novel strategy to discover protein-RNA interactions and degrade oncogenic lncRNAs was conceived and the synthesis of heterobifunctional compounds was carried out for a proof-of-concept study. Synthesis of WDR5 WIN site inhibitors allowed reproduction of reported biological activity in-house using a competitive FP assay. Linker attachment at solvent exposed positions by the introduction of an alkyne resulted in compounds with retained activity. Conjugation with thiophenone as reported RNase L recruiter was carried out using click chemistry to obtain the first reported heterobifunctional molecules aimed to induce complex formation between RNase L-RITAC-WDR5-HOTTIP as a potential anti-AML approach. Up to 17 individual synthetic steps were performed to afford each heterobifunctional molecule. Issues with poor

aqueous solubility was solved by the use of smaller WDR5 inhibitors without a biaryl fragment yielding a promising lead compound with retained activity.

Thienopyridines with various aromatic substitutions were synthesized to target HIV-1 TAR RNA. Introduction of a C-C bond to minimize loss of target binding of the original molecule allowed the attachment of an alkyne handle. Conjugation with the reported thiophenone RNase L recruiter was performed via CuAAC to obtain heterobifunctional molecules for targeted degradation of the HIV-1 RNA genome and thereby expanding the scope of RIBOTACs.

5. Perspective

For small molecule RNase L activators, synthesized 2-aminothiophenes are to be further evaluated in orthogonal assays to determine their RNase L activating potency. Reported FRET assay based on cleavage of 6-FAM labelled RNA suffer from the autofluorescence of compounds and may generate false positive results. Additionally, background levels of dimerized enzyme results in poor signal-to-noise ratio. An alternative assay to evaluate activation of RNase L with small molecules may be the use of a bioanalyzer instrument for detection of a cleavage pattern of rRNA specific to RNase L in the cellular context.^[379]

For the proof-of-concept of the RITAC strategy, validation of the bifunctional molecules synthesized from the alkyne functionalized WDR5 inhibitors needs to be performed *in cellulo* to detect the degradation of HOTTIP or other lncRNAs. Since the protein-interacting RNA sequence is unknown, a set of overlapping primers will allow identification of cleavage site(s) by RT-qPCR analysis, which will indicate approximate binding site to WDR5 and the secondary structure of the lncRNA. Knockdown of RNase L and WDR5 respectively using siRNA will serve as negative controls in cellular experiments to confirm that the observed effects are dependent on the presence of both proteins. To further determine the complete RNA interactome of WDR5, next-generation sequencing methods will be applied to detect downregulated transcripts compared to untreated cells. The effect of RITACs in cancer cells are to be studied to determine possible therapeutic applications, especially by the degradation of oncogenic lncRNAs.

For the HIV-1 TAR targeting RIBOTACs, thienopyridines designed to target the HIV-1 TAR RNA are to be evaluated, for example via differential scanning fluorimetry or microscale thermophoresis, to confirm that selected linker attachment sites are suitable for conjugation with an RNase L recruiter. Synthesized RIBOTACs are to be evaluated in cell-based assays using RT-qPCR with a set of primers for the detection of the HIV-1 genomic RNA degradation. This would similarly to the RITAC strategy yield information about cleavage site(s) and folding of the RNA. Structurally related RNAs containing hairpins with small apical loops containing 4-6 nucleotide sequences and di- or trinucleotide bulge regions can be used as controls to confirm selective binding and degradation of HIV-1 TAR. Excessive yeast tRNA in the sample may alternatively be added to confirm selective binding and degradation of HIV-1 TAR, similarly to the evaluation of

reported RIBOTACs. Promising RIBOTACs will subsequently be evaluated in viability assays to determine whether HIV-infected cells may be rescued from apoptosis induced by the degradation of viral RNA, which can be indicative of the potential to develop therapeutics based on the obtained HIV-1 TAR RIBOTACs.

6. Experimental

6.1. General Information

Commercially available starting materials, reagents and solvents purchased from ABCR, Acros, Alfa Aesar, Carl Roth, Fluorochem, Sigma Aldrich, TCI and VWR were used without further purification. Moisture sensitive solutions were prepared from solvents dried over activated molecular sieves (3 Å) under argon atmosphere in oven-dried glassware and transferred using syringes and cannulas.

Thin-layer chromatography (TLC) was performed on silica coated aluminum plates (Merck 60 F₂₅₄) and visualized under UV irradiation (254 nm), bromocresol green stain (0.04 g bromocresol green, 100 mL EtOH, aqueous 0.1 M NaOH added dropwise until solution turn blue), dinitrophenylhydrazine stain (12 g 2,4-dinitrophenylhydrazine, 60 mL concentrated sulfuric acid, 80 mL H₂O, 200 mL EtOH), iodine stain (0.5 g iodine in 25 mL silica gel) or potassium permanganate stain (1.5 g potassium permanganate, 10 g potassium carbonate, 1.25 mL 10% aqueous NaOH solution, 200 mL H₂O).

LC-MS was performed on an Agilent 1200 system equipped with a mass detector (column: Zorbax Eclipse XDB-C18 4.6 x 150 mm, particle size 5 µm). Appropriate gradients were applied by mixing H₂O (+ 0.1% TFA) and MeCN (+ 0.1% TFA).

Analytical UHPLC-MS was performed on an Agilent 1260 II Infinity system equipped with a mass detector (column: Zorbax Eclipse C18 Rapid Resolution 2.1 x 50 mm, particle size 1.8 µm). Appropriate gradients were applied by mixing H₂O (+ 0.1% TFA) and MeCN (+ 0.1% TFA).

Purification of crude products was achieved through flash column chromatography (FC, silica gel 60, 0.035-0.070 mm), automated medium pressure liquid chromatography (MPLC, Büchi Pure C-810 Flash, prepacked silica gel cartridges) with UV detection (254 nm) or preparative high-performance liquid chromatography (prep. HPLC, Büchi Pure C-850 FlashPrep, Macherey-Nagel Nucleodur C18 gravity column) with UV detection (254 nm) using indicated solvents.

NMR spectra were recorded on Bruker AV 400 Avance III HD (NanoBay), Agilent Technologies DD2, Bruker AV 500 Avance III HD (Prodigy), Bruker AV 600 Avance III HD (CryoProbe) or Bruker AV 700 Avance III HD (CryoProbe) spectrometers. Data is reported in ppm with reference to the used deuterated solvent (CDCl₃: 7.26 ppm, 77.16 ppm; DMSO-d₆: 2.50

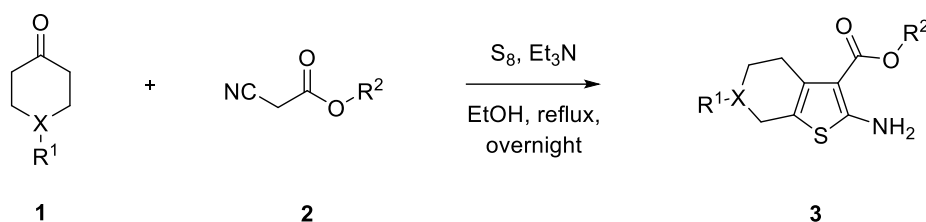
ppm, 39.52 ppm; CD₂Cl₂: 5.32 ppm, 53.84 ppm; MeOH-d₄: 3.31 ppm, 49.00 ppm; Acetone-d₆: 2.05 ppm, 29.84 ppm, 206.26 ppm).^[380] Signals were assigned based on 2D NMR correlations (¹H/¹H COSY, ¹H/¹H NOESY, ¹H/¹³C HSQC, ¹H/¹³C HMBC).

High-resolution mass spectrometry (HRMS) was performed on an LTQ Orbitrap mass spectrometer coupled to an Accela HPLC-System (HPLC column: Hypersyl GOLD, 50 mm x 1 mm, particle size 1.9 μm, ionization method: electron spray ionization (ESI)).

Microwave reactions were performed on a CEM Discover SP Activent device.

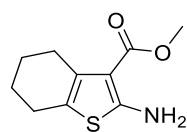
6.2. Synthesis of Thiophenes

General procedure 1 (GP1): Multicomponent Gewald reaction.



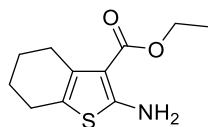
To a solution of cyclohexanone derivative **1** (3.00 mmol), cyanoacetate ester **2** (1.0 equivalent) and elemental sulfur (1.0 equivalent) in anhydrous EtOH (0.15 M) was added triethylamine (1.2 equivalents). The mixture was heated at 78 °C overnight under argon atmosphere. Solvent was evaporated under vacuum for purification by flash column chromatography to afford corresponding thiophenes.

Methyl 2-amino-4,5,6,7-tetrahydrobenzo[*b*]thiophene-3-carboxylate (**3a**)



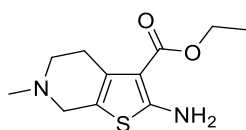
To a solution of cyclohexanone **1a** (0.99 mL, 9.58 mmol), methyl cyanoacetate **2a** (0.93 mL, 10.5 mmol) and elemental sulfur (0.37 g, 11.5 mmol) in anhydrous MeOH (10 mL) was added diethylamine (0.50 mL, 4.79 mmol). The mixture was stirred at room temperature for 24 hours under argon atmosphere. Solvent was evaporated under vacuum for purification by MPLC (PE/EtOAc 1:0 to 0:1) to afford title compound as a light-yellow solid (1.91 g, 94%). ¹H NMR (400 MHz, CDCl₃): δ 3.79 (s, 3H), 2.71 – 2.66 (m, 2H), 2.53 – 2.47 (m, 2H), 1.81 – 1.72 (m, 4H). LCMS-ESI (m/z): 212.1 [M + H]⁺. Analytical data matches with literature values.^[381]

Ethyl 2-amino-4,5,6,7-tetrahydrobenzo[*b*]thiophene-3-carboxylate (**3b**)



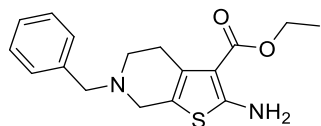
According to GP1. Cyclohexanone **1a** (0.31 mL, 3.00 mmol) and ethyl cyanoacetate **2b** (0.32 mL, 3.00 mmol) was reacted for 21 hours. Purification by flash column chromatography (PE/EtOAc 20:1) to afford title compound as a light-yellow solid (0.62 g, 91%). **¹H NMR** (700 MHz, CDCl₃): δ 5.92 (br s, 2H), 4.26 (q, *J* = 7.1 Hz, 2H), 2.70 (t, *J* = 7.3 Hz, 2H), 2.50 (t, *J* = 6.2 Hz, 2H), 1.80 – 1.76 (m, 2H), 1.76 – 1.72 (m, 2H), 1.33 (t, *J* = 7.1 Hz, 3H). **LCMS-ESI** (*m/z*): 226.1 [M + H]⁺. Analytical data matches with literature values.^[382]

Ethyl 2-amino-6-methyl-4,5,6,7-tetrahydrothieno[2,3-*c*]pyridine-3-carboxylate (**3c**)



According to GP1. *N*-methyl-4-piperidone **1b** (0.74 mL, 6.00 mmol) and ethyl cyanoacetate **2b** (0.64 mL, 6.00 mmol) was reacted for 15 hours. Purification by flash column chromatography (DCM, 5% MeOH) to afford title compound as a brown solid (0.93 g, 64%). **¹H NMR** (400 MHz, CDCl₃): δ 5.94 (s, 2H), 4.26 (q, *J* = 7.1 Hz, 2H), 3.42 (s, 2H), 2.88 – 2.85 (m, 2H), 2.71 (t, *J* = 5.8 Hz, 2H), 2.47 (s, 3 H), 1.33 (t, *J* = 7.1 Hz, 3H). **LCMS-ESI** (*m/z*): 241.1 [M + H]⁺. Analytical data matches with literature values.^[382]

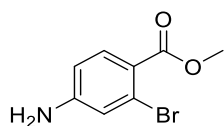
Ethyl 2-amino-6-benzyl-4,5,6,7-tetrahydrothieno[2,3-*c*]pyridine-3-carboxylate (**3d**)



According to GP1. *N*-benzyl-4-piperidone **1c** (1.11 mL, 6.00 mmol) and ethyl cyanoacetate **2b** (0.64 mL, 6.00 mmol) was reacted for 15 hours. Purification by flash column chromatography (PE/EtOAc 4:1) to afford title compound as a yellow solid (1.78 g, 94%). **¹H NMR** (400 MHz, CDCl₃): δ 7.39 – 7.24 (m, 5H), 5.93 (s, 2H), 4.24 (q, *J* = 7.1 Hz, 2H), 3.68 (s, 2H), 3.41 (s, 2H), 2.84 – 2.80 (m, 2H), 2.75 (t, *J* = 5.7 Hz, 2H), 1.32 (t, *J* = 7.1 Hz, 3H). **LCMS-ESI** (*m/z*): 317.1 [M + H]⁺. Analytical data matches with literature values.^[383]

6.3. Synthesis of Benzonitriles

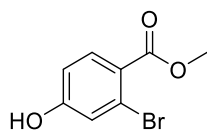
Methyl 4-amino-2-bromobenzoate (**9**)



Methyl 2-bromo-4-nitrobenzoate **8** (1.50 g, 5.77 mmol) and iron powder (1.21 g, 51.8 mmol) was added to EtOH (20.3 mL) and heated at 60 °C. Concentrated HCl (4.32 mL) was added dropwise. The mixture was heated at 78 °C for 2

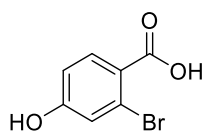
hours. H₂O (60 mL) was added to the cooled down mixture, which was neutralized to pH 7 by addition of aqueous 1 M NaOH and extracted with EtOAc (2 x 60 mL). Combined organic phases were filtered through celite and solvent evaporated under vacuum to afford title compound as a yellow solid (1.33 g, quant). ¹H NMR (400 MHz, CDCl₃): δ 7.76 (d, *J* = 8.5 Hz, 1H), 6.93 (s, 1H), 6.57 (d, *J* = 8.5 Hz, 1H), 4.07 (br s, 2H), 3.86 (s, 3H). LCMS-ESI (m/z): 230.0 [M + H]⁺. Analytical data matches with literature values.^[384]

Methyl 2-bromo-4-hydroxybenzoate (10)

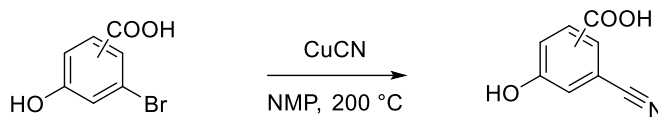


9 (1.22 g, 5.30 mmol) was mixed with H₂O (15 mL) and concentrated sulfuric acid (1.5 mL). At 0 °C was added a solution of sodium nitrite (0.40 g, 5.82 mmol) dissolved in H₂O (1.5 mL), via pipette below the surface of the reaction. The mixture was diluted with H₂O (15 mL) after 15 minutes and stirred for at room temperature 15 minutes. The mixture was heated at 100 °C for 30 minutes and then stirred at room temperature for 22 hours. The mixture was extracted with Et₂O (3 x 45 mL). Combined organic phases were concentrated under vacuum for purification by flash column chromatography (PE/EtOAc 20:1 to 9:1) to afford title compound as an orange solid (0.91 g, 75%). ¹H NMR (400 MHz, CDCl₃): δ 7.83 (d, *J* = 8.6 Hz, 1H), 7.17 (s, 1H), 6.82 (d, *J* = 8.6 Hz, 1H), 5.44 (br s, 1H), 3.90 (s, 3H). LCMS-ESI (m/z): 231.0 [M + H]⁺. Analytical data matches with literature values.^[385]

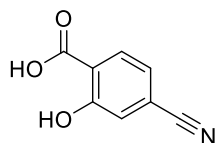
2-Bromo-4-hydroxybenzoic acid (11)



To **10** (0.50 g, 2.16 mmol) was added 30% hydrogen bromide (w/w) in acetic acid (7.00 mL) and solution was heated at 118 °C for 14 hours. The cooled down solution was poured into H₂O (35 mL) and extracted with Et₂O (2 x 35 mL). Combined organic phases were dried over MgSO₄, filtered and concentrated under vacuum for purification by MPLC (PE/EtOAc 1:0 to 0:1) to afford title compound as an off-white solid (0.31 g, 67%). ¹H NMR (400 MHz, DMSO-d₆): δ 12.75 (br s, 1H), 10.50 (br s, 1H), 7.72 (d, *J* = 8.6 Hz, 1H), 7.02 (s, 1H), 6.80 (d, *J* = 8.6 Hz, 1H). LCMS-ESI (m/z): 217.0 [M + H]⁺. Analytical data matches with literature values.^[385]

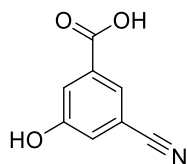
General procedure 2 (GP2): Nucleophilic aromatic substitution.

Copper(I) cyanide (1.0 equivalent) was added to a solution of bromobenzene derivative (2.50 mmol) in NMP (0.83 M). The mixture was heated at 200 °C in a microwave reactor for 2 hours. The solution was poured into 1 M aqueous HCl (25 mL) and extracted with EtOAc (3 x 20 mL). Combined organic phases were washed with brine (60 mL), dried over Na₂SO₄, filtered and solvent evaporated under vacuum to afford corresponding benzonitriles.

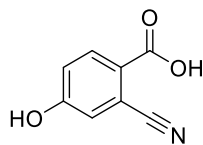
4-Cyano-2-hydroxybenzoic acid (5)

According to GP2. Purification by MPLC (PE/EtOAc 1:0 to 0:1) to afford title compound as a brown solid (0.35 g, 85%). ¹H NMR (400 MHz, DMSO-d₆): δ 10.16 (s, 1H), 7.89 (d, *J* = 8.0 Hz, 1H), 7.43 (s, 1H), 7.31 (d, *J* = 8.0 Hz, 1H).

LCMS-ESI (m/z): 164.0 [M + H]⁺. Analytical data matches with literature values.^[386]

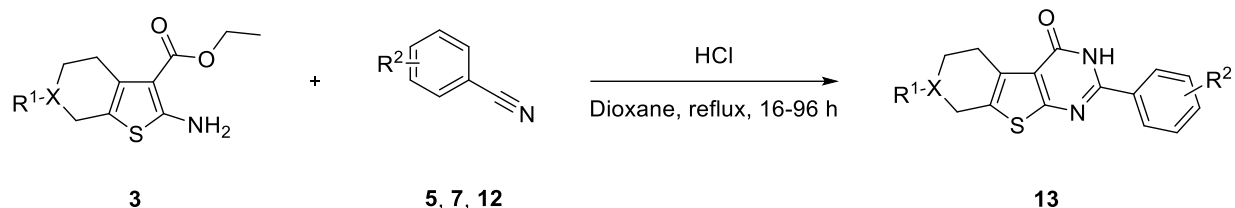
3-Cyano-5-hydroxybenzoic acid (7)

According to GP2. Title compound afforded as a brown solid (0.32 g, 79%). ¹H NMR (400 MHz, DMSO-d₆): δ 13.34 (br s, 1H), 10.57 (br s, 1H), 7.67 (s, 1H), 7.59 (s, 1H), 7.36 (s, 1H). LCMS-ESI (m/z): 164.0 [M + H]⁺. Analytical data matches with literature values.^[387]

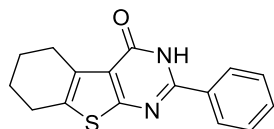
2-Cyano-4-hydroxybenzoic acid (12)

According to GP2. **11** (0.30 g, 1.38 mmol) was reacted with copper(I) cyanide (1.1 equivalents) for 4 hours. Purification by MPLC (DCM, 0-10% MeOH) afforded title compound as a brown solid (0.12 g, 65%). ¹H NMR (500 MHz, DMSO-d₆): δ 11.07 (s, 1H), 10.88 (s, 1H), 7.65 (d, *J* = 8.1 Hz, 1H), 7.12 – 7.09 (m, 2H). ¹³C NMR (126 MHz, DMSO-d₆): δ 174.2, 169.5, 163.6, 135.9, 125.5, 123.3, 120.8, 109.9. LCMS-ESI (m/z): 164.0 [M + H]⁺.

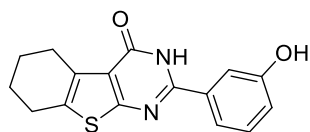
6.4. Synthesis of Thienopyrimidinones

General procedure 3 (GP3): Pyrimidinone formation.

Thiophene derivative **3** (0.44 mmol) was dissolved in anhydrous 1,4-dioxane (0.5 M) saturated with 4 M hydrochloric acid gas. Benzonitrile derivative **5**, **7** or **12** (1.1 equivalents) was added and mixture heated at 100 °C in a closed vial. The mixture was cooled to room temperature and mixed with aqueous saturated NaHCO₃ (10 mL). Aqueous phase was extracted with EtOAc (3 x 10 mL). Combined organic phases were concentrated under vacuum for purification by flash column chromatography to afford corresponding pyrimidinones.

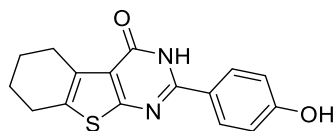
2-Phenyl-5,6,7,8-tetrahydrobenzo[4,5]thieno[2,3-*d*]pyrimidin-4(3*H*)-one (13a)

According to GP3. Reaction time 20 hours and purification by flash column chromatography (PE/EtOAc 4:1 to 0:1) to afford title compound as an off-white solid (0.12 g, 94%). ¹H NMR (400 MHz, CDCl₃): δ 11.05 (br s, 1H), 8.16 (d, *J* = 8.2 Hz, 2H), 7.56 – 7.50 (m, 3H), 3.13 – 3.08 (m, 2H), 2.84 – 2.80 (m, 2H), 1.94 – 1.87 (m, 4H). LCMS-ESI (m/z): 283.1 [M + H]⁺. Analytical data matches with literature values.^[382]

2-(3-hydroxyphenyl)-5,6,7,8-tetrahydrobenzo[4,5]thieno[2,3-*d*]pyrimidin-4(3*H*)-one (13b)

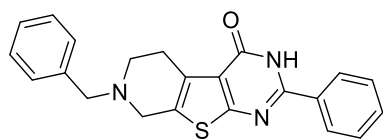
According to GP3. Reaction time 18 hours and purification by flash column chromatography (DCM, 3% MeOH) to afford title compound as a white solid (38.6 mg, 58%). ¹H NMR (400 MHz, DMSO-*d*₆): δ 12.37 (s, 1H), 9.69 (s, 1H), 7.52 (d, *J* = 7.9 Hz, 1H), 7.50 (s, 1H), 7.28 (t, *J* = 7.9 Hz, 1H), 6.93 (d, *J* = 7.9 Hz, 1H), 2.89 (t, *J* = 5.9 Hz, 2H), 2.74 (t, *J* = 5.8 Hz, 2H), 1.84 – 1.73 (m, 4H). LCMS-ESI (m/z): 299.1 [M + H]⁺.

2-(4-Hydroxyphenyl)-5,6,7,8-tetrahydrobenzo[4,5]thieno[2,3-*d*]pyrimidin-4(3*H*)-one (13c)



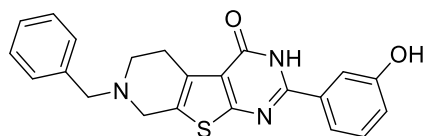
According to GP3. Reaction time 16 hours and purification by flash column chromatography (DCM, 3-10% MeOH) to afford title compound as a white solid (0.13 g, 99%). $^1\text{H NMR}$ (400 MHz, DMSO- d_6): δ 12.21 (s, 1H), 10.12 (s, 1H), 7.99 (d, $J = 8.8$ Hz, 2H), 6.84 (d, $J = 8.8$ Hz, 2H), 2.88 (t, $J = 5.9$ Hz, 2H), 2.72 (t, $J = 5.8$ Hz, 2H), 1.83 – 1.72 (m, 4H). LCMS-ESI (m/z): 299.1 [M + H] $^+$. Analytical data matches with literature values.^[382]

7-Benzyl-2-phenyl-5,6,7,8-tetrahydropyrido[4',3':4,5]thieno[2,3-*d*]pyrimidin-4(3*H*)-one (13d)



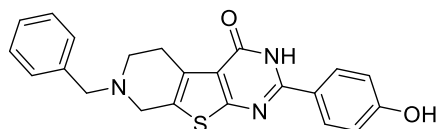
According to GP3. Reaction time 64 hours and purification by MPLC (DCM, 0-20% MeOH) to afford title compound as a pale-yellow solid (33.9 mg, 21%). $^1\text{H NMR}$ (400 MHz, DMSO- d_6): δ 12.55 (s, 1H), 8.11 (d, $J = 8.4$ Hz, 2H), 7.58 – 7.48 (m, 3H), 7.37 – 7.31 (m, 4H), 7.28 – 7.24 (m, 1H), 3.70 (s, 2H), 3.62 (s, 2H), 2.96 (t, $J = 5.8$ Hz, 2H), 2.77 (t, $J = 5.8$ Hz, 2H). LCMS-ESI (m/z): 374.2 [M + H] $^+$. Analytical data matches with literature values.^[382]

7-Benzyl-2-(3-hydroxyphenyl)-5,6,7,8-tetrahydropyrido[4',3':4,5]thieno[2,3-*d*]pyrimidin-4(3*H*)-one (13e)



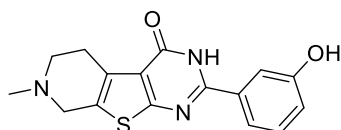
According to GP3. Reaction time 96 hours and purification by MPLC (DCM, 0-20% MeOH) to afford title compound as an off-white solid (33.7 mg, 20%). $^1\text{H NMR}$ (700 MHz, DMSO- d_6): δ 12.48 (s, 1H), 9.74 (s, 1H), 7.56 (d, $J = 7.8$ Hz, 1H), 7.53 (s, 1H), 7.39 – 7.35 (m, 4H), 7.32 (t, $J = 7.9$ Hz, 1H), 7.29 (t, $J = 6.9$ Hz, 1H), 6.96 (d, $J = 8.1$ Hz, 1H), 3.72 (s, 2H), 3.64 (s, 2H), 2.98 (t, $J = 5.8$ Hz, 2H), 2.79 (t, $J = 5.8$ Hz, 2H). $^{13}\text{C NMR}$ (176 MHz, DMSO- d_6): δ 163.9, 159.2, 158.0, 152.9, 138.6, 133.7, 130.5, 130.2, 129.8, 129.3, 128.8, 127.6, 121.0, 119.0, 118.8, 115.0, 61.3, 51.5, 49.5, 26.1. HRMS-ESI (m/z): [M + H] $^+$ calculated for C₂₂H₂₀O₂N₃S: 390.1271, found: 390.1271.

7-Benzyl-2-(4-hydroxyphenyl)-5,6,7,8-tetrahydropyrido[4',3':4,5]thieno[2,3-*d*]pyrimidin-4(3*H*)-one (13f)



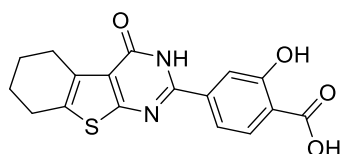
According to GP3. Reaction time 20 hours and purification by MPLC (DCM, 0-20% MeOH) to afford title compound as a pale-yellow solid (38.8 mg, 23%). **¹H NMR** (400 MHz, DMSO-*d*₆): δ 12.28 (s, 1H), 10.13 (s, 1H), 7.99 (d, *J* = 8.9 Hz, 2H), 7.37 – 7.31 (m, 4H), 7.28 – 7.24 (m, 1H), 6.84 (d, *J* = 8.9 Hz, 2H), 3.70 (s, 2H), 3.60 (s, 2H), 2.93 (t, *J* = 5.7 Hz, 2H), 2.76 (t, *J* = 5.7 Hz, 2H). **LCMS-ESI** (m/z): 390.1 [M + H]⁺. Analytical data matches with literature values.^[382]

2-(3-Hydroxyphenyl)-7-methyl-5,6,7,8-tetrahydropyrido[4',3':4,5]thieno[2,3-*d*]pyrimidin-4(3*H*)-one (13g)



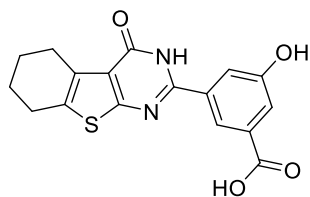
According to GP3. Reaction time 24 hours and purification by MPLC (DCM, 0-20% MeOH) to afford title compound as a beige solid (69.6 mg, 53%). **¹H NMR** (500 MHz, DMSO-*d*₆): δ 8.99 (br s, 1H), 7.75 (s, 1H), 7.70 (d, *J* = 7.7 Hz, 1H), 7.13 (t, *J* = 7.8 Hz, 1H), 6.69 (d, *J* = 7.9 Hz, 1H), 3.46 (s, 2H), 2.94 (t, *J* = 5.6 Hz, 2H), 2.60 (t, *J* = 5.8 Hz, 2H), 2.35 (s, 3H). **LCMS-ESI** (m/z): 314.1 [M + H]⁺. Analytical data matches with literature values.^[382]

2-Hydroxy-4-(4-oxo-3,4,5,6,7,8-hexahydrobenzo[4,5]thieno[2,3-*d*]pyrimidin-2-yl)benzoic acid (13h)



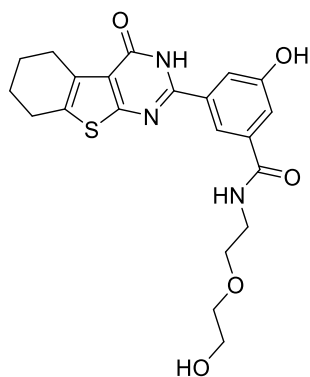
According to GP3. Reaction time 20 hours with **5** (1.0 equivalent) and crude product isolated by filtration to afford title compound as a curry-yellow solid (93.5 mg, 62%). **¹H NMR** (500 MHz, DMSO-*d*₆): δ 12.62 (s, 1H), 11.39 (br s, 1H), 7.89 (d, *J* = 8.3 Hz, 1H), 7.71 (s, 1H), 7.68 (d, *J* = 8.2 Hz, 1H), 2.92 (t, *J* = 6.1 Hz, 2H), 2.79 (t, *J* = 7.9 Hz, 2H), 1.86 – 1.76 (m, 4 H). **¹³C NMR** (126 MHz, DMSO-*d*₆): δ 171.7, 161.3, 159.5, 133.9, 131.5, 131.0, 130.2, 123.6, 122.0, 118.7, 116.6, 115.6, 66.8, 25.8, 25.1, 22.9, 22.2. **HRMS-ESI** (m/z): [M + H]⁺ calculated for C₁₇H₁₅O₄N₂S: 343.0747, found: 343.0751.

3-Hydroxy-5-(4-oxo-3,4,5,6,7,8-hexahydrobenzo[4,5]thieno[2,3-*d*]pyrimidin-2-yl)benzoic acid (13i)



According to GP3. Reaction time 18 hours with **7** (1.0 equivalent) and crude product isolated by filtration to afford title compound as a light-purple solid (79.7 mg, 52%). **¹H NMR** (700 MHz, DMSO-*d*₆): δ 13.11 (s, 1H), 12.60 (s, 1H), 10.14 (s, 1H), 8.14 (s, 1H), 7.73 (s, 1H), 7.51 (s, 1H), 2.91 (t, *J* = 5.8 Hz, 2H), 2.77 (t, *J* = 5.7 Hz, 2H), 1.85 – 1.82 (m, 2H), 1.80 – 1.77 (m, 2H). **¹³C NMR** (176 MHz, DMSO-*d*₆): δ 167.2, 163.2, 159.2, 158.2, 152.0, 134.1, 133.2, 133.0, 131.4, 121.6, 120.1, 119.2, 119.0, 25.8, 25.0, 23.0, 22.2. **HRMS-ESI** (*m/z*): [*M* + *H*]⁺ calculated for C₁₇H₁₅O₄N₂S: 343.0747, found: 343.0748.

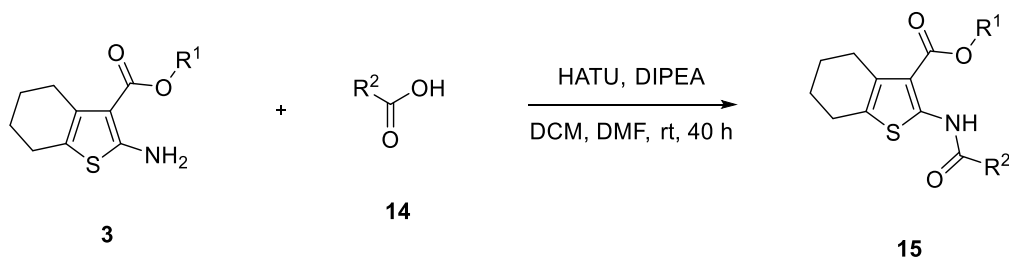
3-Hydroxy-*N*-(2-(2-hydroxyethoxy)ethyl)-5-(4-oxo-3,4,5,6,7,8-hexahydrobenzo[4,5]thieno[2,3-*d*]pyrimidin-2-yl)benzamide (**13k**)



To a solution of **13i** (10.0 mg, 29.2 μmol), *N,N*-diisopropylethylamine (15.3 μL, 87.6 μmol) and 2-(2-aminoethoxy)ethanol (5.86 μL, 58.4 μmol) in anhydrous DMF (0.29 mL) was added HATU (22.2 mg, 58.4 μmol). The mixture was stirred at room temperature for 6 hours, crude product precipitated in H₂O (2 mL) and collected by filtration to afford title compound as an off-white solid (10.7 mg, 85%). **¹H NMR** (700 MHz, DMSO-*d*₆): δ 12.37 (s, 1H), 10.04 (s, 1H), 8.46 (s, 1H), 7.99 (s, 1H), 7.62 (s, 1H), 7.41 (s, 1H), 4.59 (s, 1H), 3.56 (t, *J* = 6.0 Hz, 2H), 3.52 (t, *J* = 5.2 Hz, 2H), 3.48 – 3.44 (m, 4H), 2.92 (t, *J* = 6.4 Hz, 2H), 2.78 (t, *J* = 5.9 Hz, 2H), 1.85 – 1.82 (m, 2H), 1.80 – 1.77 (m, 2H). **¹³C NMR** (176 MHz, DMSO-*d*₆): δ 166.2, 163.3, 159.1, 158.1, 136.8, 133.7, 133.2, 131.4, 121.5, 117.7, 117.5, 117.4, 72.6, 69.4, 60.7, 40.5, 25.8, 25.0, 23.0, 22.2. **HRMS-ESI** (*m/z*): [*M* + *H*]⁺ calculated for C₂₁H₂₄O₅N₃S: 430.1431, found: 430.1431.

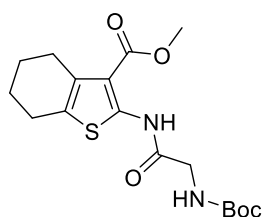
6.5. Synthesis of *N*-Boc Thiophene Dipeptides

General procedure 4 (GP4): Amino acid amide coupling.



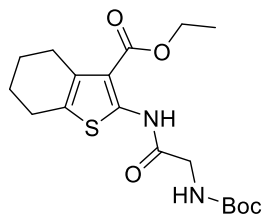
2-Aminothiophene **3** (1.00 mmol) was dissolved in a mixture of dry DCM/DMF 9:1 (0.23 M). Boc-Aa-OH derivative **14** (2.0 equivalents), *N,N*-diisopropylethylamine (3.0 equivalents) and HATU (2.0 equivalents) was added and the reaction stirred at room temperature for 40 hours. Solution was diluted with DCM (30 mL) and washed with H₂O (2 x 30 mL). Organic phase was concentrated under vacuum for purification by MPLC (PE/EtOAc 1:0 to 4:1) to afford corresponding Boc-protected dipeptides.

Methyl 2-(2-((*tert*-butoxycarbonyl)amino)acetamido)-4,5,6,7-tetrahydrobenzo[*b*]thiophene-3-carboxylate (15a)



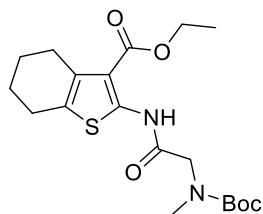
According to GP4. Title compound afforded as a yellow oil (0.35 g, quant). ¹H NMR (500 MHz, CDCl₃): δ 11.65 (s, 1H), 5.31 (s, 1H), 4.04 (s, 2H), 3.84 (s, 3H), 2.72 (t, *J* = 5.9 Hz, 2H), 2.62 (t, *J* = 5.8 Hz, 2H), 1.81 – 1.73 (m, 4 H), 1.48 (s, 9 H). ¹³C NMR (126 MHz, CDCl₃): δ 166.9, 166.6, 155.8, 146.7, 130.9, 127.0, 112.0, 51.4, 44.5, 38.7, 28.3, 26.2, 24.4, 23.9, 23.0. HRMS-ESI (*m/z*): [M + H]⁺ calculated for C₁₇H₂₅O₅N₂S: 369.1479, found: 369.1482.

Ethyl 2-(2-((*tert*-butoxycarbonyl)amino)acetamido)-4,5,6,7-tetrahydrobenzo[*b*]thiophene-3-carboxylate (15b)



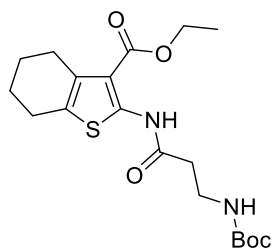
According to GP4. Title compound afforded as a white solid (0.37 g, 96%). ¹H NMR (600 MHz, CDCl₃): δ 11.70 (s, 1H), 5.19 (s, 1H), 4.31 (q, *J* = 7.1 Hz, 2H), 4.04 (s, 2H), 2.76 (t, *J* = 5.7 Hz, 2H), 2.64 (t, *J* = 5.8 Hz, 2H), 1.81 – 1.75 (m, 4 H), 1.48 (s, 9 H), 1.36 (t, *J* = 7.1 Hz, 3H). ¹³C NMR (151 MHz, DMSO-*d*₆): δ 166.7, 166.3, 155.8, 146.7, 131.0, 127.0, 112.2, 80.6, 60.4, 44.5, 28.3, 26.3, 24.4, 23.0, 22.8, 14.3. HRMS-ESI (*m/z*): [M + H]⁺ calculated for C₁₈H₂₆O₅N₂S: 383.1635, found: 383.1629.

Ethyl 2-(2-((*tert*-butoxycarbonyl)(methyl)amino)acetamido)-4,5,6,7-tetrahydrobenzo[*b*]thiophene-3-carboxylate (15c)



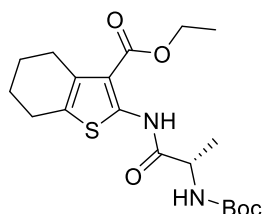
According to GP4. Title compound afforded as a light-yellow oil (0.35 g, 89%). $^1\text{H NMR}$ (700 MHz, CDCl_3): δ 11.66 (s, 1H), 4.31 (q, $J = 6.7$ Hz, 2H), 4.14 – 4.02 (m, 2H), 3.06 – 2.98 (m, 2H), 2.78 – 2.74 (m, 2H), 2.65 (t, $J = 5.8$ Hz, 2H), 1.82 – 1.75 (m, 4 H), 1.46 (s, 9 H), 1.35 (t, $J = 7.1$ Hz, 3H). $^{13}\text{C NMR}$ (176 MHz, CDCl_3): δ 166.7, 166.0, 155.2, 146.4, 127.0, 112.2, 81.0, 60.5, 60.3, 53.5, 52.8, 35.8, 27.4, 24.4, 23.8, 22.8, 14.3. **HRMS**-ESI (m/z): $[\text{M} + \text{H}]^+$ calculated for $\text{C}_{19}\text{H}_{29}\text{O}_5\text{N}_2\text{S}$: 397.1792, found: 397.1794.

Ethyl 2-(3-((tert-butoxycarbonyl)amino)propanamido)-4,5,6,7-tetrahydrobenzo[b]thiophene-3-carboxylate (15d)



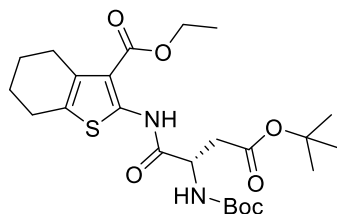
According to GP4. Title compound afforded as a yellow oil (0.34 g, 86%). $^1\text{H NMR}$ (700 MHz, CDCl_3): δ 11.29 (s, 1H), 5.18 (s, 1H), 4.32 (q, $J = 7.2$ Hz, 2H), 3.50 (q, $J = 5.9$ Hz, 2H), 2.76 (t, $J = 5.9$ Hz, 2H), 2.68 (t, $J = 5.8$ Hz, 2H), 2.64 (t, $J = 5.7$ Hz, 2H), 1.81 – 1.75 (m, 4 H), 1.42 (s, 9 H), 1.37 (t, $J = 7.1$ Hz, 3H). $^{13}\text{C NMR}$ (176 MHz, CDCl_3): δ 168.7, 166.6, 155.9, 147.0, 130.9, 126.8, 111.7, 79.4, 60.5, 36.5, 36.2, 28.4, 26.4, 24.4, 23.0, 22.8, 14.3. **HRMS**-ESI (m/z): $[\text{M} + \text{H}]^+$ calculated for $\text{C}_{19}\text{H}_{29}\text{O}_5\text{N}_2\text{S}$: 397.1792, found: 397.1793.

Ethyl (S)-2-(2-((tert-butoxycarbonyl)amino)propanamido)-4,5,6,7-tetrahydrobenzo[b]thiophene-3-carboxylate (15e)



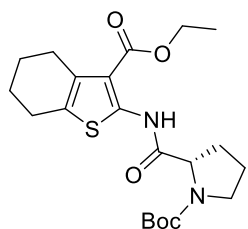
According to GP4. Title compound afforded as a white solid (0.33 g, 83%). $^1\text{H NMR}$ (700 MHz, CDCl_3): δ 11.72 (s, 1H), 5.06 (s, 1H), 4.43 – 4.41 (m, 1H), 4.32 (q, $J = 7.1$ Hz, 2H), 2.76 (t, $J = 5.9$ Hz, 2H), 2.64 (t, $J = 5.9$ Hz, 2H), 1.81 – 1.75 (m, 4H), 1.48 (s, 9H), 1.37 (t, $J = 7.1$ Hz, 3H). $^{13}\text{C NMR}$ (176 MHz, CDCl_3): δ 169.9, 166.3, 155.2, 147.0, 131.0, 127.0, 112.2, 80.4, 60.4, 50.5, 28.3, 26.4, 24.4, 23.0, 22.8, 18.5, 14.3. **HRMS**-ESI (m/z): $[\text{M} + \text{H}]^+$ calculated for $\text{C}_{19}\text{H}_{29}\text{O}_5\text{N}_2\text{S}$: 397.1792, found: 397.1794.

Ethyl (S)-2-(4-(tert-butoxy)-2-((tert-butoxycarbonyl)amino)-4-oxobutanamido)-4,5,6,7-tetrahydrobenzo[b]thiophene-3-carboxylate (15f)



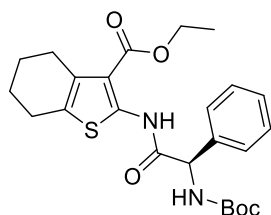
According to GP4. Title compound afforded as an orange oil (0.40 g, 80%). $^1\text{H NMR}$ (700 MHz, CDCl_3): δ 11.28 (s, 1H), 5.67 (s, 1H), 4.51 – 4.48 (m, 1H), 4.32 (q, $J = 7.1$ Hz, 2H), 3.13 – 3.09 (m, 1H), 2.94 – 2.90 (m, 1H), 2.76 (t, $J = 5.9$ Hz, 2H), 2.63 (t, $J = 5.9$ Hz, 2H), 1.81 – 1.75 (m, 4H), 1.43 (s, 9H), 1.37 (t, $J = 7.1$ Hz, 3H). $^{13}\text{C NMR}$ (176 MHz, CDCl_3): δ 169.9, 167.2, 166.5, 155.6, 146.9, 130.8, 126.9, 111.7, 82.3, 79.9, 60.5, 50.8, 38.7, 28.3, 27.9, 26.4, 24.3, 23.0, 22.8, 14.3. **HRMS-ESI** (m/z): $[\text{M} + \text{H}]^+$ calculated for $\text{C}_{24}\text{H}_{37}\text{O}_7\text{N}_2\text{S}$: 497.2316, found: 497.2315.

***tert*-Butyl (*S*)-2-((3-(ethoxycarbonyl)-4,5,6,7-tetrahydrobenzo[*b*]thiophen-2-yl)carbamoyl)pyrrolidine-1-carboxylate (15g)**



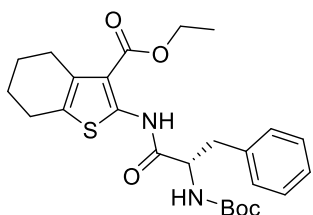
According to GP4. Title compound afforded as a colourless oil (0.25 g, 60%). $^1\text{H NMR}$ (700 MHz, CDCl_3): δ 11.60 (s, 1H), 4.53 – 4.50 (m, 1H), 4.31 (q, $J = 7.1$ Hz, 2H), 3.67 – 3.55 (m, 2H), 2.79 – 2.74 (m, 2H), 2.67 – 2.63 (m, 2H), 2.30 – 2.23 (m, 1H), 2.17 – 2.11 (m, 1H), 1.94 – 1.89 (m, 2H), 1.82 – 1.75 (m, 4H), 1.57 (s, 9H), 1.35 (t, $J = 7.1$ Hz, 3H). $^{13}\text{C NMR}$ (176 MHz, CDCl_3): δ 170.4, 166.0, 155.2, 154.3, 131.1, 127.0, 112.1, 80.6, 61.5, 60.5, 46.8, 31.4, 28.4, 26.4, 24.4, 23.9, 23.8, 23.0, 14.4. **HRMS-ESI** (m/z): $[\text{M} + \text{H}]^+$ calculated for $\text{C}_{21}\text{H}_{31}\text{O}_5\text{N}_2\text{S}$: 423.1948, found: 423.1951.

Ethyl (*R*)-2-(2-((*tert*-butoxycarbonyl)amino)-2-phenylacetamido)-4,5,6,7-tetrahydrobenzo[*b*]thiophene-3-carboxylate (15h)



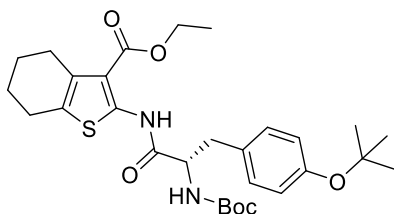
According to GP4. Title compound afforded as a yellow solid (0.34 g, 75%). $^1\text{H NMR}$ (700 MHz, CDCl_3): δ 11.61 (s, 1H), 7.42 (d, $J = 7.6$ Hz, 2H), 7.37 (t, $J = 7.6$ Hz, 2H), 7.32 (t, $J = 7.3$ Hz, 1H), 5.75 (s, 1H), 5.38 (s, 1H), 4.29 (q, $J = 6.6$ Hz, 2H), 2.75 – 2.71 (m, 2H), 2.62 (t, $J = 4.7$ Hz, 2H), 1.80 – 1.73 (m, 4H), 1.44 (s, 9H), 1.34 (t, $J = 7.1$ Hz, 3H). $^{13}\text{C NMR}$ (176 MHz, CDCl_3): δ 167.3, 166.2, 155.0, 146.6, 137.4, 131.1, 129.2, 128.7, 127.3, 127.1, 112.4, 80.3, 60.5, 59.3, 28.3, 26.3, 24.4, 23.0, 22.8, 14.3. **HRMS-ESI** (m/z): $[\text{M} + \text{H}]^+$ calculated for $\text{C}_{24}\text{H}_{31}\text{O}_5\text{N}_2\text{S}$: 459.1948, found: 459.1948.

Ethyl (S)-2-(2-((tert-butoxycarbonyl)amino)-3-phenylpropanamido)-4,5,6,7-tetrahydrobenzo[*b*]thiophene-3-carboxylate (15i)



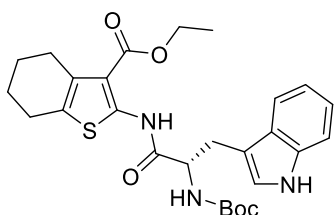
According to GP4. **3b** (0.66 g, 3.00 mmol) and Boc-L-Phe-OH **14** (1.59 g, 6.00 mmol) was reacted. Title compound afforded as a light-yellow solid (1.35 g, 95%). **¹H NMR** (700 MHz, CDCl₃): δ 11.59 (s, 1H), 7.28 (t, *J* = 7.5 Hz, 2H), 7.23 (t, *J* = 7.4 Hz, 1H), 7.18 (d, *J* = 7.5 Hz, 2H), 4.98 (s, 1H), 4.63 (s, 1H), 4.27 (q, *J* = 7.1 Hz, 2H), 3.20 (d, *J* = 6.2 Hz, 2H), 2.76 (t, *J* = 6.6 Hz, 2H), 2.65 (t, *J* = 5.9 Hz, 2H), 1.82 – 1.76 (m, 4H), 1.42 (s, 9H), 1.33 (t, *J* = 7.2 Hz, 3H). **¹³C NMR** (176 MHz, CDCl₃): δ 168.7, 166.0, 155.2, 146.5, 136.0, 131.1, 129.3, 128.9, 127.2, 127.1, 112.3, 80.5, 60.4, 55.8, 38.0, 28.2, 28.2, 26.3, 24.4, 23.0, 14.3. **HRMS-ESI** (*m/z*): [M + H]⁺ calculated for C₂₅H₃₃O₅N₂S: 473.2105, found: 473.2104.

Ethyl (S)-2-(3-(4-(tert-butoxy)phenyl)-2-((tert-butoxycarbonyl)amino)propanamido)-4,5,6,7-tetrahydrobenzo[*b*]thiophene-3-carboxylate (15j)



According to GP4. Title compound afforded as a white solid (0.51 g, 94%). **¹H NMR** (700 MHz, CDCl₃): δ 11.53 (s, 1H), 7.07 (d, *J* = 8.3 Hz, 2H), 6.89 (d, *J* = 8.3 Hz, 2H), 5.00 (s, 1H), 4.57 (s, 1H), 4.26 (q, *J* = 7.2 Hz, 2H), 3.13 (d, *J* = 6.5 Hz, 2H), 2.74 (t, *J* = 6.0 Hz, 2H), 2.64 (t, *J* = 5.8 Hz, 2H), 1.81 – 1.74 (m, 4H), 1.42 (s, 9H), 1.33 (t, *J* = 7.1 Hz, 3H), 1.29 (s, 9H). **¹³C NMR** (176 MHz, CDCl₃): δ 168.7, 166.0, 155.2, 154.4, 146.5, 131.0, 130.8, 129.7, 127.0, 124.5, 112.3, 80.4, 78.4, 60.4, 56.0, 37.6, 28.8, 28.3, 26.3, 24.4, 23.0, 22.8, 14.3. **HRMS-ESI** (*m/z*): [M + H]⁺ calculated for C₂₉H₄₁O₆N₂S: 545.2680, found: 545.2680.

Ethyl (S)-2-(2-((tert-butoxycarbonyl)amino)-3-(1*H*-indol-3-yl)propanamido)-4,5,6,7-tetrahydrobenzo[*b*]thiophene-3-carboxylate (15k)

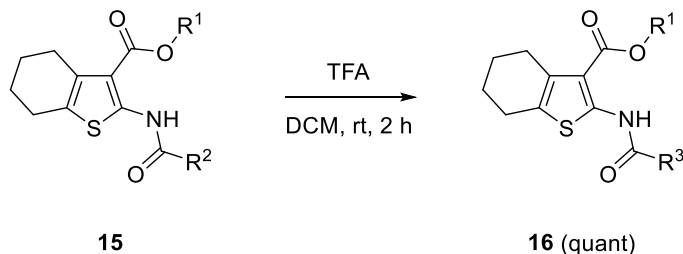


According to GP4. Title compound afforded as a yellow oil (0.50 g, 99%). **¹H NMR** (700 MHz, CDCl₃): δ 11.57 (s, 1H), 8.13 (s, 1H), 7.60 (d, *J* = 7.9 Hz, 1H), 7.33 (d, *J* = 8.1 Hz, 1H), 7.18 (t, *J* = 8.1 Hz, 1H), 7.10 (t, *J* = 8.0 Hz, 1H), 7.02 (s, 1H), 5.10 (s, 1H), 4.71 (s, 1H), 4.21 (q, *J* = 7.1 Hz, 2H), 3.46 – 3.42 (m, 1H), 3.37 – 3.32 (m, 1H), 2.72 (t, *J* = 5.7 Hz, 2H), 2.65 (t, *J* = 5.7 Hz, 2H), 1.81 – 1.74 (m, 4H), 1.43 (s, 9H), 1.28 (t, *J* = 7.1 Hz, 3H). **¹³C NMR** (176 MHz,

CDCl₃): δ 169.3, 165.8, 165.5, 146.5, 136.1, 131.1, 126.9, 123.5, 123.1, 122.3, 119.9, 118.8, 112.2, 111.1, 110.1, 60.3, 55.4, 47.3, 28.3, 27.6, 26.3, 24.4, 23.0, 22.8, 14.3. **HRMS-ESI** (m/z): [M + H]⁺ calculated for C₂₇H₃₄O₅N₃S: 512.2214, found: 512.2212.

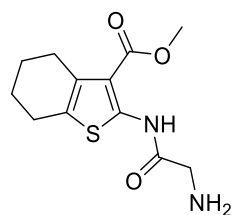
6.6. Synthesis of Thiophene Dipeptides

General procedure 5 (GP5): Boc deprotection.



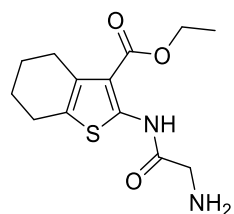
To a solution of Boc-Aa-Thiophene-OEt derivative **15** (0.76 mmol) in DCM (0.15 M) was added TFA (1:1 (v/v) to solvent). Solution was stirred at room temperature for 2 hours and concentrated under vacuum. Residue was neutralized to pH 7-10 with aqueous 1 M NaOH and extracted with EtOAc. Combined organic phases were dried over MgSO₄, filtered and concentrated under vacuum to afford corresponding dipeptides.

Methyl 2-(2-aminoacetamido)-4,5,6,7-tetrahydrobenzo[*b*]thiophene-3-carboxylate (**16a**)



According to GP5. **15a** (0.35 g, 0.95 mmol) was used as starting material. Title compound afforded as a light-yellow solid (0.25 g, quant). **¹H NMR** (500 MHz, DMSO-d₆): δ 11.13 (s, 1H), 8.29 (s, 3H), 4.10 (s, 2H), 3.83 (s, 3H), 2.70 (t, *J* = 5.4 Hz, 2H), 2.62 (t, *J* = 5.6 Hz, 2H), 1.76 – 1.70 (m, 4H). **¹³C NMR** (126 MHz, DMSO-d₆): δ 165.0, 158.2, 144.6, 131.3, 127.4, 113.2, 52.1, 41.4, 26.2, 24.1, 22.9, 22.6. **HRMS-ESI** (m/z): [M + H]⁺ calculated for C₁₂H₁₇O₃N₂S: 269.0954, found: 269.0956.

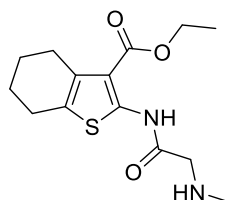
Ethyl 2-(2-aminoacetamido)-4,5,6,7-tetrahydrobenzo[*b*]thiophene-3-carboxylate (**16b**)



According to GP5. **15b** (0.40 g, 1.05 mmol) was used as starting material. Title compound afforded as a light-yellow solid (0.30 g, quant). **¹H NMR** (600 MHz, DMSO-d₆): δ 5.76 (s, 1H), 4.28 (q, *J* = 7.1 Hz, 2H), 3.38 (s, 2H), 3.33 (s, 2H), 2.72 (t, *J* = 5.7 Hz, 2H), 2.59 (t, *J* = 5.6 Hz, 2H), 1.75 – 1.70 (m, 4H),

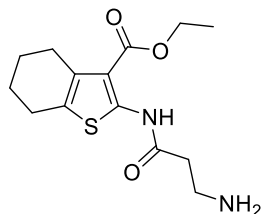
1.32 (t, $J = 7.1$ Hz, 3H). ^{13}C NMR (151 MHz, DMSO- d_6): δ 171.9, 164.8, 146.1, 131.0, 126.1, 122.7, 111.6, 60.6, 44.7, 26.3, 24.2, 23.0, 14.7. HRMS-ESI (m/z): $[\text{M} + \text{H}]^+$ calculated for $\text{C}_{13}\text{H}_{19}\text{O}_3\text{N}_2\text{S}$: 283.1111, found: 283.1109.

Ethyl 2-(2-(methylamino)acetamido)-4,5,6,7-tetrahydrobenzo[*b*]thiophene-3-carboxylate (16c)



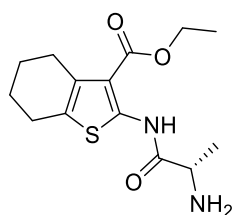
According to GP5. **15c** (0.16 g, 0.40 mmol) was used as starting material. Title compound afforded as a light-yellow oil (0.12 g, quant). ^1H NMR (700 MHz, DMSO- d_6): δ 4.29 (q, $J = 7.1$ Hz, 2H), 3.35 (s, 3H), 2.73 (t, $J = 5.3$ Hz, 2H), 2.60 (t, $J = 5.5$ Hz, 2H), 2.35 (s, 3H), 1.76 – 1.70 (m, 4H), 1.33 (t, $J = 7.1$ Hz, 3H). ^{13}C NMR (176 MHz, DMSO- d_6): δ 170.1, 164.8, 145.9, 131.1, 126.3, 111.7, 60.7, 54.4, 36.8, 26.3, 24.2, 23.0, 22.8, 14.6. HRMS-ESI (m/z): $[\text{M} + \text{H}]^+$ calculated for $\text{C}_{14}\text{H}_{21}\text{O}_3\text{N}_2\text{S}$: 297.1267, found: 297.1272.

Ethyl 2-(3-aminopropanamido)-4,5,6,7-tetrahydrobenzo[*b*]thiophene-3-carboxylate (16d)



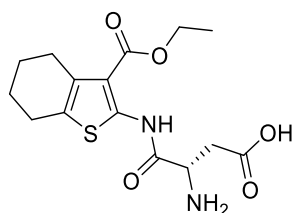
According to GP5. Title compound afforded as an orange solid (0.22 g, quant). ^1H NMR (500 MHz, DMSO- d_6): δ 11.05 (s, 1H), 7.90 (s, 3H), 4.29 (q, $J = 7.1$ Hz, 2H), 3.12 (t, $J = 6.8$ Hz, 2H), 2.89 (t, $J = 6.8$ Hz, 2H), 2.72 – 2.69 (m, 2H), 2.60 (t, $J = 5.8$ Hz, 2H), 1.76 – 1.69 (m, 4H), 1.32 (t, $J = 7.1$ Hz, 3H). ^{13}C NMR (126 MHz, DMSO- d_6): δ 167.8, 165.3, 145.9, 130.9, 126.8, 112.2, 60.9, 35.1, 33.6, 26.3, 24.2, 23.0, 22.8, 14.5. HRMS-ESI (m/z): $[\text{M} + \text{H}]^+$ calculated for $\text{C}_{14}\text{H}_{21}\text{O}_3\text{N}_2\text{S}$: 297.1267, found: 297.1272.

Ethyl (*S*)-2-(2-aminopropanamido)-4,5,6,7-tetrahydrobenzo[*b*]thiophene-3-carboxylate (16e)



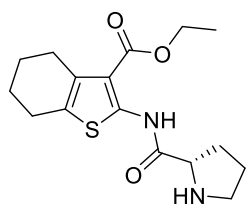
According to GP5. Title compound afforded as a yellow oil (0.22 g, quant). ^1H NMR (500 MHz, DMSO- d_6): δ 4.28 (q, $J = 7.1$ Hz, 2H), 3.55 (q, $J = 7.0$ Hz, 1H), 2.72 (t, $J = 5.5$ Hz, 2H), 2.60 (t, $J = 5.2$ Hz, 2H), 1.75 – 1.69 (m, 4H), 1.33 (t, $J = 7.1$ Hz, 3H), 1.27 (d, $J = 7.0$ Hz, 3H). ^{13}C NMR (126 MHz, DMSO- d_6): δ 174.4, 164.8, 146.3, 131.0, 126.1, 111.7, 60.6, 50.5, 26.3, 24.2, 23.0, 22.8, 22.3, 14.7. HRMS-ESI (m/z): $[\text{M} + \text{H}]^+$ calculated for $\text{C}_{14}\text{H}_{21}\text{O}_3\text{N}_2\text{S}$: 297.1267, found: 297.1271.

(S)-3-Amino-4-((3-(ethoxycarbonyl)-4,5,6,7-tetrahydrobenzo[*b*]thiophen-2-yl)amino)-4-oxobutanoic acid (16f)



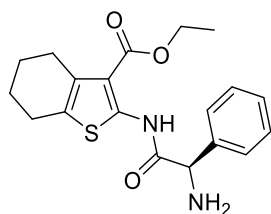
According to GP5. Title compound afforded as an off-white solid (0.25 g, quant). $^1\text{H NMR}$ (500 MHz, DMSO- d_6): δ 4.28 (q, $J = 7.1$ Hz, 2H), 3.70 – 3.67 (m, 1H), 3.10 (d, $J = 15.7$, 1H), 2.86 – 2.80 (m, 1H), 2.72 – 2.68 (m, 2H), 2.59 (t, $J = 5.5$ Hz, 2H), 1.76 – 1.69 (m, 4H), 1.31 (t, $J = 7.1$ Hz, 3H). $^{13}\text{C NMR}$ (126 MHz, DMSO- d_6): δ 165.2, 158.3, 158.0, 146.0, 142.1, 130.9, 126.5, 60.8, 50.8, 26.2, 24.2, 23.0, 22.8, 21.6, 14.6. **HRMS-ESI** (m/z): $[\text{M} + \text{H}]^+$ calculated for $\text{C}_{15}\text{H}_{21}\text{O}_5\text{N}_2\text{S}$: 341.1166, found: 341.1170.

Ethyl (S)-2-(pyrrolidine-2-carboxamido)-4,5,6,7-tetrahydrobenzo[*b*]thiophene-3-carboxylate (16g)



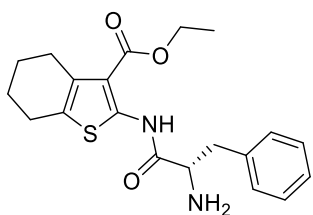
According to GP5. **15g** (0.24 g, 0.56 mmol) was used as starting material. Title compound afforded as an orange oil (0.18 g, quant). $^1\text{H NMR}$ (500 MHz, DMSO- d_6): δ 12.26 (s, 1H), 4.27 (q, $J = 7.2$ Hz, 2H), 3.84 (dd, $J = 9.3$, 5.2 Hz, 1H), 3.02 – 2.97 (m, 1H), 2.80 – 2.75 (m, 1H), 2.70 (t, $J = 5.1$ Hz, 2H), 2.57 (t, $J = 5.2$ Hz, 2H), 2.12 – 2.04 (m, 1H), 1.82 – 1.74 (m, 1H), 1.74 – 1.68 (m, 4H), 1.65 – 1.60 (m, 2H), 1.32 (t, $J = 7.1$ Hz, 3H). $^{13}\text{C NMR}$ (126 MHz, DMSO- d_6): δ 173.8, 164.6, 146.0, 131.1, 126.1, 111.8, 60.6, 60.5, 47.2, 30.9, 26.5, 26.3, 24.2, 23.0, 22.8, 14.6. **HRMS-ESI** (m/z): $[\text{M} + \text{H}]^+$ calculated for $\text{C}_{16}\text{H}_{23}\text{O}_3\text{N}_2\text{S}$: 323.1424, found: 323.1429.

Ethyl (R)-2-(2-amino-2-phenylacetamido)-4,5,6,7-tetrahydrobenzo[*b*]thiophene-3-carboxylate (16h)



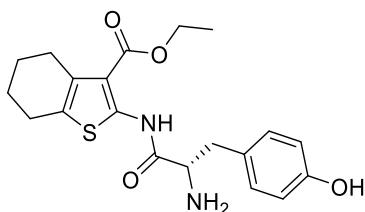
According to GP5. **15h** (0.30 g, 0.65 mmol) was used as starting material. Title compound afforded as a white solid (0.23 g, quant). $^1\text{H NMR}$ (500 MHz, DMSO- d_6): δ 7.46 (d, $J = 7.2$ Hz, 2H), 7.41 (t, $J = 7.4$ Hz, 2H), 7.36 (t, $J = 7.2$ Hz, 1H), 4.94 (s, 1H), 4.29 (q, $J = 7.1$ Hz, 2H), 2.71 (t, $J = 5.4$ Hz, 2H), 2.59 (t, $J = 5.0$ Hz, 2H), 1.75 – 1.68 (m, 4H), 1.32 (t, $J = 7.1$ Hz, 3H). $^{13}\text{C NMR}$ (126 MHz, DMSO- d_6): δ 164.9, 146.7, 139.6, 139.4, 137.7, 131.3, 129.2, 127.9, 126.8, 112.4, 60.8, 58.9, 26.8, 24.2, 23.0, 22.7, 14.6. **HRMS-ESI** (m/z): $[\text{M} + \text{H}]^+$ calculated for $\text{C}_{19}\text{H}_{23}\text{O}_3\text{N}_2\text{S}$: 359.1424, found: 359.1430.

Ethyl (S)-2-(2-amino-3-phenylpropanamido)-4,5,6,7-tetrahydrobenzo[*b*]thiophene-3-carboxylate (16i)



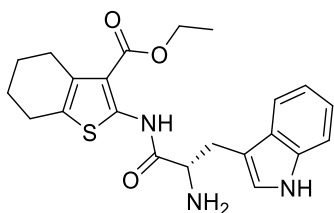
According to GP5. **15i** (1.30 g, 2.75 mmol) was used as starting material. Title compound afforded as a yellow solid (1.02 g, quant). **¹H NMR** (700 MHz, DMSO-*d*₆): δ 7.30 (t, *J* = 7.4 Hz, 2H), 7.26 (d, *J* = 7.5 Hz, 2H), 7.22 (t, *J* = 7.3 Hz, 1H), 4.25 (q, *J* = 7.0 Hz, 2H), 3.71 (dd, *J* = 9.1, 4.1 Hz, 1H), 3.15 (dd, *J* = 13.7, 4.1 Hz, 1H), 2.76 (dd, *J* = 13.8, 8.9 Hz, 1H), 2.71 (t, *J* = 5.2 Hz, 2H), 2.61 (t, *J* = 5.4 Hz, 2H), 1.76 – 1.70 (m, 4H), 1.30 (t, *J* = 7.1 Hz, 3H). **¹³C NMR** (176 MHz, DMSO-*d*₆): δ 173.0, 164.7, 146.1, 138.6, 131.1, 129.8, 128.8, 126.7, 126.3, 111.8, 60.6, 56.3, 40.3, 26.3, 24.2, 24.0, 22.8, 14.6. **HRMS-ESI** (*m/z*): [*M* + *H*]⁺ calculated for C₂₀H₂₅O₃N₂S: 373.1580, found: 373.1586.

Ethyl (S)-2-(2-amino-3-(4-hydroxyphenyl)propanamido)-4,5,6,7-tetrahydrobenzo[*b*]thiophene-3-carboxylate (16j)



According to GP5. Title compound afforded as a yellow solid (0.29 g, quant). **¹H NMR** (500 MHz, DMSO-*d*₆): δ 9.26 (s, 1H), 7.03 (d, *J* = 8.5 Hz, 2H), 6.68 (d, *J* = 8.5 Hz, 2H), 4.25 (q, *J* = 7.1 Hz, 2H), 3.76 – 3.72 (m, 1H), 3.35 (s, 1H), 3.00 (dd, *J* = 13.7, 4.5 Hz, 1H), 2.72 (t, *J* = 5.8 Hz, 2H), 2.61 (t, *J* = 5.5 Hz, 2H), 1.76 – 1.69 (m, 4H), 1.30 (t, *J* = 7.1 Hz, 3H). **¹³C NMR** (126 MHz, DMSO-*d*₆): δ 164.8, 156.5, 145.9, 131.1, 130.7, 128.1, 126.4, 115.6, 114.2, 112.0, 60.6, 60.2, 56.3, 26.3, 24.2, 23.0, 22.8, 14.6. **HRMS-ESI** (*m/z*): [*M* + *H*]⁺ calculated for C₂₀H₂₅O₄N₂S: 389.1530, found: 389.1539.

Ethyl (S)-2-(2-amino-3-(1*H*-indol-3-yl)propanamido)-4,5,6,7-tetrahydrobenzo[*b*]thiophene-3-carboxylate (16k)

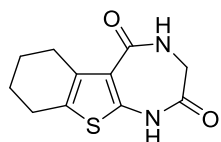


According to GP5. Title compound afforded as a yellow solid (0.33 g, quant). **¹H NMR** (500 MHz, DMSO-*d*₆): δ 10.96 (s, 1H), 7.54 (d, *J* = 7.9 Hz, 1H), 7.34 (d, *J* = 8.1 Hz, 1H), 7.21 (s, 1H), 7.07 (t, *J* = 8.2 Hz, 1H), 6.96 (t, *J* = 8.0 Hz, 1H), 4.21 (q, *J* = 6.9 Hz, 2H), 4.12 – 4.02 (m, 1H), 3.24 (dd, *J* = 14.5, 5.3 Hz, 1H), 3.05 (dd, *J* = 14.5, 7.6 Hz, 1H), 2.72 – 2.68 (m, 2H), 2.62 (t, *J* = 5.4 Hz, 2H), 1.76 – 1.68 (m, 4H), 1.27 (t, *J* = 7.1 Hz, 3H). **¹³C NMR** (126 MHz, DMSO-*d*₆):

δ 172.5, 164.8, 158.3, 145.5, 136.7, 131.1, 127.6, 126.8, 124.8, 121.6, 119.1, 119.0, 118.6, 111.9, 60.7, 29.6, 26.3, 24.2, 23.0, 22.8, 21.6, 14.6. **HRMS-ESI** (m/z): [M + H]⁺ calculated for C₂₂H₂₆O₃N₃S: 412.1689, found: 412.1691.

6.7. Synthesis of Thienodiazepines

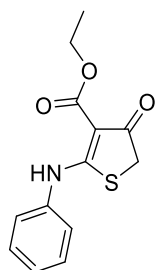
3,4,6,7,8,9-Hexahydro-1*H*-benzo[4,5]thieno[2,3-*e*][1,4]diazepine-2,5-dione (**17a**)



Aa-Thiophene-OEt derivative **16b** (0.35 mmol) was dissolved in dry DMF (0.2 M) and transferred to a flask with 60% sodium hydride dispersion in mineral oil (4.0 equivalents) under argon atmosphere. Reaction was heated at 100 °C for 24 hours. Cooled down mixture was quenched with addition of aqueous 0.1 M HCl and extracted with EtOAc (2 x 30 mL). Combined organic phases were dried over MgSO₄, filtered and solvent evaporated under vacuum for purification by MPLC (DCM, 0-12% MeOH) to afford title compound as a brown solid (42.4 mg, 51%). **¹H NMR** (700 MHz, DMSO-*d*₆): δ 10.86 (s, 1H), 8.07 (s, 1H), 3.63 (d, *J* = 5.7 Hz, 2H), 2.65 (t, *J* = 6.2 Hz, 2H), 2.60 (t, *J* = 6.2 Hz, 2H), 1.77 – 1.73 (m, 2H), 1.70 – 1.66 (m, 2H). **¹³C NMR** (176 MHz, DMSO-*d*₆): δ 170.4, 165.3, 142.4, 134.4, 127.6, 121.1, 45.5, 25.8, 24.3, 23.1, 22.4. **HRMS-ESI** (m/z): [M + H]⁺ calculated for C₁₁H₁₃O₂N₂S: 237.0692, found: 237.0693.

6.8. Synthesis of Thiophenones

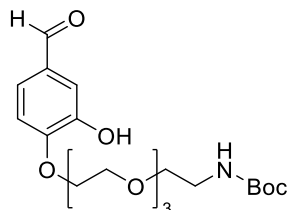
Ethyl 4-oxo-2-(phenylamino)-4,5-dihydrothiophene-3-carboxylate (**23**)



Ethyl 4-chloroacetoacetate **21** (0.61 mL, 4.52 mmol) was added to a solution of 60% sodium hydride dispersion in mineral oil (0.36 g, 9.04 mmol) in dry THF (20 mL) and the mixture was stirred at room temperature for 1 hour under argon atmosphere. A solution of phenyl isothiocyanate **22** (0.54 mL, 4.52 mmol) in dry THF (16 mL) was added dropwise and the mixture stirred for another 20 hours. Aqueous 1 M HCl (50 mL) was added and extracted with EtOAc (2 x 50 mL). Combined organic phases were dried over Na₂SO₄, filtered and concentrated under vacuum. Crude was triturated with methyl *tert*-butyl ether (20 mL) and filtered to afford title compound as a light-beige solid (0.74 g, 63%). **¹H NMR** (400 MHz, CDCl₃): δ 11.49 (s, 1H), 7.45 (t, *J* = 7.8 Hz, 2H), 7.38 – 7.33 (m, 3H), 4.38 (q, *J* = 7.1

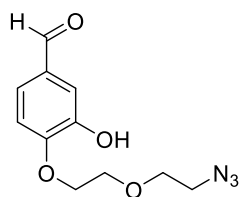
Hz, 2H), 3.64 (s, 2H), 1.41 (t, $J = 7.1$ Hz, 3H). LCMS-ESI (m/z): 264.1 $[M + H]^+$. Analytical data matches with literature values.^[388]

***tert*-Butyl (2-(2-(2-(2-(4-formyl-2-hydroxyphenoxy)ethoxy)ethoxy)ethoxy)ethyl)carbamate (20)**

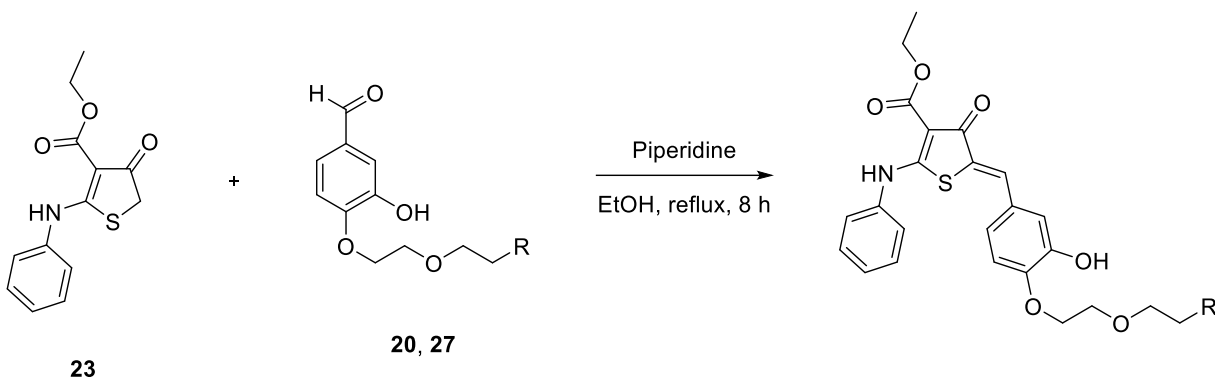


To a solution of *tert*-butyl (2-(2-(2-(2-bromoethoxy)ethoxy)ethoxy)ethyl) carbamate **19** (0.21 g, 0.59 mmol) in anhydrous DMF (1.9 mL) was added 3,4-dihydroxybenzaldehyde **18** (81.7 mg, 0.59 mmol) and potassium carbonate (81.7 mg, 0.59 mmol). The mixture was heated at 50 °C for 19 hours. Solvent was evaporated by SpeedVac (50 °C) for purification by MPLC (PE/EtOAc 1:0 to 0:1). Title compound was afforded as a yellow oil (0.13 g, 51%). ¹H NMR (400 MHz, CDCl₃): δ 9.85 (s, 1H), 7.44 (s, 1H), 7.39 (d, $J = 8.2$ Hz, 1H), 7.11 (br s, 1H), 6.98 (d, $J = 8.3$ Hz, 1H), 5.14 (br s, 1H), 4.28 – 4.25 (m, 2H), 3.91 – 3.88 (m, 2H), 3.76 – 3.73 (m, 2H), 3.71 – 3.68 (m, 2H), 3.67 – 3.61 (m, 4H), 3.55 (t, $J = 5.1$ Hz, 2H), 3.34 – 3.29 (m, 2H), 1.43 (s, 9H). Analytical data matches with literature values.^[49]

4-(2-(2-Azidoethoxy)ethoxy)-3-hydroxybenzaldehyde (27)

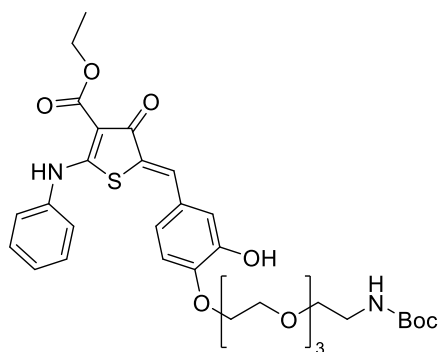


To a solution of bis(2-bromoethyl) ether **26** (1.21 mL, 9.60 mmol) in dry DMF (12 mL) was added 3,4-dihydroxybenzaldehyde **18** (0.66 g, 4.80 mmol) and potassium carbonate (0.66 g, 4.80 mmol). The mixture was heated at 50 °C for 24 hours. Sodium azide (1.25 g, 19.2 mmol) and potassium iodide (79.7 mg, 0.48 mmol) was added to the reaction mixture that was heated at 50 °C for another 21 hours. H₂O (80 mL) was added and mixture extracted with EtOAc (2 x 80 mL). Combined organic layers were dried over Na₂SO₄, filtered, and concentrated. Remaining solvent was evaporated by SpeedVac (50 °C) for purification by MPLC (PE/EtOAc 1:0 to 3:2). Title compound was afforded as a yellow oil (0.61 g, 50%). ¹H NMR (500 MHz, DMSO-*d*₆): δ 9.77 (s, 1H), 7.38 (d, $J = 8.2$ Hz, 1H), 7.27 (s, 1H), 7.14 (d, $J = 8.3$ Hz, 1H), 4.22 (t, $J = 4.6$ Hz, 2H), 3.84 (t, $J = 4.6$ Hz, 2H), 3.70 (t, $J = 5.0$ Hz, 2H), 3.44 (t, $J = 5.0$ Hz, 2H). ¹³C NMR (126 MHz, DMSO-*d*₆): δ 192.0, 153.0, 147.6, 130.4, 124.8, 114.1, 113.2, 69.9, 69.2, 68.6, 50.5. HRMS-ESI (m/z): $[M + H]^+$ calculated for C₁₁H₁₄O₄N₃: 252.0979, found: 252.0981.

General procedure 6 (GP6): Thiophenone synthesis through aldol condensation.

A mixture of aldehyde derivative **20** or **27** (0.16 mmol), **23** (1.1 equivalents) and piperidine (0.15 equivalents) in EtOH (0.15 M) was heated at 78 °C for 8 hours. Solvent was evaporated under vacuum for purification by MPLC (PE/EtOAc 1:0 to 2:3) to afford corresponding thiophenones.

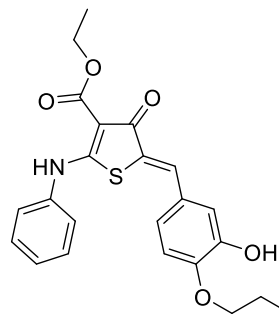
Ethyl (Z)-5-(4-((2,2-dimethyl-4-oxo-3,8,11,14-tetraoxa-5-azahexadecan-16-yl)oxy)-3-hydroxybenzylidene)-4-oxo-2-(phenylamino)-4,5-dihydrothiophene-3-carboxylate (24**)**



According to GP6. **20** (50.0 mg, 0.12 mmol) was used as starting material. Purification by MPLC (PE/EtOAc 0:1 to 1:0) afforded title compound as a yellow oil (66.6 mg, 84%). ¹H NMR (400 MHz, DMSO-d₆): δ 11.21 (s, 1H), 9.37 (s, 1H), 7.55 – 7.46 (m, 4H), 7.45 – 7.40 (m, 1H), 7.02 – 6.94 (m, 3H), 6.72 – 6.68 (m, 1H), 4.26 (q, *J* = 7.1 Hz, 2H), 4.11 – 4.08 (m, 2H), 3.74 – 3.71 (m, 2H), 3.59 – 3.54 (m, 2H),

3.53 – 3.44 (m, 6H), 3.34 (t, *J* = 6.1 Hz, 2H), 3.02 (q, *J* = 6.0 Hz, 2H), 1.34 (s, 9H), 1.27 (t, *J* = 7.1 Hz, 3H). LCMS-ESI (*m/z*): 659.3 [M + H]⁺. Analytical data matches with literature values.^[49]

Ethyl (Z)-5-(4-(2-(2-azidoethoxy)ethoxy)-3-hydroxybenzylidene)-4-oxo-2-(phenylamino)-4,5-dihydrothiophene-3-carboxylate (28**)**



According to GP6. Title compound afforded as a yellow solid (60.8 mg, 77%). $^1\text{H NMR}$ (500 MHz, DMSO-d_6): δ 11.25 (s, 1H), 9.44 (s, 1H), 7.57 – 7.51 (m, 4H), 7.49 (s, 1H), 7.48 – 7.43 (m, 1H), 7.05 – 7.02 (m, 1H), 7.01 – 6.99 (m, 1H), 6.98 (s, 1H), 4.28 (q, $J = 7.1$ Hz, 2H), 4.13 (t, $J = 4.7$ Hz, 2H), 3.79 (t, $J = 4.7$ Hz, 2H), 3.67 (t, $J = 5.5$ Hz, 2H), 3.43 (t, $J = 5.5$ Hz, 2H), 1.30 (t, $J = 7.1$ Hz, 3H). $^{13}\text{C NMR}$ (126 MHz, DMSO-d_6): δ 181.4, 175.8, 165.3, 149.2, 147.5, 138.0, 130.5, 130.1, 128.7, 126.8, 126.1, 125.1, 123.6, 116.3, 114.2, 97.3, 69.9, 69.2, 68.5, 60.0, 50.5, 14.9. **HRMS-ESI** (m/z): $[\text{M} + \text{H}]^+$ calculated for $\text{C}_{24}\text{H}_{25}\text{O}_6\text{N}_4\text{S}$: 497.1489, found: 497.1484.

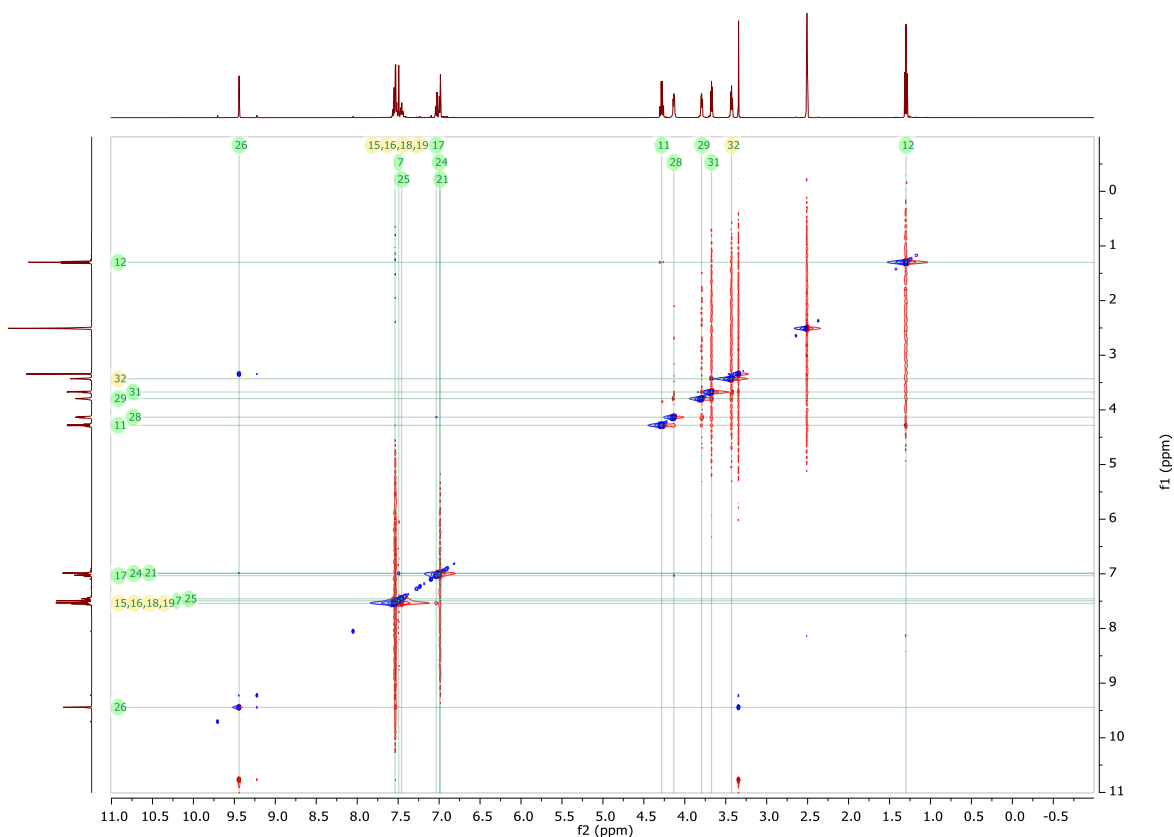


Figure 30. 2D NOESY NMR ($^1\text{H}/^1\text{H}$) of **28**.

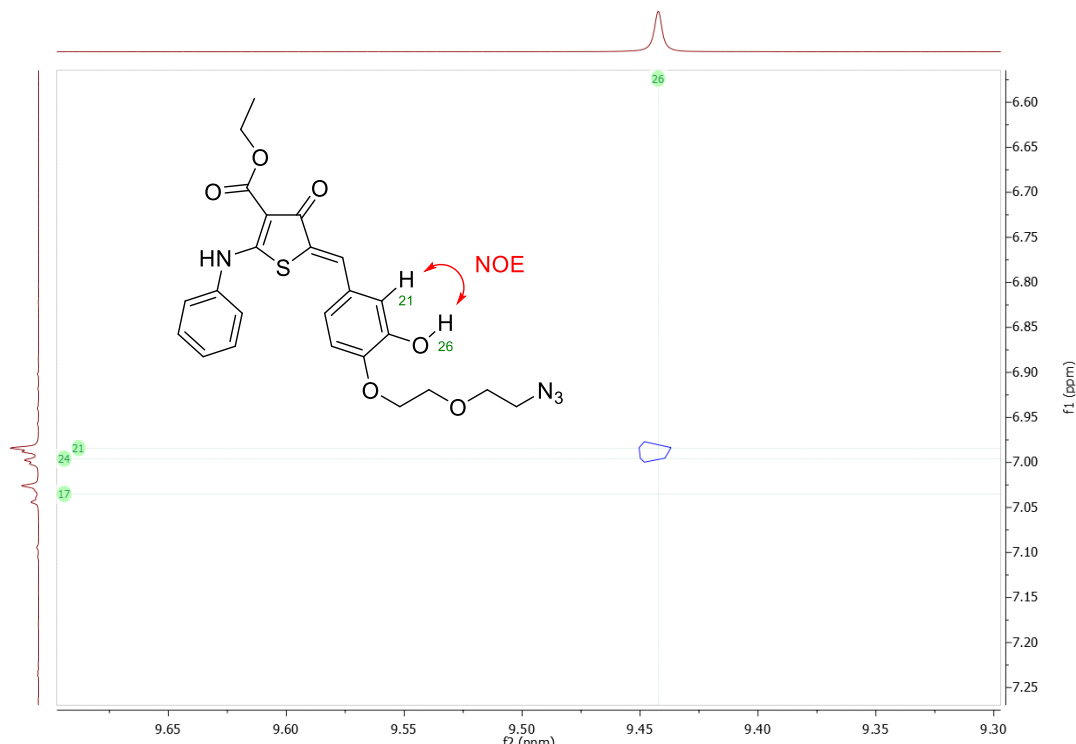
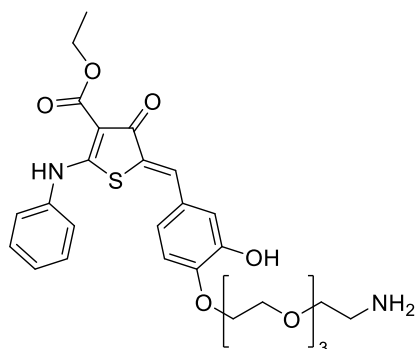


Figure 31. NOE coupling between phenol proton and aromatic ^1H singlet proving isolation of desired regioisomer of **28**.

Ethyl (Z)-5-(4-(2-(2-(2-(2-aminoethoxy)ethoxy)ethoxy)ethoxy)ethoxy)-3-hydroxybenzylidene)-4-oxo-2-(phenylamino)-4,5-dihydrothiophene-3-carboxylate (25**)**

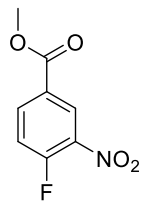


To a solution of **24** (40.0 mg, 60.7 μmol) in DCM (2 mL) was added 4 M HCl in 1,4-dioxane (0.5 mL, 2.0 mmol). The mixture was stirred at room temperature for 30 minutes. Mixture was concentrated under vacuum to afford HCl salt of title compound as a yellow oil (33.9 mg, quant). ^1H NMR (400 MHz, DMSO- d_6): δ 11.22 (s, 1H), 9.47 (s, 1H), 7.86 (br s, 3H), 7.55 – 7.38 (m, 6H), 7.02 – 6.95 (m, 3H), 4.26 (q, $J = 7.1$ Hz, 2H), 4.11 –

4.08 (m, 2H), 3.74 – 3.71 (m, 2H), 3.59 – 3.56 (m, 4H), 3.55 – 3.51 (m, 6H), 2.96 – 2.90 (m, 2H), 1.27 (t, $J = 7.1$ Hz, 3H). LCMS-ESI (m/z): 559.2 $[\text{M} + \text{H}]^+$. Analytical data matches with literature values.^[49]

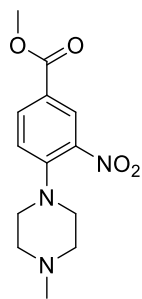
6.9. Synthesis of WDR5 Inhibitors

Methyl 4-fluoro-3-nitrobenzoate (**31**)



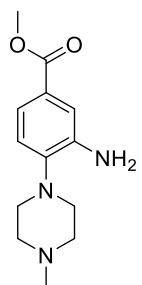
4-Fluoro-3-nitrobenzoic acid **29** (3.00 g, 16.2 mmol) was added to thionyl chloride (15 mL) and heated at 79 °C for 6 hours. Mixture was concentrated under vacuum to afford 4-fluoro-3-nitrobenzoyl chloride **30** and residue dissolved in dry DCM (20 mL). Dry MeOH (6.57 mL, 162 mmol) was added followed by triethylamine (2.70 mL, 19.4 mmol) and the solution stirred at room temperature for 30 minutes under argon atmosphere. Mixture was concentrated under vacuum to afford title compound as a light-yellow solid (3.23 g, quant over two steps). $^1\text{H NMR}$ (400 MHz, CDCl_3): δ 8.74 (d, 1H), 8.32 (d, 1H), 7.39 (m, 1H), 3.98 (s, 3H). **LCMS-ESI** (m/z): 200.1 $[\text{M} + \text{H}]^+$. Analytical data matches with literature values.^[326]

Methyl 4-(4-methylpiperazin-1-yl)-3-nitrobenzoate (**33**)



To a solution of **31** (3.19 g, 16.0 mmol) in DMF (30 mL) was added 1-methylpiperazine **32** (2.31 mL, 20.8 mmol) followed by *N,N*-diisopropylethylamine (3.62 mL, 20.8 mmol). The mixture was stirred at room temperature for 30 minutes, then diluted with EtOAc (100 mL) and washed with H_2O (3 x 50 mL). Organic phase was dried over Na_2SO_4 , filtered and concentrated under vacuum to afford title compound as a dark-red oil (4.47 g, quant). $^1\text{H NMR}$ (700 MHz, CDCl_3): δ 8.43 (s, 1H), 8.06 (d, $J = 8.7$ Hz, 1H), 7.07 (d, $J = 8.8$ Hz, 1H), 3.91 (s, 3H), 3.21 (t, $J = 4.9$ Hz, 4H), 2.58 (t, $J = 4.9$ Hz, 4H), 2.36 (s, 3H). **LCMS-ESI** (m/z): 280.1 $[\text{M} + \text{H}]^+$. Analytical data matches with literature values.^[326]

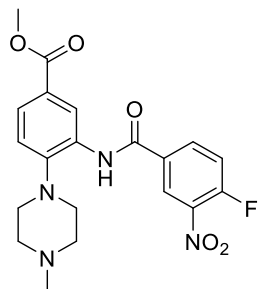
Methyl 3-amino-4-(4-methylpiperazin-1-yl)benzoate (**34**)



To a solution of **33** (3.69 g, 13.2 mmol) in EtOAc (100 mL) at room temperature was added tin(II) chloride dihydrate (8.96 g, 39.7 mmol). The mixture was heated at 77 °C with vigorous stirring for 8 hours, and subsequently cooled to room temperature. Following dilution with EtOAc (150 mL), the mixture was neutralized with aqueous saturated NaHCO_3 (200 mL) and filtered through celite. Residue was washed with EtOAc (5 x 20 mL) and the aqueous phase extracted with EtOAc (100 mL). Combined

organic phases were dried over Na₂SO₄, filtered, and concentrated under vacuum to afford title compound as a yellow solid (2.14 g, 65%). ¹H NMR (400 MHz, CDCl₃): δ 7.44 (d, *J* = 8.2 Hz, 1H), 7.39 (s, 1H), 6.99 (d, *J* = 8.2 Hz, 1H), 3.94 (s, 2H), 3.87 (s, 3H), 3.03 (t, *J* = 4.6 Hz, 4H), 2.70 – 2.58 (m, 4H), 2.40 (s, 3H). LCMS-ESI (m/z): 250.1 [M + H]⁺. Analytical data matches with literature values.^[326]

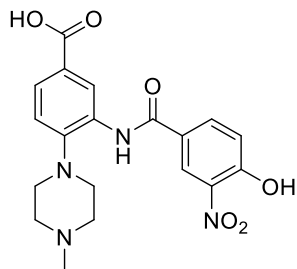
Methyl 3-(4-fluoro-3-nitrobenzamido)-4-(4-methylpiperazin-1-yl)benzoate (35)



29 (1.81 g, 9.77 mmol) was added to thionyl chloride (9 mL) and heated at 79 °C for 6 hours. Mixture was concentrated under vacuum to afford 4-fluoro-3-nitrobenzoyl chloride **30**. To a solution of **34** (1.00 g, 4.00 mmol) in dry DCM (90 mL) was added **30** (0.99 g, 4.88 mmol) dissolved in dry DCM (30 mL) at room temperature under argon atmosphere. Pyridine (0.39 mL, 4.88 mmol) was added and the mixture stirred at room temperature for

19 hours. Reaction mixture was subsequently diluted with DCM (200 mL) and washed with aqueous saturated NaHCO₃ (3 x 150 mL) then brine (200 mL). Organic phase was dried over Na₂SO₄, filtered and concentrated under vacuum for purification by flash column chromatography (DCM, 0-4% MeOH) to afford title compound as a light-yellow solid (0.94 g, 56% over two steps). ¹H NMR (400 MHz, DMSO-d₆): δ 9.94 (s, 1H), 8.70 (d, *J* = 7.2 Hz, 1H), 8.40 – 8.35 (m, 1H), 8.31 (s, 1H), 7.82 – 7.76 (m, 2H), 7.24 (d, *J* = 8.4 Hz, 1H), 3.82 (s, 3H), 3.30 – 3.28 (m, 6H), 2.99 – 2.95 (m, 4H), 2.20 (s, 3H). LCMS-ESI (m/z): 417.1 [M + H]⁺. Analytical data matches with literature values.^[326]

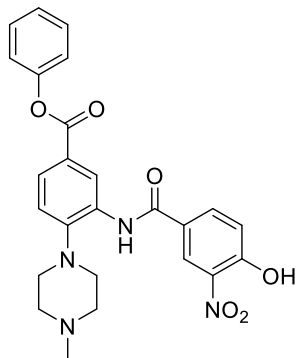
3-(4-Hydroxy-3-nitrobenzamido)-4-(4-methylpiperazin-1-yl)benzoic acid (36)



35 (0.83 g, 2.00 mmol) was dissolved in THF (40 mL) to which was dropwise added aqueous 1 M lithium hydroxide (30 mL). Mixture was stirred vigorously at room temperature for 66 hours. Mixture was acidified to pH 4-6 with addition of aqueous 1 M HCl to form a precipitate that was collected by filtration and washed with DCM (10 mL) to afford title compound as a yellow solid (0.56 g, 70%). ¹H NMR (500 MHz, DMSO-d₆): δ 9.60 (s, 1H), 8.50 (s, 1H), 8.45 (s, 1H), 8.06 (d, *J* = 8.8 Hz, 1H), 7.75 (d, *J* = 8.4 Hz, 1H), 7.27 (d, *J* = 8.4 Hz, 1H), 7.20 (d, *J* = 8.8 Hz, 1H), 3.10 (t, *J* = 4.9 Hz, 4H), 2.92 (t, *J* = 4.9 Hz, 4H), 2.53

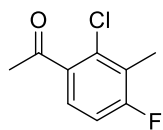
(s, 3H). ^{13}C NMR (126 MHz, DMSO- d_6): δ 167.4, 163.5, 157.9, 148.4, 137.0, 133.9, 131.9, 127.1, 126.3, 126.0, 125.4, 123.1, 121.1, 120.4, 54.3, 49.6, 44.6. HRMS-ESI (m/z): $[\text{M} + \text{H}]^+$ calculated for $\text{C}_{19}\text{H}_{21}\text{O}_6\text{N}_4$: 401.1456, found: 401.1455.

Phenyl 3-(4-hydroxy-3-nitrobenzamido)-4-(4-methylpiperazin-1-yl)benzoate (37)



A solution of **36** (33.3 mg, 83.2 μmol), HATU (37.8 mg, 99.3 μmol), HOAt (13.5 mg, 99.3 μmol), and *N,N*-diisopropylethylamine (43.2 μL , 0.25 mmol) in dry DMF (2.6 mL) was stirred for 10 minutes, then a solution of phenol (28.0 mg, 0.30 mmol) and *N,N*-diisopropylethylamine (43.2 μL , 0.25 mmol) in dry DMF (1.0 mL) was added. The mixture was stirred at room temperature for 19 hours. Mixture was diluted with DCM (20 mL) and washed with H_2O (2 x 20 mL). Organic phase was dried over Na_2SO_4 , filtered and concentrated under vacuum for purification by MPLC (DCM, 0-10% MeOH) to afford title compound as a yellow oil (24.1 mg, 61%). ^1H NMR (500 MHz, DMSO- d_6): δ 9.52 (s, 1H), 8.67 (s, 1H), 8.50 (s, 1H), 7.91 (s, 1H), 7.89 (s, 1H), 7.48 (t, $J = 7.9$ Hz, 2H), 7.35 (d, $J = 8.4$ Hz, 1H), 7.32 (t, $J = 7.4$ Hz, 1H), 7.27 (d, $J = 7.5$ Hz, 2H), 6.92 (d, $J = 9.0$ Hz, 1H), 3.03 (t, $J = 4.8$ Hz, 4H), 2.66 – 2.60 (m, 4H), 2.32 (s, 3H). ^{13}C NMR (126 MHz, DMSO- d_6): δ 164.8, 163.8, 151.2, 149.7, 136.9, 133.3, 133.3, 132.4, 130.1, 127.3, 127.3, 126.5, 126.4, 125.0, 123.8, 123.4, 122.5, 120.5, 55.1, 50.7, 45.9. HRMS-ESI (m/z): $[\text{M} + \text{H}]^+$ calculated for $\text{C}_{25}\text{H}_{25}\text{O}_6\text{N}_4$: 477.1769, found: 477.1774.

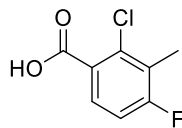
1-(2-Chloro-4-fluoro-3-methylphenyl) ethanone (40)



To a solution of 2-chloro-6-fluorotoluene **38** (11.0 mL, 90.6 mmol) and aluminum chloride (36.9 g, 0.28 mol) in dry DCM (100 mL), acetyl chloride **39** (7.31 mL, 0.10 mol) was added dropwise at 0 $^\circ\text{C}$ under argon atmosphere, then the reaction mixture was allowed to stir at room temperature for 3 hours. The mixture was poured into ice-cold H_2O (200 mL) and neutralized to pH 3-4 by addition of aqueous 1 M NaOH. The solution was extracted with DCM (2 x 200 mL), and the combined organic phases were washed with H_2O (400 mL), dried over MgSO_4 , filtered and solvent evaporated under vacuum for purification by flash column chromatography (PE/EtOAc 1:0 to 1:2) to afford title compound as a light-yellow oil (4.03

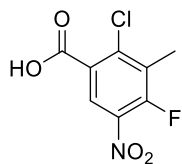
g, 24%). $^1\text{H NMR}$ (400 MHz, CDCl_3): δ 7.36 (dd, 8.6, 6.0 Hz, 1H), 7.01 (t, $J = 8.6$ Hz, 1H), 2.62 (s, 3H), 2.35 (s, 3H). Analytical data matches with literature values.^[327]

2-Chloro-4-fluoro-3-methylbenzoic acid (**41**)



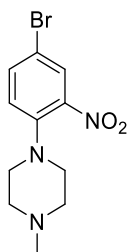
A mixture of **40** (0.11 g, 0.56 mmol), DMSO (0.24 mL, 3.38 mmol) and iodine (14.3 mg, 56.3 μmol) in chlorobenzene (1.1 mL) was stirred at 132 °C for 3 hours. 5-6 M *tert*-Butyl hydroperoxide in nonane (0.20 mL, 1.13 mmol) was added to the cooled down reaction mixture that was subsequently heated at 132 °C for another 3 hours. Reaction was quenched with addition of H_2O (3 mL) and extracted with Et_2O (3 x 3 mL). Combined organic phases were dried over Na_2SO_4 , filtered and concentrated under vacuum for purification by MPLC (PE/ EtOAc 1:0 to 1:2, with 1% AcOH) to afford title compound as a white solid (67.7 mg, 64%). $^1\text{H NMR}$ (400 MHz, DMSO-d_6): δ 13.33 (s, 1H), 7.65 (dd, $J = 8.7, 6.3$ Hz, 1H), 7.26 (t, $J = 8.6$ Hz, 1H), 2.28 (s, 3H). Analytical data matches with literature values.^[341]

2-Chloro-4-fluoro-3-methyl-5-nitrobenzoic acid (**42**)



Fuming nitric acid (0.24 mL, 3.79 mmol) was added dropwise into a solution of **41** (0.65 g, 3.45 mmol) and concentrated sulfuric acid (10 mL) under stirring at 0 °C. The reaction mixture was stirred at room temperature for 2 hours and then poured in ice-cold H_2O (50 mL). Precipitate was collected by filtration and washed with H_2O (60 mL) to afford title compound as a light-yellow solid (0.66 g, 82%). $^1\text{H NMR}$ (400 MHz, DMSO-d_6): δ 13.96 (br s, 1H), 8.35 (d, $J = 8.0$ Hz, 1H), 2.37 (s, 3H). LCMS-ESI (m/z): 234.0 $[\text{M} + \text{H}]^+$. Analytical data matches with literature values.^[327]

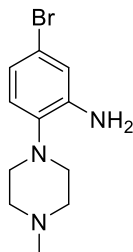
5-Bromo-2-(4-methylpiperazin-1-yl) nitrobenzene (**45**)



To a solution of 5-bromo-2-fluoronitrobenzene **44** (2.80 mL, 22.7 mmol) in DMF (30 mL) was added 1-methylpiperazine **32** (3.03 mL, 27.3 mmol) followed by *N,N*-diisopropylethylamine (4.75 mL, 27.3 mmol). The mixture was heated at 80 °C for 3 hours, and subsequently cooled to room temperature. Mixture was diluted with EtOAc (250 mL) and washed with H_2O (3 x 100 mL). Organic phase was dried over Na_2SO_4 , filtered, and concentrated under vacuum to afford title compound as a red oil (6.82 g, quant). $^1\text{H NMR}$ (500 MHz, CDCl_3): δ 7.89 (s, 1H), 7.55 (d, $J = 8.8$ Hz, 1H), 7.02 (d, $J = 8.8$ Hz, 1H), 3.06

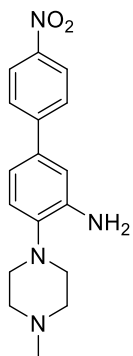
(t, $J = 4.9$ Hz, 4H), 2.56 (t, $J = 4.9$ Hz, 4H), 2.35 (s, 3H). **LCMS-ESI** (m/z): 300.0 [M + H]⁺. Analytical data matches with literature values.^[327]

5-Bromo-2-(4-methylpiperazin-1-yl)aniline (46)



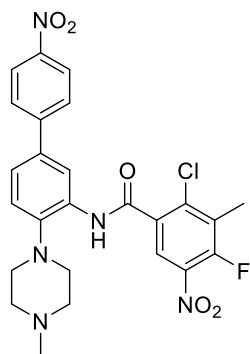
To a solution of **45** (6.78 g, 22.6 mmol) in EtOAc (150 mL) at room temperature was added tin(II) chloride dihydrate (20.4 g, 90.6 mmol). The mixture was heated at 77 °C with vigorous stirring for 3 hours, and subsequently cooled to room temperature. Following dilution with EtOAc (150 mL), the mixture was neutralized with aqueous saturated NaHCO₃ (150 mL) and filtered through celite. Residue was washed with EtOAc (2 x 50 mL) and organic phase dried over Na₂SO₄, filtered, and concentrated under vacuum to afford title compound as a light-yellow solid (4.11 g, 67%). **¹H NMR** (400 MHz, CDCl₃): δ 6.87 – 6.81 (m, 3H), 4.01 (s, 2H), 2.91 (t, $J = 4.9$ Hz, 4H), 2.62 – 2.52 (m, 4H), 2.37 (s, 3H). **LCMS-ESI** (m/z): 270.1 [M + H]⁺. Analytical data matches with literature values.^[327]

4-(4-Methylpiperazin-1-yl)-4'-nitro-[1,1'-biphenyl]-3-amine (48)



4-Nitrophenylboronic acid **47** (1.53 g, 9.14 mmol) was added to a solution of **46** (2.06 g, 7.61 mmol) in 1,4-dioxane (56 mL). Cesium carbonate (4.96 g, 15.2 mmol) in H₂O (5.6 mL) followed by bis(triphenylphosphine)palladium(II) dichloride (0.22 g, 0.31 mmol) was added to the mixture. Reaction mixture was heated at 100 °C for 20 hours under argon atmosphere. The mixture was filtered through celite and residue washed with H₂O (2 x 20 mL) then EtOAc (3 x 20 mL). Aqueous phase was extracted with EtOAc (2 x 100 mL). Filter was washed with MeOH (10 x 50 mL). Combined organic phases were dried over Na₂SO₄, filtered and concentrated under vacuum for purification by MPLC (DCM, 0-40% MeOH) to afford title compound as an orange solid (1.27 g, 54%). **¹H NMR** (500 MHz, DMSO-d₆): δ 8.27 (d, $J = 8.9$ Hz, 2H), 7.82 (d, $J = 8.9$ Hz, 2H), 7.09 (s, 1H), 7.03 – 6.97 (m, 2H), 4.90 (s, 2H), 2.90 – 2.83 (m, 4H), 2.50 – 2.44 (m, 4H), 2.25 (s, 3H). **LCMS-ESI** (m/z): 313.2 [M + H]⁺. Analytical data matches with literature values.^[327]

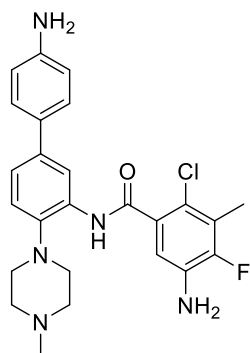
2-Chloro-4-fluoro-3-methyl-N-(4-(4-methylpiperazin-1-yl)-4'-nitro-[1,1'-biphenyl]-3-yl)-5-nitrobenzamide (49)



42 (0.63 g, 2.70 mmol) was added to thionyl chloride (20 mL) and heated at 79 °C for 6 hours. Mixture was concentrated under vacuum to afford 2-chloro-4-fluoro-3-methyl-5-nitrobenzoyl chloride **43**. To a solution of **48** (0.70 g, 2.25 mmol) in dry DCM (50 mL) was added **43** (0.68 g, 2.70 mmol) at 0 °C under argon atmosphere. Pyridine (0.22 mL, 2.70 mmol) was added and the mixture stirred at room temperature for 16 hours. Reaction mixture

was subsequently diluted with DCM (30 mL) and washed with H₂O (30 mL), aqueous saturated copper(II) sulfate pentahydrate (2 x 30 mL), H₂O (30 mL), aqueous saturated NaHCO₃ (2 x 30 mL) then brine (30 mL). Organic phase was dried over Na₂SO₄, filtered, and concentrated under vacuum to afford title compound as a brown solid (0.57 g, 48% over two steps). ¹H NMR (400 MHz, DMSO-d₆): δ 9.89 (s, 1H), 8.38 (s, 1H), 8.33 – 8.30 (m, 3H), 7.91 (d, *J* = 8.9 Hz, 2H), 7.64 (dd, *J* = 8.4, 2.3 Hz, 1H), 7.31 (d, *J* = 8.4 Hz, 1H), 3.10 – 3.04 (m, 4H), 2.86 – 2.78 (m, 4H), 2.42 (s, 3H), 2.35 (s, 3H). LCMS-ESI (m/z): 528.2 [M + H]⁺. Analytical data matches with literature values.^[327]

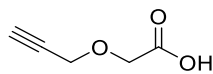
5-Amino-*N*-(4'-amino-4-(4-methylpiperazin-1-yl)-[1,1'-biphenyl]-3-yl)-2-chloro-4-fluoro-3-methylbenzamide (**50**)



To a solution of **49** (0.53 g, 1.00 mmol) in EtOAc (50 mL) at room temperature was added tin(II) chloride dihydrate (3.40 g, 15.1 mmol). The mixture was heated at 77 °C with vigorous stirring for 17 hours, and subsequently cooled to room temperature. Following dilution with EtOAc (75 mL), the mixture was neutralized with aqueous saturated NaHCO₃ (75 mL) and filtered through celite. Residue was washed with EtOAc (5 x 20 mL) and organic phase dried over Na₂SO₄, filtered and concentrated under

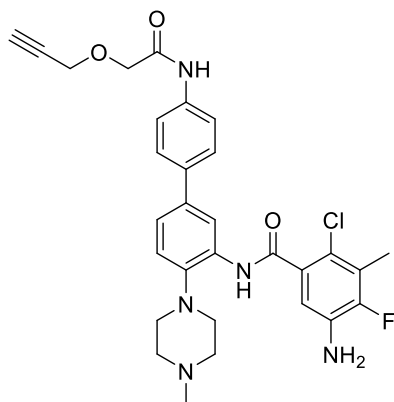
vacuum for purification by MPLC (DCM, 0-15% MeOH) to afford title compound as a yellow oil (0.25 g, 53%). ¹H NMR (400 MHz, DMSO-d₆): δ 9.20 (s, 1H), 8.28 (s, 1H), 7.29 – 7.23 (m, 4H), 6.88 (d, *J* = 9.2 Hz, 1H), 6.63 (d, *J* = 8.5 Hz, 2H), 5.47 (s, 2H), 5.18 (s, 2H), 2.83 (t, *J* = 4.7 Hz, 4H), 2.46 – 2.39 (m, 4H), 2.24 (d, *J* = 2.6 Hz, 3H), 2.19 (s, 3H). LCMS-ESI (m/z): 468.2 [M + H]⁺. Analytical data matches with literature values.^[327]

2-(Prop-2-yn-1-yloxy)acetic acid (**53**)



Propargyl alcohol **51** (0.48 mL, 8.30 mmol) in dry THF (10 mL) was added dropwise to a stirred mixture of 60% sodium hydride dispersion in mineral oil (0.66 g, 16.6 mmol) in dry THF (10 mL) at room temperature and stirred for 10 minutes under argon atmosphere. Bromoacetic acid **52** (1.15 g, 8.30 mmol) in dry THF (10 mL) was added dropwise and resulting mixture stirred at room temperature for 18 hours. Reaction was quenched with addition of H₂O (30 mL) and the mixture concentrated under vacuum. Residue was taken up in H₂O and washed with Et₂O (30 mL). Aqueous phase was acidified to pH 1 by addition of aqueous 3 M HCl and extracted with EtOAc (2 x 30 mL). Combined organic phases were dried over Na₂SO₄ and concentrated under vacuum to afford title compound as a light-yellow oil (0.76 g, 80%). ¹H NMR (400 MHz, CDCl₃): δ 10.01 (br s, 1H), 4.32 (s, 2H), 4.26 (s, 2H), 2.50 (s, 1H). Analytical data matches with literature values.^[389]

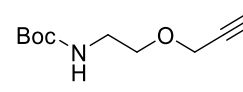
5-Amino-2-chloro-4-fluoro-3-methyl-N-(4-(4-methylpiperazin-1-yl)-4'-(2-(prop-2-yn-1-yloxy)acetamido)-[1,1'-biphenyl]-3-yl)benzamide (55)



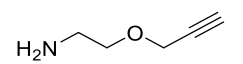
53 (21.9 mg, 0.19 mmol) was added to thionyl chloride (3 mL) and heated at 79 °C for 6 hours. Mixture was concentrated under vacuum to afford 2-(prop-2-yn-1-yloxy)acetyl chloride **54**. To a solution of **50** (50.0 mg, 0.11 mmol) in dry DMF (2.3 mL) was added **54** (25.5 mg, 0.19 mmol) dissolved in dry DMF (0.8 mL) at room temperature under argon atmosphere. Pyridine (10.4 μL, 0.13 mmol) was added and the mixture stirred at room temperature for 2 hours. Reaction mixture was subsequently diluted with EtOAc (40 mL) and washed with saturated aqueous NaHCO₃ (2 x 30 mL). Organic phase was dried over Na₂SO₄, filtered, concentrated under vacuum for purification by prep. HPLC (H₂O, 10-50% MeCN with 0.1% TFA) and lyophilization to afford TFA salt of title compound as a white solid (14.4 mg, 24% over two steps). ¹H NMR (700 MHz, DMSO-d₆): δ 9.95 (s, 1H), 9.42 (s, 1H), 8.29 (s, 1H), 7.76 (d, *J* = 8.3 Hz, 2H), 7.58 (d, *J* = 8.3 Hz, 2H), 7.47 (d, *J* = 8.2 Hz, 1H), 7.30 (d, *J* = 8.3 Hz, 1H), 6.86 (d, *J* = 9.1 Hz, 1H), 4.33 (s, 2H), 4.16 (s, 1H), 3.55 – 3.52 (m, 3H), 3.24 – 3.18 (m, 2H), 3.26 (d, *J* = 12.6 Hz, 2H), 3.05 (t, *J* = 11.5 Hz, 2H), 2.87 (s, 3H), 2.27 (s, 3H). ¹³C NMR (176 MHz, DMSO-d₆): δ 168.0, 166.0, 158.8 and 158.6 and 158.4 and 158.2 (q, ²*J*_{C-F} = 32 Hz), 150.3 and 148.9 (d, ¹*J*_{C-F} = 241 Hz), 141.9, 138.3, 136.7, 136.0 and 135.9 (d, ²*J*_{C-F} = 14

Hz), 135.2, 133.5, 133.1, 127.2, 123.6, 121.6, 121.3, 120.7, 116.2, 113.3, 80.1, 78.5, 70.0, 58.4, 53.4, 48.9, 42.8, 12.5. **¹⁹F NMR** (470 MHz, DMSO-d₆): δ -131.8. **HRMS-ESI** (m/z): [M + H]⁺ calculated for C₃₀H₃₂O₃N₅ClF: 564.2172, found: 564.2169.

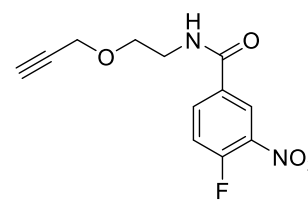
tert-Butyl (2-(prop-2-yn-1-yloxy)ethyl)carbamate (58)

 *tert*-Butyl (2-hydroxyethyl) carbamate **56** (3.10 mL, 20.0 mmol) was added dropwise to a stirred mixture of 60% sodium hydride dispersion in mineral oil (2.04 g, 51.0 mmol) in dry THF (167 ml) at 0 °C and stirred for 15 minutes under argon atmosphere. 80% Propargyl bromide **57** in toluene (2.84 mL, 25.5 mmol) was added dropwise at 0 °C and resulting mixture stirred at room temperature for 16 hours. Reaction was quenched with addition of ice-cold H₂O (250 ml) and extracted with EtOAc (2 x 200 ml). Combined organic phases were dried over Na₂SO₄, filtered and concentrated under vacuum for purification by flash column chromatography (PE/EtOAc 1:19 to 1:6) to afford title compound as an uncoloured oil (2.75 g, 69%). **¹H NMR** (400 MHz, CDCl₃): δ 4.87 (br s, 1H), 4.16 (s, 2H), 3.58 (t, *J* = 5.2 Hz, 2H), 3.34 (q, *J* = 5.2 Hz, 2H), 2.44 (s, 1H), 1.44 (s, 9H). Analytical data matches with literature values.^[390]

2-(Prop-2-yn-1-yloxy)ethan-1-amine (59)

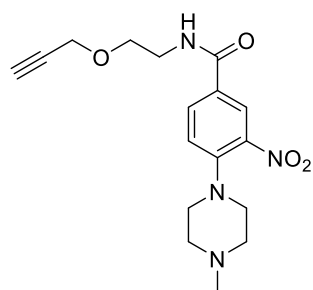
 A solution of **58** (2.70 g, 13.6 mmol) in DCM (68 mL) was treated with 4 M HCl in 1,4-dioxane (25.4 mL, 102 mmol). The reaction mixture was stirred at room temperature for 3 hours. Mixture was concentrated under vacuum to afford HCl salt of title compound as a light-yellow solid (1.84 g, quant). **¹H NMR** (600 MHz, DMSO-d₆): δ 7.91 (br s, 1H), 4.22 (s, 2H), 3.64 (t, *J* = 5.3 Hz, 2H), 3.54 (s, 1H), 3.00 (t, *J* = 5.3 Hz, 2H). Analytical data matches with literature values.^[129]

4-Fluoro-3-nitro-N-(2-(prop-2-yn-1-yloxy)ethyl)benzamide (60)

 4-Fluoro-3-nitrobenzoic acid **29** (3.01 g, 16.3 mmol) was added to thionyl chloride (15 mL) and heated at 79 °C for 6 hours. Mixture was concentrated under vacuum to afford 4-fluoro-3-nitrobenzoyl chloride **30**. To a mixture of **59** (1.84 g, 13.6 mmol) in dry DCM (13.6 mL) was added triethylamine (4.16 mL, 29.8 mmol) followed by **30** (3.31 g, 16.3 mmol) dissolved in dry DCM (13.6 mL) at 0 °C under argon atmosphere. Mixture was stirred at 0 °C for 30 minutes.

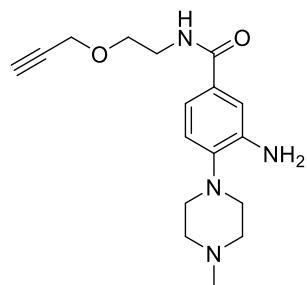
Reaction mixture was subsequently diluted with DCM (200 mL) and washed with H₂O (2 x 150 mL), aqueous 10 mM HCl (2 x 100 mL) then H₂O (100 mL). Organic phase was dried over Na₂SO₄, filtered and concentrated under vacuum for purification by MPLC (PE/EtOAc 1:0 to 0:1) to afford title compound as a yellow oil (3.05 g, 85% over two steps). **¹H NMR** (500 MHz, DMSO-d₆): δ 8.96 (t, *J* = 5.5 Hz, 1H), 8.65 (s, 1H), 8.29 (d, *J* = 8.7 Hz, 1H), 7.72 (d, *J* = 8.7 Hz, 1H), 4.18 (s, 2H), 3.60 (t, *J* = 5.7 Hz, 2H), 3.47 (t, *J* = 5.7 Hz, 2H), 3.45 (s, 1H). **¹³C NMR** (126 MHz, DMSO-d₆): δ 163.8, 157.8 and 155.6 (d, ¹*J*_{C-F} = 266 Hz), 137.1 and 137.0 (d, ²*J*_{C-F} = 8 Hz), 135.7 and 135.6 (d, ²*J*_{C-F} = 10 Hz), 131.6 and 131.5 (d, ³*J*_{C-F} = 4 Hz), 125.8 and 125.8 (d, ³*J*_{C-F} = 2 Hz), 119.4, 119.2, 80.7, 77.8, 68.0, 57.9. **¹⁹F NMR** (470 MHz, DMSO-d₆): δ -115.2. **HRMS-ESI** (m/z): [M + H]⁺ calculated for C₁₂H₁₂O₄N₂F: 267.0776, found: 267.0776.

4-(4-Methylpiperazin-1-yl)-3-nitro-*N*-(2-(prop-2-yn-1-yloxy)ethyl)benzamide (61)



To a solution of **60** (2.00 g, 7.51 mmol) in DMF (14 mL) was added 1-methylpiperazine **32** (1.08 mL, 9.77 mmol) followed by *N,N*-diisopropylethylamine (1.70 mL, 9.77 mmol). The mixture was stirred at room temperature for 1 hour, then diluted with EtOAc (50 mL) and washed with H₂O (3 x 30 mL). Organic phase was dried over Na₂SO₄, filtered, and concentrated under vacuum to afford title compound as a brown-red oil (1.98 g, 76%). **¹H NMR** (600 MHz, DMSO-d₆): δ 8.65 (t, *J* = 5.6 Hz, 1H), 8.31 (s, 1H), 8.02 (d, *J* = 8.8 Hz, 1H), 7.32 (d, *J* = 8.8 Hz, 1H), 4.16 (s, 2H), 3.57 (t, *J* = 5.9 Hz, 2H), 3.45 – 3.41 (m, 3H), 3.09 (t, *J* = 4.9 Hz, 4H), 2.43 (t, *J* = 4.9 Hz, 4H), 2.22 (s, 3H). **¹³C NMR** (151 MHz, DMSO-d₆): δ 164.6, 147.4, 140.4, 132.9, 125.9, 125.8, 120.7, 80.7, 77.7, 68.2, 57.8, 54.7, 50.7, 46.1, 39.5. **HRMS-ESI** (m/z): [M + H]⁺ calculated for C₁₇H₂₃O₄N₄: 347.1714, found: 347.1715.

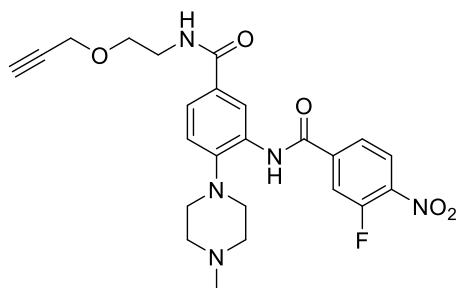
3-Amino-4-(4-methylpiperazin-1-yl)-*N*-(2-(prop-2-yn-1-yloxy)ethyl)benzamide (62)



To a solution of **61** (1.80 g, 5.2 mmol) in EtOAc (40 mL) at room temperature was added tin(II) chloride dihydrate (3.52 g, 15.6 mmol). The mixture was heated at 77 °C with vigorous stirring for 8 hours and subsequently cooled to room temperature. Following dilution with EtOAc (80 mL), the mixture was neutralized with aqueous saturated

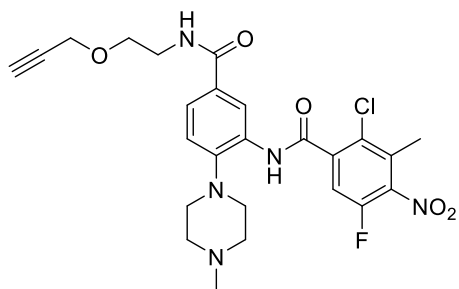
NaHCO₃ (100 mL) and filtered through celite. Residue was washed with EtOAc (5 x 10 mL) and the aqueous phase extracted with EtOAc (50 mL). Combined organic phases were dried over Na₂SO₄, filtered, and concentrated under vacuum to afford title compound as a yellow solid (1.02 g, 62%). **¹H NMR** (500 MHz, DMSO-d₆): δ 8.20 (t, *J* = 5.7 Hz, 1H), 7.17 (s, 1H), 7.06 (d, *J* = 8.2 Hz, 1H), 6.89 (d, *J* = 8.2 Hz, 1H), 4.80 (s, 2H), 4.16 (s, 2H), 3.54 (t, *J* = 6.0 Hz, 2H), 3.45 (s, 1H), 3.39 (t, *J* = 5.7 Hz, 2H), 2.87 – 2.79 (m, 4H), 2.50 – 2.42 (m, 4H), 2.23 (s, 3H). **¹³C NMR** (126 MHz, DMSO-d₆): δ 167.2, 142.2, 141.2, 130.3, 118.6, 116.1, 114.1, 80.8, 77.7, 75.8, 68.3, 57.8, 55.5, 50.3, 39.2. **HRMS-ESI** (*m/z*): [M + H]⁺ calculated for C₁₇H₂₅O₂N₄: 317.1972, found: 317.1974.

4-Fluoro-*N*-(2-(4-methylpiperazin-1-yl)-5-((2-(prop-2-yn-1-yloxy)ethyl)carbamoyl)phenyl)-3-nitrobenzamide (63)



4-Fluoro-3-nitrobenzoic acid **29** (0.28 g, 1.52 mmol) was added to thionyl chloride (1.6 mL) and heated at 79 °C for 6 hours. Mixture was concentrated under vacuum to afford 4-fluoro-3-nitrobenzoyl chloride **30**. To a solution of **62** (0.40 g, 1.26 mmol) in dry DCM (24 mL) was added **30** (0.31 g, 1.52 mmol) dissolved in dry DCM (10 mL) at room temperature under argon atmosphere. Pyridine (0.12 mL, 1.52 mmol) was added and the mixture stirred at room temperature for 18 hours. Reaction mixture was subsequently diluted with DCM (100 mL) and washed with aqueous saturated NaHCO₃ (3 x 70 mL) then brine (70 mL). Organic phase was dried over Na₂SO₄, filtered and concentrated under vacuum for purification by MPLC (DCM, 0-15% MeOH) to afford title compound as a yellow oil (0.17 g, 28% over two steps). **¹H NMR** (500 MHz, DMSO-d₆): δ 10.01 (s, 1H), 8.56 (d, *J* = 7.5 Hz, 1H), 8.50 (t, *J* = 5.7 Hz, 1H), 8.22 (s, 1H), 7.82 (d, *J* = 8.7 Hz, 1H), 7.73 (d, *J* = 8.4 Hz, 1H), 7.67 (d, *J* = 8.7 Hz, 1H), 7.24 (d, *J* = 8.5 Hz, 1H), 4.17 (s, 2H), 3.64 (s, 1H), 3.58 (t, *J* = 6.0 Hz, 2H), 3.46 – 3.43 (m, 2H), 3.00 (t, *J* = 4.8 Hz, 4H), 2.64 – 2.59 (m, 4H), 2.32 (s, 3H). **¹³C NMR** (126 MHz, DMSO-d₆): δ 166.0, 158.1, 149.1, 148.8, 137.3 and 137.2 (d, ²*J*_{C-F} = 10 Hz), 135.8 and 135.8 (d, ²*J*_{C-F} = 8 Hz), 131.7 and 129.5 (d, ¹*J*_{C-F} = 275 Hz), 131.1, 129.5, 127.4, 126.1, 125.8, 125.3, 119.9, 80.8, 77.7, 68.3, 57.8, 55.4, 55.0, 50.8, 45.8. **¹⁹F NMR** (470 MHz, DMSO-d₆): δ -114.9. **HRMS-ESI** (*m/z*): [M + H]⁺ calculated for C₂₄H₂₇O₅N₅F: 484.1991, found: 484.1985.

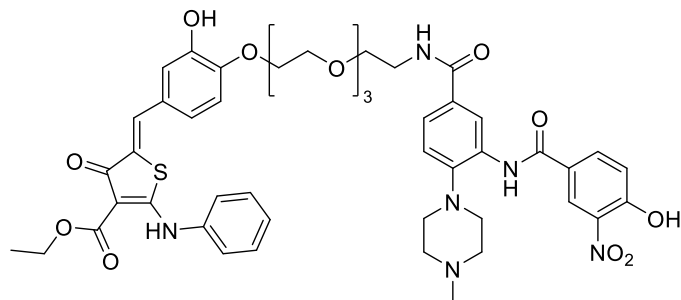
2-Chloro-4-fluoro-3-methyl-N-(2-(4-methylpiperazin-1-yl)-5-((2-(prop-2-yn-1-yloxy)ethyl)carbamoyl)phenyl)-5-nitrobenzamide (64)



2-Chloro-4-fluoro-3-methyl-5-nitrobenzoic acid **42** (0.36 g, 1.52 mmol) was added to thionyl chloride (12.8 mL) and heated at 79 °C for 6 hours. Mixture was concentrated under vacuum to afford 2-chloro-4-fluoro-3-methyl-5-nitrobenzoyl chloride **43**. To a solution of **62** (0.40 g, 1.26 mmol) in dry DCM (24 mL) was added **43** (0.38 g, 1.52 mmol) dissolved in dry DCM (10 mL) at room temperature under argon atmosphere. Pyridine (0.12 mL, 1.52 mmol) was added and the mixture stirred at room temperature for 20 hours. Reaction mixture was subsequently diluted with DCM (100 mL) and washed with aqueous saturated NaHCO₃ (3 x 70 mL) then brine (70 mL). Organic phase was dried over Na₂SO₄, filtered and concentrated under vacuum for purification by MPLC (DCM, 0-15% MeOH) to afford title compound as a yellow oil (0.11 g, 16% over two steps). ¹H NMR (500 MHz, DMSO-d₆): δ 9.86 (s, 1H), 8.50 (t, *J* = 5.7 Hz, 1H), 8.30 – 8.26 (m, 2H), 7.71 (d, *J* = 8.5 Hz, 1H), 7.19 (d, *J* = 8.5 Hz, 1H), 4.17 (s, 2H), 3.64 (s, 1H), 3.58 (t, *J* = 6.0 Hz, 2H), 3.46 – 3.40 (m, 4H), 2.97 (t, *J* = 4.7 Hz, 4H), 2.44 (s, 3H), 2.23 (s, 3H). ¹³C NMR (126 MHz, DMSO-d₆): δ 166.1, 163.5, 148.8, 137.9 and 137.8 (d, ²*J*_{C-F} = 6 Hz), 135.9 and 135.8 (d, ²*J*_{C-F} = 10 Hz), 133.9, 130.7, 129.3, 128.2, 128.1, 128.1, 125.6 and 123.5 (d, ¹*J*_{C-F} = 271 Hz), 125.2, 119.5, 80.8, 77.7, 68.3, 57.8, 55.4, 54.9, 51.2, 46.2, 13.0. ¹⁹F NMR (470 MHz, DMSO-d₆): δ -115.5. HRMS-ESI (m/z): [M + H]⁺ calculated for C₂₅H₂₈O₅N₅ClF: 532.1758, found: 532.1753.

6.10. Synthesis of RITACs

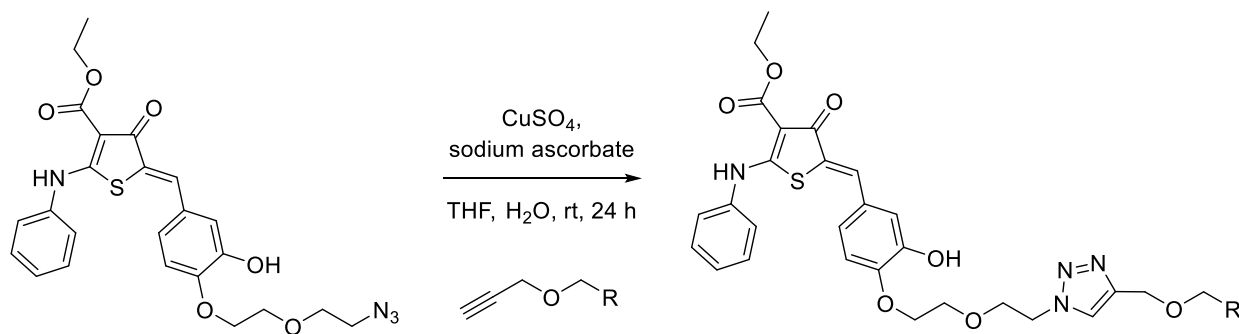
Ethyl (Z)-5-(3-hydroxy-4-((1-(3-(4-hydroxy-3-nitrobenzamido)-4-(4-methylpiperazin-1-yl)phenyl)-1-oxo-5,8,11-trioxa-2-azatriecan-13-yl)oxy)benzylidene)-4-oxo-2-(phenylamino)-4,5-dihydrothiophene-3-carboxylate (65)



A solution of **36** (50.0 mg, 0.12 mmol), HATU (40.8 mg, 0.11 mmol), HOAt (14.6 mg, 0.11 mmol), and *N,N*-diisopropylethylamine (46.8 μ L, 0.27 mmol) in dry DMF (2.8 mL) was stirred for 10 minutes, then a solution of **25** (50.0

mg, 89.5 μ mol) and *N,N*-diisopropylethylamine (46.8 μ L, 0.27 mmol) in dry DMF (1.1 mL) was added. The mixture was stirred at room temperature for 45 hours. Solvent was evaporated by SpeedVac (50 $^{\circ}$ C) for purification by prep. HPLC (H_2O , 5-95% MeCN with 0.1% TFA) and lyophilization to afford TFA salt of title compound as a yellow solid (17.3 mg, 18%). ^1H NMR (700 MHz, DMSO-d_6): δ 11.24 (s, 1H), 9.71 (s, 1H), 9.42 (s, 1H), 9.04 (br s, 1H), 8.53 (s, 1H), 8.46 (t, $J = 4.7$ Hz, 1H), 8.28 (s, 1H), 8.15 (d, $J = 8.7$ Hz, 1H), 7.72 (d, $J = 8.4$ Hz, 1H), 7.56 – 7.51 (m, 4H), 7.49 (s, 1H), 7.46 – 7.44 (m, 1H), 7.28 (t, $J = 8.2$ Hz, 2H), 7.02 – 7.00 (m, 1H), 6.98 (s, 1H), 4.28 (q, $J = 7.1$ Hz, 2H), 4.10 (t, $J = 4.7$ Hz, 2H), 3.73 (t, $J = 4.7$ Hz, 2H), 3.59 – 3.56 (m, 2H), 3.55 – 3.50 (m, 9H), 3.13 – 3.08 (m, 8H), 2.89 – 2.86 (m, 4H), 1.30 (t, $J = 7.1$ Hz, 3H). ^{13}C NMR (176 MHz, DMSO-d_6): δ 181.4, 175.8, 166.0, 165.3, 163.6, 158.4, 158.2, 155.3, 149.2, 147.5, 146.8, 138.0, 137.0, 134.4, 131.8, 130.6, 130.5, 130.1, 128.7, 126.8, 126.1, 125.8, 125.4, 125.3, 125.1, 124.9, 120.5, 119.7, 116.3, 114.3, 97.4, 70.4, 70.3, 70.2, 70.1, 69.4, 69.3, 68.4, 60.0, 48.3, 46.2, 42.9, 14.9. HRMS-ESI (m/z): $[\text{M} + \text{H}]^+$ calculated for $\text{C}_{47}\text{H}_{53}\text{O}_{13}\text{N}_6\text{S}$: 941.3386, found: 941.3395.

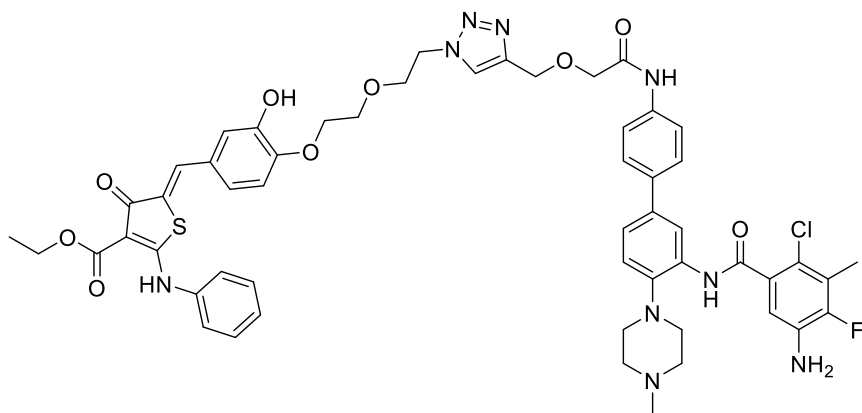
General procedure 7 (GP7): CuAAC conjugation.



28

Thiophenone **28** (96.7 μmol) and alkyne derivative (1.0 equivalent) were suspended in THF (0.125 M) and sonicated to afford a cloudy mixture. An aqueous solution of copper sulfate pentahydrate (0.2 equivalents, 0.2 M, 96.7 μL) and an aqueous solution of (+)-sodium L-ascorbate (0.2 equivalents, 0.2 M, 96.7 μL) were added in that order. The resulting reaction mixture was stirred at room temperature for 24 hours under argon atmosphere. Reaction mixture was diluted with H_2O (0.4 mL) and organic solvent evaporated under vacuum. The aqueous solution was mixed with MeCN/ H_2O (4:1, 3.5 mL) for purification by prep. HPLC ($\text{H}_2\text{O}/\text{MeCN}$, 0.1% TFA) to afford corresponding heterobifunctional molecules.

Ethyl (Z)-5-(4-(2-(2-(4-((2-((3'-(5-amino-2-chloro-4-fluoro-3-methylbenzamido)-4'-(4-methylpiperazin-1-yl)-[1,1'-biphenyl]-4-yl)amino)-2-oxoethoxy)methyl)-1H-1,2,3-triazol-1-yl)ethoxy)ethoxy)-3-hydroxybenzylidene)-4-oxo-2-(phenylamino)-4,5-dihydrothiophene-3-carboxylate (66a)

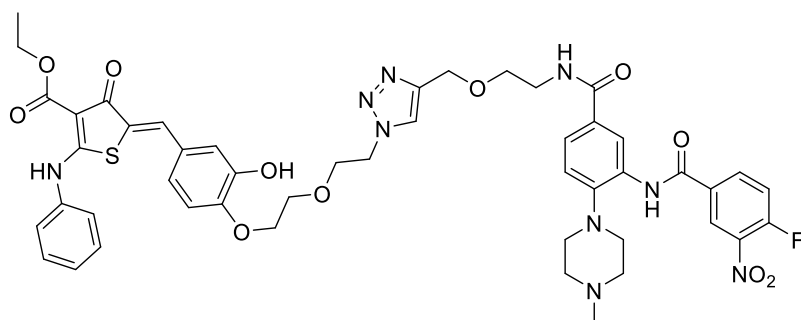


According to GP8. **28** (26.5 mg, 53.4 μmol) was reacted with **55** (30.1 mg, 53.4 μmol), purified by prep. HPLC (H_2O , MeCN 10-60% with 0.1% TFA) and lyophilized to afford TFA salt of title compound as a

yellow solid (12.2 mg, 19%). $^1\text{H NMR}$ (500 MHz, DMSO-d_6): δ 11.24 (s, 1H), 9.89 (s, 1H), 9.49 (br s, 1H), 8.28 (s, 1H), 8.18 (s, 1H), 7.75 (d, $J = 8.3$ Hz, 2H), 7.58 – 7.54 (m, 2H), 7.53 – 7.47 (m, 3H), 7.46 – 7.41 (m, 1H), 7.28 (d, $J = 8.3$ Hz, 1H), 7.00 – 6.96 (m, 3H), 6.85 (d, $J = 9.2$ Hz, 1H), 4.65 (s, 2H), 4.56 (t, $J = 5.2$ Hz, 2H), 4.27 (q, $J = 7.1$ Hz, 2H), 4.11 (s, 2H), 4.09 (t, $J = 5.9$ Hz, 2H), 3.88 (t, $J = 5.2$ Hz, 2H), 3.76 (t, $J = 4.5$ Hz, 2H), 3.55 – 3.50 (m, 2H), 3.28 – 3.16 (m, 4H), 3.03 (t, $J = 11.4$ Hz, 2H), 2.86 (s, 3H), 2.26 (s, 3H), 1.29 (t, $J = 7.0$ Hz, 3H). $^{13}\text{C NMR}$ (126 MHz, DMSO-d_6): δ 181.4, 175.8, 168.4, 166.1, 166.0, 165.3, 159.4, 158.7, 150.5, 149.1, 148.6, 147.5, 143.7, 141.9, 138.6 and 136.7 (d, $^1J_{\text{C-F}} = 251$ Hz), 138.3, 138.0, 133.5, 133.1, 130.5, 130.1, 128.7, 127.1, 126.8, 126.1, 125.2, 125.1, 123.6, 121.5 and 121.3 (d, $^2J_{\text{C-F}} = 31$ Hz), 120.6, 116.6, 116.3 and 116.1 (d, $^2J_{\text{C-F}} = 21$ Hz), 114.1, 108.8, 97.3, 73.0, 69.6, 69.3, 69.0, 68.2, 64.2, 60.0, 53.3, 49.8,

48.8, 48.7, 14.9, 12.5. ^{19}F NMR (470 MHz, DMSO- d_6): δ -131.8. HRMS-ESI (m/z): $[\text{M} + \text{H}]^+$ calculated for $\text{C}_{54}\text{H}_{56}\text{O}_9\text{N}_9\text{ClFS}$: 1060.3589, found: 1060.3599.

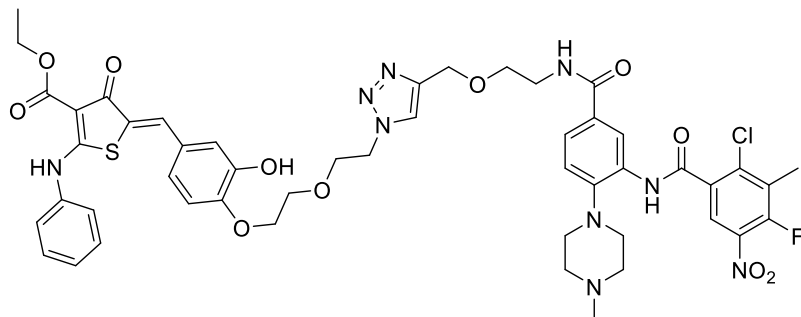
Ethyl (Z)-5-(4-(2-(2-(4-((2-(3-(4-fluoro-3-nitrobenzamido)-4-(4-methylpiperazin-1-yl)benzamido)ethoxy)methyl)-1H-1,2,3-triazol-1-yl)ethoxy)ethoxy)-3-hydroxybenzylidene)-4-oxo-2-(phenylamino)-4,5-dihydrothiophene-3-carboxylate (66b)



According to GP8. **28** (50.0 mg, 0.10 mmol) was reacted with **63** (48.7 mg, 0.10 mmol), purified by prep. HPLC (H_2O , MeCN 10-80% with 0.1% TFA) and lyophilized to afford TFA salt of

title compound as a yellow solid (13.3 mg, 12%). ^1H NMR (500 MHz, DMSO- d_6): δ 11.24 (s, 1H), 10.02 (s, 1H), 9.84 (br s, 1H), 9.48 (br s, 1H), 8.74 – 8.70 (m, 1H), 8.52 (t, $J = 5.6$ Hz, 1H), 8.41 – 8.37 (m, 1H), 8.22 (s, 1H), 8.07 (s, 1H), 7.81 – 7.72 (m, 2H), 7.56 – 7.49 (m, 4H), 7.47 (s, 1H), 7.46 – 7.41 (m, 1H), 7.27 (d, $J = 8.4$ Hz, 1H), 6.99 – 6.95 (m, 3H), 4.54 – 4.46 (m, 4H), 4.27 (q, $J = 7.1$ Hz, 2H), 4.07 (t, $J = 5.8$ Hz, 2H), 3.86 (t, $J = 5.2$ Hz, 2H), 3.74 (t, $J = 5.7$ Hz, 2H), 3.56 – 3.49 (m, 4H), 3.41 – 3.31 (m, 4H), 3.16 – 3.08 (m, 2H), 3.04 (t, $J = 12.2$ Hz, 2H), 2.85 (s, 3H), 1.29 (t, $J = 7.1$ Hz, 3H). ^{13}C NMR (126 MHz, DMSO- d_6): δ 181.4, 175.8, 175.1, 165.9, 165.3, 163.1, 155.9, 149.1, 147.5, 144.2, 141.4, 138.0, 137.1, 136.1, 131.8, 131.3, 130.5 and 130.3 (d, $^2J_{\text{C-F}} = 27$ Hz), 130.1, 128.7, 126.8, 126.5, 126.1, 125.8, 125.1 and 124.9 (d, $^2J_{\text{C-F}} = 26$ Hz), 123.6, 120.4, 119.6, 117.8, 116.9, 116.3 and 114.2 (d, $^1J_{\text{C-F}} = 265$ Hz), 106.0, 97.3, 69.3, 69.0, 68.6, 68.2, 65.4, 63.7, 60.0, 53.4, 49.7, 48.2, 42.8, 14.9. ^{19}F NMR (470 MHz, DMSO- d_6): δ -114.4. HRMS-ESI (m/z): $[\text{M} + \text{H}]^+$ calculated for $\text{C}_{48}\text{H}_{51}\text{O}_{11}\text{N}_9\text{FS}$: 980.3407, found: 980.3418.

Ethyl (Z)-5-(4-(2-(2-(4-((2-(3-(2-chloro-4-fluoro-3-methyl-5-nitrobenzamido)-4-(4-methylpiperazin-1-yl)benzamido)ethoxy)methyl)-1H-1,2,3-triazol-1-yl)ethoxy)ethoxy)-3-hydroxybenzylidene)-4-oxo-2-(phenylamino)-4,5-dihydrothiophene-3-carboxylate (66c)

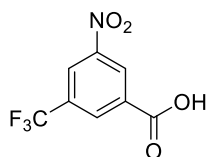


According to GP8. Purification by prep. HPLC (H₂O, MeCN 10-80% with 0.1% TFA) and lyophilized to afford TFA salt of title compound as a yellow solid (46.5 mg, 42%). ¹H NMR (500

MHz, DMSO-d₆): δ 11.25 (s, 1H), 9.91 (s, 1H), 9.48 (br s, 1H), 8.53 (t, *J* = 5.7 Hz, 1H), 8.41 (s, 1H), 8.38 (d, *J* = 7.6 Hz, 1H), 8.07 (s, 1H), 7.70 (d, *J* = 8.4 Hz, 2H), 7.56 – 7.49 (m, 4H), 7.48 – 7.42 (m, 2H), 7.23 (d, *J* = 8.4 Hz, 1H), 6.99 – 6.91 (m, 3H), 4.55 – 4.49 (m, 4H), 4.27 (q, *J* = 7.1 Hz, 2H), 4.07 (t, *J* = 4.4 Hz, 2H), 3.86 (t, *J* = 5.2 Hz, 2H), 3.74 (t, *J* = 4.4 Hz, 2H), 3.56 – 3.48 (m, 4H), 3.44 – 3.34 (m, 4H), 3.20 – 3.12 (m, 1H), 3.03 (t, *J* = 12.0 Hz, 2H), 2.84 (s, 3H), 1.29 (t, *J* = 7.1 Hz, 3H). ¹³C NMR (126 MHz, DMSO-d₆): δ 181.5, 175.8, 166.0, 165.3, 163.6, 158.8, 158.5, 154.5, 152.4, 149.1, 147.5, 146.2, 144.2, 140.4, 138.0, 136.0, 134.1, 131.2, 130.5, 130.3, 130.1, 128.7, 128.0, 126.8, 126.1, 125.2, 125.1 and 124.9 (d, ²*J*_{C-F} = 23 Hz), 124.5, 123.6 and 123.4 (d, ²*J*_{C-F} = 24 Hz), 120.1, 116.2 and 114.1 (d, ¹*J*_{C-F} = 266 Hz), 97.3, 69.3, 69.0, 68.6, 68.2, 63.7, 60.0, 55.4, 53.1, 49.7, 48.3, 42.8, 14.9, 13.0. ¹⁹F NMR (470 MHz, DMSO-d₆): δ -115.7. HRMS-ESI (m/z): [M + H]⁺ calculated for C₄₉H₅₂O₁₁N₉ClF: 1028.3174, found: 1028.3188.

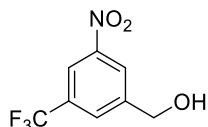
6.11. Synthesis of HIV TAR Ligands

3-Nitro-5-(trifluoromethyl)benzoic acid (68)



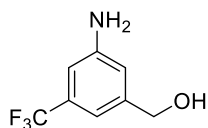
Fuming nitric acid (2.20 mL, 34.5 mmol) was added dropwise into a mixture of 3-trifluoromethylbenzoic acid **67** (2.00 g, 10.5 mmol) and concentrated sulfuric acid (10 mL) under vigorous stirring at 0 °C. The reaction mixture was stirred at room temperature for 3 hours and then poured in ice-cold H₂O (100 mL). Precipitate was collected by filtration and washed with H₂O (40 mL). Solids were redissolved in EtOAc (20 mL) and washed with H₂O (2 x 20 mL) then brine (20 mL). Organic phase was dried over Na₂SO₄ and concentrated under vacuum to afford title compound as a light-yellow solid (1.94 g, 78%). ¹H NMR (500 MHz, CDCl₃): δ 9.13 (s, 1H), 8.76 (s, 1H), 8.70 (s, 1H). Analytical data matches with literature values.^[391]

(3-Nitro-5-(trifluoromethyl)phenyl)methanol (69)



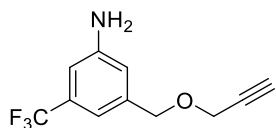
68 (1.70 g, 7.23 mmol) was dissolved in dry THF (20.4 mL) and cooled to 0 °C under argon atmosphere. A solution of 1 M borane THF complex solution in THF (14.5 mL, 14.5 mmol) was added dropwise. After stirring at 0 °C for 3 hours reaction mixture was allowed to warm to room temperature and stirred for another 18 hours. Reaction was quenched by the slow addition of aqueous saturated NaHCO₃ (50 mL), then extracted with EtOAc (2 x 50 mL). Combined organic phases were washed with H₂O (100 mL) then brine (100 mL), dried over Na₂SO₄, filtered and concentrated under vacuum to afford title compound as a yellow oil (1.60 g, quant). **¹H NMR** (500 MHz, CDCl₃): δ 8.44 (s, 1H), 8.41 (s, 1H), 7.99 (s, 1H), 4.91 (s, 2H). **LCMS-ESI** (m/z): 222.1 [M + H]⁺. Analytical data matches with literature values.^[392]

(3-Amino-5-(trifluoromethyl)phenyl)methanol (**70**)



69 (1.00 g, 4.52 mmol) in anhydrous MeOH (12.8 mL) was flushed with argon and treated with 10% palladium on activated charcoal (0.10 g, 94.0 μmol). The flask was flushed with hydrogen and allowed to stir under hydrogen atmosphere at room temperature for 18 hours. The reaction mixture was flushed with argon, filtered through celite and concentrated under vacuum to afford title compound as an oil (0.81 g, 93%). **¹H NMR** (500 MHz, CDCl₃): δ 6.98 (s, 1H), 6.84 (s, 1H), 6.82 (s, 1H), 4.66 (s, 2H), 3.87 (br s, 2H). **LCMS-ESI** (m/z): 192.0 [M + H]⁺. Analytical data matches with literature values.^[393]

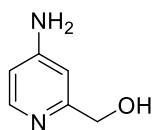
3-((Prop-2-yn-1-yloxy)methyl)-5-(trifluoromethyl)aniline (**71**)



70 (0.70 g, 3.66 mmol) in dry THF (14.6 mL) was added dropwise to 60% sodium hydride dispersion in mineral oil (0.18 g, 4.39 mmol) at 0 °C and stirred for 30 minutes under argon atmosphere. 80% Propargyl bromide **57** in toluene (0.48 mL, 4.39 mmol) was added dropwise and resulting mixture stirred at room temperature for 19 hours. Reaction was quenched with addition of H₂O (15 mL) and extracted with EtOAc (2 x 15 mL). Combined organic phases were dried over Na₂SO₄, filtered and concentrated under vacuum for purification by MPLC (PE/EtOAc 1:0 to 3:2) to afford title compound as a yellow oil (0.67 g, 80%). **¹H NMR** (500 MHz, CDCl₃): δ 6.98 (s, 1H), 6.85 (s, 1H), 6.84 (s, 1H), 4.56 (s, 2H), 4.20 (s, 2H), 2.48 (s, 1H). **¹³C NMR** (126 MHz, CDCl₃): δ 146.7, 139.6, 132.2 and 132.0 and 131.7 and 131.4 (q, ²J_{C-F} = 32 Hz), 127.3 and 125.1 and 123.0 and

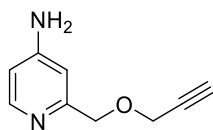
120.8 (q, $^1J_{\text{C-F}} = 272$ Hz), 117.2, 114.6 and 114.6 and 114.6 and 114.5 (q, $^3J_{\text{C-F}} = 4$ Hz), 111.1 and 111.0 and 111.0 and 111.0 (q, $^3J_{\text{C-F}} = 4$ Hz), 79.3, 75.0, 70.9, 57.4. **^{19}F NMR** (470 MHz, CDCl_3): δ -62.9. **HRMS-ESI** (m/z): $[\text{M} + \text{H}]^+$ calculated for $\text{C}_{11}\text{H}_{11}\text{ON}_4\text{F}_3$: 230.0787, found: 230.0791.

(4-Aminopyridin-2-yl)methanol (73)



To lithium aluminum hydride (0.62 g, 16.4 mmol) was slowly added dry THF (6 mL) at 0 °C under argon atmosphere. To the mixture was slowly added methyl-4-aminopicolinate **72** (1.00 g, 6.57 mmol) in dry THF (28 mL) at 0 °C. The reaction mixture was heated at 50 °C for 18 hours. Reaction mixture was cooled to 0 °C and quenched by sequential addition of H_2O (0.6 mL), 15% aqueous NaOH (0.6 mL) and H_2O (1.9 mL). Mixture was stirred at room temperature before filtration through celite and residue washed with THF (20 mL), water (20 mL) then MeOH (10 mL). Organic solvents were removed under vacuum and aqueous phase saturated with sodium chloride, then extracted with EtOAc (3 x 100 mL) then DCM (2 x 100 mL). Combined organic phases were dried over Na_2SO_4 , filtered and concentrated under vacuum to afford title compound as a light-yellow solid (0.69 g, 85%). **^1H NMR** (400 MHz, DMSO-d_6): δ 7.84 (d, $J = 5.5$ Hz, 1H), 6.57 (s, 1H), 6.28 (d, $J = 5.6$ Hz, 1H), 5.91 (s, 2H), 5.08 (s, 1H), 4.31 (s, 2H). **LCMS-ESI** (m/z): 125.2 $[\text{M} + \text{H}]^+$. Analytical data matches with literature values.^[394]

2-((Prop-2-yn-1-yloxy)methyl)pyridin-4-amine (74)

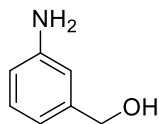


73 (0.50 g, 4.03 mmol) in dry THF (16.2 mL) was added dropwise to 60% sodium hydride dispersion in mineral oil (0.19 g, 4.83 mmol) at 0 °C and stirred for 30 minutes under argon atmosphere. 80% Propargyl bromide **57** in toluene (0.53 mL, 4.83 mmol) was added dropwise and resulting mixture stirred at room temperature for 17 hours. Reaction was quenched with addition of H_2O (10 mL) and extracted with EtOAc (2 x 20 mL) then DCM (20 mL). Combined organic phases were dried over Na_2SO_4 , filtered and concentrated under vacuum for purification by MPLC (DCM, 0-20% MeOH) to afford title compound as a brown oil (0.25 g, 38%). **^1H NMR** (700 MHz, DMSO-d_6): δ 7.90 (d, $J = 5.6$ Hz, 1H), 6.54 (s, 1H), 6.36 (d, $J = 5.6$ Hz, 1H), 6.01 (s, 2H), 4.38 (s, 2H), 4.22 (s, 2H), 3.47 (s, 1H).

^{13}C NMR (176 MHz, DMSO- d_6): δ 157.8, 155.3, 149.3, 108.1, 106.4, 80.7, 77.8, 72.5, 57.7.

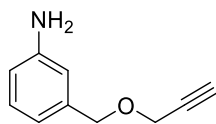
HRMS-ESI (m/z): $[\text{M} + \text{H}]^+$ calculated for $\text{C}_9\text{H}_{11}\text{ON}_2$: 163.0866, found: 163.0867.

3-Aminobenzyl alcohol (76)

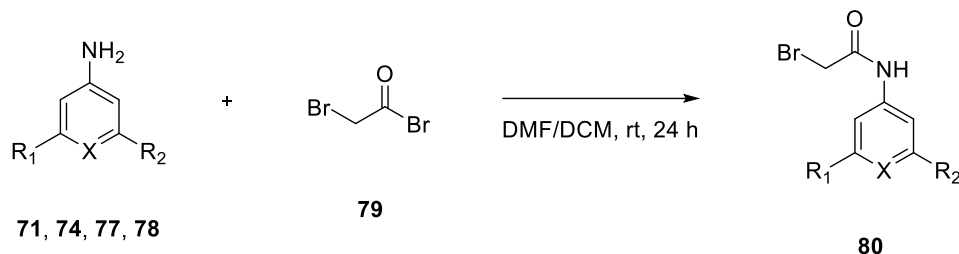


To lithium aluminum hydride (0.42 g, 11.1 mmol) was slowly added dry THF (5 mL) at 0 °C under argon atmosphere. To the mixture was slowly added 3-aminobenzoic acid **75** (1.00 g, 7.29 mmol) in dry THF (25 mL) at 0 °C. The reaction mixture was stirred vigorously at 66 °C for 17 hours. Reaction mixture was cooled to 0 °C and quenched by sequential addition of H_2O (0.4 mL), 15% aqueous NaOH (0.4 mL) and H_2O (1.3 mL). Mixture was stirred at room temperature before filtration through celite and residue washed with H_2O (10 mL). Filtrate was extracted with EtOAc (2 x 15 mL). Combined organic phases were dried over Na_2SO_4 , filtered and concentrated under vacuum to afford title compound as a brown solid (0.84 g, 93%). ^1H NMR (500 MHz, CDCl_3): δ 7.15 (t, $J = 7.7$ Hz, 1H), 6.74 (d, $J = 7.5$ Hz, 1H), 6.72 (s, 1H), 6.62 (d, $J = 7.9$ Hz, 2H), 4.61 (s, 2H). LCMS-ESI (m/z): 124.1 $[\text{M} + \text{H}]^+$. Analytical data matches with literature values.^[395]

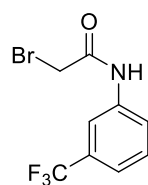
3-((Prop-2-yn-1-yloxy)methyl)aniline (77)



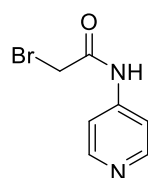
76 (0.70 g, 5.68 mmol) in dry THF (22.7 mL) was added dropwise to 60% sodium hydride dispersion in mineral oil (0.27 g, 6.82 mmol) at 0 °C and stirred for 30 minutes under argon atmosphere. 80% Propargyl bromide **57** in toluene (0.75 mL, 6.82 mmol) was added dropwise and resulting mixture stirred at room temperature for 21 hours. Reaction was quenched with addition of H_2O (25 mL) and extracted with EtOAc (2 x 25 mL). Combined organic phases were dried over Na_2SO_4 , filtered and concentrated under vacuum for purification by MPLC (PE/EtOAc 1:0 to 3:2) to afford title compound as a yellow oil (0.70 g, 76%). ^1H NMR (700 MHz, CDCl_3): δ 7.14 (t, $J = 7.7$ Hz, 1H), 6.75 (d, $J = 7.6$ Hz, 1H), 6.71 (s, 1H), 6.64 (d, $J = 8.0$ Hz, 2H), 4.53 (s, 2H), 4.16 (s, 2H), 2.46 (s, 1H). ^{13}C NMR (176 MHz, CDCl_3): δ 146.4, 138.5, 129.4, 118.5, 114.8, 114.7, 79.8, 74.5, 71.5, 57.0. HRMS-ESI (m/z): $[\text{M} + \text{H}]^+$ calculated for $\text{C}_{10}\text{H}_{12}\text{ON}$: 162.0913, found: 162.0913.

General procedure 8 (GP8): Synthesis of bromoacetamides.

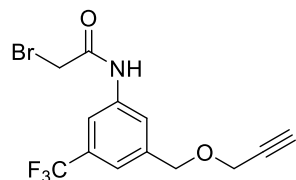
To a stirred solution of aniline derivative **71**, **74**, **77** or **78** (1.74 mmol) in dry DCM or DMF (0.42 M) at 0 °C was added bromoacetyl bromide **79** (2.0 equivalents) dropwise under argon atmosphere. Reaction mixture was stirred at room temperature for 24 hours. Precipitation in Et₂O afforded corresponding bromoacetamides.

2-Bromo-N-(3-(trifluoromethyl)phenyl)acetamide (80a)

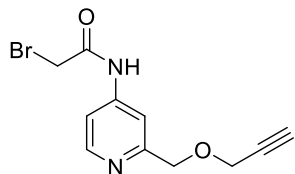
According to GP8. 3-(Trifluoromethyl)aniline **78a** (0.27 mL, 2.13 mmol) was reacted with **79** (0.37 mL, 4.26 mmol) in DCM. Precipitation in Et₂O (20 mL) was collected to afford title compound as a white solid. LCMS-ESI (m/z): 282.0 [M + H]⁺. Analytical data matches with literature values.^[365]

2-Bromo-N-(pyridin-4-yl)acetamide (80b)

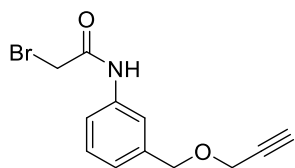
According to GP8. 4-Aminopyridine **78b** (0.20 g, 2.13 mmol) was reacted with **79** (0.37 mL, 4.26 mmol) in DMF. Precipitation in DCM (40 mL) gave product in supernatant, which was further precipitated in Et₂O (200 mL). Product was observed in pellet, which was collected to afford title compound as a brown solid. LCMS-ESI (m/z): 215.0 [M + H]⁺. Analytical data matches with literature values.^[365]

2-Bromo-N-(3-((prop-2-yn-1-yloxy)methyl)-5-(trifluoromethyl)phenyl)acetamide (80c)

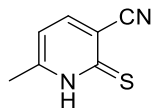
According to GP8. **71** (0.40 g, 1.75 mmol) was reacted with **79** (0.30 mL, 3.50 mmol) in DCM. Precipitation in Et₂O (24 mL) gave product in supernatant, which was concentrated under vacuum to afford title compound as a yellow oil. HRMS-ESI (m/z): [M + H]⁺ calculated for C₁₃H₁₂O₂NBrF₃: 349.9998, found: 350.0001.

2-Bromo-N-(2-((prop-2-yn-1-yloxy)methyl)pyridin-4-yl)acetamide (80d)

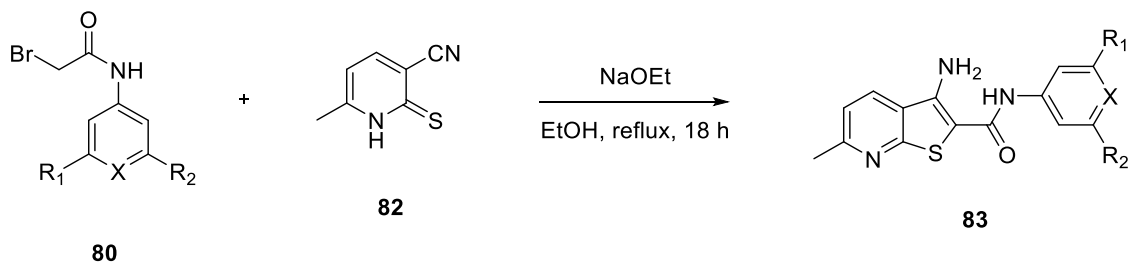
According to GP8. **74** (0.23 g, 1.42 mmol) was reacted with **79** (0.25 mL, 2.84 mmol) in DMF. Precipitation in DCM (32 mL) gave product in supernatant, which was further precipitated in Et₂O (160 mL). Product was observed in pellet, which was collected to afford title compound as a brown solid. **HRMS**-ESI (m/z): [M + H]⁺ calculated for C₁₁H₁₂O₂N₂Br: 283.0077, found: 283.0081.

2-Bromo-N-(3-((prop-2-yn-1-yloxy)methyl)phenyl)acetamide (80e)

According to GP8. **77** (0.28 g, 1.74 mmol) was reacted with **79** (0.30 mL, 3.48 mmol) in DCM. Precipitation in Et₂O (20 mL) gave product in supernatant, which was concentrated under vacuum to afford title compound as a brown oil. **HRMS**-ESI (m/z): [M + H]⁺ calculated for C₁₂H₁₃O₂NBr: 282.0124, found: 282.0130.

6-Methyl-2-thioxo-1,2-dihydropyridine-3-carbonitrile (82)

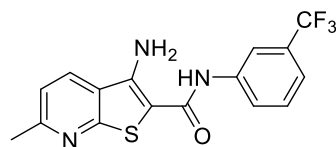
A mixture of 2-chloro-6-methylnicotinonitrile **81** (2.00 g, 13.1 mmol), and thiourea (3.16 g, 41.6 mmol) in *n*-butanol (33 mL) was heated at 118 °C for 3 hours. After cooling to room temperature, the formed precipitate was collected by filtration and rinsed with cold *n*-butanol (25 mL) to afford title compound as a yellow solid (1.97 g, quant). **¹H NMR** (700 MHz, DMSO-d₆): δ 14.10 (s, 1H), 8.00 (d, *J* = 7.7 Hz, 1H), 6.73 (d, *J* = 8.0 Hz, 1H), 2.39 (s, 3H). **LCMS**-ESI (m/z): 151.1 [M + H]⁺. Analytical data matches with literature values.^[365]

General procedure 9 (GP9): Thienopyridine formation.

To a suspension of **82** (1.06 equivalents) in anhydrous EtOH (0.16 M) was added bromoacetamide derivative **80** (1.07 mmol) and 21% sodium ethoxide in EtOH (2.2 equivalents). Reaction mixture

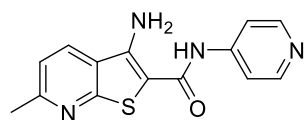
was heated at 78 °C for 18 hours in a closed vial. Mixture was concentrated under vacuum for purification by MPLC (PE/EtOAc 1:0 to 0:1) to afford corresponding thienopyridines.

3-Amino-6-methyl-*N*-(3-(trifluoromethyl)phenyl)thieno[2,3-*b*]pyridine-2-carboxamide (83a)



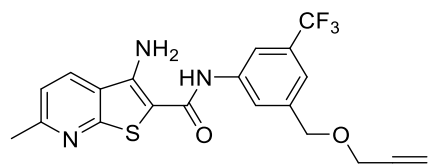
According to GP9. Title compound afforded as a yellow solid (11.2 mg, <10% over two steps). $^1\text{H NMR}$ (500 MHz, DMSO- d_6): δ 9.71 (s, 1H), 8.41 (d, $J = 8.3$ Hz, 1H), 8.23 (s, 1H), 7.99 (d, $J = 8.2$ Hz, 1H), 7.56 (t, $J = 8.0$ Hz, 1H), 7.49 (s, 2H), 7.41 (d, $J = 8.0$ Hz, 1H), 7.35 (d, $J = 8.4$ Hz, 1H), 2.61 (s, 3H). **LCMS-ESI** (m/z): 352.0 [$M + H$] $^+$. Analytical data matches with literature values.^[365]

3-Amino-6-methyl-*N*-(pyridin-4-yl)thieno[2,3-*b*]pyridine-2-carboxamide (83b)



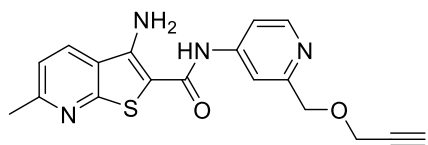
According to GP9. **80b** (68.8 mg, 0.32 mmol) was reacted with **82** (51.1 mg, 0.34 mmol). Title compound afforded as a yellow solid (86.7 mg, 90% over two steps). $^1\text{H NMR}$ (700 MHz, DMSO- d_6): δ 9.73 (s, 1H), 8.44 – 8.41 (m, 3H), 7.77 (d, $J = 6.5$ Hz, 2H), 7.54 (s, 2H), 7.36 (d, $J = 8.3$ Hz, 1H), 2.61 (s, 3H). **LCMS-ESI** (m/z): 285.1 [$M + H$] $^+$. Analytical data matches with literature values.^[365]

3-Amino-6-methyl-*N*-(3-((prop-2-yn-1-yloxy)methyl)-5-(trifluoromethyl)phenyl)thieno[2,3-*b*]pyridine-2-carboxamide (83c)



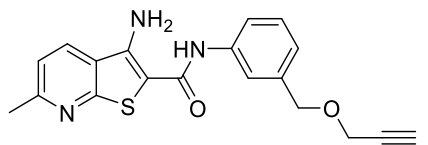
According to GP9. Purification by MPLC (PE, 5-60% EtOAc) to afford title compound as a light-yellow solid (0.10 g, 23% over two steps). $^1\text{H NMR}$ (500 MHz, DMSO- d_6): δ 10.72 (s, 1H), 8.12 (d, $J = 7.9$ Hz, 1H), 7.99 (s, 1H), 7.77 (s, 1H), 7.36 (s, 1H), 7.19 (d, $J = 7.9$ Hz, 1H), 4.60 (s, 2H), 4.24 (s, 2H), 4.21 (s, 2H), 3.54 (s, 1H), 2.43 (s, 1H). $^{13}\text{C NMR}$ (126 MHz, DMSO- d_6): δ 167.2, 162.9, 160.4, 142.2, 140.7, 140.3, 130.1, 129.9, 127.8, 125.6, 123.4, 121.7, 119.8, 119.0, 116.3, 114.7, 103.4, 80.4, 78.2, 70.3, 57.7, 35.2, 24.9. $^{19}\text{F NMR}$ (470 MHz, DMSO- d_6): δ -61.4. **HRMS-ESI** (m/z): [$M + H$] $^+$ calculated for $\text{C}_{20}\text{H}_{17}\text{O}_2\text{N}_4\text{F}_3\text{S}$: 420.0988, found: 420.0989.

3-Amino-6-methyl-N-(2-((prop-2-yn-1-yloxy)methyl)pyridin-4-yl)thieno[2,3-*b*]pyridine-2-carboxamide (83d)



According to GP9. **80d** (0.37 g, 1.30 mmol) was reacted with **82** (0.21 g, 1.38 mmol). Purification by MPLC (DCM, 0-10% MeOH) to afford title compound as a yellow solid (0.17 g, 37% over two steps). **¹H NMR** (700 MHz, DMSO-*d*₆): δ 10.80 (s, 1H), 8.39 (d, *J* = 5.6 Hz, 1H), 8.11 (d, *J* = 7.9 Hz, 1H), 7.65 (s, 1H), 7.53 (d, *J* = 5.6 Hz, 1H), 7.18 (d, *J* = 7.9 Hz, 1H), 4.57 (s, 2H), 4.28 (s, 2H), 4.21 (s, 2H), 3.51 (s, 1H), 2.42 (s, 3H). **¹³C NMR** (176 MHz, DMSO-*d*₆): δ 167.8, 162.9, 160.3, 158.8, 149.9, 147.1, 142.2, 119.8, 116.3, 112.5, 110.8, 103.4, 80.4, 78.1, 71.9, 58.0, 35.4, 24.9. **HRMS-ESI** (*m/z*): [*M* + *H*]⁺ calculated for C₁₈H₁₇O₂N₄S: 353.1067, found: 353.1070.

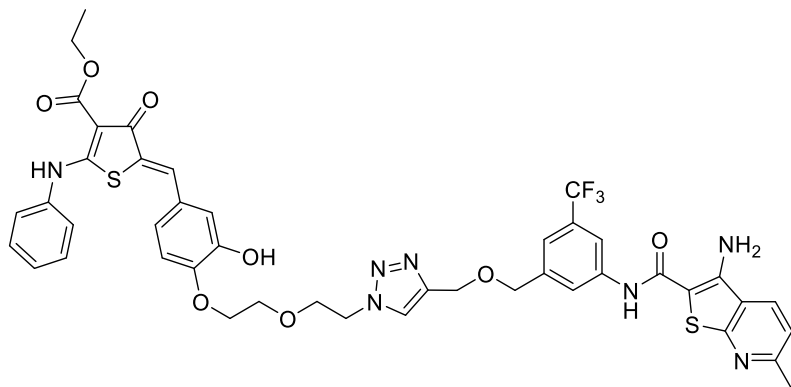
3-Amino-6-methyl-N-(3-((prop-2-yn-1-yloxy)methyl)phenyl)thieno[2,3-*b*]pyridine-2-carboxamide (83e)



According to GP9. Purification by MPLC (PE, 20-50% EtOAc) afforded title compound as a white solid (0.20 g, 58% over two steps). **¹H NMR** (500 MHz, DMSO-*d*₆): δ 10.36 (s, 1H), 8.11 (d, *J* = 7.9 Hz, 1H), 7.59 (s, 1H), 7.51 (d, *J* = 8.1 Hz, 1H), 7.30 (t, *J* = 7.8 Hz, 1H), 7.19 (d, *J* = 7.9 Hz, 1H), 7.01 (d, *J* = 7.6 Hz, 1H), 4.49 (s, 2H), 4.19 (s, 2H), 4.18 (s, 2H), 3.51 (s, 1H), 2.46 (s, 3H). **¹³C NMR** (126 MHz, DMSO-*d*₆): δ 166.5, 162.9, 160.5, 142.1, 139.5, 138.7, 129.3, 123.1, 119.8, 118.8, 118.8, 116.3, 103.4, 80.6, 78.0, 71.1, 57.3, 35.2, 25.0. **HRMS-ESI** (*m/z*): [*M* + *H*]⁺ calculated for C₁₉H₁₈O₂N₃S: 352.1114, found: 352.1117.

6.12. Synthesis of RIBOTACs

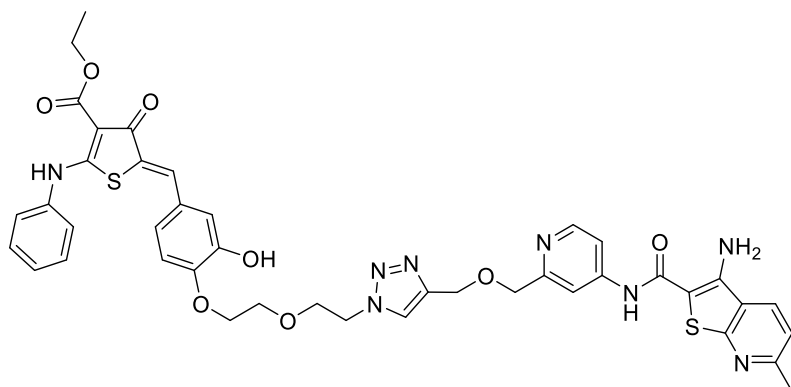
Ethyl (Z)-5-(4-(2-(2-(4-(((3-(3-amino-6-methylthieno[2,3-*b*]pyridine-2-carboxamido)-5-(trifluoromethyl)benzyl)oxy)methyl)-1*H*-1,2,3-triazol-1-yl)ethoxy)ethoxy)-3-hydroxybenzylidene)-4-oxo-2-(phenylamino)-4,5-dihydrothiophene-3-carboxylate (84a)



According to GP7. **28** (54.9 mg, 0.11 mmol) was reacted with **83c** (46.4 mg, 0.11 mmol), purified by prep. HPLC (H₂O, MeCN 20-80% with 0.1% TFA) and lyophilized to afford TFA salt of title compound as a yellow solid (50.8 mg, 45%). ¹H NMR (500

MHz, DMSO-d₆): δ 11.24 (s, 1H), 10.68 (s, 1H), 9.46 (br s, 1H), 8.12 (s, 1H), 8.09 (d, *J* = 7.9 Hz, 1H), 7.97 (s, 1H), 7.73 (s, 1H), 7.54 – 7.48 (m, 4H), 7.47 (s, 1H), 7.45 – 7.41 (m, 1H), 7.30 (s, 1H), 7.15 (d, *J* = 8.0 Hz, 1H), 6.98 – 6.94 (m, 3H), 4.58 – 4.54 (m, 6H), 4.27 (q, *J* = 7.1 Hz, 2H), 4.18 (s, 2H), 4.08 (t, *J* = 4.5 Hz, 2H), 3.88 (t, *J* = 5.2 Hz, 2H), 3.76 (t, *J* = 4.5 Hz, 2H), 2.40 (s, 3H), 1.29 (t, *J* = 7.1 Hz, 3H). ¹³C NMR (126 MHz, DMSO-d₆): δ 181.4, 175.8, 167.1, 165.4, 162.9, 160.4, 149.1, 147.5, 146.5, 145.2, 143.9, 142.1, 141.2, 140.3, 138.0, 130.5, 130.1, 129.8, 128.6, 126.8, 126.1, 125.1, 125.1, 123.5, 121.5, 119.8, 118.8, 118.8, 118.7, 116.3, 114.6, 114.1, 103.4, 97.3, 70.6, 69.3, 69.0, 68.2, 63.5, 60.0, 49.8, 35.2, 24.9, 14.9. ¹⁹F NMR (470 MHz, DMSO-d₆): δ -61.4. HRMS-ESI (m/z): [M + H]⁺ calculated for C₄₄H₄₁O₈N₇F₃S₂: 916.2405, found: 916.2410.

Ethyl (Z)-5-(4-(2-(2-(4-(((4-(3-amino-6-methylthieno[2,3-*b*]pyridine-2-carboxamido)pyridin-2-yl)methoxy)methyl)-1*H*-1,2,3-triazol-1-yl)ethoxy)ethoxy)-3-hydroxybenzylidene)-4-oxo-2-(phenylamino)-4,5-dihydrothiophene-3-carboxylate (84b)

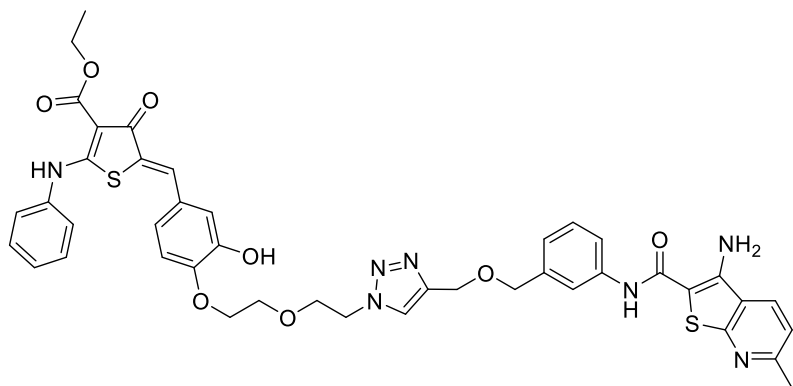


According to GP7. **28** (44.0 mg, 88.5 μmol) was reacted with **83d** (31.2 mg, 88.5 μmol), purified by prep. HPLC (H₂O, MeCN 10-60% with 0.1% TFA) and lyophilized to afford TFA salt of title compound as a yellow solid (28.9 mg, 34%). ¹H NMR (500

MHz, DMSO-d₆): δ 11.44 (s, 1H), 11.24 (s, 1H), 9.50 (br s, 1H), 8.51 (d, *J* = 6.4 Hz, 1H), 8.15 (s, 1H), 8.10 (d, *J* = 7.9 Hz, 1H), 7.85 (s, 1H), 7.78 (d, *J* = 6.4 Hz, 1H), 7.56 – 7.49 (m, 4H), 7.46 –

7.41 (m, 2H), 7.16 (d, $J = 7.9$ Hz, 1H), 6.97 – 6.92 (m, 3H), 4.70 (s, 2H), 4.65 (s, 2H), 4.55 (t, 2H), 4.27 (q, 2H), 4.24 (s, 2H), 4.08 (m, 2H), 3.87 (t, 2H), 3.76 (m, 2H), 2.36 (s, 3H), 1.29 (t, 3H). ^{13}C NMR (126 MHz, DMSO- d_6): δ 181.4, 175.8, 168.8, 165.3, 162.9, 160.0, 158.7, 149.1, 147.5, 143.4, 142.2, 138.0, 130.4, 130.1, 128.7, 126.8, 126.1, 125.4, 125.1, 123.5, 119.9, 116.3, 116.2, 114.1, 113.2, 111.6, 103.4, 97.3, 69.2, 69.0, 68.2, 64.1, 60.0, 49.8, 35.6, 24.8, 14.9. HRMS-ESI (m/z): $[\text{M} + \text{H}]^+$ calculated for $\text{C}_{42}\text{H}_{41}\text{O}_8\text{N}_8\text{S}_2$: 849.2483, found: 849.2491.

Ethyl (Z)-5-(4-(2-(2-(4-((3-(3-aminobenzo[*b*]thiophene-2-carboxamido)phenethoxy)methyl)-1*H*-1,2,3-triazol-1-yl)ethoxy)ethoxy)-3-hydroxybenzylidene)-4-oxo-2-(phenylamino)-4,5-dihydrothiophene-3-carboxylate (84c)



According to GP7. **28** (54.8 mg, 0.11 mmol) was reacted with **83e** (38.8 mg, 0.11 mmol), purified by prep. HPLC (H_2O , MeCN 10-60% with 0.1% TFA) and lyophilized to afford TFA salt of title compound as a yellow solid (51.3 mg, 48%). ^1H NMR (500

MHz, DMSO- d_6): δ 11.24 (s, 1H), 10.33 (s, 1H), 9.45 (br s, 1H), 8.09 – 8.06 (m, 2H), 7.56 – 7.46 (m, 7H), 7.45 – 7.41 (m, 1H), 7.24 (t, $J = 7.8$ Hz, 1H), 7.15 (d, $J = 7.9$ Hz, 1H), 6.98 – 6.95 (m, 4H), 4.54 (t, $J = 5.1$ Hz, 2H), 4.51 (s, 2H), 4.45 (s, 2H), 4.27 (q, $J = 7.1$ Hz, 2H), 4.16 (s, 2H), 4.07 (t, $J = \text{Hz}$, 2H), 3.88 (t, $J = 5.2$ Hz, 2H), 3.75 (t, $J = 4.5$ Hz, 2H), 2.42 (s, 3H), 1.29 (t, $J = 7.1$ Hz, 3H). ^{13}C NMR (126 MHz, DMSO- d_6): δ 181.4, 175.8, 171.6, 166.4, 165.3, 162.9, 160.5, 149.1, 147.5, 144.1, 142.1, 139.5, 139.3, 138.0, 130.6, 130.1, 129.2, 128.7, 126.8, 126.1, 125.4, 125.1, 124.9, 123.6, 123.0, 119.7, 118.7, 116.3, 114.2, 103.4, 97.3, 71.5, 69.3, 69.0, 68.2, 63.3, 60.0, 49.8, 35.2, 24.9, 14.9. HRMS-ESI (m/z): $[\text{M} + \text{H}]^+$ calculated for $\text{C}_{43}\text{H}_{42}\text{O}_8\text{N}_7\text{S}_2$: 848.2531, found: 848.2531.

6.13. Biochemical Evaluation

RNase L FRET activation assay

Performed by Lydia Borgelt and Neele Haacke. RNase L was expressed as monomer in *E. coli* and purified. The FRET-based RNA cleavage assay to determine activation of RNase L was established according to literature^[49, 223] and adapted to 384 well plate format. In assay buffer (0.1 M KCl, 25 mM Tris, 10 mM MgCl₂, 2 mM glutathione, 2.5 μM ATP, pH 7.4) was incubated at room temperature for 60 minutes at final concentrations of 5 nM monomeric RNase L with 50 nM labelled RNA probe (6-FAM-5'-UUAUCAAUUCUUAUUUGCCCCAUUUUUUUGGUUUA-3'-IQ4) and varied concentrations of 2-5A (25 nM) or compounds (60 or 130 μM) diluted from 20 mM DMSO stock solutions. Fluorescence intensity measurements (excitation wavelength: 489 nm, emission wavelength: 525 nm) were performed with two technical replicates using a TECAN Spark plate reader. Half maximal effective concentrations (EC₅₀) values were determined with non-linear regression fit using GraphPad Prism 7 software.

WDR5 competitive FP assay

Performed by Jen-Yao Chang. WDR5 was expressed in *E. coli* and purified by the protein chemistry facility at Max Planck Institute of Molecular Physiology in Dortmund. The competitive FP assay was established according to literature^[315] and adapted to 384 well plate format. In assay buffer (0.1 M phosphate, 25 mM KCl, 0.01% Triton X-100, pH 6.5) was premixed WDR5 with 5-FAM-labelled MLL1 peptide (10mer-Thr-FAM: ARTEVHLRKS, Ahx-Ahx linker). Compounds in assay buffer with 8% DMSO were added 1:1 (v/v) in dilution series and incubated at room temperature for 60 minutes at final concentrations of 4 nM WDR5, 0.6 nM 5-FAM-labelled MLL1 peptide and 4% DMSO. FP measurements (excitation wavelength: 485 nm, emission wavelength: 535 nm) were performed with two technical replicates using a TECAN Spark plate reader. Half maximal inhibitory concentrations (IC₅₀) values were determined with non-linear regression fit using GraphPad Prism 7 software.

7. References

- [1] E. Valeur, S. M. Guéret, H. Adihou, R. Gopalakrishnan, M. Lemurell, H. Waldmann, T. N. Grossmann, A. T. Plowright, *Angew. Chem. Int. Ed.* **2017**, *56*, 10294-10323.
- [2] E. Valeur, F. Narjes, C. Ottmann, A. T. Plowright, *MedChemComm* **2019**, *10*, 1550-1568.
- [3] A. L. Hopkins, C. R. Groom, *Nat. Rev. Drug Discov.* **2002**, *1*, 727-730.
- [4] K. D. Warner, C. E. Hajdin, K. M. Weeks, *Nat. Rev. Drug Discov.* **2018**, *17*, 547-558.
- [5] M. Esteller, *Nat. Rev. Genet.* **2011**, *12*, 861-874.
- [6] D. Wiener, S. Schwartz, *Nat. Rev. Genet.* **2021**, *22*, 119-131.
- [7] Guillermo A. Bermejo, G. M. Clore, Charles D. Schwieters, *Structure* **2016**, *24*, 806-815.
- [8] R. P. Rambo, J. A. Tainer, *RNA* **2010**, *16*, 638-646.
- [9] K. Kappel, K. Zhang, Z. Su, A. M. Watkins, W. Kladwang, S. Li, G. Pintilie, V. V. Topkar, R. Rangan, I. N. Zheludev, J. D. Yesselman, W. Chiu, R. Das, *Nat. Methods* **2020**, *17*, 699-707.
- [10] M. D. Disney, B. G. Dwyer, J. L. Childs-Disney, *Cold Spring Harb. Perspect. Biol.* **2018**, *10*, a034769.
- [11] R. Juliano, M. R. Alam, V. Dixit, H. Kang, *Nucleic Acids Res.* **2008**, *36*, 4158-4171.
- [12] S. Andersson, M. Antonsson, M. Elebring, R. Jansson-Löfmark, L. Weidolf, *Drug Discov. Today* **2018**, *23*, 1733-1745.
- [13] T. A. Vickers, J. R. Wyatt, S. M. Freier, *Nucleic Acids Res.* **2000**, *28*, 1340-1347.
- [14] G. F. Deleavey, J. K. Watts, M. J. Damha, *Curr. Protoc. Nucleic Acid Chem.* **2009**, *39*.
- [15] Y. Huang, *Mol. Ther. Nucleic Acids* **2017**, *6*, 116-132.
- [16] S. Wittrisch, N. Klöting, K. Mörl, R. Chakaroun, M. Blüher, A. G. Beck-Sickinger, *Mol. Metab.* **2020**, *31*, 163-180.
- [17] E. A. Orellana, S. Tenneti, L. Rangasamy, L. T. Lyle, P. S. Low, A. L. Kasinski, *Sci. Transl. Med.* **2017**, *9*, eaam9327.
- [18] L. Knerr, T. P. Prakash, R. Lee, W. J. Drury Iii, M. Nikan, W. Fu, E. Pirie, L. D. Maria, E. Valeur, A. Hayen, M. Ölwegård-Halvarsson, J. Broddefalk, C. Ämmälä, M. E. Østergaard, J. Meuller, L. Sundström, P. Andersson, D. Janzén, R. Jansson-Löfmark, P. P. Seth, et al., *J. Am. Chem. Soc.* **2021**, *143*, 3416-3429.
- [19] K. Tatiparti, S. Sau, S. K. Kashaw, A. K. Iyer, *Nanomaterials* **2017**, *7*, 77-94.

- [20] M. L. Stephenson, P. C. Zamecnik, *Proc. Natl. Acad. Sci. USA* **1978**, *75*, 285-288.
- [21] K. Jiang, *Nat. Med.* **2013**, *19*, 252-252.
- [22] X.-H. Liang, H. Sun, J. G. Nichols, S. T. Crooke, *Mol. Ther.* **2017**, *25*, 2075-2092.
- [23] J. Kim, C. Hu, C. Moufawad El Achkar, L. E. Black, J. Douville, A. Larson, M. K. Pendergast, S. F. Goldkind, E. A. Lee, A. Kuniholm, A. Soucy, J. Vaze, N. R. Belur, K. Fredriksen, I. Stojkowska, A. Tsytsykova, M. Armant, R. L. DiDonato, J. Choi, L. Cornelissen, et al., *New Engl. J. Med.* **2019**, *381*, 1644-1652.
- [24] J. Scharner, I. Aznarez, *Mol. Ther.* **2021**, *29*, 540-554.
- [25] M. M. Zhang, R. Bahal, T. P. Rasmussen, J. E. Manautou, X.-b. Zhong, *Biochem. Pharmacol.* **2021**, 114432.
- [26] S. T. Crooke, *Antisense Nucleic Acid Drug Dev.* **1998**, *8*, vii-viii.
- [27] S. T. Crooke, R. S. Geary, *Br. J. Clin. Pharmacol.* **2013**, *76*, 269-276.
- [28] M. Scoto, R. Finkel, E. Mercuri, F. Muntoni, *Lancet Child Adolesc. Health* **2018**, *2*, 600-609.
- [29] M. D. Benson, M. Waddington-Cruz, J. L. Berk, M. Polydefkis, P. J. Dyck, A. K. Wang, V. Planté-Bordeneuve, F. A. Barroso, G. Merlini, L. Obici, M. Scheinberg, T. H. Brannagan, W. J. Litchy, C. Whelan, B. M. Drachman, D. Adams, S. B. Heitner, I. Conceição, H. H. Schmidt, G. Vita, et al., *New Engl. J. Med.* **2018**, *379*, 22-31.
- [30] F. Muntoni, D. Frank, V. Sardone, J. Morgan, F. Schnell, J. Charleston, C. Desjardins, R. Phadke, C. Sewry, L. Popplewell, M. Guglieri, K. Bushby, P. Carlier, C. Clark, G. Dickson, J.-Y. Hogrel, V. Straub, E. Mercuri, T. Voit, E. Kaye, et al., *Neurology* **2018**, *90*.
- [31] J. L. Witztum, D. Gaudet, S. D. Freedman, V. J. Alexander, A. Digenio, K. R. Williams, Q. Yang, S. G. Hughes, R. S. Geary, M. Arca, E. S. G. Stroes, J. Bergeron, H. Soran, F. Civeira, L. Hemphill, S. Tsimikas, D. J. Blom, L. O'Dea, E. Bruckert, *New Engl. J. Med.* **2019**, *381*, 531-542.
- [32] S. Dhillon, *Drugs* **2020**, *80*, 1027-1031.
- [33] K. R. Wagner, N. L. Kuntz, E. Koenig, L. East, S. Upadhyay, B. Han, P. B. Shieh, *Muscle Nerve* **2021**, *64*, 285-292.
- [34] D. Adams, A. Gonzalez-Duarte, W. D. O'Riordan, C.-C. Yang, M. Ueda, A. V. Kristen, I. Tournev, H. H. Schmidt, T. Coelho, J. L. Berk, K.-P. Lin, G. Vita, S. Attarian, V. Planté-

- Bordeneuve, M. M. Mezei, J. M. Campistol, J. Buades, T. H. Brannagan, B. J. Kim, J. Oh, et al., *New Engl. J. Med.* **2018**, *379*, 11-21.
- [35] M. Balwani, E. Sardh, P. Ventura, P. A. Peiró, D. C. Rees, U. Stölzel, D. M. Bissell, H. L. Bonkovsky, J. Windyga, K. E. Anderson, C. Parker, S. M. Silver, S. B. Keel, J.-D. Wang, P. E. Stein, P. Harper, D. Vassiliou, B. Wang, J. Phillips, A. Ivanova, et al., *New Engl. J. Med.* **2020**, *382*, 2289-2301.
- [36] L. J. Scott, S. J. Keam, *Drugs* **2021**, *81*, 277-282.
- [37] Colleen M. Connelly, Michelle H. Moon, John S. Schneekloth, *Cell Chem. Biol.* **2016**, *23*, 1077-1090.
- [38] C. S. Eubanks, A. E. Hargrove, *Biochemistry* **2019**, *58*, 199-213.
- [39] F. A. Abulwerdi, J. S. Schneekloth, *Methods* **2016**, *103*, 188-195.
- [40] Q. Vicens, E. Westhof, *ChemBioChem* **2003**, *4*, 1018-1023.
- [41] J. L. Childs-Disney, M. Wu, A. Pushechnikov, O. Aminova, M. D. Disney, *ACS Chem. Biol.* **2007**, *2*, 745-754.
- [42] M. D. Disney, L. P. Labuda, D. J. Paul, S. G. Poplawski, A. Pushechnikov, T. Tran, S. P. Velagapudi, M. Wu, J. L. Childs-Disney, *J. Am. Chem. Soc.* **2008**, *130*, 11185-11194.
- [43] S. P. Velagapudi, S. J. Seedhouse, M. D. Disney, *Angew. Chem. Int. Ed.* **2010**, *49*, 3816-3818.
- [44] S. P. Velagapudi, S. M. Gallo, M. D. Disney, *Nat. Chem. Biol.* **2014**, *10*, 291-297.
- [45] M. D. Disney, A. M. Winkelsas, S. P. Velagapudi, M. Southern, M. Fallahi, J. L. Childs-Disney, *ACS Chem. Biol.* **2016**, *11*, 1720-1728.
- [46] S. P. Velagapudi, M. D. Cameron, C. L. Haga, L. H. Rosenberg, M. Lafitte, D. R. Duckett, D. G. Phinney, M. D. Disney, *Proc. Natl. Acad. Sci. USA* **2016**, *113*, 5898-5903.
- [47] S. P. Velagapudi, Y. Luo, T. Tran, H. S. Haniff, Y. Nakai, M. Fallahi, G. J. Martinez, J. L. Childs-Disney, M. D. Disney, *ACS Cent. Sci.* **2017**, *3*, 205-216.
- [48] M. G. Costales, C. L. Haga, S. P. Velagapudi, J. L. Childs-Disney, D. G. Phinney, M. D. Disney, *J. Am. Chem. Soc.* **2017**, *139*, 3446-3455.
- [49] M. G. Costales, H. Aikawa, Y. Li, J. L. Childs-Disney, D. Abegg, D. G. Hoch, S. Pradeep Velagapudi, Y. Nakai, T. Khan, K. W. Wang, I. Yildirim, A. Adibekian, E. T. Wang, M. D. Disney, *Proc. Natl. Acad. Sci. USA* **2020**, *117*, 2406-2411.

- [50] H. S. Haniff, L. Knerr, X. Liu, G. Crynen, J. Boström, D. Abegg, A. Adibekian, E. Lekah, K. W. Wang, M. D. Cameron, I. Yildirim, M. Lemurell, M. D. Disney, *Nat. Chem.* **2020**, *12*, 952-961.
- [51] M. G. Costales, D. G. Hoch, D. Abegg, J. L. Childs-Disney, S. P. Velagapudi, A. Adibekian, M. D. Disney, *J. Am. Chem. Soc.* **2019**, *141*, 2960-2974.
- [52] S. G. Rzuczek, L. A. Colgan, Y. Nakai, M. D. Cameron, D. Furling, R. Yasuda, M. D. Disney, *Nat. Chem. Biol.* **2017**, *13*, 188-193.
- [53] H. S. Haniff, A. Graves, M. D. Disney, *ACS Comb. Sci.* **2018**, *20*, 482-491.
- [54] Y. Luo, M. D. Disney, *ChemBioChem* **2014**, *15*, 2041-2044.
- [55] J. L. Chen, P. Zhang, M. Abe, H. Aikawa, L. Zhang, A. J. Frank, T. Zembryski, C. Hubbs, H. Park, J. Withka, C. Steppan, L. Rogers, S. Cabral, M. Pettersson, T. T. Wager, M. A. Fountain, G. Rumbaugh, J. L. Childs-Disney, M. D. Disney, *J. Am. Chem. Soc.* **2020**, *142*, 8706-8727.
- [56] H. S. Haniff, Y. Tong, X. Liu, J. L. Chen, B. M. Suresh, R. J. Andrews, J. M. Peterson, C. A. O'Leary, R. I. Benhamou, W. N. Moss, M. D. Disney, *ACS Cent. Sci.* **2020**, *6*, 1713-1721.
- [57] R. I. Benhamou, A. J. Angelbello, R. J. Andrews, E. T. Wang, W. N. Moss, M. D. Disney, *ACS Chem. Biol.* **2020**, *15*, 485-493.
- [58] A. Mehta, S. Sonam, I. Gouri, S. Loharch, D. K. Sharma, R. Parkesh, *Nucleic Acids Res.* **2014**, *42*, D132-D141.
- [59] S. Kumar Mishra, A. Kumar, *Database* **2016**, *2016*.
- [60] B. S. Morgan, B. G. Sanaba, A. Donlic, D. B. Karloff, J. E. Forte, Y. Zhang, A. E. Hargrove, *ACS Chem. Biol.* **2019**, *14*, 2691-2700.
- [61] K. D. Warner, P. Homan, K. M. Weeks, A. G. Smith, C. Abell, A. R. Ferré-D'Amaré, *Chem. Biol.* **2014**, *21*, 591-595.
- [62] J. A. Howe, H. Wang, T. O. Fischmann, C. J. Balibar, L. Xiao, A. M. Galgoci, J. C. Malinverni, T. Mayhood, A. Villafania, A. Nahvi, N. Murgolo, C. M. Barbieri, P. A. Mann, D. Carr, E. Xia, P. Zuck, D. Riley, R. E. Painter, S. S. Walker, B. Sherborne, et al., *Nature* **2015**, *526*, 672-677.

- [63] G. Baranello, B. T. Darras, J. W. Day, N. Deconinck, A. Klein, R. Masson, E. Mercuri, K. Rose, M. El-Khairi, M. Gerber, K. Gorni, O. Khwaja, H. Kletzl, R. S. Scalco, T. Seabrook, P. Fontoura, L. Servais, *New Engl. J. Med.* **2021**, *384*, 915-923.
- [64] K. F. Blount, R. R. Breaker, *Nat. Biotechnol.* **2006**, *24*, 1558-1564.
- [65] V. Panchal, R. Brenk, *Antibiotics* **2021**, *10*, 45-66.
- [66] M. Sivaramakrishnan, K. D. McCarthy, S. Campagne, S. Huber, S. Meier, A. Augustin, T. Heckel, H. Meistermann, M. N. Hug, P. Birrer, A. Moursy, S. Khawaja, R. Schmucki, N. Berntenis, N. Giroud, S. Golling, M. Tzouros, B. Banfai, G. Duran-Pacheco, J. Lamerz, et al., *Nat. Commun.* **2017**, *8*, 1476-1488.
- [67] J. Wang, P. G. Schultz, K. A. Johnson, *Proc. Natl. Acad. Sci. USA* **2018**, *115*, E4604-E4612.
- [68] J. R. Thomas, P. J. Hergenrother, *Chem. Rev.* **2008**, *108*, 1171-1224.
- [69] A. L. Garner, *Future Med. Chem.* **2019**, *11*, 2487-2490.
- [70] M. G. Costales, J. L. Childs-Disney, H. S. Haniff, M. D. Disney, *J. Med. Chem.* **2020**, *63*, 8880-8900.
- [71] F. Lovering, J. Bikker, C. Humblet, *J. Med. Chem.* **2009**, *52*, 6752-6756.
- [72] P. G. Dougherty, A. Sahni, D. Pei, *Chem. Rev.* **2019**, *119*, 10241-10287.
- [73] P. C. Gareiss, K. Sobczak, B. R. McNaughton, P. B. Palde, C. A. Thornton, B. L. Miller, *J. Am. Chem. Soc.* **2008**, *130*, 16254-16261.
- [74] J. Pai, S. Hyun, J. Y. Hyun, S.-H. Park, W.-J. Kim, S.-H. Bae, N.-K. Kim, J. Yu, I. Shin, *J. Am. Chem. Soc.* **2016**, *138*, 857-867.
- [75] D. Bose, S. Nahar, M. K. Rai, A. Ray, K. Chakraborty, S. Maiti, *Nucleic Acids Res.* **2015**, *43*, 4342-4352.
- [76] K. Sakamoto, K. Otake, T. Umemoto, *Bioorg. Med. Chem. Lett.* **2017**, *27*, 826-828.
- [77] S. Pomplun, Z. P. Gates, G. Zhang, A. J. Quartararo, B. L. Pentelute, *J. Am. Chem. Soc.* **2020**, *142*, 19642-19651.
- [78] Z. Athanassiou, R. L. A. Dias, K. Moehle, N. Dobson, G. Varani, J. A. Robinson, *J. Am. Chem. Soc.* **2004**, *126*, 6906-6913.
- [79] A. Davidson, T. C. Leeper, Z. Athanassiou, K. Patora-Komisarska, J. Karn, J. A. Robinson, G. Varani, *Proc. Natl. Acad. Sci. USA* **2009**, *106*, 11931-11936.

- [80] I. A. Belashov, D. W. Crawford, C. E. Cavender, P. Dai, P. C. Beardslee, D. H. Mathews, B. L. Pentelute, B. R. McNaughton, J. E. Wedekind, *Nucleic Acids Res.* **2018**, *46*, 6401-6415.
- [81] A. Kuepper, N. McLoughlin, S. Neubacher, E. Collado-Camps, N. Chandran, S. Mukherjee, L. Bethge, J. Bujnicki, R. Brock, S. Heinrichs, T. Grossmann, *ChemRxiv* **2020**, 13325264.
- [82] N. M. McLoughlin, A. Kuepper, S. Neubacher, T. N. Grossmann, *Chem. Eur. J.* **2021**, *27*, 10477-10483.
- [83] S. D. Auweter, F. C. Oberstrass, F. H. T. Allain, *Nucleic Acids Res.* **2006**, *34*, 4943-4959.
- [84] T. S. Bayer, L. N. Booth, S. M. Knudsen, A. D. Ellington, *RNA* **2005**, *11*, 1848-1857.
- [85] R. Valverde, L. Edwards, L. Regan, *FEBS J.* **2008**, *275*, 2712-2726.
- [86] P. Linder, E. Jankowsky, *Nat. Rev. Mol. Cell Biol.* **2011**, *12*, 505-516.
- [87] P. L. Graumann, M. A. Marahiel, *Trends Biochem. Sci.* **1998**, *23*, 286-290.
- [88] K. Nakaminami, D. T. Karlson, R. Imai, *Proc. Natl. Acad. Sci. USA* **2006**, *103*, 10122-10127.
- [89] M. Cassandri, A. Smirnov, F. Novelli, C. Pitolli, M. Agostini, M. Malewicz, G. Melino, G. Raschellà, *Cell Death Discov.* **2017**, *3*, 17071-17082.
- [90] L. R. Saunder, G. N. Barber, *FASEB J.* **2003**, *17*, 961-983.
- [91] B. Tian, P. C. Bevilacqua, A. Diegelman-Parente, M. B. Mathews, *Nat. Rev. Mol. Cell Biol.* **2004**, *5*, 1013-1023.
- [92] G. Masliah, P. Barraud, F. H. T. Allain, *Cell. Mol. Life Sci.* **2013**, *70*, 1875-1895.
- [93] D. P. Reich, B. L. Bass, *Cold Spring Harb. Perspect. Biol.* **2019**, *11*, a035352.
- [94] G. Dreyfuss, V. N. Kim, N. Kataoka, *Nat. Rev. Mol. Cell Biol.* **2002**, *3*, 195-205.
- [95] S. Gerstberger, M. Hafner, T. Tuschl, *Nat. Rev. Genet.* **2014**, *15*, 829-845.
- [96] M. W. Hentze, A. Castello, T. Schwarzl, T. Preiss, *Nat. Rev. Mol. Cell Biol.* **2018**, *19*, 327-341.
- [97] M. Roos, U. Pradère, R. P. Ngondo, A. Behera, S. Allegrini, G. Civenni, J. A. Zagalak, J.-R. Marchand, M. Menzi, H. Towbin, J. Scheuermann, D. Neri, A. Caflisch, C. V. Catapano, C. Ciaudo, J. Hall, *ACS Chem. Biol.* **2016**, *11*, 2773-2781.
- [98] D. Lim, W. G. Byun, J. Y. Koo, H. Park, S. B. Park, *J. Am. Chem. Soc.* **2016**, *138*, 13630-13638.

- [99] H. L. Lightfoot, E. A. Miska, S. Balasubramanian, *Org. Biomol. Chem.* **2016**, *14*, 10208-10216.
- [100] D. A. Lorenz, T. Kaur, S. A. Kerk, E. E. Gallagher, J. Sandoval, A. L. Garner, *ACS Med. Chem. Lett.* **2018**, *9*, 517-521.
- [101] L. Wang, R. G. Rowe, A. Jaimes, C. Yu, Y. Nam, D. S. Pearson, J. Zhang, X. Xie, W. Marion, G. J. Heffron, G. Q. Daley, P. Sliz, *Cell Rep.* **2018**, *23*, 3091-3101.
- [102] D. Lim, W. G. Byun, S. B. Park, *ACS Med. Chem. Lett.* **2018**, *9*, 1181-1185.
- [103] W. G. Byun, D. Lim, S. B. Park, *ChemBioChem* **2020**, *21*, 818-824.
- [104] L. Borgelt, F. Li, P. Hommen, P. Lampe, J. Hwang, G. L. Goebel, S. Sievers, P. Wu, *ACS Med. Chem. Lett.* **2021**, *12*, 893-898.
- [105] K. Cheng, X. Wang, H. Yin, *J. Am. Chem. Soc.* **2011**, *133*, 3764-3767.
- [106] D. Ustianenko, H.-S. Chiu, T. Treiber, S. M. Weyn-Vanhentenryck, N. Treiber, G. Meister, P. Sumazin, C. Zhang, *Mol. Cell* **2018**, *71*, 271-283.
- [107] Y. Nam, C. Chen, Richard I. Gregory, James J. Chou, P. Sliz, *Cell* **2011**, *147*, 1080-1091.
- [108] J. Balzeau, M. R. Menezes, S. Cao, J. P. Hagan, *Front. Genet.* **2017**, *8*.
- [109] J. Choe, M. S. Kelker, I. A. Wilson, *Science* **2005**, *309*, 581-585.
- [110] J. K. Bell, I. Botos, P. R. Hall, J. Askins, J. Shiloach, D. M. Segal, D. R. Davies, *Proc. Natl. Acad. Sci. USA* **2005**, *102*, 10976-10980.
- [111] L. Liu, I. Botos, Y. Wang, J. N. Leonard, J. Shiloach, D. M. Segal, D. R. Davies, *Science* **2008**, *320*, 379-381.
- [112] M. A. Anwar, M. Shah, J. Kim, S. Choi, *Med. Res. Rev.* **2019**, *39*, 1053-1090.
- [113] R. K. Bedi, D. Huang, S. A. Eberle, L. Wiedmer, P. Śledź, A. Caflisch, *ChemMedChem* **2020**, *15*, 744-748.
- [114] E. Yankova, W. Blackaby, M. Albertella, J. Rak, E. De Braekeleer, G. Tsagkogeorga, E. S. Pilka, D. Aspris, D. Leggate, A. G. Hendrick, N. A. Webster, B. Andrews, R. Fosbeary, P. Guest, N. Irigoyen, M. Eleftheriou, M. Gozdecka, J. M. L. Dias, A. J. Bannister, B. Vick, et al., *Nature* **2021**, *593*, 597-601.
- [115] G. Minuesa, C. Antczak, D. Shum, C. Radu, B. Bhinder, Y. Li, H. Djaballah, M. G. Kharas, *Comb. Chem. High Throughput Screen* **2014**, *17*, 596-609.
- [116] C. C. Clingman, L. M. Deveau, S. A. Hay, R. M. Genga, S. M. D. Shandilya, F. Massi, S. P. Ryder, *eLife* **2014**, *3*, e02848.

- [117] L. Lan, C. Appelman, A. R. Smith, J. Yu, S. Larsen, R. T. Marquez, H. Liu, X. Wu, P. Gao, A. Roy, A. Anbanandam, R. Gowthaman, J. Karanicolas, R. N. De Guzman, S. Rogers, J. Aubé, M. Ji, R. S. Cohen, K. L. Neufeld, L. Xu, *Mol. Oncol.* **2015**, *9*, 1406-1420.
- [118] L. Lan, H. Liu, A. R. Smith, C. Appelman, J. Yu, S. Larsen, R. T. Marquez, X. Wu, F. Y. Liu, P. Gao, R. Gowthaman, J. Karanicolas, R. N. De Guzman, S. Rogers, J. Aubé, K. L. Neufeld, L. Xu, *BMC Cancer* **2018**, *18*, 809-822.
- [119] C. Yi, G. Li, D. N. Ivanov, Z. Wang, M. X. Velasco, G. Hernández, S. Kaundal, J. Villarreal, Y. K. Gupta, M. Qiao, C. G. Hubert, M. J. Hart, L. O. F. Penalva, *RNA Biol.* **2018**, *15*, 1420-1432.
- [120] G. Minuesa, S. K. Albanese, W. Xie, Y. Kazansky, D. Worroll, A. Chow, A. Schurer, S.-M. Park, C. Z. Rotsides, J. Taggart, A. Rizzi, L. N. Naden, T. Chou, S. Gourkanti, D. Cappel, M. C. Passarelli, L. Fairchild, C. Adura, J. F. Glickman, J. Schulman, et al., *Nat. Commun.* **2019**, *10*, 2691-2705.
- [121] L. Lan, J. Liu, M. Xing, A. R. Smith, J. Wang, X. Wu, C. Appelman, K. Li, A. Roy, R. Gowthaman, J. Karanicolas, A. D. Somoza, C. C. C. Wang, Y. Miao, R. De Guzman, B. R. Oakley, K. L. Neufeld, L. Xu, *Cancers* **2020**, *12*, 2221-2238.
- [122] N. V. Jammi, L. R. Whitby, P. A. Beal, *Biochem. Biophys. Res. Commun.* **2003**, *308*, 50-57.
- [123] B. K. Jha, I. Polyakova, P. Kessler, B. Dong, B. Dickerman, G. C. Sen, R. H. Silverman, *J. Biol. Chem.* **2011**, *286*, 26319-26326.
- [124] S. Dabo, P. Maillard, M. Collados Rodriguez, M. D. Hansen, S. Mazouz, D.-J. Bigot, M. Tible, G. Janvier, O. Helynck, P. Cassonnet, Y. Jacob, J. Bellalou, A. Gatignol, R. C. Patel, J. Hugon, H. Munier-Lehmann, E. F. Meurs, *Sci. Rep.* **2017**, *7*, 16129-16143.
- [125] G. M. Bol, F. Vesuna, M. Xie, J. Zeng, K. Aziz, N. Gandhi, A. Levine, A. Irving, D. Korz, S. Tantravedi, M. R. Heerma van Voss, K. Gabrielson, E. A. Bordt, B. M. Polster, L. Cope, P. van der Groep, A. Kondaskar, M. A. Rudek, R. S. Hosmane, E. van der Wall, et al., *EMBO Mol. Med.* **2015**, *7*, 648-669.
- [126] A. Brai, F. Martelli, V. Riva, A. Garbelli, R. Fazi, C. Zamperini, A. Pollutri, L. Falsitta, S. Ronzini, L. Maccari, G. Maga, S. Giannecchini, M. Botta, *J. Med. Chem.* **2019**, *62*, 2333-2347.

- [127] A. Brai, S. Ronzini, V. Riva, L. Botta, C. Zamperini, M. Borgini, C. I. Trivisani, A. Garbelli, C. Pennisi, A. Boccuto, F. Saladini, M. Zazzi, G. Maga, M. Botta, *Molecules* **2019**, *24*, 3988-4005.
- [128] S. Nakao, M. Nogami, M. Iwatani, T. Imaeda, M. Ito, T. Tanaka, M. Tawada, S. Endo, D. R. Cary, M. Ohori, Y. Imaeda, T. Kawamoto, S. Aparicio, A. Nakanishi, S. Araki, *Biochem. Biophys. Res. Commun.* **2020**, *523*, 795-801.
- [129] A. Brai, A. Boccuto, M. Monti, S. Marchi, I. Vicenti, F. Saladini, C. I. Trivisani, A. Pollutri, C. M. Trombetta, E. Montomoli, V. Riva, A. Garbelli, E. M. Nola, M. Zazzi, G. Maga, E. Dreassi, M. Botta, *ACS Med. Chem. Lett.* **2020**, *11*, 956-962.
- [130] V. Riva, A. Garbelli, A. Brai, F. Casiraghi, R. Fazi, C. I. Trivisani, A. Boccuto, F. Saladini, I. Vicenti, F. Martelli, M. Zazzi, S. Giannecchini, E. Dreassi, M. Botta, G. Maga, *J. Med. Chem.* **2020**, *63*, 9876-9887.
- [131] A. Brai, V. Riva, F. Saladini, C. Zamperini, C. I. Trivisani, A. Garbelli, C. Pennisi, A. Giannini, A. Boccuto, F. Bugli, M. Martini, M. Sanguinetti, M. Zazzi, E. Dreassi, M. Botta, G. Maga, *Eur. J. Med. Chem.* **2020**, *200*, 112319-112330.
- [132] T. Tanaka, T. Ishii, D. Mizuno, T. Mori, R. Yamaji, Y. Nakamura, S. Kumazawa, T. Nakayama, M. Akagawa, *Free Radical Biol. Med.* **2011**, *50*, 1324-1335.
- [133] G. C. Kost, M. Y. Yang, L. Li, Y. Zhang, C. Y. Liu, D. J. Kim, C. H. Ahn, Y. B. Lee, Z. R. Liu, *J. Cell. Biochem.* **2015**, *116*, 1595-1601.
- [134] T. Taniguchi, Y. Iizumi, M. Watanabe, M. Masuda, M. Morita, Y. Aono, S. Toriyama, M. Oishi, W. Goi, T. Sakai, *Cell Death Dis.* **2016**, *7*, e2211.
- [135] M.-E. Bordeleau, A. Mori, M. Oberer, L. Lindqvist, L. S. Chard, T. Higa, G. J. Belsham, G. Wagner, J. Tanaka, J. Pelletier, *Nat. Chem. Biol.* **2006**, *2*, 213-220.
- [136] N. J. Moerke, H. Aktas, H. Chen, S. Cantel, M. Y. Reibarkh, A. Fahmy, John D. Gross, A. Degterev, J. Yuan, M. Chorev, J. A. Halperin, G. Wagner, *Cell* **2007**, *128*, 257-267.
- [137] N.-C. Meisner, M. Hintersteiner, K. Mueller, R. Bauer, J.-M. Seifert, H.-U. Naegeli, J. Ottl, L. Oberer, C. Guenat, S. Moss, N. Harrer, M. Woisetschlaeger, C. Buehler, V. Uhl, M. Auer, *Nat. Chem. Biol.* **2007**, *3*, 508-515.
- [138] Y. Kotake, K. Sagane, T. Owa, Y. Mimori-Kiyosue, H. Shimizu, M. Uesugi, Y. Ishihama, M. Iwata, Y. Mizui, *Nat. Chem. Biol.* **2007**, *3*, 570-575.

- [139] M. Seiler, A. Yoshimi, R. Darman, B. Chan, G. Keaney, M. Thomas, A. A. Agrawal, B. Caleb, A. Csibi, E. Sean, P. Fekkes, C. Karr, V. Klimek, G. Lai, L. Lee, P. Kumar, S. C.-W. Lee, X. Liu, C. Mackenzie, C. Meeske, et al., *Nat. Med.* **2018**, *24*, 497-504.
- [140] G. M. Burslem, B. E. Smith, A. C. Lai, S. Jaime-Figueroa, D. C. McQuaid, D. P. Bondeson, M. Toure, H. Dong, Y. Qian, J. Wang, A. P. Crew, J. Hines, C. M. Crews, *Cell Chem. Biol.* **2018**, *25*, 67-77.
- [141] B. Z. Stanton, E. J. Chory, G. R. Crabtree, *Science* **2018**, *359*, eaao5902.
- [142] A. Ursu, J. L. Childs-Disney, A. J. Angelbello, M. G. Costales, S. M. Meyer, M. D. Disney, *ACS Chem. Biol.* **2020**, *15*, 2031-2040.
- [143] R. S. Murante, L. A. Henricksen, R. A. Bambara, *Proc. Natl. Acad. Sci. USA* **1998**, *95*, 2244-2249.
- [144] C. Rinaldi, M. J. A. Wood, *Nat. Rev. Neurol.* **2018**, *14*, 9-21.
- [145] M. De Vivo, M. Dal Peraro, M. L. Klein, *J. Am. Chem. Soc.* **2008**, *130*, 10955-10962.
- [146] J. Kurreck, *Eur. J. Biochem.* **2003**, *270*, 1628-1644.
- [147] A. Fire, S. Xu, M. K. Montgomery, S. A. Kostas, S. E. Driver, C. C. Mello, *Nature* **1998**, *391*, 806-811.
- [148] T. Treiber, N. Treiber, G. Meister, *Nat. Rev. Mol. Cell Biol.* **2019**, *20*, 5-20.
- [149] R. L. Setten, J. J. Rossi, S.-p. Han, *Nat. Rev. Drug Discov.* **2019**, *18*, 421-446.
- [150] J. T. Marques, B. R. G. Williams, *Nat. Biotechnol.* **2005**, *23*, 1399-1405.
- [151] A. L. Jackson, P. S. Linsley, *Nat. Rev. Drug Discov.* **2010**, *9*, 57-67.
- [152] E. Fakhr, F. Zare, L. Teimoori-Toolabi, *Cancer Gene Ther.* **2016**, *23*, 73-82.
- [153] H. W. Pley, K. M. Flaherty, D. B. McKay, *Nature* **1994**, *372*, 68-74.
- [154] K. J. Young, F. Gill, J. A. Grasby, *Nucleic Acids Res.* **1997**, *25*, 3760-3760.
- [155] A. Ke, K. Zhou, F. Ding, J. H. D. Cate, J. A. Doudna, *Nature* **2004**, *429*, 201-205.
- [156] N. B. Suslov, S. DasGupta, H. Huang, J. R. Fuller, D. M. J. Lilley, P. A. Rice, J. A. Piccirilli, *Nat. Chem. Biol.* **2015**, *11*, 840-846.
- [157] M. Ma, L. Benimetskaya, I. Lebedeva, J. Dignam, G. Takle, C. A. Stein, *Nat. Biotechnol.* **2000**, *18*, 58-61.
- [158] S. Schubert, D. C. Gül, H. P. Grunert, H. Zeichhardt, V. A. Erdmann, J. Kurreck, *Nucleic Acids Res.* **2003**, *31*, 5982-5992.
- [159] T. R. Cech, O. C. Uhlenbeck, *Nature* **1994**, *372*, 39-40.

- [160] K. Kim, F. Liu, *Biochim. Biophys. Acta* **2007**, 1769, 603-612.
- [161] D. L. Makino, F. Halbach, E. Conti, *Nat. Rev. Mol. Cell Biol.* **2013**, 14, 654-660.
- [162] R. Goraczniak, M. A. Behlke, S. I. Gunderson, *Nat. Biotechnol.* **2009**, 27, 257-263.
- [163] L. Spraggon, L. Cartegni, *Int. J. Cell Biol.* **2013**, 2013, 846510-846520.
- [164] R. I. Benhamou, A. J. Angelbello, E. T. Wang, M. D. Disney, *Cell Chem. Biol.* **2020**, 27, 223-231.
- [165] R. N. Zuckermann, D. R. Corey, P. G. Schultz, *J. Am. Chem. Soc.* **1988**, 110, 1614-1615.
- [166] R. N. Zuckermann, P. G. Schultz, *Proc. Natl. Acad. Sci. USA* **1989**, 86, 1766-1770.
- [167] D. R. Corey, D. Pei, P. G. Schultz, *Biochemistry* **1989**, 28, 8277-8286.
- [168] R. N. Zuckermann, P. G. Schultz, *J. Am. Chem. Soc.* **1988**, 110, 6592-6594.
- [169] S. Kanaya, C. Nakai, A. Konishi, H. Inoue, E. Ohtsuka, M. Ikehara, *J. Biol. Chem.* **1992**, 267, 8492-8498.
- [170] N. L. Mironova, D. V. Pyshnyi, E. M. Ivanova, M. A. Zenkova, H. J. Gross, V. V. Vlassov, *Nucleic Acids Res.* **2004**, 32, 1928-1936.
- [171] J. J. Turner, S. Jones, M. M. Fabani, G. Ivanova, A. A. Arzumanov, M. J. Gait, *Blood Cells Mol. Dis.* **2007**, 38, 1-7.
- [172] Y. Staroseletz, A. Williams, K. K. Burusco, I. Alibay, V. V. Vlassov, M. A. Zenkova, E. V. Bichenkova, *Biomaterials* **2017**, 112, 44-61.
- [173] Y. Staroseletz, B. Amirloo, A. Williams, A. Lomzov, Kepa K. Burusco, D. J. Clarke, T. Brown, M. A. Zenkova, Elena V. Bichenkova, *Nucleic Acids Res.* **2020**, 48, 10662-10679.
- [174] M. Gebrezgiabher, W. A. Zalloum, D. J. Clarke, S. M. Miles, A. A. Fedorova, M. A. Zenkova, E. V. Bichenkova, *J. Biomol. Struct. Dyn.* **2021**, 39, 2555-2574.
- [175] O. A. Patutina, E. V. Bichenkova, S. K. Miroshnichenko, N. L. Mironova, L. T. Trivoluzzi, K. K. Burusco, R. A. Bryce, V. V. Vlassov, M. A. Zenkova, *Biomaterials* **2017**, 122, 163-178.
- [176] O. A. Patutina, S. K. Miroshnichenko, N. L. Mironova, A. V. Sen'kova, E. V. Bichenkova, D. J. Clarke, V. V. Vlassov, M. A. Zenkova, *Front. Pharmacol.* **2019**, 10.
- [177] B. J. Calnan, B. Tidor, S. Biancalana, D. Hudson, A. D. Frankel, *Science* **1991**, 252, 1167.
- [178] S. S. Chavali, C. E. Cavender, D. H. Mathews, J. E. Wedekind, *J. Am. Chem. Soc.* **2020**, 142, 19835-19839.

- [179] A. Williams, Y. Staroseletz, M. A. Zenkova, L. Jeannin, H. Aojula, E. V. Bichenkova, *Bioconj. Chem.* **2015**, *26*, 1129-1143.
- [180] O. A. Patutina, M. A. Bazhenov, S. K. Miroshnichenko, N. L. Mironova, D. V. Pyshnyi, V. V. Vlassov, M. A. Zenkova, *Sci. Rep.* **2018**, *8*, 14990-15004.
- [181] J. A. Doudna, E. Charpentier, *Science* **2014**, *346*, 1258096.
- [182] I. M. Slaymaker, P. Mesa, M. J. Kellner, S. Kannan, E. Brignole, J. Koob, P. R. Feliciano, S. Stella, O. O. Abudayyeh, J. S. Gootenberg, J. Strecker, G. Montoya, F. Zhang, *Cell Rep.* **2019**, *26*, 3741-3751.
- [183] D. B. T. Cox, J. S. Gootenberg, O. O. Abudayyeh, B. Franklin, M. J. Kellner, J. Joung, F. Zhang, *Science* **2017**, *358*, 1019-1027.
- [184] G. J. Knott, J. A. Doudna, *Science* **2018**, *361*, 866-869.
- [185] L. Guan, M. D. Disney, *Angew. Chem. Int. Ed.* **2013**, *52*, 1462-1465.
- [186] B. M. Aveline, I. E. Kochevar, R. W. Redmond, *J. Am. Chem. Soc.* **1996**, *118*, 10113-10123.
- [187] S. G. Chaulk, J. P. Pezacki, A. M. MacMillan, *Biochemistry* **2000**, *39*, 10448-10453.
- [188] L. Guan, Y. Luo, W. W. Ja, M. D. Disney, *Bioorg. Med. Chem. Lett.* **2018**, *28*, 2794-2796.
- [189] T. D. Tullius, *Annu. Rev. Biophys. Biophys. Chem.* **1989**, *18*, 213-237.
- [190] C. H. B. Chen, D. S. Sigman, *J. Am. Chem. Soc.* **1988**, *110*, 6570-6572.
- [191] J. Hall, D. Hüsken, U. Pielers, H. E. Moser, R. Häner, *Chem. Biol.* **1994**, *1*, 185-190.
- [192] S. Matsuda, A. Ishikubo, A. Kuzuya, M. Yashiro, M. Komiyama, *Angew. Chem. Int. Ed.* **1998**, *37*, 3284-3286.
- [193] W. S. Bowen, W. E. Hill, J. S. Lodmell, *Methods* **2001**, *25*, 344-350.
- [194] K. Michaelis, M. Kalesse, *Angew. Chem. Int. Ed.* **1999**, *38*, 2243-2245.
- [195] J. C. Joyner, J. A. Cowan, *J. Am. Chem. Soc.* **2011**, *133*, 9912-9922.
- [196] A. Sreedhara, J. D. Freed, J. A. Cowan, *J. Am. Chem. Soc.* **2000**, *122*, 8814-8824.
- [197] A. Sreedhara, A. Patwardhan, J. A. Cowan, *Chem. Commun.* **1999**, 1147-1148.
- [198] E. Riguet, S. Tripathi, B. Chaubey, J. Désiré, V. N. Pandey, J.-L. Décout, *J. Med. Chem.* **2004**, *47*, 4806-4809.
- [199] B. Chaubey, S. Tripathi, J. Désiré, I. Baussanne, J.-L. Décout, V. N. Pandey, *Oligonucleotides* **2007**, *17*, 302-313.

- [200] S. Mikutis, M. Gu, E. Sendinc, M. E. Hazemi, H. Kiely-Collins, D. Aspris, G. S. Vassiliou, Y. Shi, K. Tzelepis, G. J. L. Bernardes, *ACS Cent. Sci.* **2020**, *6*, 2196-2208.
- [201] R. Breslow, *Acc. Chem. Res.* **1991**, *24*, 317-324.
- [202] N. G. Beloglazova, A. Y. Epanchintsev, V. N. Sil'nikov, M. A. Zenkova, V. V. Vlasov, *Mol. Biol.* **2002**, *36*, 581-588.
- [203] S. M. Hecht, *Bioconj. Chem.* **1994**, *5*, 513-526.
- [204] D. L. Boger, T. Honda, *J. Am. Chem. Soc.* **1994**, *116*, 5647-5656.
- [205] C. J. Thomas, A. O. Chizhov, C. J. Leitheiser, M. J. Rishel, K. Konishi, Z.-F. Tao, S. M. Hecht, *J. Am. Chem. Soc.* **2002**, *124*, 12926-12927.
- [206] C. J. Leitheiser, K. L. Smith, M. J. Rishel, S. Hashimoto, K. Konishi, C. J. Thomas, C. Li, M. M. McCormick, S. M. Hecht, *J. Am. Chem. Soc.* **2003**, *125*, 8218-8227.
- [207] Q. Ma, Z. Xu, B. R. Schroeder, W. Sun, F. Wei, S. Hashimoto, K. Konishi, C. J. Leitheiser, S. M. Hecht, *J. Am. Chem. Soc.* **2007**, *129*, 12439-12452.
- [208] B. J. Carter, E. de Vroom, E. C. Long, G. A. van der Marel, J. H. van Boom, S. M. Hecht, *Proc. Natl. Acad. Sci. USA* **1990**, *87*, 9373-9377.
- [209] A. T. Abraham, J.-J. Lin, D. L. Newton, S. Rybak, S. M. Hecht, *Chem. Biol.* **2003**, *10*, 45-52.
- [210] A. J. Angelbello, M. D. Disney, *ChemBioChem* **2018**, *19*, 43-47.
- [211] A. J. Angelbello, M. E. DeFeo, C. M. Glinkerman, D. L. Boger, M. D. Disney, *ACS Chem. Biol.* **2020**, *15*, 849-855.
- [212] P. E. Vorobjev, J. B. Smith, I. A. Pyshnaya, A. S. Levina, V. F. Zarytova, E. Wickstrom, *Bioconj. Chem.* **2003**, *14*, 1307-1313.
- [213] A. J. Angelbello, S. G. Rzuczek, K. K. McKee, J. L. Chen, H. Olafson, M. D. Cameron, W. N. Moss, E. T. Wang, M. D. Disney, *Proc. Natl. Acad. Sci. USA* **2019**, *116*, 7799-7804.
- [214] R. I. Benhamou, M. Abe, S. Choudhary, S. M. Meyer, A. J. Angelbello, M. D. Disney, *J. Med. Chem.* **2020**, *63*, 7827-7839.
- [215] Y. Li, M. D. Disney, *ACS Chem. Biol.* **2018**, *13*, 3065-3071.
- [216] X. Liu, H. S. Haniff, J. L. Childs-Disney, A. Shuster, H. Aikawa, A. Adibekian, M. D. Disney, *J. Am. Chem. Soc.* **2020**, *142*, 6970-6982.
- [217] M. Knight, P. J. Cayley, R. H. Silverman, D. H. Wreschner, C. S. Gilbert, R. E. Brown, I. M. Kerr, *Nature* **1980**, *288*, 189-192.

- [218] M. R. Player, P. F. Torrence, *Pharmacol. Ther.* **1998**, *78*, 55-113.
- [219] A. Zhou, B. A. Hassel, R. H. Silverman, *Cell* **1993**, *72*, 753-765.
- [220] A. Zhou, R. J. Molinaro, K. Malathi, R. H. Silverman, *J. Interferon Cytokine Res.* **2005**, *25*, 595-603.
- [221] N. Tanaka, M. Nakanishi, Y. Kusakabe, Y. Goto, Y. Kitade, K. T. Nakamura, *EMBO J.* **2004**, *23*, 3929-3938.
- [222] R. H. Silverman, D. D. Jung, N. L. Nolan-Sorden, C. W. Dieffenbach, V. P. Kedar, D. N. SenGupta, *J. Biol. Chem.* **1988**, *263*, 7336-7341.
- [223] C. S. Thakur, B. K. Jha, B. Dong, J. Das Gupta, K. M. Silverman, H. Mao, H. Sawai, A. O. Nakamura, A. K. Banerjee, A. Gudkov, R. H. Silverman, *Proc. Natl. Acad. Sci. USA* **2007**, *104*, 9585-9590.
- [224] B. Dong, R. H. Silverman, *J. Biol. Chem.* **1995**, *270*, 4133-4137.
- [225] H. Huang, E. Zeqiraj, B. Dong, Babal K. Jha, Nicole M. Duffy, S. Orlicky, N. Thevakumaran, M. Talukdar, Monica C. Pillon, Derek F. Ceccarelli, Leo C. K. Wan, Y.-C. Juang, Daniel Y. L. Mao, C. Gaughan, Margo A. Brinton, Andrey A. Perelygin, I. Kourinov, A. Guarné, Robert H. Silverman, F. Sicheri, *Mol. Cell* **2014**, *53*, 221-234.
- [226] D. H. Wreschner, J. W. McCauley, J. J. Skehel, I. M. Kerr, *Nature* **1981**, *289*, 414-417.
- [227] G. Floyd-Smith, E. Slattery, P. Lengyel, *Science* **1981**, *212*, 1030-1032.
- [228] Y. Han, J. Donovan, S. Rath, G. Whitney, A. Chitrakar, A. Korennykh, *Science* **2014**, *343*, 1244-1248.
- [229] J. Donovan, S. Rath, D. Kolet-Mandrikov, A. Korennykh, *RNA* **2017**, *23*, 1660-1671.
- [230] L. Rusch, A. Zhou, R. H. Silverman, *J. Interferon Cytokine Res.* **2000**, *20*, 1091-1100.
- [231] M. A. Siddiqui, S. Mukherjee, P. Manivannan, K. Malathi, *Int. J. Mol. Sci.* **2015**, *16*, 17611-17636.
- [232] K. Kubota, K. Nakahara, T. Ohtsuka, S. Yoshida, J. Kawaguchi, Y. Fujita, Y. Ozeki, A. Hara, C. Yoshimura, H. Furukawa, H. Haruyama, K. Ichikawa, M. Yamashita, T. Matsuoka, Y. Iijima, *J. Biol. Chem.* **2004**, *279*, 37832-37841.
- [233] R. H. Silverman, S. R. Weiss, *J. Interferon Cytokine Res.* **2014**, *34*, 455-463.
- [234] S. A. Adah, S. F. Bayly, H. Cramer, R. H. Silverman, P. F. Torrence, *Curr. Med. Chem.* **2001**, *8*, 1189-1212.

- [235] M. G. Costales, Y. Matsumoto, S. P. Velagapudi, M. D. Disney, *J. Am. Chem. Soc.* **2018**, *140*, 6741-6744.
- [236] M. G. Costales, B. Suresh, K. Vishnu, M. D. Disney, *Cell Chem. Biol.* **2019**, *26*, 1180-1186.
- [237] S. M. Meyer, C. C. Williams, Y. Akahori, T. Tanaka, H. Aikawa, Y. Tong, J. L. Childs-Disney, M. D. Disney, *Chem. Soc. Rev.* **2020**, *49*, 7167-7199.
- [238] P. Zhang, X. Liu, D. Abegg, T. Tanaka, Y. Tong, R. I. Benhamou, J. Baisden, G. Crynen, S. M. Meyer, M. D. Cameron, A. K. Chatterjee, A. Adibekian, J. L. Childs-Disney, M. D. Disney, *J. Am. Chem. Soc.* **2021**, *143*, 13044-13055.
- [239] K. Lesiak, S. Khamnei, P. F. Torrence, *Bioconj. Chem.* **1993**, *4*, 467-472.
- [240] P. F. Torrence, R. K. Maitra, K. Lesiak, S. Khamnei, A. Zhou, R. H. Silverman, *Proc. Natl. Acad. Sci. USA* **1993**, *90*, 1300-1304.
- [241] A. Maran, R. K. Maitra, A. Kumar, B. Dong, W. Xiao, G. Li, B. R. Williams, P. F. Torrence, R. H. Silverman, *Science* **1994**, *265*, 789-792.
- [242] R. K. Maitra, G. Li, W. Xiao, B. Dong, P. F. Torrence, R. H. Silverman, *J. Biol. Chem.* **1995**, *270*, 15071-15075.
- [243] W. Xiao, G. Li, R. K. Maitra, A. Maran, R. H. Silverman, P. F. Torrence, *J. Med. Chem.* **1997**, *40*, 1195-1200.
- [244] W. Xiao, G. Li, M. R. Player, R. K. Maitra, C. F. Waller, R. H. Silverman, P. F. Torrence, *J. Med. Chem.* **1998**, *41*, 1531-1539.
- [245] H. Cramer, M. R. Player, P. F. Torrence, *Bioorg. Med. Chem. Lett.* **1999**, *9*, 1049-1054.
- [246] N. M. Cirino, G. Li, W. Xiao, P. F. Torrence, R. H. Silverman, *Proc. Natl. Acad. Sci. USA* **1997**, *94*, 1937-1942.
- [247] M. R. Player, D. L. Barnard, P. F. Torrence, *Proc. Natl. Acad. Sci. USA* **1998**, *95*, 8874-8879.
- [248] D. W. Leaman, F. J. Longano, J. R. Okicki, K. F. Soike, P. F. Torrence, R. H. Silverman, H. Cramer, *Virology* **2002**, *292*, 70-77.
- [249] S. Kondo, Y. Kondo, G. Li, R. H. Silverman, J. K. Cowell, *Oncogene* **1998**, *16*, 3323-3330.
- [250] D. M. Kushner, J. M. Paranjape, B. Bandyopadhyay, H. Cramer, D. W. Leaman, A. W. Kennedy, R. H. Silverman, J. K. Cowell, *Gynecol. Oncol.* **2000**, *76*, 183-192.

- [251] J. M. Paranjape, D. Xu, D. M. Kushner, J. Okicki, D. J. Lindner, H. Cramer, R. H. Silverman, D. W. Leaman, *Oligonucleotides* **2006**, *16*, 225-238.
- [252] I. Robbins, G. Mitta, S. Vichier-Guerre, R. Sobol, A. Ubysz, B. Rayner, B. Lebleu, *Biochimie* **1998**, *80*, 711-720.
- [253] A. Maran, C. F. Waller, J. M. Paranjape, G. Li, W. Xiao, K. Zhang, M. E. Kalaycio, R. K. Maitra, A. E. Lichtin, W. Brugger, P. F. Torrence, R. H. Silverman, *Blood* **1998**, *92*, 4336-4343.
- [254] Player, R. K. Maitra, R. H. Silverman, P. F. Torrence, *Antiviral Chem. Chemother.* **1998**, *9*, 225-231.
- [255] X. Su, W. Ma, B. Cheng, Q. Wang, Z. Guo, D. Zhou, X. Tang, *BioRxiv* **2021**, 433849.
- [256] Y. Hu, D. Stumpfe, J. Bajorath, *J. Med. Chem.* **2017**, *60*, 1238-1246.
- [257] R. W. Huigens Iii, K. C. Morrison, R. W. Hicklin, T. A. Flood Jr, M. F. Richter, P. J. Hergenrother, *Nat. Chem.* **2013**, *5*, 195-202.
- [258] M. Grigalunas, A. Burhop, A. Christoforow, H. Waldmann, *Curr. Opin. Chem. Biol.* **2020**, *56*, 111-118.
- [259] K. Gewald, *Angew. Chem.* **1961**, *73*, 114.
- [260] G. Kazuhiro, H. Masao, I. Hiroshi, *Biochem. Pharmacol.* **1977**, *26*, 11-18.
- [261] M. Bandini, A. Melloni, F. Piccinelli, R. Sinisi, S. Tommasi, A. Umami-Ronchi, *J. Am. Chem. Soc.* **2006**, *128*, 1424-1425.
- [262] A. Di Fenza, M. Tancredi, C. Galoppini, P. Rovero, *Tetrahedron Lett.* **1998**, *39*, 8529-8532.
- [263] T. Ohshima, Y. Hayashi, K. Agura, Y. Fujii, A. Yoshiyama, K. Mashima, *Chem. Commun.* **2012**, *48*, 5434-5436.
- [264] A.-Z. Irini, B. Wilfred, D. Stevan W., W. Noel, T. Sean C., K. Albert W., R. Ana-Lucia, S. Shashank, Z. Hongyu, G. Jorge, G. Alan F., L. Huanqiu, T. Christina M., Z. Min, WO 2010/135560 A1, **2010**.
- [265] S. W. Gordon-Wylie, E. Teplin, J. C. Morris, M. I. Trombley, S. M. McCarthy, W. M. Cleaver, G. R. Clark, *Cryst. Growth Des.* **2004**, *4*, 789-797.
- [266] B. G. Whitehouse, R. C. Cooke, *Chemosphere* **1982**, *11*, 689-699.
- [267] A. Veseli, S. Žakelj, A. Kristl, *Drug Dev. Ind. Pharm.* **2019**, *45*, 1717-1724.
- [268] G. M. Castanedo, D. P. Sutherlin, *Tetrahedron Lett.* **2001**, *42*, 7181-7184.

- [269] S. Bräse, C. Gil, K. Knepper, V. Zimmermann, *Angew. Chem. Int. Ed.* **2005**, *44*, 5188-5240.
- [270] M. S. Gadd, A. Testa, X. Lucas, K.-H. Chan, W. Chen, D. J. Lamont, M. Zengerle, A. Ciulli, *Nat. Chem. Biol.* **2017**, *13*, 514-521.
- [271] S. B. Alabi, C. M. Crews, *J. Biol. Chem.* **2021**, *296*, 100647-100663.
- [272] A. Donlic, B. S. Morgan, J. L. Xu, A. Liu, C. Roble Jr., A. E. Hargrove, *Angew. Chem. Int. Ed.* **2018**, *57*, 13242-13247.
- [273] F. A. Abulwerdi, W. Xu, A. A. Ageeli, M. J. Yonkunas, G. Arun, H. Nam, J. S. Schneekloth, T. K. Dayie, D. Spector, N. Baird, S. F. J. Le Grice, *ACS Chem. Biol.* **2019**, *14*, 223-235.
- [274] Y. Shi, S. Parag, R. Patel, A. Lui, M. Murr, J. Cai, N. A. Patel, *Cell Chem. Biol.* **2019**, *26*, 319-330.
- [275] A. Donlic, M. Zafferani, G. Padroni, M. Puri, Amanda E. Hargrove, *Nucleic Acids Res.* **2020**, *48*, 7653-7664.
- [276] M. Guttman, J. L. Rinn, *Nature* **2012**, *482*, 339-346.
- [277] M. Huarte, *Nat. Med.* **2015**, *21*, 1253-1261.
- [278] Y. Dou, T. A. Milne, A. J. Ruthenburg, S. Lee, J. W. Lee, G. L. Verdine, C. D. Allis, R. G. Roeder, *Nat. Struct. Mol. Biol.* **2006**, *13*, 713-719.
- [279] S. M. Southall, P.-S. Wong, Z. Odho, S. M. Roe, J. R. Wilson, *Mol. Cell* **2009**, *33*, 181-191.
- [280] A. D. Guarnaccia, W. P. Tansey, *J. Clin. Med.* **2018**, *7*, 21-37.
- [281] S.-L. Chen, Z.-Y. Qin, F. Hu, Y. Wang, Y.-J. Dai, Y. Liang, *Genes* **2019**, *10*, 621-632.
- [282] A. V. Krivtsov, S. A. Armstrong, *Nat. Rev. Cancer* **2007**, *7*, 823-833.
- [283] J. Xu, L. Li, J. Xiong, A. Dekker, A. Ye, H. Karatas, L. Liu, H. Wang, Z. S. Qin, S. Wang, Y. Dou, *Cell Discov.* **2016**, *2*, 16008-16018.
- [284] A. Schuetz, A. Allali-Hassani, F. Martín, P. Loppnau, M. Vedadi, A. Bochkarev, A. N. Plotnikov, C. H. Arrowsmith, J. Min, *EMBO J.* **2006**, *25*, 4245-4252.
- [285] Z. Han, L. Guo, H. Wang, Y. Shen, X. W. Deng, J. Chai, *Mol. Cell* **2006**, *22*, 137-144.
- [286] J.-F. Couture, E. Collazo, R. C. Trievel, *Nat. Struct. Mol. Biol.* **2006**, *13*, 698-703.
- [287] A. J. Ruthenburg, W. Wang, D. M. Graybosch, H. Li, C. D. Allis, D. J. Patel, G. L. Verdine, *Nat. Struct. Mol. Biol.* **2006**, *13*, 704-712.

- [288] J.-J. Song, R. E. Kingston, *J. Biol. Chem.* **2008**, *283*, 35258-35264.
- [289] A. Patel, V. Dharmarajan, M. S. Cosgrove, *J. Biol. Chem.* **2008**, *283*, 32158-32161.
- [290] Z. Fu, C. Chen, Q. Zhou, Y. Wang, Y. Zhao, X. Zhao, W. Li, S. Zheng, H. Ye, L. Wang, Z. He, Q. Lin, Z. Li, R. Chen, *Cancer Lett.* **2017**, *410*, 68-81.
- [291] W. He, G. Zhong, N. Jiang, B. Wang, X. Fan, C. Chen, X. Chen, J. Huang, T. Lin, *J. Clin. Invest.* **2018**, *128*, 861-875.
- [292] J. A. Gomez, Orly L. Wapinski, Yul W. Yang, J.-F. Bureau, S. Gopinath, Denise M. Monack, Howard Y. Chang, M. Brahic, K. Kirkegaard, *Cell* **2013**, *152*, 743-754.
- [293] T.-T. Sun, J. He, Q. Liang, L.-L. Ren, T.-T. Yan, T.-C. Yu, J.-Y. Tang, Y.-J. Bao, Y. Hu, Y. Lin, D. Sun, Y.-X. Chen, J. Hong, H. Chen, W. Zou, J.-Y. Fang, *Cancer Discov.* **2016**, *6*, 784-801.
- [294] X. Guo, Y. Xu, Z. Wang, Y. Wu, J. Chen, G. Wang, C. Lu, W. Jia, J. Xi, S. Zhu, Z. Jiapaer, X. Wan, Z. Liu, S. Gao, J. Kang, *Cell Stem Cell* **2018**, *22*, 893-908.
- [295] T. Rossi, M. Pistoni, V. Sancisi, G. Gobbi, F. Torricelli, B. Donati, S. Ribisi, M. Gugnoni, A. Ciarrocchi, *Mol. Cancer Res.* **2020**, *18*, 140-152.
- [296] Y. W. Yang, R. A. Flynn, Y. Chen, K. Qu, B. Wan, K. C. Wang, M. Lei, H. Y. Chang, *eLife* **2014**, *3*, e02046.
- [297] S. Subhash, K. Mishra, V. S. Akhade, M. Kanduri, T. Mondal, C. Kanduri, *Nucleic Acids Res.* **2018**, *46*, 9384-9400.
- [298] Lance R. Thomas, Q. Wang, Brian C. Grieb, J. Phan, Audra M. Foshage, Q. Sun, Edward T. Olejniczak, T. Clark, S. Dey, S. Lorey, B. Alicie, Gregory C. Howard, B. Cawthon, Kevin C. Ess, Christine M. Eischen, Z. Zhao, Stephen W. Fesik, William P. Tansey, *Mol. Cell* **2015**, *58*, 440-452.
- [299] J. D. Macdonald, S. Chacón Simon, C. Han, F. Wang, J. G. Shaw, J. E. Howes, J. Sai, J. P. Yuh, D. Camper, B. M. Alicie, J. Alvarado, S. Nikhar, W. Payne, E. R. Aho, J. A. Bauer, B. Zhao, J. Phan, L. R. Thomas, O. W. Rossanese, W. P. Tansey, et al., *J. Med. Chem.* **2019**, *62*, 11232-11259.
- [300] S. Chacón Simon, F. Wang, L. R. Thomas, J. Phan, B. Zhao, E. T. Olejniczak, J. D. Macdonald, J. G. Shaw, C. Schlund, W. Payne, J. Creighton, S. R. Stauffer, A. G. Waterson, W. P. Tansey, S. W. Fesik, *J. Med. Chem.* **2020**, *63*, 4315-4333.
- [301] S. Guil, M. Esteller, *Nat. Struct. Mol. Biol.* **2012**, *19*, 1068-1075.

- [302] J. Wysocka, T. Swigut, T. A. Milne, Y. Dou, X. Zhang, A. L. Burlingame, R. G. Roeder, A. H. Brivanlou, C. D. Allis, *Cell* **2005**, *121*, 859-872.
- [303] K. C. Wang, Y. W. Yang, B. Liu, A. Sanyal, R. Corces-Zimmerman, Y. Chen, B. R. Lajoie, A. Protacio, R. A. Flynn, R. A. Gupta, J. Wysocka, M. Lei, J. Dekker, J. A. Helms, H. Y. Chang, *Nature* **2011**, *472*, 120-124.
- [304] Y. Cheng, I. Jutooru, G. Chadalapaka, J. C. Corton, S. Safe, *Oncotarget* **2015**, *6*, 10840-10852.
- [305] Z. Li, X. Zhao, Y. Zhou, Y. Liu, Q. Zhou, H. Ye, Y. Wang, J. Zeng, Y. Song, W. Gao, S. Zheng, B. Zhuang, H. Chen, W. Li, H. Li, H. Li, Z. Fu, R. Chen, *J. Transl. Med.* **2015**, *13*, 84-99.
- [306] R. Zhao, Y. Zhang, X. Zhang, Y. Yang, X. Zheng, X. Li, Y. Liu, Y. Zhang, *Mol. Cancer* **2018**, *17*, 68-72.
- [307] Y. Wang, Z. Li, S. Zheng, Y. Zhou, L. Zhao, H. Ye, X. Zhao, W. Gao, Z. Fu, Q. Zhou, Y. Liu, R. Chen, *Oncotarget* **2015**, *6*, 35684-35698.
- [308] Y. J. Lee, H. Oh, E. Kim, B. Ahn, J. H. Lee, Y. Lee, Y. S. Chae, S. G. Kang, C. H. Kim, *Pathol. Res. Pract.* **2019**, *215*, 152649-152654.
- [309] P. Zhang, H. Lee, J. S. Brunzelle, J.-F. Couture, *Nucleic Acids Res.* **2012**, *40*, 4237-4246.
- [310] V. Dharmarajan, J.-H. Lee, A. Patel, D. G. Skalnik, M. S. Cosgrove, *J. Biol. Chem.* **2012**, *287*, 27275-27289.
- [311] Z. Odho, S. M. Southall, J. R. Wilson, *J. Biol. Chem.* **2010**, *285*, 32967-32976.
- [312] V. Avdic, P. Zhang, S. Lanouette, A. Groulx, V. Tremblay, J. Brunzelle, J.-F. Couture, *Structure* **2011**, *19*, 101-108.
- [313] B. A. Bayard, J. B. Gabrion, *Biochem. J.* **1993**, *296*, 155-160.
- [314] W. Al-Ahmadi, L. al-Haj, F. A. Al-Mohanna, R. H. Silverman, K. S. A. Khabar, *Oncogene* **2009**, *28*, 1782-1791.
- [315] H. Karatas, E. C. Townsend, D. Bernard, Y. Dou, S. Wang, *J. Med. Chem.* **2010**, *53*, 5179-5185.
- [316] H. Karatas, E. C. Townsend, F. Cao, Y. Chen, D. Bernard, L. Liu, M. Lei, Y. Dou, S. Wang, *J. Am. Chem. Soc.* **2013**, *135*, 669-682.

- [317] F. Cao, Elizabeth C. Townsend, H. Karatas, J. Xu, L. Li, S. Lee, L. Liu, Y. Chen, P. Ouillette, J. Zhu, Jay L. Hess, P. Atadja, M. Lei, Zhaohui S. Qin, S. Malek, S. Wang, Y. Dou, *Mol. Cell* **2014**, *53*, 247-261.
- [318] H. Karatas, Y. Li, L. Liu, J. Ji, S. Lee, Y. Chen, J. Yang, L. Huang, D. Bernard, J. Xu, E. C. Townsend, F. Cao, X. Ran, X. Li, B. Wen, D. Sun, J. A. Stuckey, M. Lei, Y. Dou, S. Wang, *J. Med. Chem.* **2017**, *60*, 4818-4839.
- [319] T. D. Brown, K. A. Whitehead, S. Mitragotri, *Nat. Rev. Mater.* **2020**, *5*, 127-148.
- [320] G. Senisterra, H. Wu, A. Allali-Hassani, G. A. Wasney, D. Barsyte-Lovejoy, L. Dombrowski, A. Dong, K. T. Nguyen, D. Smil, Y. Bolshan, T. Hajian, H. He, A. Seitova, I. Chau, F. Li, G. Poda, J. F. Couture, P. J. Brown, R. Al-Awar, M. Schapira, et al., *Biochem. J.* **2013**, *449*, 151-159.
- [321] Y. Bolshan, M. Getlik, E. Kuznetsova, G. A. Wasney, T. Hajian, G. Poda, K. T. Nguyen, H. Wu, L. Dombrowski, A. Dong, G. Senisterra, M. Schapira, C. H. Arrowsmith, P. J. Brown, R. Al-awar, M. Vedadi, D. Smil, *ACS Med. Chem. Lett.* **2013**, *4*, 353-357.
- [322] F. Grebien, M. Vedadi, M. Getlik, R. Giambruno, A. Grover, R. Avellino, A. Skucha, S. Vittori, E. Kuznetsova, D. Smil, D. Barsyte-Lovejoy, F. Li, G. Poda, M. Schapira, H. Wu, A. Dong, G. Senisterra, A. Stukalov, K. V. M. Huber, A. Schönegger, et al., *Nat. Chem. Biol.* **2015**, *11*, 571-578.
- [323] D.-D. Li, W.-L. Chen, Z.-H. Wang, Y.-Y. Xie, X.-L. Xu, Z.-Y. Jiang, X.-J. Zhang, Q.-D. You, X.-K. Guo, *Eur. J. Med. Chem.* **2016**, *124*, 480-489.
- [324] F. Wang, K. O. Jeon, J. M. Salovich, J. D. Macdonald, J. Alvarado, R. D. Gogliotti, J. Phan, E. T. Olejniczak, Q. Sun, S. Wang, D. Camper, J. P. Yuh, J. G. Shaw, J. Sai, O. W. Rossanese, W. P. Tansey, S. R. Stauffer, S. W. Fesik, *J. Med. Chem.* **2018**, *61*, 5623-5642.
- [325] J. Tian, K. B. Teuscher, E. R. Aho, J. R. Alvarado, J. J. Mills, K. M. Meyers, R. D. Gogliotti, C. Han, J. D. Macdonald, J. Sai, J. G. Shaw, J. L. Sensintaffar, B. Zhao, T. A. Rietz, L. R. Thomas, W. G. Payne, W. J. Moore, G. M. Stott, J. Kondo, M. Inoue, et al., *J. Med. Chem.* **2020**, *63*, 656-675.
- [326] D.-D. Li, Z.-H. Wang, W.-L. Chen, Y.-Y. Xie, Q.-D. You, X.-K. Guo, *Bioorg. Med. Chem.* **2016**, *24*, 6109-6118.
- [327] D.-D. Li, W.-L. Chen, X.-L. Xu, F. Jiang, L. Wang, Y.-Y. Xie, X.-J. Zhang, X.-K. Guo, Q.-D. You, H.-P. Sun, *Eur. J. Med. Chem.* **2016**, *118*, 1-8.

- [328] M. Getlik, D. Smil, C. Zepeda-Velázquez, Y. Bolshan, G. Poda, H. Wu, A. Dong, E. Kuznetsova, R. Marcellus, G. Senisterra, L. Dombrovski, T. Hajian, T. Kiyota, M. Schapira, C. H. Arrowsmith, P. J. Brown, M. Vedadi, R. Al-awar, *J. Med. Chem.* **2016**, *59*, 2478-2496.
- [329] A.-A. Rima, I. Methvin, J. Babu, L. Yong, M. Ahmed, P. Gennady, S. Pandiaraju, U. David, W. Brian, Z.-V. C. Armando, WO 2017/147700 A1, **2017**.
- [330] A.-A. Rima, I. Methvin, J. Babu, L. Yong, M. Ahmed, P. Gennady, P. Michael, S. J. Kathleen, S. Pandiaraju, U. David, W. Brian, Z.-V. C. Armando, WO 2017/147701 A1, **2017**.
- [331] A.-A. Rima, I. Methvin, J. Babu, L. Yong, M. Ahmed, P. Gennady, S. Pandiaraju, U. David, W. Brian, Z.-V. C. Armando, WO 2019/046944 A1, **2019**.
- [332] C. Weilin, G. Xiaoke, L. Dongdong, W. Zhihui, Y. Qidong, WO 2019/205687 A1, **2019**.
- [333] C. Weilin, C. Xin, G. Jing, G. Xiaoke, J. Zhengyu, L. Dongdong, X. Jun, X. Xiaoli, Y. Qidong, WO 2020/172932 A1, **2020**.
- [334] W. Chen, X. Chen, D. Li, J. Zhou, Z. Jiang, Q. You, X. Guo, *J. Med. Chem.* **2021**, *64*, 8221-8245.
- [335] E. R. Aho, J. Wang, R. D. Gogliotti, G. C. Howard, J. Phan, P. Acharya, J. D. Macdonald, K. Cheng, S. L. Lorey, B. Lu, S. Wenzel, A. M. Foshage, J. Alvarado, F. Wang, J. G. Shaw, B. Zhao, A. M. Weissmiller, L. R. Thomas, C. R. Vakoc, M. D. Hall, et al., *Cell Rep.* **2019**, *26*, 2916-2928.
- [336] A. D. Guarnaccia, K. L. Rose, J. Wang, B. Zhao, T. M. Popay, C. E. Wang, K. Guerrazzi, S. Hill, C. M. Woodley, T. J. Hansen, S. L. Lorey, J. G. Shaw, W. G. Payne, A. M. Weissmiller, E. T. Olejniczak, S. W. Fesik, Q. Liu, W. P. Tansey, *Cell Rep.* **2021**, *34*, 108636-108650.
- [337] Aoife C. McMahon, R. Rahman, H. Jin, James L. Shen, A. Fieldsend, W. Luo, M. Rosbash, *Cell* **2016**, *165*, 742-753.
- [338] W.-L. Chen, D.-D. Li, Z.-H. Wang, X.-L. Xu, X.-J. Zhang, Z.-Y. Jiang, X.-K. Guo, Q.-D. You, *Bioorg. Chem.* **2018**, *76*, 380-385.
- [339] J. Jian, L. Dongxu, L. Jing, W. Gang, Y. Xufen, WO 2019/246570 A1, **2019**.
- [340] A. Dölle, B. Adhikari, A. Krämer, J. Weckesser, N. Berner, L.-M. Berger, M. Diebold, M. M. Szewczyk, D. Barsyte-Lovejoy, C. H. Arrowsmith, J. Gebel, F. Löhr, V. Dötsch, M.

- Eilers, S. Heinzlmeir, B. Kuster, C. Sottriffer, E. Wolf, S. Knapp, *J. Med. Chem.* **2021**, *64*, 10682-10710.
- [341] L. Xu, S. Wang, B. Chen, M. Li, X. Hu, B. Hu, L. Jin, N. Sun, Z. Shen, *Synlett* **2018**, *29*, 1505-1509.
- [342] D. P. Bondeson, B. E. Smith, G. M. Burslem, A. D. Buhimschi, J. Hines, S. Jaime-Figueroa, J. Wang, B. D. Hamman, A. Ishchenko, C. M. Crews, *Cell Chem. Biol.* **2018**, *25*, 78-87.
- [343] V. V. Rostovtsev, L. G. Green, V. V. Fokin, K. B. Sharpless, *Angew. Chem. Int. Ed.* **2002**, *41*, 2596-2599.
- [344] S. D. Edmondson, B. Yang, C. Fallan, *Bioorg. Med. Chem. Lett.* **2019**, *29*, 1555-1564.
- [345] A. Pike, B. Williamson, S. Harlfinger, S. Martin, D. F. McGinnity, *Drug Discov. Today* **2020**, *25*, 1793-1800.
- [346] C. Cantrill, P. Chaturvedi, C. Rynn, J. Petrig Schaffland, I. Walter, M. B. Wittwer, *Drug Discov. Today* **2020**, *25*, 969-982.
- [347] Y. Atilaw, V. Poongavanam, C. Svensson Nilsson, D. Nguyen, A. Giese, D. Meibom, M. Erdelyi, J. Kihlberg, *ACS Med. Chem. Lett.* **2021**, *12*, 107-114.
- [348] C. Martinand, C. Montavon, T. Salehzada, M. Silhol, B. Lebleu, C. Bisbal, *J. Virol.* **1999**, *73*, 290-296.
- [349] L. O. Kallings, *J. Intern. Med.* **2008**, *263*, 218-243.
- [350] J. M. Brenchley, T. W. Schacker, L. E. Ruff, D. A. Price, J. H. Taylor, G. J. Beilman, P. L. Nguyen, A. Khoruts, M. Larson, A. T. Haase, D. C. Douek, *J. Exp. Med.* **2004**, *200*, 749-759.
- [351] M. Ooms, T. E. M. Abbink, C. Pham, B. Berkhout, *Nucleic Acids Res.* **2007**, *35*, 5253-5261.
- [352] S. R. King, *Ann. Emergency Med.* **1994**, *24*, 443-449.
- [353] S. Nekhai, K.-T. Jeang, *Future Microbiol.* **2006**, *1*, 417-426.
- [354] Brandon S. Razooky, A. Pai, K. Aull, Igor M. Rouzine, Leor S. Weinberger, *Cell* **2015**, *160*, 990-1001.
- [355] D. L. Ouellet, I. Plante, P. Landry, C. Barat, M.-È. Janelle, L. Flamand, M. J. Tremblay, P. Provost, *Nucleic Acids Res.* **2008**, *36*, 2353-2365.

- [356] Z. Klase, R. Winograd, J. Davis, L. Carpio, R. Hildreth, M. Heydarian, S. Fu, T. McCaffrey, E. Meiri, M. Ayash-Rashkovsky, S. Gilad, Z. Bentwich, F. Kashanchi, *Retrovirology* **2009**, *6*, 18-34.
- [357] A. Narayanan, S. Iordanskiy, R. Das, R. Van Duyne, S. Santos, E. Jaworski, I. Guendel, G. Sampey, E. Dalby, M. Iglesias-Ussel, A. Popratiloff, R. Hakami, K. Kehn-Hall, M. Young, C. Subra, C. Gilbert, C. Bailey, F. Romerio, F. Kashanchi, *J. Biol. Chem.* **2013**, *288*, 20014-20033.
- [358] M. H. Malim, M. Emerman, *Cell Host Microbe* **2008**, *3*, 388-398.
- [359] J. M. Watts, K. K. Dang, R. J. Gorelick, C. W. Leonard, J. W. Bess Jr, R. Swanstrom, C. L. Burch, K. M. Weeks, *Nature* **2009**, *460*, 711-716.
- [360] R. T. Mitsuyasu, T. C. Merigan, A. Carr, J. A. Zack, M. A. Winters, C. Workman, M. Bloch, J. Lalezari, S. Becker, L. Thornton, B. Akil, H. Khanlou, R. Finlayson, R. McFarlane, D. E. Smith, R. Garsia, D. Ma, M. Law, J. M. Murray, C. von Kalle, et al., *Nat. Med.* **2009**, *15*, 285-292.
- [361] T. I. Cornu, C. Mussolino, M. C. Müller, C. Wehr, W. V. Kern, T. Cathomen, *Hum. Gene Ther.* **2020**, *32*, 52-65.
- [362] L. Xu, J. Wang, Y. Liu, L. Xie, B. Su, D. Mou, L. Wang, T. Liu, X. Wang, B. Zhang, L. Zhao, L. Hu, H. Ning, Y. Zhang, K. Deng, L. Liu, X. Lu, T. Zhang, J. Xu, C. Li, et al., *New Engl. J. Med.* **2019**, *381*, 1240-1247.
- [363] G. Hütter, D. Nowak, M. Mossner, S. Ganepola, A. Müßig, K. Allers, T. Schneider, J. Hofmann, C. Kücherer, O. Blau, I. W. Blau, W. K. Hofmann, E. Thiel, *New Engl. J. Med.* **2009**, *360*, 692-698.
- [364] J. Sztuba-Solinska, S. R. Shenoy, P. Gareiss, L. R. H. Krumpke, S. F. J. Le Grice, B. R. O’Keefe, J. S. Schneekloth, *J. Am. Chem. Soc.* **2014**, *136*, 8402-8410.
- [365] F. A. Abulwerdi, M. D. Shortridge, J. Sztuba-Solinska, R. Wilson, S. F. J. Le Grice, G. Varani, J. S. Schneekloth, *J. Med. Chem.* **2016**, *59*, 11148-11160.
- [366] X.-D. Li, L. Liu, L. Cheng, *Org. Biomol. Chem.* **2018**, *16*, 9191-9196.
- [367] V. Cecchetti, C. Parolin, S. Moro, T. Pecere, E. Filipponi, A. Calistri, O. Tabarrini, B. Gatto, M. Palumbo, A. Fravolini, *J. Med. Chem.* **2000**, *43*, 3799-3802.
- [368] S. Richter, C. Parolin, B. Gatto, C. Del Vecchio, E. Brocca-Cofano, A. Fravolini, G. Palù, M. Palumbo, *Antimicrob. Agents Chemother.* **2004**, *48*, 1895-1899.

- [369] S. N. Richter, B. Gatto, O. Tabarrini, A. Fravolini, M. Palumbo, *Bioorg. Med. Chem. Lett.* **2005**, *15*, 4247-4251.
- [370] G. Manfroni, B. Gatto, O. Tabarrini, S. Sabatini, V. Cecchetti, G. Giaretta, C. Parolin, C. Del Vecchio, A. Calistri, M. Palumbo, A. Fravolini, *Bioorg. Med. Chem. Lett.* **2009**, *19*, 714-717.
- [371] B. Gatto, O. Tabarrini, S. Massari, G. Giaretta, S. Sabatini, C. Del Vecchio, C. Parolin, A. Fravolini, M. Palumbo, V. Cecchetti, *ChemMedChem* **2009**, *4*, 935-938.
- [372] O. Tabarrini, S. Massari, D. Daelemans, F. Meschini, G. Manfroni, L. Bottega, B. Gatto, M. Palumbo, C. Pannecouque, V. Cecchetti, *ChemMedChem* **2010**, *5*, 1880-1892.
- [373] J. Desantis, S. Massari, A. Sosic, G. Manfroni, R. Cannalire, T. Felicetti, C. Pannecouque, B. Gatto, O. Tabarrini, *Open J. Med. Chem.* **2019**, *13*, 16-28.
- [374] N. N. Patwardhan, L. R. Ganser, G. J. Kapral, C. S. Eubanks, J. Lee, B. Sathyamoorthy, H. M. Al-Hashimi, A. E. Hargrove, *MedChemComm* **2017**, *8*, 1022-1036.
- [375] N. N. Patwardhan, Z. Cai, A. Umuhire Juru, A. E. Hargrove, *Org. Biomol. Chem.* **2019**, *17*, 9313-9320.
- [376] N. N. Patwardhan, Z. Cai, C. N. Newson, A. E. Hargrove, *Org. Biomol. Chem.* **2019**, *17*, 1778-1786.
- [377] A. Umuhire Juru, Z. Cai, A. Jan, A. E. Hargrove, *Chem. Commun.* **2020**, *56*, 3555-3558.
- [378] L. R. Ganser, M. L. Kelly, N. N. Patwardhan, A. E. Hargrove, H. M. Al-Hashimi, *J. Mol. Biol.* **2020**, *432*, 1297-1304.
- [379] R. H. Silverman, J. J. Skehel, T. C. James, D. H. Wreschner, I. M. Kerr, *J. Virol.* **1983**, *46*, 1051-1055.
- [380] G. R. Fulmer, A. J. M. Miller, N. H. Sherden, H. E. Gottlieb, A. Nudelman, B. M. Stoltz, J. E. Bercaw, K. I. Goldberg, *Organometallics* **2010**, *29*, 2176-2179.
- [381] H. The Dang, E. Chorell, H. Uvell, J. S. Pinkner, S. J. Hultgren, F. Almqvist, *Org. Biomol. Chem.* **2014**, *12*, 1942-1956.
- [382] L. Ouyang, L. Zhang, J. Liu, L. Fu, D. Yao, Y. Zhao, S. Zhang, G. Wang, G. He, B. Liu, *J. Med. Chem.* **2017**, *60*, 9990-10012.
- [383] L. Aurelio, C. Valant, H. Figler, B. L. Flynn, J. Linden, P. M. Sexton, A. Christopoulos, P. J. Scammells, *Bioorg. Med. Chem.* **2009**, *17*, 7353-7361.

- [384] K.-Y. Jung, K. Vanommeslaeghe, M. E. Lanning, J. L. Yap, C. Gordon, P. T. Wilder, A. D. MacKerell, S. Fletcher, *Org. Lett.* **2013**, *15*, 3234-3237.
- [385] G. Liu, B. G. Szczepankiewicz, Z. Pei, Z. Xin, T. K. Oost, D. A. Janowick, WO 02/18323 A2, **2002**.
- [386] T. Rieth, N. Tober, D. Limbach, T. Haspel, M. Sperner, N. Schupp, P. Wicker, S. Glang, M. Lehmann, H. Detert, *Molecules* **2020**, *25*, 5761-5779.
- [387] K. Liu, L. Wu, Y. Xie, G. Zhou, WO 2015/094913 A1, **2015**.
- [388] M. Xu, J. Zhu, Y. Diao, H. Zhou, X. Ren, D. Sun, J. Huang, D. Han, Z. Zhao, L. Zhu, Y. Xu, H. Li, *J. Med. Chem.* **2013**, *56*, 7911-7924.
- [389] M. Jezowska, D. Honcharenko, A. Ghidini, R. Strömberg, M. Honcharenko, *Bioconj. Chem.* **2016**, *27*, 2620-2628.
- [390] A. Ghilardi, D. Pezzoli, M. C. Bellucci, C. Malloggi, A. Negri, A. Sganappa, G. Tedeschi, G. Candiani, A. Volonterio, *Bioconj. Chem.* **2013**, *24*, 1928-1936.
- [391] G. Karabanovich, J. Němeček, L. Valášková, A. Carazo, K. Konečná, J. Stolaříková, A. Hrabálek, O. Pavliš, P. Pávek, K. Vávrová, J. Roh, V. Klimešová, *Eur. J. Med. Chem.* **2017**, *126*, 369-383.
- [392] A. E. Gould, R. Adams, S. Adhikari, K. Aertgeerts, R. Afroze, C. Blackburn, E. F. Calderwood, R. Chau, J. Chouitar, M. O. Duffey, D. B. England, C. Farrer, N. Forsyth, K. Garcia, J. Gaulin, P. D. Greenspan, R. Guo, S. J. Harrison, S.-C. Huang, N. Iartchouk, et al., *J. Med. Chem.* **2011**, *54*, 1836-1846.
- [393] A. Degnan, G. O. Tora, R. Ramkumar, J. L. Ditta, K. W. Gillman, WO 2007/121389 A2, **2007**.
- [394] G. K. Newton, M. R. Stewart, T. R. Perrior, S. R. Crosby, A. Hopkins, G. Negoita-Giras, K. Jenkins, WO 2014/128486 A1, **2014**.
- [395] N. Umezawa, N. Matsumoto, S. Iwama, N. Kato, T. Higuchi, *Bioorg. Med. Chem.* **2010**, *18*, 6340-6350.

8. Appendix

8.1. List of Abbreviations

2-5A	2'-5' Polyadenylate
μM	Micromolar
μm	Micrometer
AcOH	Acetic acid
ADP	Adenosine diphosphate
Ago2	Argounate 2
AHP	Acute hepatic porphyria
Ahx	6-Amino hexanoic acid
AIDS	Acquired immunodeficiency syndrome
ALAS1	Delta-aminolevulinate synthase 1
AlCl_3	Aluminium trichloride
AML	Acute myeloid leukemia
apoB	Apolipoprotein B-100
apoC	Apolipoprotein C-III
ARM	Arginine-rich motif
ASO	Antisense oligonucleotide
ATP	Adenosine triphosphate
BCR-ABL	Breakpoint cluster region-Abelson proto-oncogene
BH_3	Borane
BLACAT2	Bladder cancer-associated transcript 2

Cas13	CRISPR-associated protein 13
CCR5	C-C chemokine receptor type 5
CD ₅₀	Half-maximal inhibitory band intensity concentration
CLN7	Ceroid lipofuscinosis-7
cLog P	Calculated Log P
CMV	Cytomegalovirus
COSY	Correlation spectroscopy
COVID-19	Coronavirus disease 2019
CRISPR	Clustered regularly interspaced short palindromic repeats
crRNA	CRISPR RNA
CSD	Cold-shock domain
CuAAC	Copper-catalyzed azide-alkyne cycloaddition
DC ₅₀	Half-maximal degradation concentration
DGCR8	DiGeorge syndrome critical region 8
DIPEA	<i>N,N</i> -diisopropylethylamine
DMA	Dimethylacetamide
DMD	Duchenne muscular dystrophy
DMPK	Dystrophia myotonica protein kinase
DMSO	Dimethylsulfoxide
DNA	Deoxyribonucleic acid
dsRNA	Double stranded RNA
E. Coli	Escherichia coli
EC ₅₀	Half-maximal effective concentration
EDTA	Ethylenediaminetetraacetic acid

EGS	External guide sequence
EIC	Extracted ion chromatogram
EM	Electron microscopy
ESI	Electrospray ionization
FAM	Carboxyfluorescein
FCS	Familial chylomicronemia syndrome
F_{norm}	Fluorescence normalized to negative and positive controls
FP	Fluorescence polarization
FRET	Fluorescence resonance energy transfer
GCInc1	Gastric cancer-associated lncRNA1
H3K4me3	Trimethylation of histone H3 at lysine 4
HAO1	Hydroxyacid oxidase 1
hATTR	Hereditary transthyretin amyloidosis
HATU	Hexafluorophosphate azabenzotriazole tetramethyl uronium
HEPN	Higher eukaryotes and prokaryotes nucleotide-binding
HIV	Human immunodeficiency virus
HMBC	Heteronuclear multiple bond correlation
HOAt	1-Hydroxy-7-azabenzotriazole
HOBt	1-Hydroxybenzotriazole
HoFH	Homozygous familial hypercholesterolaemia
HOTTIP	HOXA transcript at the distal tip
HOXA	Homeobox A
HPLC	High performance liquid chromatography

HPT	<i>N</i> -hydroxypyridine-2(1 <i>H</i>)-thione
HRMS	High resolution mass spectrometry
HSQC	Heteronuclear single quantum coherence
HTS	High-throughput screening
Hz	Hertz
IC ₅₀	Half-maximal inhibitory concentration
IQ4	Fourth generation instant quenchers
K _D	Dissociation constant
kDa	Kilodalton
KH	K homology
K _i	Inhibition constant
KI	Potassium iodide
LC-MS	Liquid chromatography-mass spectrometry
<i>let-7</i>	Lethal-7
LiAlH ₄	Lithium aluminum hydride
LIN28	Abnormal cell lineage protein 28
Linc1405	Long intergenic non-coding RNA 1405
lncRNA	Long non-coding RNA
MBNL1	Muscle blind-like splicing regulator 1
METTL	Methyltransferase-like
miRNA	MicroRNA
MLL1	Mixed lineage leukemia 1

mM	Millimolar
mm	Millimeter
mP	Millipolarization
MPLC	Medium pressure liquid chromatography
mRNA	Messenger RNA
MS	Mass spectrometry
MSI	Musashi
MTBE	Methyl <i>tert</i> -butyl ether
MW	Molecular weight
MYC	Myelocytomatosis oncogene
ncRNA	Non-coding RNA
NeST	Nettoie salmonella pas Theilers's
nM	Nanomolar
nm	Nanometer
NMP	<i>N</i> -Methyl-2-pyrrolidone
NMR	Nuclear magnetic resonance
NOESY	Nuclear Overhauser effect spectroscopy
OAS	Oligoadenylate synthesase
OICR	Ontario institute of cancer research
Pd(OH) ₂ /C	Palladium hydroxide on charcoal
Pd(PPh ₃) ₂ Cl ₂	Bis(triphenylphosphine)palladium(II) dichloride
Pd/C	Palldium on charcoal
PDB	Protein data bank

PE	Petroleum ether
PEG	Polyethylene glycol
PH1	Primary hyperoxaluria type 1
PKR	RNA-dependent protein kinase
PPi	Pyrophosphate
PPI	Protein-protein interaction
ppm	Parts per million
pre-crRNA	Precursor CRISPR RNA
pre-miRNA	Precursor microRNA
pre-mRNA	Precursor messenger RNA
pre-rRNA	Precursor ribosomal RNA
pre-tRNA	Precursor transport RNA
pri-miRNA	Primary microRNA
PROTAC	Proteolysis targeting chimera
PS	Phosphorothioate
PtO ₂ /C	Palladium oxide on charcoal
Quant	Quantitative
RAIN	RUNX2-associated intergenic lncRNA
RbBP5	Retinoblastoma binding protein 5
RBD	RNA-binding domain
RBP	RNA-binding protein
RIBOTAC	Ribonuclease targeting chimera
RISC	RNA-induced silencing complex
RITAC	RNA interactome targeting chimera

RNA	Ribonucleic acid
RNA-Seq	RNA sequencing
RNAi	RNA interference
RNase H	Ribonuclease H
RNase L	Ribonuclease L
RNase P	Ribonuclease P
rpm	Rounds per minute
RRM	RNA recognition motif
rRNA	Ribosomal RNA
RSV	Respiratory syncytial virus
rt	Room temperature
RT-qPCR	Reverse transcription-quantitative polymerase chain reaction
S ₈	Elemental sulfur
SAR	Structure-activity relationship
SARS-CoV-2	Severe acute respiratory syndrome coronavirus-2
SET1	Su(var)3-9, Enhancer-of-zeste and Trithorax 1
siRNA	Small interfering RNA
SMA	Spinal muscular atrophy
SMN2	Survival of motor neuron 2
SNase	Staphylococcal nuclease
snRNA	Small nuclear RNA
ssDNA	Single stranded DNA
ssRNA	Single stranded RNA

TAR	Transactivation response
Tat	Trans-activator of transcription
TBHP	<i>tert</i> -Butyl hydroxy peroxide
TFA	Trifluoroacetic acid
TLC	Thin-layer chromatography
TLR	Toll-like receptor
TRBP	TAR RNA-binding protein
tRNA	Transfer RNA
TTR	Transthyretin
U1 snRNP	U1 small nuclear ribonucleoprotein
UHPLC	Ultra-high-performance liquid chromatography
UTR	Untranslated region
UV	Ultraviolet
VEGF-165	Vascular endothelial growth factor 165
WBM	WDR5-binding motif
WDR5	WD (Trp-Asp)-40 repeat protein 5
WIN	WDR5-interaction
ZFD	Zinc-finger domain

8.2. Acknowledgements

First of all, I would like to thank Prof. Dr. Herbert Waldmann for initiating the Chemical Genomics Centre and always sharing a great amount of wisdom and enthusiasm for science. I truly appreciate performing research in the department of chemical biology, a collaborative and interdisciplinary environment serving as great training of scientists.

I am grateful for the opportunity to work on exciting and challenging projects with Dr. Peng Wu.

I thank Dr. Andreas Brunschweiler for accepting my request of being second examiner.

I would also like to thank the representants from the funding companies AstraZeneca, Merck and Pfizer for giving input and advice on projects. The valuable connection to pharmaceutical industry has added another layer of motivation to generate impactful science and advance the development of medicines for future generations.

I am also thankful for collaborators accepting a CGC-wide project spanning across three groups. Dr. Peter 't Hart for sharing knowledge on the RNA-binding protein WDR5 and Jen-Yao Chang for evaluating presented compounds in a competitive FP assay. I thank Dr. Jochen Imig in advance for planning RT-qPCR experiments to provide evidence for targeted RNA degradation using presented RITACs and RIBOTACs in cells. Lydia Borgelt and Neele Haacke for establishing and evaluating presented compounds in RNase L activation assays.

I highly appreciate the useful input from Dr. Stéphanie Guéret, Dr. Malte Gersch, Dr. Sebastian Loscher and Dr. Andrei Ursu on my research projects.

Thank you, Caitlin Davies and Lydia Borgelt, for proofreading my thesis.

I acknowledge analytical departments at the Max Planck Institute of Molecular Physiology and TU Dortmund for characterization of presented compounds by NMR and HRMS.

For the financial support, I thank the Max Planck Society for funding my doctoral studies with a fellowship.

Last but not least, I want to thank my family and friends supporting this journey. It has been especially important during these challenging times caused by the SARS-CoV-2 pandemic. You have brought necessary distraction and motivation to complete this chapter of my research career.

8.3. Eidesstattliche Versicherung (Affidavit)

Stenbratt, Carl Leonard

Name, Vorname
(Surname, first name)

215951

Matrikel-Nr.
(Enrolment number)

Belehrung:

Wer vorsätzlich gegen eine die Täuschung über Prüfungsleistungen betreffende Regelung einer Hochschulprüfungsordnung verstößt, handelt ordnungswidrig. Die Ordnungswidrigkeit kann mit einer Geldbuße von bis zu 50.000,00 € geahndet werden. Zuständige Verwaltungsbehörde für die Verfolgung und Ahndung von Ordnungswidrigkeiten ist der Kanzler/die Kanzlerin der Technischen Universität Dortmund. Im Falle eines mehrfachen oder sonstigen schwerwiegenden Täuschungsversuches kann der Prüfling zudem exmatrikuliert werden, § 63 Abs. 5 Hochschulgesetz NRW.

Die Abgabe einer falschen Versicherung an Eides statt ist strafbar.

Wer vorsätzlich eine falsche Versicherung an Eides statt abgibt, kann mit einer Freiheitsstrafe bis zu drei Jahren oder mit Geldstrafe bestraft werden, § 156 StGB. Die fahrlässige Abgabe einer falschen Versicherung an Eides statt kann mit einer Freiheitsstrafe bis zu einem Jahr oder Geldstrafe bestraft werden, § 161 StGB.

Die oben stehende Belehrung habe ich zur Kenntnis genommen:

Official notification:

Any person who intentionally breaches any regulation of university examination regulations relating to deception in examination performance is acting improperly. This offence can be punished with a fine of up to EUR 50,000.00. The competent administrative authority for the pursuit and prosecution of offences of this type is the chancellor of the TU Dortmund University. In the case of multiple or other serious attempts at deception, the candidate can also be unenrolled, Section 63, paragraph 5 of the Universities Act of North Rhine-Westphalia.

The submission of a false affidavit is punishable.

Any person who intentionally submits a false affidavit can be punished with a prison sentence of up to three years or a fine, Section 156 of the Criminal Code. The negligent submission of a false affidavit can be punished with a prison sentence of up to one year or a fine, Section 161 of the Criminal Code.

I have taken note of the above official notification.

Ort, Datum
(Place, date)

Unterschrift
(Signature)

Titel der Dissertation:
(Title of the thesis):

**RNA Degradation using Small Molecule-
Based Recruiters of RNase L**

Ich versichere hiermit an Eides statt, dass ich die vorliegende Dissertation mit dem Titel selbstständig und ohne unzulässige fremde Hilfe angefertigt habe. Ich habe keine anderen als die angegebenen Quellen und Hilfsmittel benutzt sowie wörtliche und sinngemäße Zitate kenntlich gemacht.

Die Arbeit hat in gegenwärtiger oder in einer anderen Fassung weder der TU Dortmund noch einer anderen Hochschule im Zusammenhang mit einer staatlichen oder akademischen Prüfung vorgelegen.

I hereby swear that I have completed the present dissertation independently and without inadmissible external support. I have not used any sources or tools other than those indicated and have identified literal and analogous quotations.

The thesis in its current version or another version has not been presented to the TU Dortmund University or another university in connection with a state or academic examination.*

*Please be aware that solely the German version of the affidavit ("Eidesstattliche Versicherung") for the PhD thesis is the official and legally binding version.

Ort, Datum
(Place, date)

Unterschrift
(Signature)